Synthesis, Characterization and Modification of Hyperbranched Polyether Polyol Copolymers

Dissertation zur Erlangung des Grades
“Doktor der Naturwissenschaften (Dr. rer. nat.)”
im Promotionsfach Chemie
am Fachbereich Chemie, Pharmazie und Geowissenschaften
der Johannes Gutenberg-Universität
in Mainz

Jan Seiwert
geb. in Saarlouis
Mainz, den 03.06.2016

Dekan:

1. Berichterstatter:

2. Berichterstatter:

Datum der mündlichen Prüfung:29.06.2016

Die jetzt als Dissertation vorgelegte Arbeit wurde im Zeitraum von Mai 2013 bis Juni 2016 am Institut für Organische Chemie der Johannes Gutenberg-Universität Mainz angefertigt.

Hiermit versichere ich gemäß § 10 Abs. 3d der Promotionsordnung vom 24.07.2007

a) Ich habe die jetzt als Dissertation vorgelegte Arbeit selbst angefertigt und alle benutzten Hilfsmittel (Literatur, Apparaturen, Material) in der Arbeit angegeben.
b) Ich habe oder hatte die jetzt als Dissertation vorgelegte Arbeit nicht als Prüfungsarbeit für eine staatliche oder andere wissenschaftliche Prüfung eingereicht.
c) Ich hatte weder die jetzt als Dissertation eingereichte Arbeit noch Teile davon bei einer anderen Fakultät bzw. einem anderen Fachbereich als Dissertation eingereicht.

D77 (Dissertation Johannes Gutenberg-Universität Mainz)

“Yeah Science!”

(Jesse Pinkman, Breaking Bad)

ACKNOWLEDGEMENT / DANKSAGUNG

An dieser Stelle möchte ich mich gerne bei den vielen Menschen bedanken, die zum Gelingen dieser Arbeit beigetragen haben.

TABLE OF CONTENTS

MOTIVATION AND OBJECTIVES

Poly(alkylene oxide)s are a versatile and conveniently accessible class of polymers. Their linear polyether backbones are chemically inert in a wide range of conditions and flexible with low glass transition temperatures. Although different poly(alkylene oxide) comprise the same polyether backbone, their materials properties and thereby their fields of application differ tremendously depending on the presence and length of an alkyl side chain. Poly(ethylene oxide) (PEO) is the gold standard polymer for pharmaceutical applications as it is water-soluble, non-toxic, and able to prolong the circulation time of drugs by providing a "stealth effect" against the immune system. PEO is also a widely used additive for food and cosmetic products. Poly(propylene oxide) (PPO) on the other hand is rather hydrophobic and employed in many formulations for polyurethanes. Poly(1,2-butylene oxide) (PBO) is a less widespread material, but has found commercial application as an oil-soluble lubricant. Amphiphilic block copolymers of PEO and substituted poly(alkylene oxide)s have surfactant properties and are widely used in industrial applications, personal care products and pharmaceuticals. PEO, PPO and PBO are produced on a large industrial scale from readily available alkylene oxide monomers.

This thesis aims at combining the useful properties of linear poly(alkylen oxide)s with the advantages of a hyperbranched topology. In contrast to linear polymers, hyperbranched polymers exhibit dendrimer-like features such as a high number of functional end groups, a compact structure, and low viscosity in melt and in solution. In contrast to perfectly branched dendrimers, they are usually obtained in one-step polymerizations, generally resulting in irregular branching and broad molecular weight distributions. Hyperbranched polyglycerol is one of the few established hyperbranched polymers that can be prepared with control over molecular weight and narrow to moderate molecular weight distributions using slow addition of the glycidol (G) monomer. Its applications, however, are restricted because polyglycerol is highly hydrophilic with limited solubility in most organic solvents, and has a significantly less flexible polyether backbone than linear poly(alkylene oxide)s. Copolymerization of EO, PO or BO with glycidol as a branching agent provides a synthetic toolbox for adjusting the degree of branching, the number of hydroxyl functionalities, the solubility profile, and the thermal properties of the resulting materials. Controlled synthesis of these hyper-branched poly(alkylene oxide)s and elucidation of their complex branched structure are key challenges adressed in this thesis.

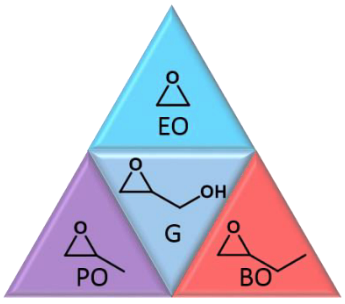

In summary, the following objectives were pursued in this thesis:

1) A main focus of this thesis is on the creation of a synthetic toolbox for hyperbranched poly(alkylene oxide)s that permits systematic variation of molecular weight, branching and solubility of the resulting materials. Already established batch procedures for the copolymerization of ethylene oxide and propylene oxide with glycidol as a branching agent only provided limited control over molecular weight and yielded hydrophiphilic materials mainly. Therefore the concept is further developed by introducing 1,2-butylene oxide as a hydrophobic comonomer to give access to more apolar hyperbranched polyether polyols. Slow monomer addition (SMA) procedures for the low-boiling alkylene oxide monomers are developed to enable polymerization with control over the molecular weight, a key challenge for the synthesis of hyperbranched polymers.

2) Anionic ring-opening copolymerization of glycidol with linear AB monomers leads to complex, irregularly branched polymer structures. A particular emphasis is placed on the detailed structure elucidation of the different copolymers synthesized, both individually and in comparison with each other. Precise information about the molecular weight and the microstructure of the hyperbranched copolymers prepared is the key to optimizing synthetic routes and to establishing and understanding structure-property relationships. Absolute molecular weight determination of hyperbranched polymers and examination of their monomer sequence distribution are challenges hardly solved to date.

3) Another important objective of this thesis is to capitalize on the high functionality of hyperbranched polyether polyols for applications as multifunctional macroinitiators for the core-first synthesis of multiarm star copolymers with a hyperbranched polyether core. Immortal copolymerization of carbon dioxide with epoxides and controlled radical polymerization of styrene are explored for the synthesis of linear hydrophobic arms. Following this concept, novel core-shell architectures can be accessed which have potential applications as unimolecular nanocontainers with adjustable core and shell.

4) Finally, this thesis aims at the development of thioether-functional polyether polyols. To achieve this, glycidol is copolymerized with a thioether-bearing epoxide monomer. The resulting materials offer great potential for post-polymerization modification due the high number of hydroxyl groups and the versatile chemistry of the thioether moieties. Thioether-containing polymers are known for their redox-switchable water solubility and their ability to form polyelectrolytes via alkylation.

ABSTRACT

This thesis aims to develop and improve the synthesis, characterization and modification of hyperbranched polyether polyol copolymers based on glycidol as a branching agent and other epoxide monomers, particularly ethylene oxide (EO), propylene oxide (PO) and 1,2-butylene oxide (BO).

Chapter 1.1 summarizes the state of the art concerning the synthesis of star-shaped and hyperbranched polymers from ethylene oxide, propylene oxide and 1,2-butylene oxide. Core-first and arm-first strategies for the preparation of star, star block and miktoarm star architectures are presented. Different methods of introducing branch-on-branch topologies are discussed. **Chapter 1.2** provides an overview of the synthesis, properties, and applications of poly(propylene oxide), poly(butylene oxide) and higher poly(alkylene oxide)s in general.

Novel synthetic strategies and detailed characterization methods for hyperbranched poly(alkylene oxide)s are presented in **chapter 2**. The copolymerization kinetics of the multibranching ring-opening anionic copolymerization of glycidol with different alkylene oxides is investigated by online ^{1}H NMR kinetic experiments in **chapter 2.1**. Reactivity ratios are calculated and related to the molecular weight distribution and the degrees of branching of the respective copolymers, implying a change from a hyperbranched to a hyperstar structure with increasing alkylene chain length of the alkylene oxide comonomer.

Chapter 2.2 focuses on the synthesis of hyperbranched poly(ethylene oxide) (*hb*PEO) copolymers with limited extent of control over the molar mass by variation of the solvent and the absolute molar mass characterization of these materials. For this purpose, analytical ultracentrifugation (AUC), intrinsic viscosity, translational diffusion measurements and SEC were combined. It is demonstrated that the use of linear PEO for the SEC calibration results in significantly underestimation of the molar masses of *hb*PEO. Absolute molar mass values up to 1.7 x 10^{6} g mol^{-1} are obtained by copolymerization in dioxane as an emulsifying solvent.

First results from applying the slow monomer addition (SMA) technique for the synthesis of *hb*PEO are shown in **chapter 2.3**. A special reactor setup is employed to add gaseous EO and glycidol continuously in a safe manner. In contrast to previous batch procedures, well-defined *hb*PEO copolymers are obtained with control over the degree of polymerization.

In **chapter 2.4** the synthesis of hyperbranched poly(butylene oxide) polyols by anionic copolymerization of 1,2-butylene oxide and glycidol is introduced. Systematic variation of the composition results in a series of moderately distributed copolymers, albeit with limited molecular weights in the solvent-free batch process. Considerably higher molecular weights are obtained under slow monomer addition conditions. By alteration of the comonomer ratio, glass transition temperatures and aqueous solubility of the hyperbranched copolymers can be tailored, resulting in well-defined cloud point temperatures.

The application of hyperbranched poly(alkylene oxide)s for the synthesis of different kinds of multiarm star copolymers is presented in **chapter 3**. **Chapter 3.1** capitalizes on hyperbranched poly(propylene oxide) polyols as multifunctional initiators for the copolymerization of propylene oxide with CO_2. Poly(propylene carbonate) (PPC) star copolymers with 14 and 28 arms, respectively, are obtained. These materials exhibit low glass transition temperatures ranging from -8 to 10 °C, approximately 30 °C lower than the glass transition temperatures of linear PPC. The terminal hydroxyl groups are capable of forming urethanes with phenylisocyanate, rendering the star copolymers potential building blocks for polyurethane networks.

Chapter 3.2 further elaborates on the synthesis of polycarbonate multiarm star polymers. *Hb*PEO and hyperbranched poly(butylene oxide) polyols are used to initiate the copolymerization of CO_2 with PO and BO, respectively. The influence of the core polymer and different comonomers for the CO_2 copolymerization on the polycarbonate star formation is studied. Amphiphilic core-shell structures able to encapsulate hydrophilic guest molecules are prepared.

The three-step synthesis of ultra-high molecular weight polystyrene hyperstar copolymers with a hyperbranched PEO core is presented in **chapter 3.3**. *Hb*PEO is modified with initiator groups for atom transfer radical polymerization (ATRP) and subsequently used for the controlled radical polymerization of styrene. Separation of the polystyrene arms from the polyether core allows individual characterization of the polystyrene arms and confirms narrow to moderate dispersities.

Chapter 4 focuses on the multibranching copolymerization of glycidol with a thioether-functional comonomer, 2-(methylthio)ethyl glycidyl ether (MTEGE). The resulting materials provide various options for orthogonal post-polymerization modification. Oxidation of the thioethers enables tailoring the copolymers' solubility profile. Furthermore, the thioethers can be selectively alkoxylated with epoxides, resulting in functional hyperbranched polyelectrolytes. These moieties also tolerate urethane functionalization of the glycerol units.

ZUSAMMENFASSUNG

Ziel dieser Dissertation ist die Entwicklung und Verbesserung der Synthese, Charakterisierung und Funktionalisierung von hyperverzweigten Polyether-Polyol-Copolymeren auf der Basis von Glycidol als Verzweigungseinheit und anderen Epoxid-Comonomeren, insbesondere Ethylenoxid (EO), Propylenoxid (PO) und 1,2-Butylenoxid (BO). **Kapitel 1.1** fasst den Stand der Technik auf dem Gebiet sternförmiger und hyperverzweigter Polyether zusammen, die aus Ethylenoxid, Propylenoxid und 1,2-Butyleneoxid aufgebaut sind. „Core-first" und "Arm-first" Strategien für die Synthese von Stern-, Stern-Block- und Miktoarm-Stern- Architekturen werden gezeigt. Verschiedene Methoden zur Darstellung dendritischer Polyether-Strukturen werden diskutiert. **Kapitel 1.2** bietet einen allgemeinen Überblick über die Synthese, Eigenschaften und Anwendungsmöglichkeiten von Poly(propylenoxid), Poly(1,2-butylenoxid) und höheren Poly(alkylenoxid)en.

In **Kapitel 2** werden neue Synthesestrategien und detaillierte Charakterisierungsmethoden für hyperverzweigte Poly(alkylenoxid)e präsentiert. Die Copolymerisationskinetik der verzweigenden, ringöffnenden Copolymerisation von Glycidol mit unterschiedlichen Alkylenoxiden wird in **Kapitel 2.1** mittels online ^{1}H NMR Kinetik-Experimenten untersucht. Copolymerisationsparameter werden berechnet und in Beziehung zu den Molekulargewichtsverteilungen sowie den Verzweigungsgraden der einzelnen Copolymere gesetzt. Mit zunehmender Länge der Alkylkette des Alkylenoxids lässt sich bei den Copolymeren eine Änderung von einer hyperverzweigten zu einer hypersternartigen Struktur feststellen. **Kapitel 2.2** legt den Fokus auf die Synthese von hyperverzweigtem Poly(ethylenoxid) (*hb*PEO) mit begrenzter Kontrolle über die erreichbaren Molekulargewichte durch die Wahl des Lösungsmittels und die Bestimmung absoluter Molekulargewichte für diese Materialien. Zur Untersuchung werden analytische Ultrazentrifugation, Viskosimetrie, Diffusionsexperimente und GPC kombiniert. Es wird demonstriert, dass die Verwendung von linearen PEO-Standards für die GPC zu einer signifikanten Unterschätzung der Molekulargewichte von *hb*PEO führt. Absolute Molekulargewichte bis zu 1.7×10^{6} g mol^{-1} werden für Copolymere bestimmt, die durch Copolymerisation in Dioxan erhalten werden. **Kapitel 2.3** zeigt erste Ergebnisse der Anwendung der langsamen Monomerzugabe für die Synthese von *hb*PEO. Ein spezieller Reaktor-Aufbau wird verwendet um die sichere, kontinuierliche Zugabe von gasförmigem Ethylenoxid und flüssigem Glycidol zu ermöglichen. Im Gegensatz zu früheren Batch-Verfahren können auf diese Weise zum ersten Mal definierte *hb*PEO-Copolymere mit Kontrolle über den Polymerisationsgrad hergestellt werden. In **Kapitel 2.4** wird die Synthese von hyperverzweigten Poly(butylenoxid)-Polyolen durch

anionische Copolymerisation von 1,2-Butylenoxid mit Glycidol vorgestellt. Im Lösungsmittel-freien Batch-Verfahren wird durch systematische Variation der Zusammensetzung eine Reihe mäßig breit verteilter Copolymere mit begrenzten Molekulargewichten erhalten. Deutlich höhere Molekulargewichte sind unter Anwendung langsamer Monomerzugabe zugänglich. Durch Änderung der Copolymer-Zusammensetzung lassen sich Glasübergangstemperaturen und Wasserlöslichkeit steuern. So werden thermoresponsive Polymere mit einstellbaren Trübungstemperaturen erhalten.

In **Kapitel 3** wird die Anwendung hyperverzweigter Poly(alkylenoxid)e für die Synthese unterschiedlicher Multiarm-Stern-Copolymere präsentiert. **Kapitel 3.1** zeigt die Verwendung von hyperverzweigten Poly(propylenoxid)-Polyolen als multifunktionellen Makroinitiatoren für die Copolymerisation von Propylenoxid mit CO_2. Poly(propylencarbonat)-Stern-Copolymere mit 14 bzw. 28 Armen werden erhalten. Diese Materialien weisen niedrige Glasübergangstemperaturen im Bereich von -8 bis 10 °C auf, die etwa 30 °C unter den Glasübergangstemperaturen linearer Poly(propylencarbonat)e liegen. Die endständigen Hydroxylgruppen sind in der Lage Urethane zu bilden, womit diese Stern-Copolymere mögliche Bausteine für Polyurethan-Netzwerke darstellen. **Kapitel 3.2** erweitert und verbessert die Synthese von Polycarbonat-Multiarm-Stern-Copolymeren. *Hb*PEO- und hyperverzweigte Poly(butylenoxid)-Polyole werden eingesetzt um die Copolymerisation von CO_2 mit PO oder BO zu initiieren. Der Einfluss der Kern-Polymere und unterschiedlicher Comonomere für die CO_2-Copolymerisation auf die Bildung der Polycarbonat-Multiarm-Sterne wird untersucht. Es werden amphiphile Kern-Schale-Strukturen erhalten, die in der Lage sind hydrophile Gastmoleküle einzulagern. In **Kapitel 3.3** wird die dreistufige Synthese von Polystyrol-Multiarm-Stern-Copolymeren mit *hb*PEO-Kern gezeigt, die ultrahohe Molekulargewichte aufweisen. *Hb*PEO wird mit ATRP-Initiatorgruppen (Atom Transfer Radical Polymerization) funktionalisiert und anschließend für die kontrollierte radikalische Polymerisation von Styrol eingesetzt. Abspaltung der Polystyrol-Arme vom Polyether-Kern ermöglicht die individuelle Charakterisierung der Polystyrol-Arme. Enge bis mäßig breite Molekulargewichtsverteilungen werden gefunden.

Kapitel 4 legt den Fokus auf die verzweigende Copolymerisation von Glycidol mit einem Thioether-funktionellen Comonomer, dem 2-(Methylthio)ethylglycidylether (MTEGE). Die resultierenden Materialien bieten verschiedene Optionen für orthogonale Post-Polymerisation-Modifikationen. Oxidation der Thioether ermöglicht die Beeinflussung der Wasserlöslichkeit der Copolymere. Desweiteren können die Thioether-Gruppen selektiv durch Epoxide alkoxyliert werden um funktionelle, hyperverzweigte Polyelektrolyte zu erhalten. Die Thioether-Gruppen tolerieren außerdem die Funktionalisierung der Glycerin-Einheiten zu Urethanen.

GRAPHICAL ABSTRACT

2 SYNTHESIS AND CHARACTERIZATION OF HYPERBRANCHED POLY(ALKYLENE OXIDE)S

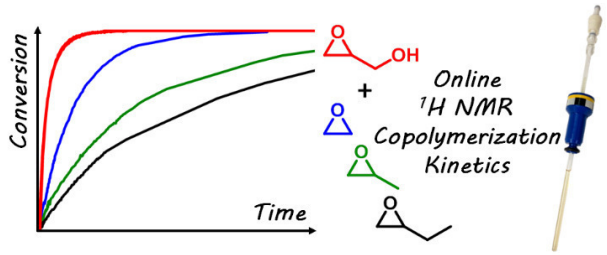

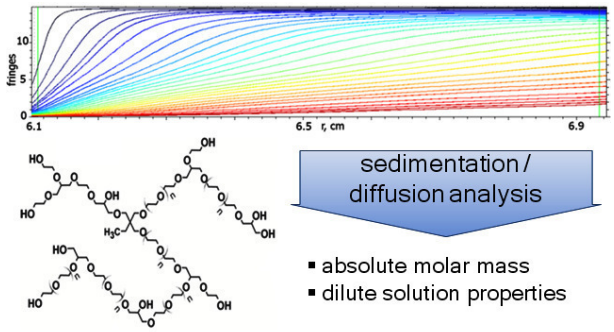

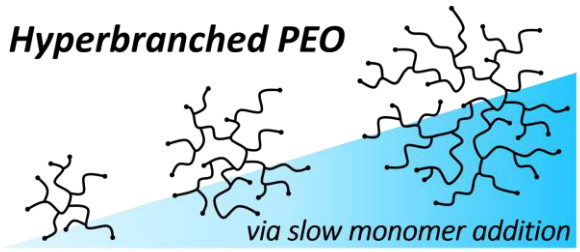

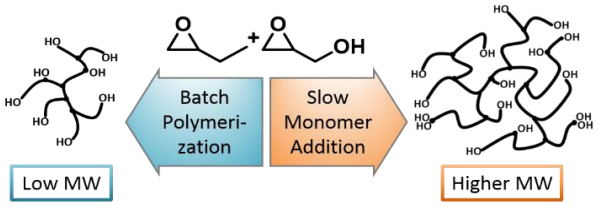

3 HYPERBRANCHED POLY(ALKYLENE OXIDE)S AS MACROINITIATORS FOR MULTIARM STAR COPOLYMERS

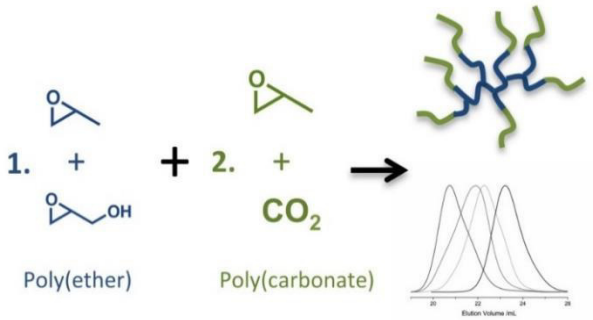

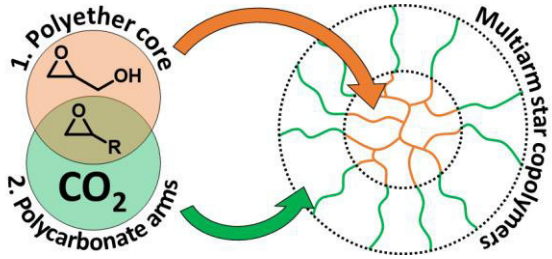

4 HETEROFUNCTIONAL HYPERBRANCHED POLYETHER POLYOS

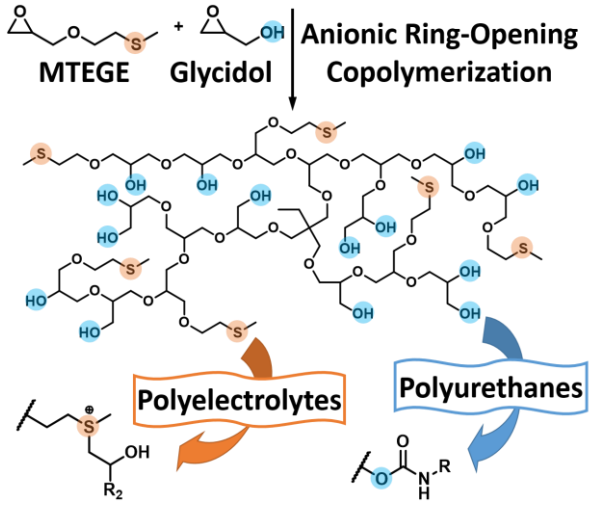

1

INTRODUCTION

Sections 1.1 and 1.2 are contributions by the author of this thesis that were published in *Chemical Reviews*, **2016**, *116*, 2170−2243 (Special Issue: Frontiers in Macromolecular and Supramolecular Science) as part of

Polymerization of Ethylene Oxide, Propylene Oxide, and Other Alkylene Oxides: Synthesis, Novel Polymer Architectures, and Bioconjugation

Jana Herzberger[1,2], Kerstin Niederer[1], Hannah Pohlit[1,2,3,4], Jan Seiwert[1], Matthias Worm[1,3], Frederik R. Wurm[3,5], Holger Frey[1,2,]*

[1] Institute of Organic Chemistry, Johannes Gutenberg-University Mainz, Duesbergweg 10-14, 55128 Mainz, Germany

[2] Graduate School Materials Science in Mainz, Staudingerweg 9, 55128 Mainz, Germany

[3] Max Planck Graduate Center, Staudingerweg 6, 55128 Mainz, Germany

[4] Department of Dermatology, University Medical Center, Langenbeckstraße 1, 55131 Mainz, Germany

[5] Max Planck Institute for Polymer Research, Ackermannweg 10, 55128 Mainz, Germany

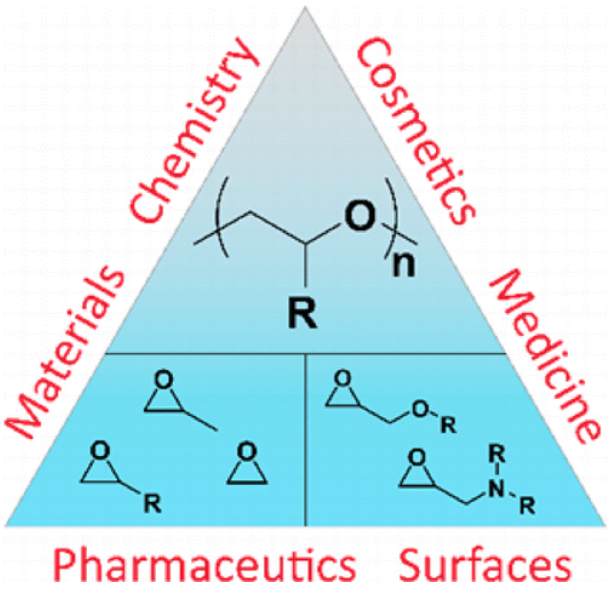

1.1 Star-Shaped and Hyperbranched Poly(alkylene oxide)s

Star-shaped, hyperbranched and dendritic polyethers exhibit unique properties that distinguish them from linear polymers, such as multiple functional end groups, a compact structure, low viscosities both in bulk and solution and a strongly reduced degree of crystallization in comparison to their linear counterparts. These properties are key to numerous advanced applications.

Star Polymers

Star-shaped polymers can be obtained by two fundamentally different synthetic strategies: the "core-first" (CF) and the "arm-first" (AF) approach. The "core-first" procedure utilizes a multifunctional initiating core-molecule to start the chain growth of the arms. Defined molecules or polymers with a predetermined number of initiating sites or multifunctional cross-linked or dendritic polymers are commonly employed for the core. In the "arm-first" process, end groups of living or functionalized, prefabricated polymer chains are either attached to a multifunctional core or connected via a (cross)linking procedure.

A very detailed and comprehensive review on star-shaped polymers with poly(ethylene glycol) (PEG) / poly(ethylene oxide) (PEO) arms was given by Lapienis in 2009.[1] Therefore, in the current review, mainly recent developments in the synthesis of PEG-based star polymers (Table 1), star-shaped block copolymers (Table 2), and miktoarm star copolymers (Table 3) since 2009 will be covered. Furthermore, star-shaped polymers containing poly(propylene oxide) (PPO) or poly(1,2-butylene oxide) PBO are summarized in Table 4. Star polymers based on commercially available, four- and eight-armed PEG stars are not considered.

In recent years only few core-first syntheses of PEG star polymers have been reported. Most of them rely on the anionic ring-opening polymerization (AROP) of ethylene oxide (EO). The harsh, strongly alkaline reaction conditions, however, limit the synthetic scope with respect to suitable core molecules and copolymers. Multiarm stars were obtained from hyperbranched polyglycerol and characterized in detail by MALDI-ToF MS.[2] Use of beta-cyclodextrin as an initiator gave access to 14-arm and 21-arm *star*PEG.[3] Tonhauser et al. introduced iron-containing, water-soluble AB_2 miktoarm stars via living anionic polymerization of vinylferrocene (VFc), followed by benzyl glycidyl ether termination, hydrogenative deprotection and subsequent AROP of EO.[4] By Glaser coupling, Huang et al. obtained polystyrene (PS) and polyisoprene (PIP) macroinitiators with two

hydroxyl iniation sites at the center for the ensuing EO polymerization, resulting in amphiphilic A_2B_2 miktoarm star structures.[5] Wang et al. used an orthofunctional core, having four hydroxyl and four allyl moieties, for the preparation of A_4B_4 miktoarm star copolymers. In the first step, PEG arms were synthesized and end-capped. Subsequent thiol−ene click reaction converted the allyl groups into initiating sites for the polymerization of poly(ε-caprolactone) (PCL), polystyrene, and poly(tert-butyl acrylate).[6] The only report on cationic ring-opening polymerization (CROP) of EO in this area deals with the synthesis of a three-arm *star*(PCL-*b*-PEG).[7]

Due to the demanding handling of ethylene oxide and the restrictions regarding functional group tolerance, the “arm-first” method and prefabricated PEG polymers are more commonly employed than the “core-first” approach. Click couplings, especially the copper-catalyzed azide−alkyne cycloaddition, but also thiol−ene and Diels−Alder reactions, have been identified as a convenient method to attach prefabricated PEG chains.[8-12] Since click reactions take place under mild conditions and tolerate a great amount of functional groups, they have found to be particularly useful for the preparation of miktoarm stars.[13-25] Controlled radical polymerization techniques, such as atom transfer radical polymerization (ARTP) and reversible addition-fragmentation chain transfer polymerization (RAFT), have also been explored extensively as a synthetic tool for arm-first star polymer synthesis.[26-33] After end functionalizing PEG with a suitable initiator group, cross-linking polymerization of divinyl monomers leads to star architectures. In analogy, ring-opening metathesis polymerization (ROMP) was applied using bis-norbonene monomers.[34] Functional cross-linkers gave access to PEG stars with acid-labile, redox-cleavable, cationic, and fluorinated core, respectively (see Figure 1).

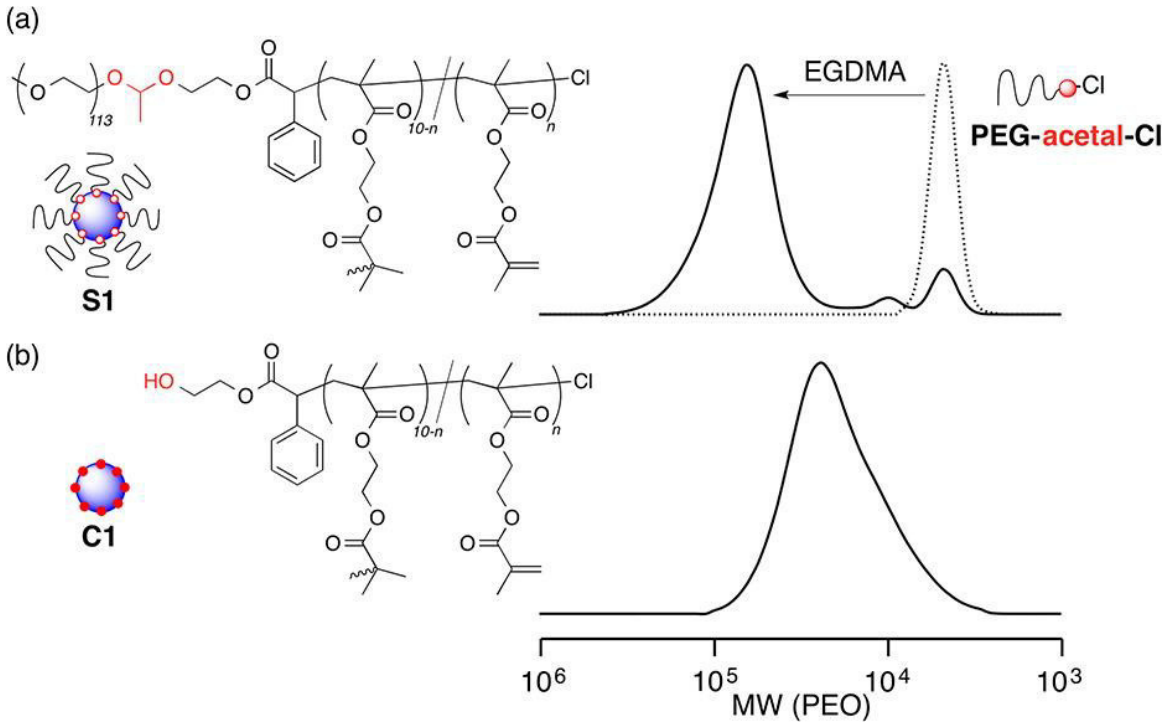

Figure 1. Cleavage of an acetal-linked multiarm star polymer with P(EGDMA) core and PEG arms. (Adapted with permission from Terashima, T.; Nishioka, S.; Koda, Y.; Takenaka, M.; Sawamoto, M. *J. Am. Chem. Soc*. 2014, 136, 10254−10257.[30] Copyright 2014 American Chemical Society.)

A particular research focus is currently on the development of biodegradable materials. Numerous star-shaped poly(ε-caprolactone)s, polylactides (PLA) and polyamides have been modified with PEG chains as a hydrophilic outer block to impart aqueous solubility. Mostly, the connection was established simply via esterification. These core−shell architectures are mostly designed for encapsulation and release of hydrophobic guest molecules with potential applications as drug carriers in mind.[35-44]

Several works capitalize on the combination of hyperbranched polymer cores and prefabricated PEG blocks to gain facile access to multiarm star polymers and star block polymers.[11,12,41,42,45-49] Cross-linked PS, polyethylenimine, polyesters, and specially designed conjugated polymers have been employed as core molecules.

Table 1. List of star-shaped PEG polymers (Reported since 2010).

Number of arms	Core molecule	Arm attachment method	Ref.
3	1,3,5-tri(azobenzeneethynyl)benzene	AF, sonogashira coupling	50
3 / 6 / 12	polyester dendrimer	AF, azide-alkyne click	8
4	dityrosine	AF, esterification	51
4	phthalocyanine	AF, cyclotetramerization of phthalonitrile	52
8	octakis(hydridodimethylsiloxy)-octasilsesquioxane	AF, hydrosilylation	53
9	nonaazido-dendrimer	AF, azide-alkyne click	9
14 / 21	beta-cyclodextrin	CF, AROP	3
Multi	hyperbranched PG	CF, AROP	2
Multi	PS-*co*-PDVB	AF, azide-alkyne click	45
Multi	hyperbranched polyacetal	AF, hydrazone formation	48
Multi	hyperbranched conjugated polymer	AF, hydrazone formation	46
Multi	hyperbranched conjugated polymer	AF, esterification	47
Multi	hyperbranched P(γ-benzyl L-glutamate)	AF, amidation	49
Multi	PDVB	AF, cross-linking ATRP / free radical polymerization	26
Multi	P(EGDMA-*co*-DMAEMA) / P(EGDMA-*co*-disulfideDMA)	AF, cross-linking ATRP	27
Multi	P(dimethylammonium DEMA)	AF, cross-linking ATRP	28
Multi	P[EGDMA-*co*-DMAEMA-*co*-(perfluoroalkyl methacrylate)]	AF, cross-linking ATRP	29
Multi	P(EGDMA) / P(PEGDMA), arms attached via acetal linker	AF, cross-linking ATRP	30
Multi	P(EGDMA)	AF, cross-linking eATRP	31
Multi	P[*N*,*N*'-methylene bis(acrylamide)]	AF, cross-linking reversible-deactivation radical pol. (RDRP)	32

Table 1 (continued). List of star-shaped PEG polymers (Reported since 2010).

Multi	P(EGDMA) / P(disulfideDMA) / P(ketalDMA)	AF, cross-linking RAFT	33
Multi	acid-labile bis-norbornene cross-linker	AF, cross-linking ROMP	34

Table 2. List of Novel Star-Shaped PEG Block Copolymers (Reported Since 2010).

Number of arms	**Core molecule**	**Arm A**	**Arm B**	**Method**	**Ref.**
3	trimethylolpropane (TMP)	PCL	PEG	CF, CROP	7
3	phenyl	polyisobutene	PEG	AF, esterification	54
3 / 4	glycerol triacrylate/ bisTMP tetraacrylate	poly (ω-undecenyl acrylate)	PEG	AF, Heck coupling	55
4	a)	PCL	PEG	AF, azide-alkyne click	14
4	cystamine	b)	PEG	AF, thiol-yne click	10
4	Pentaerythritol (PETH)	PCL	c)	AF, amidation	56
4	PETH	PLA	PEG	AF, esterification	57
4	porphyrine	PLA	PEG	AF, esterification	43
4	porphyrine	PCL	PEG	AF, esterification	35
4/ 6	PETH / diPETH	PCL	PEG	AF, esterification	36
7	beta cyclodextrin	PCL-*co*-carbonate	PEG	AF, esterification	37
A_4B_8	PETH	PCL-diol	PEG	AF, esterification	38
8	d)	poly(benzyl L-aspartate)	PEG	AF, amidation	39
16/ 32	poly(amidoamine) dendrimer	poly(L-lysine)	PEG	AF, esterification	40
Multi	polydivinylbenzene (PDVB)	PS	PEG	AF, azide-alkyne click	11

Table 2 (continued). List of Novel Star-Shaped PEG Block Copolymers (Reported Since 2010).

Multi	PS-*co*-PDVB	PMMA	PEG	AF, Diels-Alder click	12
Multi	hyperbranched poly(ethylenimine)	poly(L-lysine)	PEG	AF, urethane formation	41
Multi	hyperbranched Boltorn H40	e)	PEG	AF, esterification	42
Multi	poly[(4,4'-bioxep-ane)-7,7'-dione]	PCL	PEG	AF, cross-linking ROP	44

[a] 2-(benzyloxycarbonyl)-2-methylpropane-1,3-diyl bis[3-hydroxy-2-(hydroxymethyl)-2-methylpropanoate], [b] poly(ε-benzyl-oxycarbonyl-L-lysine), [c] PEG-glycyrrhetinic acid, [d] polyhedral oligomeric silsesquioxanes (POSS), [e] biodegradable photo-luminescent polymer

Table 3. List of PEG Containing Miktoarm Star Copolymers (Reported Since 2010).

Number of arms	**Core**	**Arm A**	**Arm B**	**Arm C**	**Method**	**Ref.**
AB_2	-	PVFc	PEG	-	CF, AROP	4
AB_2	-	PEG	PS/ P*t*BuA	-	AF, azide-alkyne click	13
AB_2	-	PEG	PCL	-	AF, Diels-Alder click	14
AB_2	-	PS/ P*t*BuA	PEG	-	AF, nitroxide radical coupling	13
AB_3	cholic acid	PEG	PCL	-	AF, azide-alkyne click	15
AB_3	PETH triazide	a)	PEG	-	AF, azide-alkyne click	16
AB_3/ AB_4	PETH triazide / PETH tetrazide	PE	PEG	-	AF, azide-alkyne click	17
A_2B_2	coupled propargyl (propyl glycol)	PS/ PI	PEG	-	CF, AROP	5
A_2B_2	calixarene	PCL	PEG	-	AF, azide-alkyne click	18
A_4B_4	$(OH)_4$/ $(Allyl)_4$	PEG	PCL/ PS/ P*t*BuA	-	CF, AROP	6

Table 3 (continued). List of PEG Containing Miktoarm Star Copolymers (Reported Since 2010).

$A_{14}B_7$	beta cyclodextrin	PCL	PEG	-	AF, azide-alkyne click	19
A_8B_4	resorcinarene	PEG	PCL	-	AF, azide-alkyne click	20
ABC	-	PEG	PS	PCl	AF, azide-alkyne click	21
ABC	b)	PS	PCL	PEG	AF, Diels-Alder click	22
ABC	beta cyclodextrin/ adamantane (supramolecular)	PEG	c)	PMMA	AF, azide-alkyne click	23
ABC	-	PEG	PS	d)	AF, azide-alkyne click	24
ABC	-	PS-pyrene	PEG	PMMA	AF, esterification	58
ABCDE	-	PEG	PCL	PS + e)	AF, azide-alkyne click	25
Multi	P(*N*,*N*'-methylene bis(acrylamide))	PEG	f)	-	AF, cross-linking RDRP	32
Multi	hyperbranched Boltorn H30	PEG	PCL	-	AF, esterification	59

[a] Azobenzene-substituted methacrylate, [b] 1-(allyloxy)-3-azidopropan-2-yl (anthracen-9-ylmethyl) succinate, [c] poly(2-dimethylamino-ethylmethacrylate), [d] poly[6-(4-methoxy-azobenzene-4'-oxy) hexyl methacrylate], [e] Arm D: PLA, Arm E: poly(acrylic acid), [f] poly(*N*-isopropylacrylamide)

PPO-containing star polymers are commercially used as building blocks for polyurethane soft foams. Reports on novel star-shaped architectures consisting of propylene oxide and higher alkylene oxides, however, are rare. In core first approaches, six-arm *star*[PPO-*b*-P(2,2-dimethyltrimethylene carbonate)] with p-*tert*-butyl-calix[6]arene core,[60] multi-arm *star*PPO and *star*(PPO-*b*-PEG) with hyperbranched polyglycerol core have been introduced.[61,62] Using phosphonium catalysts, three-arm *star*PBO copolymers with polycarbonate and polyester blocks, and four-arm *star*PBO with 1,2,4,5-benzenetetramethanol core were synthesized by anionic ring-opening polymerization.[63,64]

Table 4. List of Star-Shaped PPO/PBO Polymers and Block Copolymers.

Number of arms	Core molecule	Arm A	Arm B	Method	Ref.
6	p-*tert*-butyl-calix[6]arene	PPO	a)	CF, AROP	60
Multi	hyperbranched polyglycerol	PPO	-	CF, AROP	61
Multi	hyperbranched polyglycerol	PPO	PEG	CF, AROP	62
3	TMP	PBO	b)	CF, AROP	63
4	1,2,4,5-benzene tetramethanol	PBO	-	CF, AROP	64

[a)] poly(2,2-dimethyl-trimethylene carbonate), [b)] PEG-*b*-poly(trimethylene carbonate)-*b*-poly(δ-valerolactone)

Branched and Hyperbranched PEG, PPO, and PBO Derivatives

Since 1990, hyperbranched polymers have attracted steadily growing attention. They belong to the class of dendritic polymers, i.e., they are characterized by a tree-like branch-on-branch topology. They resemble dendrimers, which are well-defined, perfectly branched macromolecules that have attracted vast attention because of their compact, globular structure in bulk and solution, and a very large number of end groups available for further modification. Since dendrimer preparation requires generation-wise construction in demanding multistep syntheses, hyperbranched polymers have been explored as less defined, but easily accessible materials. The perfectly branched, but tediously prepared dendrimer structure is traded off for a convenient polymerization that goes along with an irregular, statistical branching and a polydisperse molecular weight distribution.[65] In order to characterize the structure of a hyperbranched polymer, the degree of branching (DB) is a decisive variable which can assume values between zero (linear) and one (perfectly branched).[66,67]

Table 5 lists (hyper)branched polymers containing in-chain linear poly(alkylene glycol) segments. Reviews on hyperbranched polyethers in general have been provided by our group.[68,69] In addition to the advances in polyether chemistry, numerous branched poly(PEG acrylates) and poly(PEG methacrylates) have been synthesized in recent years using radical polymerization techniques, such as the so-called “Strathclyde methodology” and the controlled radical homopolymerization of PEG diacrylate.[70,71]

Hawker and co-workers reported the first oligo(ethylene glycol)-based hyperbranched polymers. They synthesized poly(ether esters), consisting of oligo(ethylene glycol) segments and aromatic

branching points, via polycondensation of AB_2–type methyl 3,5-bis[oligo(ethylene glycol)]benzoate macromonomers.[72] The authors observed an elevated Lithium ion conductivity compared to linear PEG. The amorphous structure due to the branched topology leads to an increased chain and Lithium ion mobility. Similar poly(ether esters) were prepared by Long et al. via polycondensation of telechelic PEG oligomers as an A_2-type macromonomer with 1,3,5-benzenetricarbonyl trichloride as a B_3-type comonomer.[73] Furthermore, the A_2 + B_3 polycondensation route was used by Patel to synthesize flame retardant, highly branched polyurethanes from PEG, diisocyanate, castor oil and tris(bisphenol A) mono phosphate.[74] Shibasaki et al. obtained poly(propylene oxide)-based A_2B_3-type hyperbranched copolymers using 3-armed 4-*N*-methylbenzamide pentamers as branching agents.[75]

Several dendrimer-like iterative approaches toward branch-on-branch PEG architectures have been reported, all of them pursuing divergent synthesis strategies. In an elegant work, Taton et al. introduced dendrimer-like PEG structures by sequential anionic EO polymerization, allyl chloride termination and subsequent bishydroxylation of the chain ends.[76] This leads to extremely well-defined, demanding PEG-dendrimer structures with very low polydispersity in the range of 1.08−1.15. The synthetic strategy is shown in Figure 2.

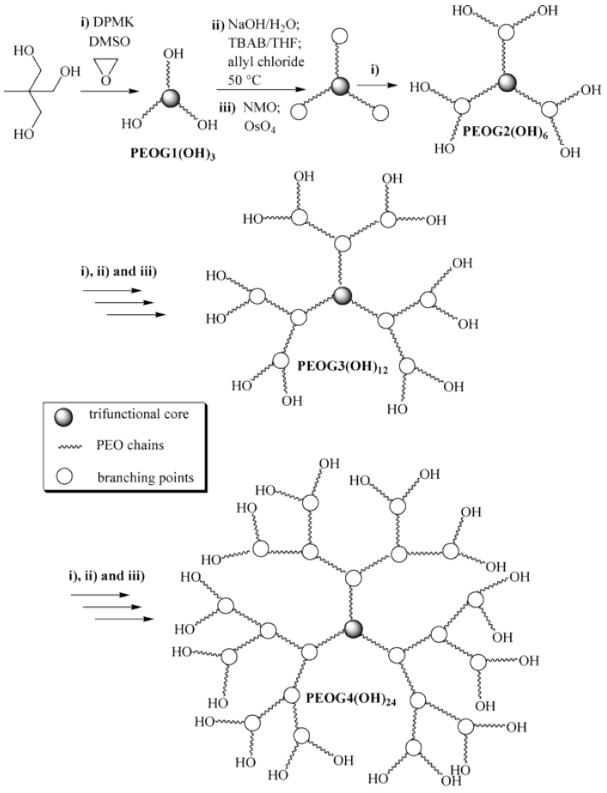

Figure 2. Synthetic strategy toward dendrimer-like PEG by Taton et al. (Adapted with permission from Feng, X.-S.; Taton, D.; Chaikof, E. L.; Gnanou, Y. *J. Am. Chem. Soc.* 2005, *127*, 10956.[76] Copyright 2005 American Chemical Society.)

Inspired by this approach, Deffieux and coauthors obtained second and third generation dendritic PEG structures by iterative azide–alkyne click coupling of α-azido-functional PEG with propargylated tetrakis(4-hydroxyphenyl) porphyrin zinc(II) and subsequent attachment of further porphyrin branching points via etherification.[77] Singlet oxygen production and photo stability were tested to investigate the first, second and third generation polymers' suitability for use as photo sensitizers and to establish differences between the generations. Dworak and Walach performed repeated anionic block copolymerization of EO and ethoxyethyl glycidyl ether (EEGE), an acetal-protected glycidol derivative, followed by acidic deprotection to generate multiple hydroxyl initiation sites.[78]

Short PEG segments (DP = 10) resulted in amorphous materials while longer linear chains led to crystallization. Branched polymers with long PEG segments (DP = 50) exhibited enhanced uptake and transport of a hydrophilic dye into a methylene chloride solution, compared to linear and star-shaped PEG.

Several promising synthetic works rely on the copolymerization of ethylene oxide with unprotected glycidol (G) as a branching agent, resulting in hyperbranched structures with mere polyether scaffold. The glycidol molecule possesses both a polymerizable epoxide ring and an alcohol moiety that is capable of initiating the growth of another chain in an anionic or cationic polymerization. Therefore, glycidol is often described as a latent AB_2 monomer and represents a cyclic "inimer".

Dworak and co-workers reported the repeated anionic block copolymerization of EO and glycidol.[79] The hyperbranching polymerization of glycidol on a PEG macroinitiator, however, was found to produce significant amounts of hyperbranched polyglycerol homopolymer. In a multistep, one-pot reaction, Taton et al. also synthesized multiblock copolymers, consisting of linear PEG chains interrupted by oligomeric poly(propylene oxide)-*co*-polyglycerol or poly(allyl glycidyl ether)-*co*-polyglycerol branching segments.[80] In 2001, Tsvetanov and co-workers obtained high molecular weight random copolymers of EO and G by simultaneously bubbling EO through and adding G to a calcium amide-alkoxide initiator suspension.[81] This procedure only permitted limited glycidol incorporation up to 3% and resulted in very broad molecular weight distributions (PDIs ranging from 3 to 13). Under different reaction conditions, the controlled copolymerization of this comonomer combination was realized by our group. We synthesized hyperbranched PEG with narrow molecular weight distributions, adjustable composition and tunable degree of branching by random anionic copolymerization in a batch process (see Scheme 1).[82]

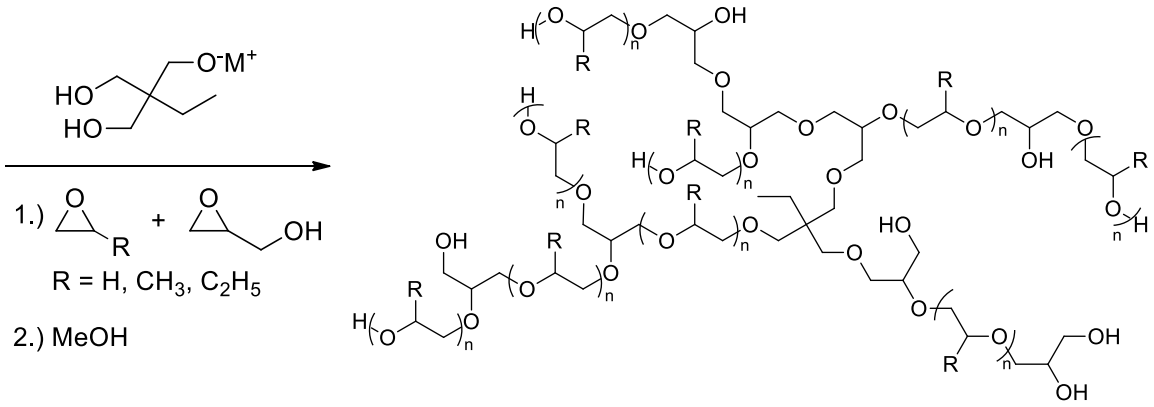

Scheme 1. Hyperbranched Poly(alkylene glycol)s by copolymerization of alkylene oxides with glycidol.[82,84,85]

Contrary to the linear anionic polymerization, the resulting molar masses do not depend on the ratio of monomer to initiator. Limited control over the degree of polymerization was achieved by varying the polarity of the reaction media. The access to well-defined hyperbranched PEG copolymers of a wide range of molecular weights enabled a combined investigation by analytical ultracentrifugation, viscometry, translational diffusion measurements and size exclusion chromatography to establish the hydrodynamic properties of these structures. The obtained scaling relations imply an approximately globular, dendrimer-like structure. For the first time, sedimentation and diffusion analysis was employed to tackle the challenge of absolute molar mass characterization of hyperbranched polymers, revealing up to 25 times higher values compared to SEC data using linear standards. The characterization data demonstrate that the copolymerization of EO and glycidol can lead to molecular weights in the range of 10^6 g mol^{-1}.[83]

Hyperbranched poly(propylene oxide)-*co*-polyglycerol and poly(1,2-butylene oxide)-*co*-polyglycerol were synthesized in a similar manner, but without solvent, leading to moderately distributed, albeit low molecular weight polymers with thermoresponsive properties in aqueous solution.[84,85] By variation of the comonomer ratio, lower critical solution temperatures (LCST) and glass transition temperatures were tailored in a systematic manner. Monitoring the batch copolymerization of BO with G by in situ NMR spectroscopy, our group found a tapered structure with a hyperbranched PG-rich core and PBO arms. Hyperbranched poly(1,2-butylene oxide)-*co*-polyglycerol copolymers with elevated molecular weights up to Mw = 35000 g mol^{-1} could be prepared under slow monomer addition conditions.

Among other polyglycerol copolymers, Royappa et al. reported various cationic copolymerizations of glycidol with propylene oxide and 1,2-butylene oxide, respectively, using boron trifluoride etherate. However, no information regarding degree of branching and amount of comonomer incorporated was given.[86]

Using glycidyl methacrylate as a branching agent and potassium hydride as a catalyst, Zhu et al. prepared long-chain hyperbranched PEG by proton-transfer copolymerization with telechelic PEG, albeit with broad molecular weight distribution. Polymer cytotoxicity and hydrolysis of the ester bonds under physiological conditions were studied.[87]

Table 5. List of dendritic PEG and poly(alkylene glycol) derivatives

Polymerization method	**Initiator**	**Linear (macro-) monomer unit**	**Branching agent**	**Ref.**
AB_2 polycondensation	-	-	methyl 3,5-bis[oligo-(ethylene glycol)]benzoate	72
$A_2 + B_3$ polycondensation	-	PEG	1,3,5-benzenetricarbonyl trichloride	73
$A_2 + B_3$ polycondensation	castor oil	PEG + diisocyanate	tris(bisphenol A) monophosphate	74
$A_2 + B_3$ polycondensation	-	PPO	3-armed *star*-penta-(4-*N*-methylbenzamide)	75
multistep anionic polymerization	a)	EO	allyl chloride + OsO_4	76
multistep anionic block copolymerization	PETH	EO	EEGE + deprotection	78
multistep azide-alkyne click coupling		PEG	Zn(II) tetraphenylporphyrin	77
anionic block copolymerization	PEG + CsOH	EO	glycidol	79
anionic block copolymerization	a)	EO + PO	glycidol	80
random anionic copolymerization	b)	EO	glycidol	81
random anionic copolymerization	c)	EO	glycidol	82, 83
random anionic copolymerization	TMP + KO*t*Bu	PO	glycidol	84
random anionic copolymerization	TMP + CsOH	BO	glycidol	85

Table 5 (continued). List of dendritic PEG and poly(alkylene glycol) derivatives

random cationic copolymerization	BF_3:OEt_2	PO / BO	glycidol	86
Proton-transfer polymerization	KH	PEG	glycidyl methacrylate	87

[a)] Trimethylolethane + diphenylmethylpotassium, [b)] calcium amide-alkoxide, [c)] TMP + potassium naphthalenide

References

1. Lapienis, G. Star-Shaped Polymers Having PEO Arms. *Prog. Polym. Sci*. **2009**, *34*, 852−892.
2. Doycheva, M.; Berger-Nicoletti, E.; Wurm, F.; Frey, H. Rapid Synthesis and MALDI-ToF Characterization of Poly(ethylene oxide) Multiarm Star Polymers. *Macromol. Chem. Phys*. **2010**, *211*, 35−44.
3. Huin, C.; Eskandani, Z.; Badi, N.; Farcas, A.; Bennevault-Celton, V.; Guégan, P. Anionic Ring-Opening Polymerization of Ethylene Oxide in DMF with Cyclodextrin Derivatives as new Initiators. *Carbohydr. Polym*. **2013**, *94*, 323−331.
4. Tonhauser, C.; Mazurowski, M.; Rehahn, M.; Gallei, M.; Frey, H. Water-Soluble Poly(vinylferrocene)-b-Poly(ethylene oxide) Diblock and Miktoarm Star Polymers. *Macromolecules* **2012**, *45*, 3409−3418.
5. Wang, G.; Fan, X.; Huang, J. Synthesis of 4μ-PS_2PEO_2, 4μ-PS_2PCl_2, 4μ-PI_2PEO_2, and 4μ-PI_2PCl_2 Star-Shaped Copolymers by the Combination of Glaser Coupling with Living Anionic Polymerization and Ring-Opening Polymerization. *J. Polym. Sci., Part A: Polym. Chem.* **2010**, *48*, 5313−5321.
6. Guo, Q.; Liu, C.; Tang, T.; Huang, J.; Zhang, X.; Wang, G. Synthesis of Amphiphilic A_4B_4 Star-Shaped Copolymers by Mechanisms Transformation Combining with Thiol-ene Reaction. *J. Polym. Sci., Part A: Polym. Chem*. **2013**, *51*, 4572−4583.
7. Jiang, G.; Xu, H. Synthesis and Evaluation of a Star Amphiphilic Block Copolymer from Poly(ε-Caprolactone) and Poly(ethylene oxide) as Load and Release Carriers for Guest Molecules. *J. Appl. Polym. Sci.* **2010**, *118*, 1372−1379.
8. Li, Y.; Zhang, B.; Hoskins, J. N.; Grayson, S. M. Synthesis, Purification, and Characterization of "Perfect" Star Polymers via "Click" Coupling. *J. Polym. Sci., Part A: Polym. Chem*. **2012**, *50*, 1086−1101.

9. Li, N.; Echeverría, M.; Moya, S.; Ruiz, J.; Astruc, D. "Click" Synthesis of Nona-PEG-Branched Triazole Dendrimers and Stabilization of Gold Nanoparticles That Efficiently Catalyze p-Nitrophenol Reduction. *Inorg. Chem*. **2014**, *53*, 6954−6961.
10. Chang, X.; Liu, L.; Guan, Y.; Dong, C.-M. Disulfide-Centered Star-Shaped Polypeptide-PEO Block Copolymers for Reduction-Triggered Drug Release. *J. Polym. Sci., Part A: Polym. Chem*. **2014**, *52*, 2000−2010.
11. Durmaz, H.; Dag, A.; Erdogan, E.; Demirel, A. L.; Hizal, G.; Tunca, U. Multiarm Star Block and Multiarm Star Mixed-Block Copolymers via Azide-Alkyne Click Reaction. *J. Polym. Sci., Part A: Polym. Chem*. **2010**, *48*, 99−108.
12. Durmaz, H.; Dag, A.; Gursoy, D.; Demirel, A. L.; Hizal, G.; Tunca, U. Multiarm Star Triblock Terpolymers Via Sequential Double Click Reactions. *J. Polym. Sci., Part A: Polym. Chem*. **2010**, *48*, 1557−1564.
13. Kulis, J.; Jia, Z.; Monteiro, M. J. One-Pot Synthesis of Mikto Three-Arm AB_2 Stars Constructed from Linear and Macrocyclic Polymer Chains. *Macromolecules* **2012**, *45*, 5956−5966.
14. Bahadori, F.; Dag, A.; Durmaz, H.; Cakir, N.; Onyuksel, H.; Tunca, U.; Topcu, G.; Hizal, G. Synthesis and Characterization of Biodegradable Amphiphilic Star and Y-Shaped Block Copolymers as Potential Carriers for Vinorelbine. *Polymers* **2014**, *6*, 214−242.
15. Doganci, E.; Gorur, M.; Uyanik, C.; Yilmaz, F. Synthesis of AB_3-Type Miktoarm Star Polymers with Steroid Core via a Combination of"Click" Chemistry and Ring Opening Polymerization Techniques. *J. Polym. Sci., Part A: Polym. Chem*. **2014**, *52*, 3390−3399.
16. Blasco, E.; Schmidt, B.; Barner-Kowollik, C.; Pinol, M.; Oriol, L. A Novel Photoresponsive Azobenzene-Containing Miktoarm Star Polymer: Self-Assembly and Photoresponse Properties. *Macromolecules* **2014**, *47*, 3693−3700.
17. Liu, R.; Li, Z. Y.; Wang, W. J.; Yuan, D.; Meng, C. F.; Wu, Q.; Zhu, F. M. Synthesis and Self-Assembly of Amphiphilic Star-Block Copolymers Consisting of Polyethylene and Poly(ethylene glycol) Segments. *J. Appl. Polym. Sci*. **2013**, *129*, 2216−2223.
18. Gou, P.-F.; Zhu, W.-P.; Shen, Z.-Q. Calixarene-Centered Amphiphilic A_2B_2 Miktoarm Star Copolymers Based on Poly(ε-Caprolactone) and Poly(ethylene glycol): Synthesis and Self-Assembly Behaviors in Water. *J. Polym. Sci., Part A: Polym. Chem*. **2010**, *48*, 5643−5651.
19. Gou, P.-F.; Zhu, W.-P.; Shen, Z.-Q. Synthesis, Self-Assembly, and Drug-Loading Capacity of Well-Defined Cyclodextrin-Centered Drug-Conjugated Amphiphilic $A_{14}B_7$ Miktoarm Star Copolymers Based on Poly(ε-caprolactone) and Poly(ethylene glycol). *Biomacromolecules* **2010**, *11*, 934−943.

20. Gao, C.; Wang, Y.; Gou, P.; Cai, X.; Li, X.; Zhu, W.; Shen, Z. Synthesis and Characterization of Resorcinarene-Centered Amphiphilic A_8B_4 Miktoarm Star Copolymers Based on Poly(ε-caprolactone) and Poly(ethylene glycol) by Combination of Crop and "Click" Chemistry. *J. Polym. Sci., Part A: Polym. Chem*. **2013**, *51*, 2824−2833.
21. Khanna, K.; Varshney, S.; Kakkar, A. Designing Miktoarm Polymers Using a Combination of "Click" Reactions in Sequence with Ring-Opening Polymerization. *Macromolecules* **2010**, *43*, 5688−5698.
22. Iskin, B.; Yilmaz, G.; Yagci, Y. Synthesis of ABC Type Miktoarm Star Copolymers by Triple Click Chemistry. *Polym. Chem*. **2011**, *2*, 2865−2871.
23. Huan, X.; Wang, D.; Dong, R.; Tu, C.; Zhu, B.; Yan, D.; Zhu, X. Supramolecular ABC Miktoarm Star Terpolymer Based on Host−Guest Inclusion Complexation. *Macromolecules* **2012**, *45*, 5941−5947.
24. Sun, W.; He, X.; Gao, C.; Liao, X.; Xie, M.; Lin, S.; Yan, D. Novel Amphiphilic and Photo-Responsive ABC_3-Miktoarm Star Terpolymers: Synthesis, Self-Assembly and Photo-Responsive Behavior. *Polym. Chem*. **2013**, *4*, 1939−1949.
25. Liu, H.; Miao, K.; Zhao, G.; Li, C.; Zhao, Y. Synthesis of an Amphiphilic PEG-PCl-PSt-PLLA-PAA Star Quintopolymer and its Self-Assembly for pH-Sensitive Drug Delivery. *Polym. Chem*. **2014**, *5*, 3071−3080.
26. Li, W.; Matyjaszewski, K. Uniform PEO Star Polymers Synthesized in Water via Free Radical Polymerization or Atom Transfer Radical Polymerization. *Macromol. Rapid Commun*. **2011**, *32*, 74−81.
27. Cho, H. Y.; Srinivasan, A.; Hong, J.; Hsu, E.; Liu, S.; Shrivats, A.; Kwak, D.; Bohaty, A. K.; Paik, H.-J.; Hollinger, J. O.; et al. Synthesis of Biocompatible PEG-Based Star Polymers with Cationic and Degradable Core for siRNA Delivery. *Biomacromolecules* **2011**, *12*, 3478−3486.
28. Fukae, K.; Terashima, T.; Sawamoto, M. Cation-Condensed Microgel-Core Star Polymers as Polycationic Nanocapsules for Molecular Capture and Release in Water. *Macromolecules* **2012**, *45*, 3377−3386.
29. Koda, Y.; Terashima, T.; Sawamoto, M. Fluorous Microgel Star Polymers: Selective Recognition and Separation of Polyfluorinated Surfactants and Compounds in Water. *J. Am. Chem. Soc*. **2014**, *136*, 15742−15748.
30. Terashima, T.; Nishioka, S.; Koda, Y.; Takenaka, M.; Sawamoto, M. Arm-Cleavable Microgel Star Polymers: A Versatile Strategy for Direct Core Analysis and Functionalization. *J. Am. Chem. Soc*. **2014**, *136*, 10254−10257.

31. Park, S.; Cho, H. Y.; Wegner, K. B.; Burdynska, J.; Magenau, A. J. D.; Paik, H.-J.; Jurga, S.; Matyjaszewski, K. Star Synthesis Using Macroinitiators Via Electrochemically Mediated Atom Transfer Radical Polymerization. *Macromolecules* **2013**, *46*, 5856−5860.
32. McKenzie, T. G.; Wong, E. H. H.; Fu, Q.; Lam, S. J.; Dunstan, D. E.; Qiao, G. G. Highly Efficient and Versatile Formation of Biocompatible Star Polymers in Pure Water and Their Stimuli-Responsive Self-Assembly. *Macromolecules* **2014**, *47*, 7869−7877.
33. Syrett, J. A.; Haddleton, D. M.; Whittaker, M. R.; Davis, T. P.; Boyer, C. Functional, Star Polymeric Molecular Carriers, Built from Biodegradable Microgel/Nanogel Cores. *Chem. Commun*. **2011**, *47*, 1449−1451.
34. Gao, A. X.; Liao, L.; Johnson, J. A. Synthesis of Acid-Labile PEG and PEG-Doxorubicin-Conjugate Nanoparticles via Brush-First ROMP. *ACS Macro Lett*. **2014**, *3*, 854−857.
35. Feng, Z.; Zhi-Ming, W.; Ya-Fei, H.; Xiao-Hui, D.; Yan-Ru, G.; Jian-Ming, P.; Yong-Sheng, Y.; Sun, L. Synthesis, Self-Assembly, and Drug Release Behavior of Star-Shaped Poly(ε-caprolactone)-*b*-Poly-(ethylene oxide) Block Copolymer with Porphyrin Core. *J. Appl. Polym. Sci*. **2014**, *131*, 40996.
36. Lim, H. J.; Lee, H.; Kim, K. H.; Huh, J.; Ahn, C.-H.; Kim, J. W. Effect of Molecular Architecture on Micellization, Drug Loading and Releasing of Multi-Armed Poly(ethylene glycol)-*b*-Poly(ε-caprolactone) Star Polymers. *Colloid Polym. Sci*. **2013**, *291*, 1817−1827.
37. Gou, P.-F.; Zhu, W.-P.; Shen, Z.-Q. Drug-Grafted Seven-Arm Amphiphilic Star Poly(ε-caprolactone-co-carbonate)-*b*-Poly(ethylene glycol)s Based on a Cyclodextrin Core: Synthesis and Self-Assembly Behavior in Water. *Polym. Chem*. **2010**, *1*, 1205.
38. Nabid, M. R.; Tabatabaei Rezaei, S. J.; Sedghi, R.; Niknejad, H.; Entezami, A. A.; Oskooie, H. A.; Heravi, M. M. Self-Assembled Micelles of Well-Defined Pentaerythritol-Centered Amphiphilic A_4B_8 Star-Block Copolymers Based on PCL and PEG for Hydrophobic Drug Delivery. *Polymer* **2011**, *52*, 2799−2809.
39. Pu, Y.; Zhang, L.; Zheng, H.; He, B.; Gu, Z. Synthesis and Drug Release of Star-Shaped Poly(benzyl L-aspartate)-*block*-Poly(ethylene glycol) Copolymers with POSS Cores. *Macromol. Biosci*. **2014**, *14*, 289−297.
40. Lam, S. J.; Sulistio, A.; Ladewig, K.; Wong, E. H. H.; Blencowe, A.; Qiao, G. G. Peptide-Based Star Polymers as Potential siRNA Carriers. *Aust. J. Chem*. **2014**, *67*, 592.
41. Yan, Y.; Wei, D.; Li, J.; Zheng, J.; Shi, G.; Luo, W.; Pan, Y.; Wang, J.; Zhang, L.; He, X.; et al. A Poly(L-lysine)-Based Hydrophilic Star Block Copolymer as a Protein Nanocarrier with Facile Encapsulation and pH-Responsive Release. *Acta Biomater*. **2012**, *8*, 2113−2120.

42. Chen, G.; Wang, L.; Cordie, T.; Vokoun, C.; Eliceiri, K. W.; Gong, S. Multi-Functional Self-Fluorescent Unimolecular Micelles for Tumor-Targeted Drug Delivery and Bioimaging. *Biomaterials* **2015**, *47*, 41−50.
43. Dai, X.-H.; Wang, Z.-M.; Gao, L.-Y.; Pan, J.-M.; Wang, X.-H.; Yan, Y.-S.; Liu, D.-M. Star-Shaped Poly(L-lactide)-*b*-Poly(ethylene glycol) with Porphyrin Core: Synthesis, Self-Assembly, Drug-Release Behavior and Singlet Oxygen Research. *New J. Chem*. **2014**, *38*, 3569.
44. Gu, D.; Ladewig, K.; Klimak, M.; Haylock, D.; McLean, K. M.; O'Connor, A. J.; Qiao, G. G. Amphiphilic Core Cross-Linked Star Polymers as Water-Soluble, Biocompatible and Biodegradable Unimolecular Carriers for Hydrophobic Drugs. *Polym. Chem*. **2015**, *6*, 6475−6487.
45. Rodionov, V.; Gao, H.; Scroggins, S.; Unruh, D. A.; Avestro, A.-J.; Fréchet, J. M. J. Easy Access to a Family of Polymer Catalysts from Modular Star Polymers. *J. Am. Chem. Soc*. **2010**, *132*, 2570−2572.
46. Qiu, F.; Tu, C.; Chen, Y.; Shi, Y.; Song, L.; Wang, R.; Zhu, X.; Zhu, B.; Yan, D.; Han, T. Control of the Optical Properties of a Star Copolymer with a Hyperbranched Conjugated Polymer Core and Poly(ethylene glycol) Arms by Self-Assembly. *Chem. - Eur. J*. **2010**, *16*, 12710−12717.
47. Qiu, F.; Wang, D.; Zhu, Q.; Zhu, L.; Tong, G.; Lu, Y.; Yan, D.; Zhu, X. Real-Time Monitoring of Anticancer Drug Release with Highly Fluorescent Star-Conjugated Copolymer as a Drug Carrier. *Biomacromolecules* **2014**, *15*, 1355−1364.
48. Chen, R.; Wang, L. Synthesis of an Amphiphilic Hyperbranched Polymer as a Novel pH-Sensitive Drug Carrier. *RSC Adv*. **2015**, *5*, 20155−20159.
49. Whitton, G.; Gauthier, M. Arborescent Micelles: Dendritic Poly(γ-benzyl L-glutamate) Cores Grafted with Hydrophilic Chain Segments. *J. Polym. Sci., Part A: Polym. Chem*. **2016**, *54*, 1197-1209.
50. Xie, Z.; He, H.; Deng, Y.; Wang, X.; Liu, C. Three-Arm Star Compounds Composed of 1,3,5-Tri(azobenzeneethynyl)Benzene Cores and Flexible PEO Arms: Synthesis, Optical Functions, Hybrid Ormosil Gel Glasses. *J. Mater. Chem. C* **2013**, *1*, 1791.
51. Lee, D.-I.; Kim, C.-J.; Lee, C.-H.; Ahn, I.-S. Synthesis of a Fluorescent and Star-Shaped 4-Arm PEG with Different Functional Groups at its Ends. *J. Ind. Eng. Chem*. **2012**, *18*, 1186−1190.
52. Mineo, P.; Alicata, R.; Micali, N.; Villari, V.; Scamporrino, E. Water-Soluble Star Polymers with a Phthalocyanine as the Core and Poly(ethylene glycol) Chains as Branches. *J. Appl. Polym. Sci*. **2012**, *126*, 1359−1368.

53. Pozza, G. M. E.; Harris, H.; Barthel, M. J.; Vitz, J.; Schubert, U. S.; Lutz, P. J. Macromonomers as Well-Defined Building Blocks in the Synthesis of Hybrid Octafunctional Star-Shaped Poly(ethylene oxide)s. *Macromol. Chem. Phys*. **2012**, *213*, 2181−2191.
54. Rother, M.; Barqawi, H.; Pfefferkorn, D.; Kressler, J.; Binder, W. H. Synthesis and Organization of Three-Arm-Star PIB-PEO Block Copolymers at the Air/Water Interface: Langmuir- and Langmuir-Blodgett Film Investigations. *Macromol. Chem. Phys*. **2010**, *211*, 204−214.
55. De Espinosa, L. M.; Winkler, M.; Meier, M. A. R. Acyclic Diene Metathesis Polymerization and Heck Polymer-Polymer Conjugation for the Synthesis of Star-Shaped Block Copolymers. *Macromol. Rapid Commun*. **2013**, *34*, 1381−1386.
56. Zhang, Y.; Zhao, Q.; Shao, H.; Zhang, S.; Han, X. Synthesis and Characterization of Star-Shaped Block Copolymer *s*PCL-*b*-PEG-GA. *Adv. Mater. Sci. Eng*. **2014**, *2014*, 1−6.
57. Lin, Y.; Zhang, A. Synthesis and Characterization of Star-Shaped Poly(D,L-lactide)-*block*-Poly(ethylene glycol) Copolymers. *Polym. Bull*. **2010**, *65*, 883−892.
58. Durmaz, H.; Dag, A.; Tunca, U.; Hizal, G. Synthesis and Characterization of Pyrene Bearing Amphiphilic Miktoarm Star Polymer and its Noncovalent Interactions with Multiwalled Carbon Nanotubes. *J. Polym. Sci., Part A: Polym. Chem*. **2012**, *50*, 2406−2414.
59. Lagunas, C.; Fernandez-Francos, X.; Ferrando, F.; Flores, M.; Serra, A.; Morancho, J.; Salla, J.; Ramis, X. New Epoxy Thermosets Modified with Amphiphilic Multiarm Star Polymers as Toughness Enhancer. *React. Funct. Polym*. **2014**, *83*, 132−143.
60. Zhu, W.; Ling, J.; Shen, Z. Synthesis and Characterization of Amphiphilic Star-Shaped Polymers with Calix[6]Arene Cores. *Macromol. Chem. Phys*. **2006**, *207*, 844−849.
61. Sunder, A.; Mülhaupt, R.; Frey, H. Hyperbranched Polyether−Polyols Based on Polyglycerol: Polarity Design by Block Copolymerization with Propylene Oxide. *Macromolecules* **2000**, *33*, 309−314.
62. Knischka, R.; Lutz, P. J.; Sunder, A.; Mülhaupt, R.; Frey, H. Functional Poly(ethylene oxide) Multiarm Star Polymers: Core-First Synthesis Using Hyperbranched Polyglycerol Initiators. *Macromolecules* **2000**, *33*, 315−320.
63. Zhao, J.; Pahovnik, D.; Gnanou, Y.; Hadjichristidis, N. One-Pot Synthesis of Linear- and Three-Arm Star-Tetrablock Quarterpolymers via Sequential Metal-Free Ring-Opening Polymerization Using a "Catalyst Switch" Strategy. *J. Polym. Sci., Part A: Polym. Chem*. **2015**, *53*, 304−312.
64. Isono, T.; Kamoshida, K.; Satoh, Y.; Takaoka, T.; Sato, S.-I.; Satoh, T.; Kakuchi, T. Synthesis of Star- and Figure-Eight-Shaped Polyethers by *t*-BuP_4-Catalyzed Ring-Opening Polymerization of Butylene Oxide. *Macromolecules* **2013**, *46*, 3841−3849.

65. Flory, P. J. Molecular Size Distribution in Three Dimensional Polymers 0.6. Branched Polymers Containing A-R-B_{f-1} Type Units. *J. Am. Chem. Soc*. **1952**, *74*, 2718−2723.
66. Hawker, C.; Lee, R.; Frechet, J. One-Step Synthesis of Hyperbranched Dendritic Polyesters. *J. Am. Chem. Soc*. **1991**, *113*, 4583−4588.
67. Hölter, D.; Burgath, A.; Frey, H. Degree of Branching in Hyperbranched Polymers. *Acta Polym*. **1997**, *48*, 30−35.
68. Schömer, M.; Schüll, C.; Frey, H. Hyperbranched Aliphatic Polyether Polyols. *J. Polym. Sci., Part A: Polym. Chem*. **2013**, *51*, 995−1019.
69. Schüll, C.; Wilms, D.; Frey, H.; Matyjaszewski, K.; Möller, M. *Polymer Science: A Comprehensive Reference* **2012**, *4*, 571−596.
70. Smeets, N. Amphiphilic Hyperbranched Polymers from the Copolymerization of a Vinyl and Divinyl Monomer: The Potential of Catalytic Chain Transfer Polymerization. *Eur. Polym. J*. **2013**, *49*, 2528−2544.
71. Zhao, T.; Zhang, H.; Zhou, D.; Gao, Y.; Dong, Y.; Greiser, U.; Tai, H.; Wang, W. Water-Soluble Hyperbranched Polymers from Controlled Radical Homopolymerization of PEG Diacrylate. *RSC Adv*. **2015**, *5*, 33823−33830.
72. Hawker, C. J.; Chu, F.; Pomery, P. J.; Hill, D. J. T. Hyperbranched Poly(ethylene glycol)s: A New Class of Ion-Conducting Materials. *Macromolecules* **1996**, *29*, 3831−3838.
73. Unal, S.; Lin, Q.; Mourey, T. H.; Long, T. E. Tailoring the Degree of Branching: Preparation of Poly(ether ester)s via Copolymerization of Poly(ethylene glycol) Oligomers (A_2) and 1,3,5-Benzenetricarbonyl Trichloride (B_3). *Macromolecules* **2005**, *38*, 3246−3254.
74. Patel, R. H.; Patel, K. S. Synthesis and Characterization of Flame Retardant Hyperbranched Polyurethanes for Nano-Composite and Nano-Coating Applications. *Prog. Org. Coat*. **2015**, *88*, 283−292.
75. Masukawa, S.; Kikkawa, T.; Fujimori, A.; Oishi, Y.; Shibasaki, Y. Synthesis of A_2B_3-Type Hyperbranched Copolymers Based on a 3-Armed Unimolecular 4-*N*-Methylbenzamide Pentamer and Poly(propylene oxide). *Chem. Lett*. **2015**, *44*, 536−538.
76. Feng, X.-S.; Taton, D.; Chaikof, E. L.; Gnanou, Y. Toward an Easy Access to Dendrimer-Like Poly(ethylene oxide)s. *J. Am. Chem. Soc*. **2005**, *127*, 10956−10966.
77. Wirotius, A.-L.; Ibarboure, E.; Scarpantonio, L.; Schappacher, M.; McClenaghan, N. D.; Deffieux, A. Hydrosoluble Dendritic Poly(ethylene oxide)s with Zinc Tetraphenylporphyrin Branching Points as Photosensitizers. *Polym. Chem*. **2013**, *4*, 1903−1912.

78. Dworak, A.; Wałach, W. Synthesis, Characterization and Properties of Functional Star and Dendritic Block Copolymers of Ethylene Oxide and Glycidol with Oligoglycidol Branching Units. *Polymer* **2009**, *50*, 3440−3447.
79. Walach, W.; Trzebicka, B.; Justynska, J.; Dworak, A. High Molecular Arborescent Poly(oxyethylene) with Hydroxyl Containing Shell. *Polymer* **2004**, *45*, 1755−1762.
80. Feng, X.; Taton, D.; Chaikof, E. L.; Gnanou, Y. Fast Access to Dendrimer-Like Poly(ethylene oxide)s through Anionic Ring-Opening Polymerization of Ethylene Oxide and Use of Nonprotected Glycidol as Branching Agent. *Macromolecules* **2009**, *42*, 7292−7298.
81. Dimitrov, P.; Hasan, E.; Rangelov, S.; Trzebicka, B.; Dworak, A.; Tsvetanov, C. B. High Molecular Weight Functionalized Poly(ethylene oxide). *Polymer* **2002**, *43*, 7171−7178.
82. Wilms, D.; Schömer, M.; Wurm, F.; Hermanns, M. I.; Kirkpatrick, C. J.; Frey, H. Hyperbranched PEG by Random Copolymerization of Ethylene Oxide and Glycidol. *Macromol. Rapid Commun*. **2010**, *31*, 1811−1815.
83. Perevyazko, I.; Seiwert, J.; Schömer, M.; Frey, H.; Schubert, U. S.; Pavlov, G. M. Hyperbranched Poly(ethylene glycol) Copolymers: Absolute Values of the Molar Mass, Properties in Dilute Solution, and Hydrodynamic Homology. *Macromolecules* **2015**, *48*, 5887−5898.
84. Schömer, M.; Seiwert, J.; Frey, H. Hyperbranched Poly(propylene oxide): A Multifunctional Backbone-Thermoresponsive Polyether Polyol Copolymer. *ACS Macro Lett*. **2012**, *1*, 888−891.
85. Seiwert, J.; Leibig, D.; Kemmer-Jonas, U.; Bauer, M.; Perevyazko, I.; Preis, J.; Frey, H. Hyperbranched Polyols via Copolymerization of 1,2-Butylene Oxide and Glycidol: Comparison of Batch Synthesis and Slow Monomer Addition. *Macromolecules* **2016**, *49*, 38-47.
86. Royappa, A.; Dalal, N.; Giese, M. Amphiphilic Copolymers of Glycidol with Nonpolar Epoxide Comonomers. *J. Appl. Polym. Sci*. **2001**, *82*, 2290−2299.
87. Pang, Y.; Liu, J.; Wu, J.; Li, G.; Wang, R.; Su, Y.; He, P.; Zhu, X.; Yan, D.; Zhu, B. Synthesis, Characterization, and in vitro Evaluation of Long-Chain Hyperbranched Poly(ethylene glycol) as Drug Carrier. *Bioconjugate Chem*. **2010**, *21*, 2093−2102.

1.2 Polymerization of Propylene Oxide, 1,2-Butylene Oxide and Higher 1,2-Alkylene Oxide Monomers

While poly(ethylene oxide) (PEO) has unique biomedical applications due to its remarkable watersolubility, substituted poly(alkylene oxide)s, particularly poly(propylene oxide) (PPO), play an important role as hydrophobic, chemically inert, amorphous and flexible polyether compounds in the industrial fabrication of polyurethane foams, for nonionic surfactants or lubricants. This chapter summarizes recent innovations in the area of alkylene oxide polymerization. Polymerization techniques established before 1990 are summarized in comprehensive book volumes.[1-3]

Among the alkylene oxides, ethylene oxide (EO), propylene oxide (PO), and 1,2-butylene oxide (BO) are available on large industrial scale. Twenty-five million tons of ethylene oxide and 8 million tons of propylene oxide were produced in 2014 (Source: BASF SE), whereas the world annual production of butylene oxide is on the kiloton scale.[3] The epoxides are synthesized from the readily available steam cracking products ethene, propene, and 1-butene. Hexene oxide and higher α-olefin oxide homologues, however, are solely commercialized as fine chemicals. Therefore, poly(alkylene oxide)s beyond poly(butylene oxide) (PBO) are of little industrial interest, and the majority of studies are performed in academia, mainly to explore modern polymerization strategies, while only limited attention has been devoted to the examination of their materials properties so far.[4-7]

In general, with increasing alkyl chain length, epoxide monomers exhibit lowered reactivity compared to ethylene oxide and glycidyl ethers.[8-10] In contrast to the ROP of EO, the asymmetric substitution pattern of the other 1,2-alkylene oxides results in two different modes of ring-opening and three kinds of monomer unit connections in the corresponding polymer chain (see Scheme 1).

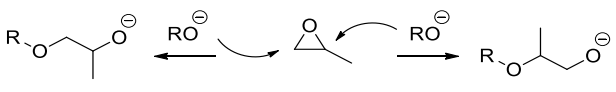

Scheme 1: Anionic ring-opening reaction of a substituted epoxide by methylene (left) or methine attack (right)

Anionic alkylene oxide polymerization largely results in regioregular head-to-tail connections (mainly due to steric reasons), whereas irregular combinations of head-to-tail, head-to-head and tail-to-tail linkages are present in poly(alkylene glycol)s obtained by cationic polymerization due

to the stability of the respective carbocations. The microstructure can be characterized by ^{13}C NMR spectroscopy (Figure 1).[11-13]

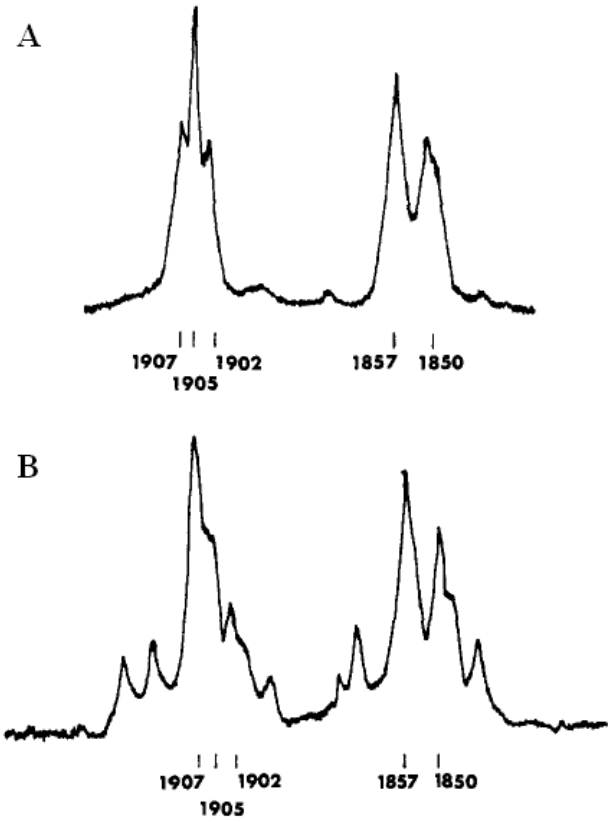

Figure 1. 13C NMR spectrum with methine and methylene carbon signal pattern of atactic, head-to-tail-linked PPO (A) and PPO with irregular microstructure (B). (Adapted with permission from Oguni, N.; Lee, K.; Tani, H. *Macromolecules* 1972, *5*, 819.[11] Copyright 1972 American Chemical Society.)

Besides this isomerism in the microstructure of the polymer backbone, also different stereoisomers can occur due to the asymmetric substituted methine carbon of the ring. Recently, an excellent and comprehensive review by Coates et al. summarized the state of the art in stereoselective epoxide polymerization and its potential for unusual polyether structures.[14] Therefore, this aspect is not covered in detail herein. In order to achieve stereoselectivity, a large range of metal catalysts have been synthesized and investigated, with focus on aluminum, zinc, iron and cobalt based systems, using porphyrin, calixarene or salen complexes (Scheme 2). All catalysts shown in Scheme 2 and the majority of other stereoselective catalysts produce poly-(propylene oxide) with semi-isotactic microstructure. These optically active polymers are semicrystalline, in contrast to stereoirregular PPO, which exhibits an amorphous structure.

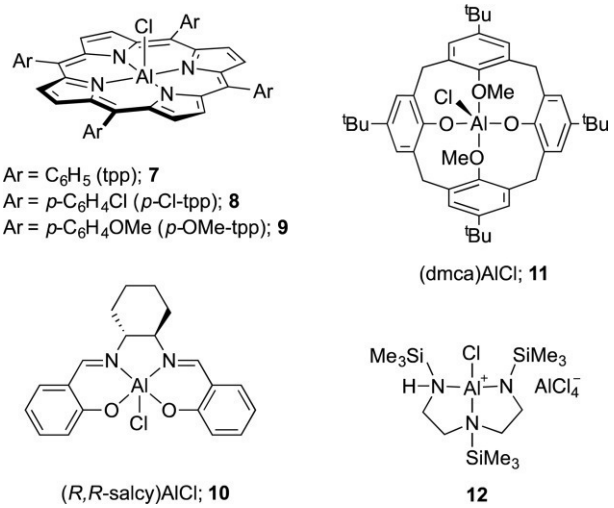

Scheme 2. Aluminum complexes with porphyrin (7,8,9), salen (10), calixarene (11), and silylamine (12) lLigands for stereoselective polymerization of propylene oxide (PO). (Adapted with permission from Childers, M.; Longo, J.; Van Zee, N.; LaPointe, A.; Coates, G. *Chem. Rev.* 2014, 114, 8129.[14] Copyright 2014 American Chemical Society.)

Anionic polymerization of substituted alkylene oxides using alkali metal alkoxide or hydroxide initiators comes with the drawback of competing chain transfer reactions (Scheme 3). The strongly alkaline alkoxide can, besides acting as a nucleophile that opens the ring, act as a base and abstract a proton from the alkyl substituent at the epoxide ring, generating an instable carbanion. The ensuing rearrangement results in an allyl alkoxide that is capable of initiating a new polymer chain with an unsaturated chain end. This side-reaction limits the achievable molecular weights of PPOs by conventional anionic polymerization (T > 90 °C) to approximately 6000 g mol^{-1}.[1] Sterically hindered epoxides such as 2,3-dimethyl-2,3-butylene oxide undergo almost quantitative elimination to allyl alcohols when treated with catalytic amounts of base. To avoid this issue, cationic ring-opening polymerization is often employed for polymerizing disubstituted epoxide monomers like cyclohexene oxide, despite the well-known disadvantages of this method, such as the lack of control over molecular weights and polydispersity.

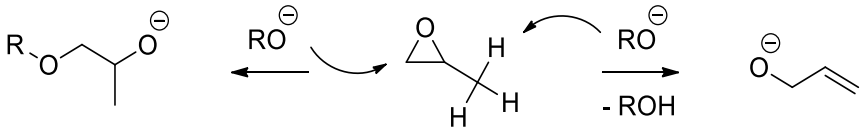

Scheme 3: Propagation and chain transfer reaction in the anionic polymerization of propylene oxide, limiting achievable molecular weights.

Aiming at an improvement of the low monomer reactivity and at reducing chain transfer reactions in the anionic polymerization of 1,2-alkylene oxides, tremendous progress has been made in the last two decades. Allgaier et al. employed crown ethers to complex potassium counterions to increase the nucleophilicity of the chain ends. The accompanying increase of basicity did not affect the polymerization negatively, because reaction conditions below room temperature were chosen. With side reactions minimized, PBO, poly(hexene oxide) (PHO), poly(octane oxide), and poly(dodecene oxide) with high molecular weights up to 65000 g mol^{-1} and narrow MWDs became accessible.[7,15] Deuterated analogues were synthesized in order to examine the effect of the side-chain length on the unperturbed chain dimensions and hydrogen dynamics via neutron scattering.[16,17] Also copolymerization of different alkylene oxides has been performed for some comonomer pairs. Anionic copolymerization of EO and BO was conducted using in situ NMR spectroscopy to determine the copolymerization kinetics;[18] strongly tapered compositional profiles were found. Xiong et al. employed Allgaier's polymerization strategy in order to prepare gradient and block side-chain liquid crystalline copolymers from butylene oxide.[19]

Increased propagation rates for anionic PO and BO polymerization can be achieved using phosphazene bases as catalysts. *t*-Bu-P_4 was found to both accelerate the reaction and to enable polymerization in a living manner without chain transfer.[20-22] Capitalizing on this method, Hadjichristidis and co-workers developed a catalyst switch strategy by which PBO block copolymers with polyesters or polycarbonates could be obtained.[23-25] For the preparation of the polyester/polycarbonate block, an excess of diphenyl phosphate was introduced to the reaction mixture before adding the cyclic carbonate or lactone monomer. Phosphazene base-promoted anionic polymerization also gave access to brush copolymers consisting of a polyacrylamide main chain and poly(alkylene oxide) side chains via a "grafting from" approach (Figure 2).[26]

Kappe and co-workers studied the polymerization of alkylene oxides (up to hexane oxide) in the microwave, resulting in low molecular weight polymers, however with fast reaction kinetics. Both oligomers and side products from transfer reactions were studied in detail by SEC.[27-29] Employing PEG monomethyl ether as an iniatior, they obtained amphiphilic block copolymers. Short, hydrophobic PBO or PHO segments sufficed to form micelles in aqueous solution.[30]

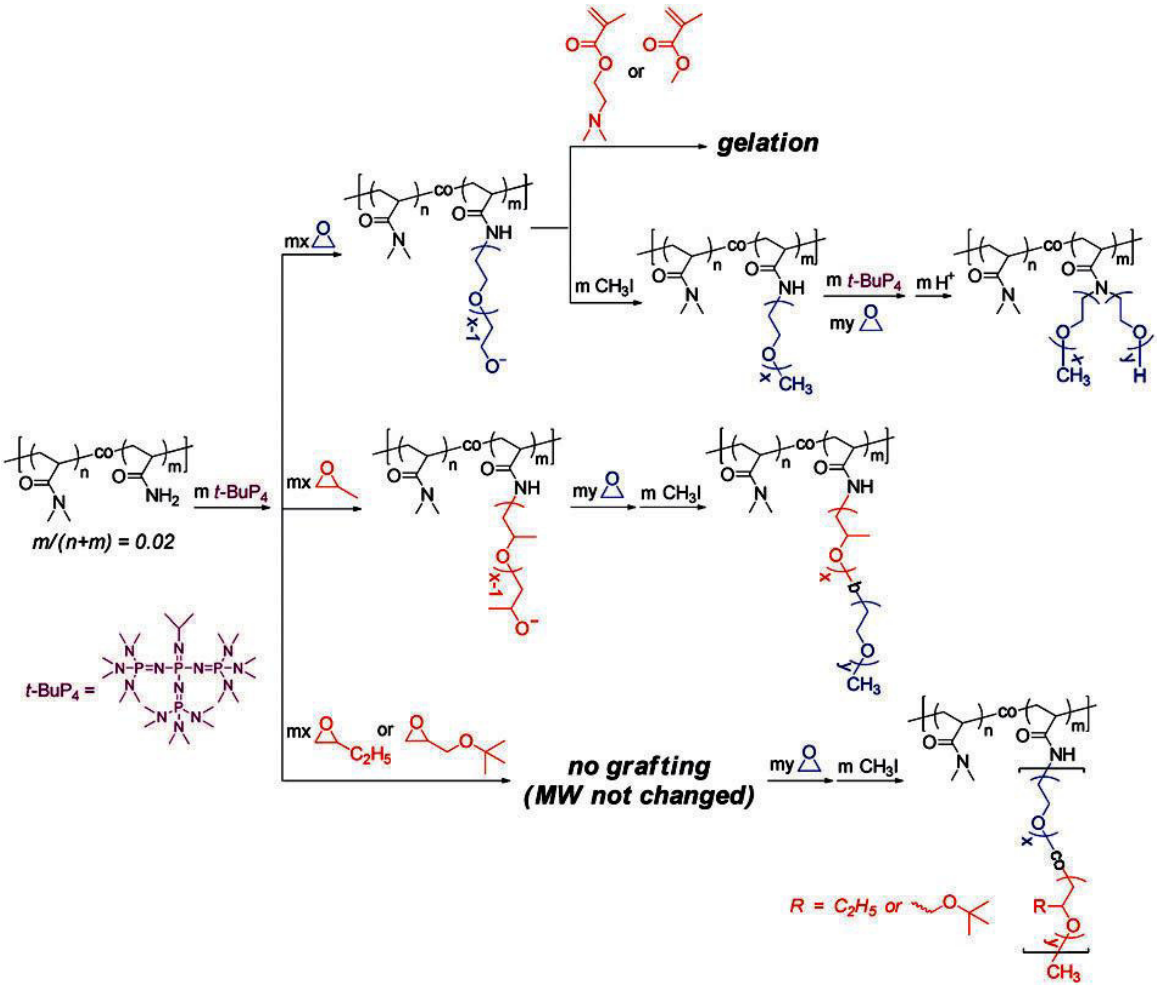

Figure 2. Phosphazene base-mediated synthesis of brush polymers with polyacrylamide backbone and polyether side chains. (Adapted with permission from Zhao, J.; Alamri, H.; Hadjichristidis, N. *Chem. Commun.* 2013, *49*, 7079.[26] Copyright 2013 Royal Society of Chemistry.)

By suspension polymerization using a calcium amide/alkoxide initiator system, Petrov and coworkers synthesized amorphous PO and BO homopolymers and PEO-*co*-PPO copolymers exhibiting low degrees of crystallinity. Without control over the degree of polymerization, high molecular weights in the range of several hundred kDa and MWDs between 2.3 and 3.2 were obtained.[31] The materials were cross-linked photochemically with *N*,*N*′-methylenebis(acrylamide) and tested as polymer gel electrolytes in dye-sensitized solar cells. A solar cell containing a chemically cross-linked PEO-*co*-PPO copolymer with 21% PPO content maintained high power conversion efficiency for at least twice the lifetime of a conventional physical PEO gel electrolyte (Figure 3).

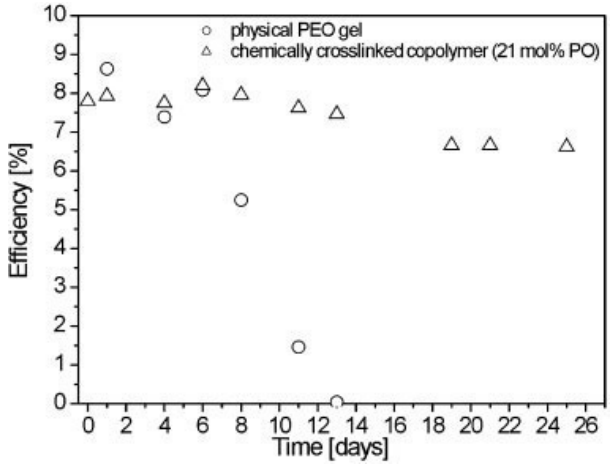

Figure 3. Power conversion effiency over time of dye-sensitized solar cells containing physical PEO gel and chemically cross-linked PEO-*co*-PPO, respectively. (Adapted with permission from Petrov, P.; Berlinova, I. V.; Tsvetanov, C.; Rosselli, S.; Schmid, A.; Zilaei, A.; Miteva, T.; Dürr, M.; Yasuda, A.; Nelles, G. *Macromol. Mater.* Eng. 2008, *293*, 598.[31] Copyright 2008 Wiley.)

The activated monomer technique, developed by Deffieux and Carlotti, uses efficient trialkylaluminum catalyst systems and ammonium salt initiators. It allows for minimizing chain transfer reactions during the polymerization of alkylene oxides. PO, BO, 1,2-hexene oxide, and 1,2-octadecene oxide were polymerized rapidly and in a controlled manner, resulting in well-defined polymers with molecular weights up to several ten thousand g/mol.[32-34] This strategy gave direct access to α-azido,ω-hydroxy-PPO.[35] By combining protonated phosphazene-base alkoxide initatiors with triisobutylaluminum, the same group synthesized telechelic PPO polyols.[36]

Via *N*-heterocyclic carbene-catalyzed polymerization, Taton et al. were able to prepare α,ω-difunctionalized PPO with MWs up to 7000 g mol^{-1} without the use of additional solvents.[37] Recently, Limbach et al. introduced imidazol(in)ium carbonates as more stable precatalysts which released the *N*-heterocyclic carbene upon heating,[38] demonstrating controlled synthesis of telechelic PPOs. In contrast, copolymerization of PO with ε-caprolactone and (S,S)-lactide, respectively, resulted in decreased conversion and broadened MWD. Carbene-mediated polymerization of higher alkylene oxide monomers has not been explored yet.

The most prominent polyalkylene glycol surfactants are block copolymers consisting of hydrophilic PEG and hydrophobic PPO segments that are discussed in a separate section of the Chemical Reviews article (not included in this thesis). In search of an alternative for poloxamers and similar EO-PO block copolymers, Booth and co-workers synthesized a great variety of linear and cyclic diblock and triblock, as well as gradient polymers from EO and BO. Polymerizations were performed in bulk, using alcohol-potassium alkoxide mixtures as initiators, resulting in narrow

molecular weight distributions. In general, rather short PBO blocks were synthesized.[39-42] Several groups extensively explored the materials properties of the copolymers, focusing on the dependence of micellization and gelation behavior on the block architecture.[43-50] Following the trend in hydrophobicity, copolymers of EO and BO exhibit lower critical micelle concentrations than copolymers of EO with PO, even if the hydrophobic block is shorter (Figure 4). In this context one may emphasize that low molecular weight PPO homopolymers are water-soluble below a critical solution temperature.[51,52]

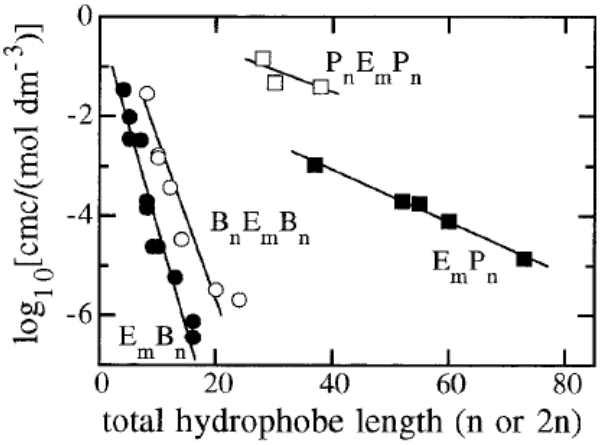

Figure 4. Critical micelle concentration of amphiphilic diblock and triblock copolymers in aqueous solution at 30 °C, versus PBO (B) and PPO (P) block length, respectively. (PEO (E) block length constant.) (Adapted with permission from Booth, C.; Attwood, D. *Macromol. Rapid Commun.* 2000, *21*, 501.[43] Copyright 2000 Wiley.)

Bates and co-workers modified the reaction protocol of Booth et al. by using THF as a solvent and completely deprotonated potassium alkoxides as initiators. This strategy enabled the synthesis of narrowly distributed PBO-*b*-PEO and low molecular weight PHO-*b*-PEO block copolymers with low monomer conversion.[5,53] The resulting materials were successfully tested for potential application as toughenersin cured epoxy resins.[54] Higher molecular weight PBO-*b*-PEO and PHO-*b*-PEO block copolymers were obtained by Carlotti et al. via the activated monomer method, and their self-organization in aqueous solution was investigated.[55] As expected from the high hydrophobicity of PHO, they observed very low critical micelle concentrations. Depending on the block lengths and molar ratio of hydrophilic and hydrophobic segments, spherical micelles or vesicles (polymersomes) or both in coexistence were observed.

Multihydroxyfunctional polyalkylene glycol amphiphiles can be accessed by replacing the PEG segments with linear or hyperbranched polyglycerol (PG), retaining the hydrophobic PPO blocks. Following the first report on linear−dendritic PPO−PG block copolymers,[56] linear diblock, triblock, and gradient copolymers were synthesized via polymerization and subsequent deprotection of

ethoxyethyl glycidyl ether (EEGE).[57-60] Incorporation of small amounts G already lead to water-soluble materials. Carlotti et al. were able to synthesize gradient copolymers of EEGE and *tert*-butyl glycidyl ether with PO and BO, respectively, with elevated molecular weights up to 85000 g mol^{-1} by the activated monomer strategy.[61] Kakuchi and co-workers combined the protected PG derivatives poly(benzyl glycidyl ether) and poly(*tert*-butyl glycidyl ether) with PBO segments, using phosphazene base-catalyzed polymerization.[22]

More than 60 years ago, random copolymers of EO and PO were commercialized as water-soluble polyalkylene glycol (PAG) lubricants by Union Carbide.[62] EO/PO random copolymers do not show such low surface tensions as the corresponding PEO-*b*-PPO block copolymers, avoiding undesired foaming when in use. Their properties in aqueous solution have been investigated by François and co-workers.[63]

Similar to the solubilization of hydrophobic compounds in water via PEGylation, oil-soluble gasoline additives were synthesized by butoxylation of hydrophilic amides.[64] Recently, Dow Chemical released oil-soluble PAGs, based on PBO and PPO-*co*-PBO copolymers as performance additives in hydrocarbon lubricants.[65]

As part of their work on epoxide-termination of living carbanionic polystyrene polymerization and subsequent AROP of epoxides, Quirk et al. prepared block copolymers which contained PPO as a semipolar segment.[66] Inspired by this, Bates and co-workers combined PBO with polyolefins and investigated the phase behavior of the completely hydrophobic, but phase-separated block copolymers.[67]

Noh and co-workers employed cationic ring-opening polymerization to copolymerize BO with epichlorohydrin.[68] In a postpolymerization modification step, they etherified the chloride groups to obtain stimuli-responsive poly(ferrocenyl glycidyl ether)-PBO copolymers.

Apart from its use in polyether chemistry, PO features prominently in the preparation of “green” polycarbonate. Driven by the global trend toward green chemistry and biodegradable materials, the copolymerization of PO (and other epoxides) with carbon dioxide has become a focus of major attention. Numerous reviews on the research in this area have been published in recent years.[14,69-78]

References

1. Gagnon, S. D. in *Encyclopedia of Polymer Science and Technology*; John Wiley & Sons, Inc.: **2002**.
2. Price, C. Polyethers. *Acc. Chem. Res.* **1974**, *7*, 294−301.
3. Bailey, F. E., Koleske, J. V. *Alkylene Oxides and Their Polymers*; Surfactant Science Ser. Vol. 35; CRC Press: Boca Raton, FL, **1990**.
4. Cracknell, R. Oil Soluble Polyethers in Automotive Crankcase Lubricants. *Lubr. Eng.* **1993**, *49*, 129−136.
5. Thio, Y.; Wu, J.; Bates, F. Epoxy Toughening Using Low Molecular Weight Poly(hexylene oxide)-Poly(ethylene oxide) Diblock Copolymers. *Macromolecules* **2006**, *39*, 7187−7189.
6. Hamley, I.; O'Driscoll, B.; Lotze, G.; Moulton, C.; Allgaier, J.; Frielinghaus, H. Highly Asymmetric Phase Diagram of a Poly(1,2-octylene oxide)-Poly(ethylene oxide) Diblock Copolymer System Comprising a Brush-Like Poly(1,2-octylene oxide) Block. Macromol*. Rapid Commun.* **2009**, *30*, 2141−2146.
7. Gerstl, C.; Schneider, G.; Pyckhout-Hintzen, W.; Allgaier, J.; Richter, D.; Alegria, A.; Colmenero, J. Segmental and Normal Mode Relaxation of Poly(alkylene oxide)s Studied by Dielectric Spectroscopy and Rheology. *Macromolecules* **2010**, *43*, 4968−4977.
8. Ponomarenko, V. A.; Khomutov, A. M.; Ilchenko, S. I.; Ignatenk, A. V. Influence of Substituted Groups on Anionic Polymerization of Alpha-Oxides. *Vysokomol. Soedin. A* **1971**, *13*, 1546−1556.
9. Ponomarenko, V. A.; Khomutov, A. M.; Ilchenko, S. I.; Ignatenk, A. V.; Khomutov, N. M. Influence of Substituted Groups on Reactivity of Monosubstituted Ethylene Oxide During Coordination-Anionic Copolymerization. *Vysokomol. Soedin. A* **1971**, *13*, 1551−1561.
10. Stolarzewicz, A.; Neugebauer, D. Influence of Substituent on the Polymerization of Oxiranes by Potassium Hydride. *Macromol. Chem. Phys.* **1999**, *200*, 2467−2470.
11. Oguni, N.; Lee, K.; Tani, H. Microstructure Analysis of Poly(propylene oxide) by ^{13}C Nuclear Magnetic Resonance Spectroscopy. *Macromolecules* **1972**, *5*, 819−820.
12. Schilling, F.; Tonelli, A. Carbon-13 NMR Determination of Poly(propylene oxide) Microstructure. *Macromolecules* **1986**, *19*, 1337−1343.
13. Chisholm, M. H.; Navarro-Llobet, D. NMR Assignments of Regioregular Poly(propylene oxide) at the Triad and Tetrad Level. *Macromolecules* **2002**, *35*, 2389−2392.
14. Childers, M.; Longo, J.; Van Zee, N.; LaPointe, A.; Coates, G. Stereoselective Epoxide Polymerization and Copolymerization. *Chem. Rev.* **2014**, *114*, 8129−8152.

15. Allgaier, J.; Willbold, S.; Chang, T. Synthesis of Hydrophobic Poly(alkylene oxide)s and Amphiphilic Poly(alkylene oxide) Block Copolymers. *Macromolecules* **2007**, *40*, 518−525.
16. Gerstl, C.; Schneider, G.; Pyckhout-Hintzen, W.; Allgaier, J.; Willbold, S.; Hofmann, D.; Disko, U.; Frielinghaus, H.; Richter, D. Chain Conformation of Poly(alkylene oxide)s Studied by Small-Angle Neutron Scattering. *Macromolecules* **2011**, *44*, 6077−6084.
17. Gerstl, C.; Schneider, G.; Fuxman, A.; Zamponi, M.; Frick, B.; Seydel, T.; Koza, M.; Genix, A.; Allgaier, J.; Richter, D.; et al. Quasielastic Neutron Scattering Study on the Dynamics of Poly(alkylene oxide)s. *Macromolecules* **2012**, *45*, 4394−4405.
18. Zhang, W.; Allgaier, J.; Zorn, R.; Willbold, S. Determination of the Compositional Profile for Tapered Copolymers of Ethylene Oxide and 1,2-Butylene Oxide by in-Situ-NMR. *Macromolecules* **2013**, *46*, 3931−3938.
19. Liu, Y.; Wei, W.; Xiong, H. Gradient and Block Side-Chain Liquid Crystalline Polyethers. *Polym. Chem.* **2015**, *6*, 583−590.
20. Rexin, O.; Mülhaupt, R. Anionic Ring-Opening Polymerization of Propylene Oxide in the Presence of Phosphonium Catalysts. *J. Polym. Sci., Part A: Polym. Chem.* **2002**, *40*, 864−873.
21. Rexin, O.; Mülhaupt, R. Anionic Ring-Opening Polymerization of Propylene Oxide in the Presence of Phosphonium Catalysts at Various Temperatures. *Macromol. Chem. Phys.* **2003**, *204*, 1102−1109.
22. Misaka, H.; Tamura, E.; Makiguchi, K.; Kamoshida, K.; Sakai, R.; Satoh, T.; Kakuchi, T. Synthesis of End-Functionalized Polyethers by Phosphazene Base-Catalyzed Ring-Opening Polymerization of 1,2- Butylene Oxide and Glycidyl Ether. *J. Polym. Sci., Part A: Polym. Chem.* **2012**, *50*, 1941−1952.
23. Zhao, J.; Pahovnik, D.; Gnanou, Y.; Hadjichristidis, N. One-Pot Synthesis of Linear- and Three-Arm Star-Tetrablock Quarterpolymers via Sequential Metal-Free Ring-Opening Polymerization Using a “Catalyst Switch” Strategy. *J. Polym. Sci., Part A: Polym. Chem.* **2015**, *53*, 304−312.
24. Zhao, J.; Pahovnik, D.; Gnanou, Y.; Hadjichristidis, N. Phosphazene-Promoted Metal-Free Ring-Opening Polymerization of Ethylene Oxide Initiated by Carboxylic Acid. *Macromolecules* **2014**, *47*, 1693−1698.
25. Zhao, J.; Hadjichristidis, N. Polymerization of 5-Alkyl δ-Lactones Catalyzed by Diphenyl Phosphate and Their Sequential Organocatalytic Polymerization with Monosubstituted Epoxides. *Polym. Chem.* **2015**, *6*, 2659−2668.
26. Zhao, J.; Alamri, H.; Hadjichristidis, N. A Facile Metal-Free ”Grafting-from” Route from Acrylamide-Based Substrate toward Complex Macromolecular Combs. *Chem. Commun*. **2013**, *49*, 7079−7081.

27. Malik, M.; Trathnigg, B.; Kappe, C. Selectvity of PEO-block-PPO Diblock Copolymers in the Microwave-Accelerated, Anionic Ring-Opening Polymerization of Propylene Oxide with PEG as Intiator. *Macromol. Chem. Phys.* **2007**, *208*, 2510−2524.
28. Malik, M.; Trathnigg, B.; Kappe, C. Microwave Assisted Synthesis and Characterization of End Functionalized Poly(propylene oxide) as Model Compounds. *Eur. Polym. J.* **2008**, *44*, 144−154.
29. Malik, M.; Trathnigg, B.; Kappe, C. Microwave-Assisted Polymerization of Higher Alkylene Oxides. *Eur. Polym. J.* **2009**, *45*, 899−910.
30. Dulle, M.; Malik, M.; Trathnigg, B.; Glatter, O. Self-Assembly and Structural Analysis of Multiblock Poly(oxyalkylene) Copolymers. *Macromolecules* **2010**, *43*, 7868−7871.
31. Petrov, P.; Berlinova, I. V.; Tsvetanov, C.; Rosselli, S.; Schmid, A.; Zilaei, A.; Miteva, T.; Durr, M.; Yasuda, A.; Nelles, G. High-Molecular-Weight Polyoxirane Copolymers and Their Use in High-Performance Dye-Sensitized Solar Cells. *Macromol. Mater. Eng.* **2008**, *293*, 598−604.
32. Labbé, A.; Carlotti, S.; Billouard, C.; Desbois, P.; Deffieux, A. Controlled High-Speed Anionic Polymerization of Propylene Oxide Initiated by Onium Salts in the Presence of Triisobutylaluminum. *Macromolecules* **2007**, *40*, 7842−7847.
33. Rejsek, V.; Sauvanier, D.; Billouard, C.; Desbois, P.; Deffieux, A.; Carlotti, S. Controlled Anionic Homo- and Copolymerization of Ethylene Oxide and Propylene Oxide by Monomer Activation. *Macromolecules* **2007**, *40*, 6510−6514.
34. Gervais, M.; Brocas, A.-L.; Deffieux, A.; Ibarboure, E.; Carlotti, S. Rapid and Controlled Synthesis of Hydrophobic Polyethers by Monomer Activation. *Pure Appl. Chem.* **2012**, *84*, 2103−2111.
35. Gervais, M.; Labbé, A. l.; Carlotti, S.; Deffieux, A. Direct Synthesis of α-Azido, ω-Hydroxypolyethers by Monomer-Activated Anionic Polymerization. *Macromolecules* **2009**, *42*, 2395−2400.
36. Brocas, A.-L.; Deffieux, A.; Le Malicot, N.; Carlotti, S. Combination of Phosphazene Base and Triisobutylaluminum for the Rapid Synthesis of Polyhydroxy Telechelic Poly(propylene oxide). *Polym. Chem.* **2012**, *3*, 1189−1195.
37. Raynaud, J.; Ottou, W. N.; Gnanou, Y.; Taton, D. Metal-Free and Solvent-Free Access to α,ω-Heterodifunctionalized Poly(propylene oxide)s by *N*-Heterocyclic Carbene-Induced Ring Opening Polymerization. *Chem. Commun*. **2010**, *46*, 3203−3205.
38. Lindner, R.; Lejkowski, M. L.; Lavy, S.; Deglmann, P.; Wiss, K. T.; Zarbakhsh, S.; Meyer, L.; Limbach, M. Ring-Opening Polymerization and Copolymerization of Propylene Oxide Catalyzed by *N*-Heterocyclic Carbenes. *ChemCatChem* **2014**, *6*, 618−625.

39. Sun, W.; Ding, J.; Mobbs, R.; Heatley, F.; Attwood, D.; Booth, C. Preparation of a Diblock Copoly(oxybutylene oxyethylene) and Study of Its Micellisation and Surface-Properties in Dilute Aqueous-Solution. *Colloids Surf*. **1991**, *54*, 103−111.
40. Luo, Y.; Nicholas, C.; Attwood, D.; Collett, J.; Price, C.; Booth, C. Micellization and Gelation of Block-Copoly(oxyethylene oxybutylene oxyethylene) $E_{58}B_{17}E_{58}$. *Colloid Polym. Sci*. **1992**, *270*, 1094−1105.
41. Yan, Z.; Yang, Z.; Price, C.; Booth, C. Cyclization of Poly(ethylene glycol)s and Related Block-Copolymers. *Makromol. Chem., Rapid Commun*. **1993**, *14*, 725−732.
42. Dickson, S.; Yu, G.; Heatley, F.; Booth, C. Reactivity Ratios for the Anionic Copolymerization of Ethylene-Oxide and Butylene Oxide in Bulk. *Eur. Polym. J*. **1993**, *29*, 281−286.
43. Booth, C.; Attwood, D. Effects of Block Architecture and Composition on the Association Properties of Poly(oxyalkylene) Copolymers in Aqueous Solution. *Macromol. Rapid Commun.* **2000**, *21*, 501−527.
44. Booth, C.; Attwood, D.; Price, C. Self-Association of Block Copoly(oxyalkylene)s in Aqueous Solution. Effects of Composition, Block Length and Block Architecture. *Phys. Chem. Chem. Phys.* **2006**, *8*, 3612−3622.
45. Liang, G.-D.; Xu, J.-T.; Fan, Z.-Q.; Mai, S.-M.; Ryan, A. J. Effect of Substrate and Molecular Weight on the Stability of Thin Films of Semicrystalline Block Copolymers. *Langmuir* **2007**, *23*, 3673−3679.
46. Ribeiro, M. E. N. P.; de Oliveira, S. A.; Ricardo, N. M. P. S.; Mai, S.-M.; Attwood, D.; Yeates, S. G.; Booth, C. Diblock Copolymers of Ethylene Oxide and 1,2-Butylene Oxide in Aqueous Solution: Formation of Unimolecular Micelles. *Int. J. Pharm*. **2008**, *362*, 193−196.
47. Kelarakis, A.; Chaibundit, C.; Krysmann, M. J.; Havredaki, V.; Viras, K.; Hamley, I. W. Interactions of an Anionic Surfactant with Poly(oxyalkylene) Copolymers in Aqueous Solution. *J. Colloid Interface Sci.* **2009**, *330*, 67−72.
48. Smart, T. P.; Ryan, A. J.; Howse, J. R.; Battaglia, G. Homopolymer Induced Aggregation of Poly(ethylene oxide)$_n$-*b*-Poly(Butylene Oxide)$_m$ Polymersomes. *Langmuir* **2010**, *26*, 7425−7430.
49. Cambón, A.; Rey-Rico, A.; Mistry, D.; Brea, J.; Loza, M. I.; Attwood, D.; Barbosa, S.; Alvarez-Lorenzo, C.; Concheiro, A.; Taboada, P.; et al. Doxorubicin-Loaded Micelles of Reverse Poly(butylene oxide)−Poly(ethylene oxide)−Poly(butylene oxide) Block Copolymers as Efficient "Active" Chemotherapeutic Agents. *Int. J. Pharm*. **2013**, *445*, 47−57.
50. Cambón, A.; Figueroa-Ochoa, E.; Juárez, J.; Villar-Álvarez, E.; Pardo, A.; Barbosa, S.; Soltero, J. F. A.; Taboada, P.; Mosquera, V. Complex Self-Assembly of Reverse Poly(butylene oxide)-

Poly(ethylene oxide)-Poly(butylene oxide) Triblock Copolymers with Long Hydrophobic and Extremely Lengthy Hydrophilic Blocks. *J. Phys. Chem. B* **2014**, *118*, 5258−5269.

51. Mortensen, K.; Schwahn, D.; Janssen, S. Pressure-Induced Melting of Micellar Crystal. *Phys. Rev. Lett.* **1993**, *71*, 1728−1731.
52. Schild, H. G.; Tirrell, D. A. Microcalorimetric Detection of Lower Critical Solution Temperatures in Aqueous Polymer Solutions*. J. Phys. Chem.* **1990**, *94*, 4352−4356.
53. Wu, J.; Thio, Y.; Bates, F. Structure and Properties of PBO-PEO Diblock Copolymer Modified Epoxy. *J. Polym. Sci., Part B: Polym. Phys*. **2005**, *43*, 1950−1965.
54. Thio, Y.; Wu, J.; Bates, F. The Role of Inclusion Size in Toughening of Epoxy Resins by Spherical Micelles. *J. Polym. Sci., Part B: Polym. Phys.* **2009**, *47*, 1125−1129.
55. Brocas, A.-L.; Gervais, M.; Carlotti, S.; Pispas, S. Amphiphilic Diblock Copolymers Based on Ethylene Oxide and Epoxides Bearing Aliphatic Side Chains. *Polym. Chem*. **2012**, *3*, 2148.
56. Istratov, V.; Kautz, H.; Kim, Y.-K.; Schubert, R.; Frey, H. Linear-Dendritic Nonionic Poly(propylene oxide)-Polyglycerol Surfactants. *Tetrahedron* **2003**, *59*, 4017−4024.
57. Dimitrov, P.; Rangelov, S.; Dworak, A.; Tsvetanov, C. Synthesis and Associating Properties of Poly(ethoxyethyl glycidyl ether)/Poly(propylene oxide) Triblock Copolymers. *Macromolecules* **2004**, *37*, 1000−1008.
58. Halacheva, S.; Rangelov, S.; Tsvetanov, C. Poly(glycidol)-Based Analogues to Pluronic Block Copolymers. Synthesis and Aqueous Solution Properties. *Macromolecules* **2006**, *39*, 6845−6852.
59. Halacheva, S.; Rangelov, S.; Tsvetanov, C.; Garamus, V. Aqueous Solution Properties of Polyglycidol-Based Analogues of Pluronic Copolymers. Influence of the Poly(propylene oxide) Block Molar Mass. *Macromolecules* **2010**, *43*, 772−781.
60. Schömer, M.; Frey, H. Water-Soluble ”Poly(propylene oxide)” by Random Copolymerization of Propylene Oxide with a Protected Glycidol Monomer. *Macromolecules* **2012**, *45*, 3039−3046.
61. Gervais, M.; Brocas, A.-L.; Cendejas, G.; Deffieux, A.; Carlotti, S. Synthesis of Linear High Molar Mass Glycidol-Based Polymers by Monomer-Activated Anionic Polymerization. *Macromolecules* **2010**, *43*, 1778−1784.
62. Matlock, P. L.; Brown, W. L.; Clinton, N. A. in *Synthetic Lubricants and High- Performance Functional Fluids, Revised and Expanded*, 2nd ed.; Rudnick, L. R., Shubkin, R. L., Eds.; CRC Press: Boca Raton, FL, **1999**.
63. Louai, A.; Sarazin, D.; Pollet, G.; Francois, J.; Moreaux, F. Properties of Ethylene Oxide-Propylene Oxide Statistical Copolymers in Aqueous-Solution. *Polymer* **1991**, *32*, 703−712.

64. Lin, J.; Wu, J.; Ho, Y. Synthesis and in Situ Transformation of Poly(oxybutylene) Amides by Butoxylation. *J. Appl. Polym. Sci.* **2001**, *82*, 435−445.
65. Greaves, M.; Zaugg-Hoozemans, E.; Khelidj, N.; van Voorst, R.; Meertens, R. Performance Properties of Oil-Soluble Synthetic Polyalkylene Glycols. *Lubr. Sci*. **2012**, *24*, 251−262.
66. Quirk, R. P.; Lizarraga, G. M. Anionic Synthesis of Well-Defined Poly[(styrene)-block-(propylene oxide)] Block Copolymers. *Macromol. Chem. Phys*. **2000**, *201*, 1395−1404.
67. Zhou, N.; Lodge, T.; Bates, F. Phase Behavior of Polyisoprene-Poly(butylene oxide) and Poly(ethylene-*alt*-propylene)-Poly(butylene oxide) Block Copolymers. *Soft Matter* **2010**, *6*, 1281−1290.
68. Cho, B.-S.; Kim, J.-S.; Lee, J.-M.; Kweon, J.-O.; Noh, S.-T. Synthesis and Characterization of Poly(ferrocenyl glycidyl ether)-1,2-Butylene Oxide Copolymers. *Macromol. Res.* **2014**, *22*, 826−831.
69. Sugimoto, H.; Inoue, S. Copolymerization of Carbon Dioxide and Epoxide. *J. Polym. Sci*., *Part A: Polym. Chem*. **2004**, *42*, 5561−5573.
70. Darensbourg, D. Making Plastics from Carbon Dioxide: Salen Metal Complexes as Catalysts for the Production of Polycarbonates from Epoxides and CO_2. *Chem. Rev*. **2007**, *107*, 2388−2410.
71. Luinstra, G. Poly(propylene carbonate), Old Copolymers of Propylene Oxide and Carbon Dioxide with New Interests: Catalysis and Material Properties. *Polym. Rev.* **2008**, *48*, 192−219.
72. Qin, Y.; Wang, X. Carbon Dioxide-Based Copolymers: Environmental Benefits of PPC, an Industrially Viable Catalyst. *Biotechnol. J*. **2010**, *5*, 1164−1180.
73. Kember, M.; Buchard, A.; Williams, C. Catalysts for CO_2/Epoxide Copolymerisation. *Chem*. *Commun*. **2011**, *47*, 141−163.
74. Lu, X.; Ren, W.; Wu, G. CO_2 Copolymers from Epoxides: Catalyst Activity, Product Selectivity, and Stereochemistry Control. *Acc. Chem. Res.* **2012**, *45*, 1721−1735.
75. Darensbourg, D.; Wilson, S. What's New with CO_2? Recent Advances in its Copolymerization with Oxiranes. *Green Chem*. **2012**, *14*, 2665−2671.
76. Lu, X.; Darensbourg, D. Cobalt Catalysts for the Coupling of CO_2 and Epoxides to Provide Polycarbonates and Cyclic Carbonates. *Chem. Soc. Rev.* **2012**, *41*, 1462−1484.
77. Taherimehr, M.; Pescarmona, P. Green Polycarbonates Prepared by the Copolymerization of CO_2 with Epoxides. *J. Appl. Polym. Sci*. **2014**, *131*, 41141.
78. Paul, S.; Zhu, Y.; Romain, C.; Brooks, R.; Saini, P.; Williams, C. Ring-Opening Copolymerization (ROCOP): Synthesis and Properties of Polyesters and Polycarbonates. *Chem*. *Commun*. **2015**, *51*, 6459−6479.

2

SYNTHESIS AND CHARACTERIZATION OF HYPERBRANCHED POLY(ALKYLENE OXIDE)S

2.1 Online NMR Copolymerization Kinetics of Glycidol with Ethylene Oxide, Propylene Oxide and 1,2-Butylene Oxide: From Hyperbranched to Hyperstar Topology

Daniel Leibig[1,2,‡], Jan Seiwert[1,‡], Johannes Liermann[1], Holger Frey[1,2,]*

[1] Institute of Organic Chemistry, Johannes Gutenberg University, Duesbergweg 10-14, 55128 Mainz, Germany

[2] Graduate School Materials Science in Mainz, Staudinger Weg 9, 55128 Mainz, Germany

[‡] Daniel Leibig and Jan Seiwert contributed equally to this work.

Submitted.

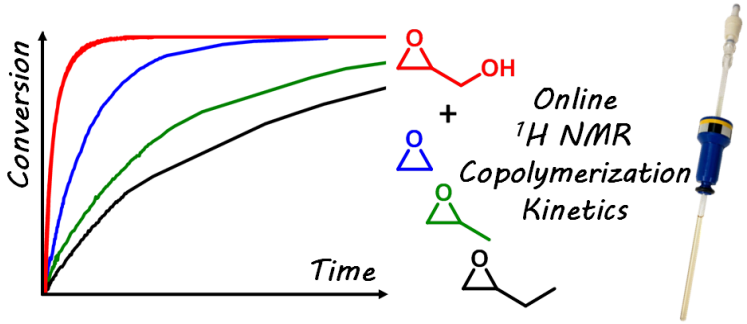

Abstract

The reaction kinetics of the multibranching anionic ring-opening copolymerization of glycidol (a cyclic latent AB_2 monomer) with ethylene oxide (EO), propylene oxide (PO) and 1,2-butylene oxide (BO) in dimethyl sulfoxide was examined. Online ^{1}H NMR spectroscopy was employed for in-situ monitoring of the individual monomer consumption during the entire course of the copolymerisation. Varying the counter ion, both cesium alkoxide and potassium alkoxide initiated copolymerization were studied and compared. From the individual monomer consumptions, reactivity ratios were calculated. The reactivity ratio of the alkylene oxides decreases from 0.44 to 0.11 with increasing alkyl chain length on going from EO to BO. Glycidol was found to exhibit higher reactivity ratios in each combination ranging from 2.34 to 7.94. Different counter ions rather influence the absolute reaction rates than the relative monomer reactivity. Furthermore, the calculated reactivity ratios were related to the molecular weight distribution and the degrees of branching of the respective copolymers, implying a change from a hyperbranched to a hyperstar structure with increasing side chain length of the alkylene comonomer.

Introduction

Hyperbranched polymers combine dendrimer-like materials properties, such as an amorphous nature and a high number of functional end groups with facile synthetic accessibility. Since Flory introduced the theoretical concepts for hyperbranched structures in 1952,[1] a considerable amount of theoretical work has been devoted to understanding and predicting the reaction kinetics of multibranching polymerizations, varying reaction parameters.[2–13] However, only in few works experimental data on polymerization kinetics have been reported. Several multibranching polycondensation and self-condensing vinyl polymerization reactions, mainly homopolymerizations, were investigated.[14–23] Classical characterization methods such as NMR spectroscopy, gas chromatography and mass spectrometry, respectively, have been employed to monitor the polymerization progress.

In recent years, our group has established *in-situ* NMR spectroscopy as a convenient tool to follow copolymerization kinetics in real time during the entire course of a reaction. This method has granted insight into the reactivity ratios and copolymer sequences for the anionic ring-opening copolymerization of ethylene oxide (EO) with different glycidyl ethers and glycidyl amines,[24–28] as well as the copolymerization of propylene oxide (PO) with acetal-protected glycidol.[29] Allgaier *et al.* studied the copolymerization of ethylene oxide and 1,2-butylene oxide (BO) in the same

manner, revealing a strongly tapered microstructure.[30] Poly(alkylene oxide)s are chemically stable, mostly non-toxic materials comprising flexible polyether chains. Their fields of application strongly depend on the materials properties of the respective polymer. The water-soluble and semi-crystalline poly(ethylene oxide) features prominently in biomedical, cosmetic and food products, whereas the hydrophobic and amorphous poly(propylene oxide) is a widely used building block for polyurethanes.

The reaction kinetics of the multibranching anionic polymerization of glycidol has been hardly studied to date. In 1966, Sandler and Berg vaguely observed a higher reactivity of glycidol in comparison with propylene oxide.[31] Copolymerization of glycidol has only been investigated by *in-situ* NMR spectroscopy in two reports to date. Kim and coworkers monitored the copolymerization of glycidol and an unusual redox-degradable glycidyl ether by quantitative ^{13}C NMR measurements.[32] This technique, however, requires polymerization in bulk to compensate for the low natural abundance of the ^{13}C isotope.[33] It is therefore unsuitable for the polymerization of volatile monomers such as ethylene oxide above their boiling points in the NMR tube. Furthermore, the established synthetic procedure for the anionic polymerization of glycidol and its copolymerization with glycidyl ethers involves slow addition of the monomer(s) to achieve control over molecular weights and molecular weight distribution.[34,35] These particular conditions could not be transferred to an *in-situ* NMR kinetic experiment so far.

In recent years our group introduced simple batch procedures for the copolymerization of the readily available alkylene oxide monomers ethylene oxide, propylene oxide and 1,2-butylene oxide (BO) with glycidol, resulting in moderately distributed hyperbranched polyether polyols with mostly low molecular weights (Scheme 1).[36–39] In the recently reported procedures, hyperbranched anologues of the commercially widely used poly(alkylene) oxide homopolymers were obtained, which feature tunable solubility, multiple hydroxyl end groups, low viscosity and an amorphous structure. We also performed a first kinetic experiment to determine the reactivity ratios of the system glycidol/BO and found a strongly tapered structure, raising the general question: At what rates does glycidol polymerize compared to common alkylene oxides?

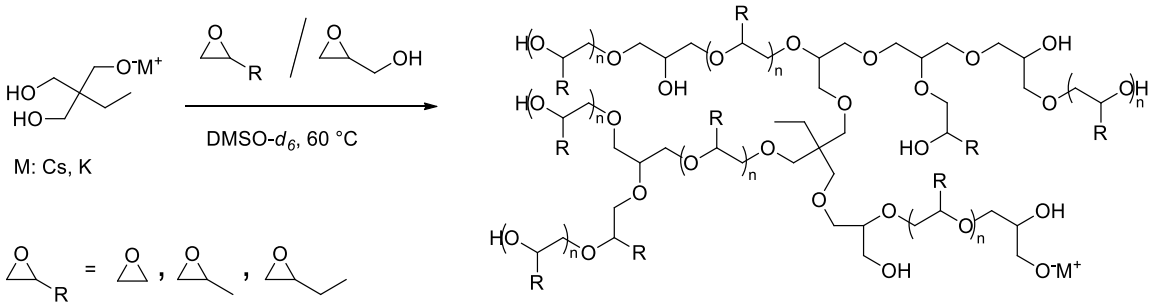

Scheme 1. Synthesis of hyperbranched copolymers from glycidol with EO, PO and BO, carried out in an NMR tube in this work.

In this work, we study the anionic copolymerization kinetics of the cyclic, latent AB_2-monomer glycidol with the common epoxide monomers EO, PO and BO in deuterated dimethyl sulfoxide by *in-situ* ^{1}H NMR spectroscopy. From the monomer consumption during the copolymerization, we determine reactivity ratios of the three different comonomer combinations, using the Fineman-Ross formalism and discuss the consequences for the resulting branched polyether structure. The influence of the counterion is investigated by comparing potassium and cesium alkoxide initiated copolymerization. From the reactivity ratios conclusions regarding the (hyper)branched structures have been derived.

Experimental part

Materials

DMSO-d_6 was purchased from Deutero GmbH (Kastellaun). Other solvents and reagents were purchased from Sigma Aldrich and Acros Organics and used as received, unless stated otherwise. Propylene oxide (99.5%), 1,2-butylene oxide (99%) and glycidol (96%) were dried over calcium hydride (CaH_2) and distilled in vacuum directly prior to use.

Instrumentation

NMR spectroscopy. ^{1}H NMR spectra were recorded at 400 MHz and ^{13}C NMR at 100 MHz on a Bruker Advance III HD 400 (5 mm BBFO-SmartProbe with z-gradient and ATM) and are referenced internally to residual signals of the deuterated solvent. Details of the *in-situ* NMR technique are given below.

Analytical Size-exclusion chromatography. An Agilent 1100 series including a PSS HEMA column combination ($10^6/10^4/10^2$ Å porosity) and UV and RI detector, was used as an integrated

instrument for SEC measurements in DMF (containing 0.25 g L^{-1} of lithium bromide as an additive). Calibration was achieved with poly(ethylene glycol) standards provided by Polymer Standards Service (PSS).

Preparative Size-exclusion chromatography. Sample fractioning by SEC was performed in $CHCl_3$, at 25 °C and a flow rate of 3.5 mL min^{-1} using a LC-91XX Next Series Recycling Preparative HPLC Anlage by *Japan Analytical Industry Co. Ltd.*. It was equipped with a Jaigel-2H column (upper exclusion limit $5 \cdot 10^3$ g mol^{-1}) and a UV and RI detector. Calibration was achieved with polystyrene standards provided by Polymer Standards Service (PSS).

In-situ NMR-monitoring of the copolymerizations

4.0 mg (0.03 mmol, 1.0 eq.) 1,1,1-Tris(hydroxymethyl)propane (TMP) and either 1.7 mg (0.01 mmol 0.3 eq.) cesium hydroxide monohydrate or 1.1 mg (0.01 mmol 0.3 eq.) potassium methoxide were placed in a Schlenk tube and dissolved in methanol. Benzene was added and the initiator salt was dried in vacuum overnight. All ensuing operations were performed under protective gas atmosphere. The initiator salt was dissolved in 0.5 mL DMSO-d_6. The solution was transferred to an NMR tube equipped with a Teflon stopcock and frozen. 60 µL (0.9 mmol, 30 eq.) glycidol and 0.6 mmol, (20 eq.) of the comonomer ethylene oxide, propylene oxide or butylene oxide, respectively, were added. In case of ethylene oxide, the monomer was transferred from a lecture bottle to a graduated ampoule and subsequently into the NMR tube via distillation in vacuum. The tube was evacuated and sealed; the solution was warmed to room temperature, mixed and then placed in the NMR spectrometer at 60 °C. Spectra were recorded with 16 scans at 2-minute intervals during the first hour, then at 5-minute intervals for 2 hours, and at 10-minute intervals within the next 15 hours. If necessary, the intervals were extended afterwards.

Hb(PEO-co-PG)

^{1}H NMR (400 MHz, DMSO-d_6, δ): 4.81 – 4.35 (m, br, OH); 4.10 – 3.06 (m, O-CH, O-CH_2); 1.36 – 1.18 (m, 2H, CH_3-CH_2 (TMP)); 0.89 – 0.68 (m, 3H, CH_3 (TMP)).

^{13}C-NMR (DMSO-d_6, 100 MHz, δ): 80.25 – 79.45 (m, CH $G_{1,3\text{-Linear}}$); 78.52 – 77.42 (m, CH $G_{\text{Dendritic}}$); 73.22 – 72.10 (m,, 2 CH_2 $G_{1,4\text{-Linear}}$); 72.04 – 69.62 (m, 2 CH_2 $G_{\text{Dendritic}}$, 2 CH_2 EO_{Linear}, *C*H_2-CH_2-OH EO_{Terminal}, CH G_{Terminal}, CH_2 G_{Terminal}); 69.61 – 68.37 (m, CH_2 $G_{1,3\text{-Linear}}$, CH-OH $G_{1,4\text{-Linear}}$); 63.39 – 62.96 (CH_2-OH G_{Terminal}); 60.87 – 60.07 (m, CH_2-OH EO_{Terminal}, CH_2-OH $G_{1,3\text{-Linear}}$).

Hb(PPO-co-PG)

^{1}H-NMR (DMSO-d_6, 400 MHz, δ): 4.55 – 4.33 (m, br, OH); 4.08 – 3.02 (m, O-CH, O-CH_2); 1.56 – 1.12 (m, CH_3-CH_2 (BO & TMP)); 0.87 (t, CH_3 (BO); 0.79 (t, CH_3 (TMP)).

^{13}C-NMR (DMSO-d_6, 100 MHz, δ): 80.6 – 79.0 (CH $G_{1,3\text{-Linear}}$, CH BO_{Linear}); 78.8 – 77.4 (CH $G_{Dendritic}$); 75.8 – 75.0 (CH_2 $BO_{Terminal}$); 74.6 – 73.6 (CH_2 BO_{Linear}) 73.2 – 72.1 (2 CH_2 $G_{1,4\text{-Linear}}$); 72.0 – 69.9 (2 CH_2 $G_{Dendritic}$, CH $G_{Terminal}$, CH $G_{Terminal}$, CH_2 $BO_{Terminal}$); 69.9 – 68.3 (CH_2 $G_{1,3\text{-Linear}}$, CH-OH $G_{1,4\text{-Linear}}$); 63.5 – 62.8 (CH_2-OH $G_{Terminal}$); 61.4 – 60.6 (CH_2-OH $G_{1,3\text{-Linear}}$).

Hb(PBO-co-PG)

^{1}H-NMR (DMSO-d_6, 400 MHz, δ): 4.55 – 4.33 (m, br, OH); 4.08 – 3.02 (m, O-CH, O-CH_2); 1.56 – 1.12 (m, CH_3-CH_2 (BO & TMP)); 0.87 (t, CH_3 (BO); 0.79 (t, CH_3 (TMP)).

^{13}C-NMR (DMSO-d_6, 100 MHz, δ): 80.6 – 79.0 (CH $G_{1,3\text{-Linear}}$, CH BO_{Linear}); 78.8 – 77.4 (CH $G_{Dendritic}$); 75.8 – 75.0 (CH_2 $BO_{Terminal}$); 74.6 – 73.6 (CH_2 BO_{Linear}) 73.2 – 72.1 (2 CH_2 $G_{1,4\text{-Linear}}$); 72.0 – 69.9 (2 CH_2 $G_{Dendritic}$, CH $G_{Terminal}$, CH $G_{Terminal}$, CH_2 $BO_{Terminal}$); 69.9 – 68.3 (CH_2 $G_{1,3\text{-Linear}}$, CH-OH $G_{1,4\text{-Linear}}$); 63.5 – 62.8 (CH_2-OH $G_{Terminal}$); 61.4 – 60.6 (CH_2-OH $G_{1,3\text{-Linear}}$).

Results and Discussion

The synthetic protocols for the anionic ring-opening copolymerization of glycidol with ethylene oxide, propylene oxide and butylene oxide, respectively, in the NMR tube were adapted from the corresponding batch procedures that were introduced in recent works by our group.[36–38]

In order to enable safe polymerization in the NMR spectrometer, the copolymerizations of all monomer combinations were performed in deuterated DMSO at 60 °C. Samples were prepared in a teflon-sealed NMR tube under high vacuum (10^{-3} bar) and introduced into the preheated NMR spectrometer. The kinetic measurements were started after the sample temperature had remained constant at 60 °C for 120 s. During the first hour, the time interval between spectra recordings was 2 minutes. The interval was increased to 5 min for the next 2 h and to 10 min for 15 h afterwards, due to the decrease of the reaction rate with time. All spectra were recorded with 16 scans and a relaxation time of 1s between the individual scans to ensure comparability of the data. In the following, the data obtained will first be discussed separately for copolymerization of EO, PO and BO with glycidol and subsequently, all combinations studied will be compared.

Hb(PEO-co-PG). Consumption of both EO and glycidol was determined by following the decrease of the individual monomer signals over the course of the polymerization. By monitoring the four methylene protons of ethylene oxide (δ = 2.61 ppm, s) and the methine proton of glycidol (δ = 2.99 ppm, m), the respective conversion rates were followed. An exemplary selection of NMR spectra is shown in Figure 1, revealing the decreasing monomer signals and the concurrent increase of the broad characteristic polymer signal of the polyether backbone in the range of 3.3 to 3.9 ppm. The decrease of the monomer signal intensity can be translated to the single monomer consumption. It is obvious that glycidol (highlighted in red) is consumed faster than the comonomer EO (highlighted in blue).

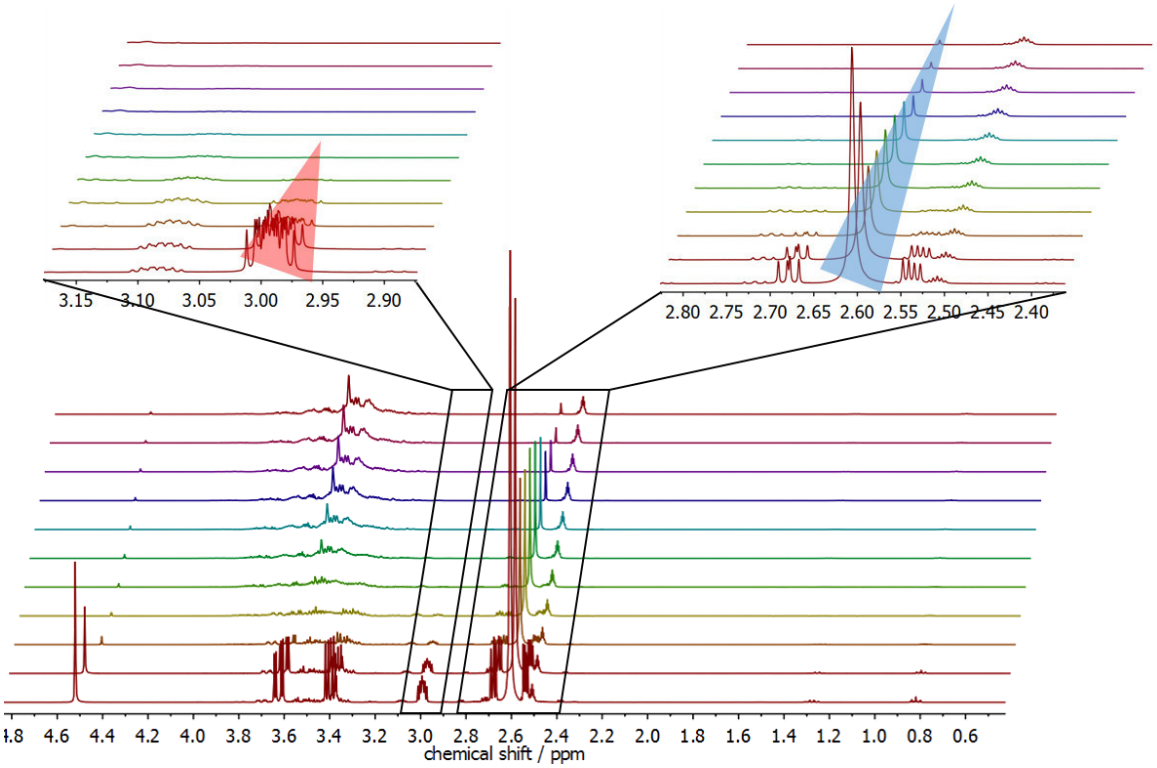

Figure 1. Online ^{1}H NMR copolymerization kinetics of ethylene oxide and glycidol in DMSO-d_6. Bottom: Overlay of spectra of the online ^{1}H NMR kinetics study. Top: Zoom-in, showing the decrease of the monomer signal of glycidol (red) and ethylene oxide (blue).

The normalized single monomer conversion is plotted versus the total monomer consumption in Figure 2. The residual monomer concentration was normalized by the intersection with c(G) = c(EO). In contrast to the generally accepted validity of reactivity ratios for radical copolymerizations, data from anionic copolymerizations are often criticized with respect to their limited significance, because the reaction rates may vary drastically with solvent polarity and counterion employed. In order to generalize our conclusions, all copolymerizations in this work have been performed with both cesium alkoxide and potassium alkoxide initiation, respectively,

to investigate the dependence of the reactivity ratios on the counterion. Cesium alkoxide initiated copolymerization of EO and G was found to proceed at a faster reaction rate and 99% conversion was achieved after 40 h. Potassium alkoxide initiation, on the other hand, leads to a slightly longer reaction time of approximately 55 h (Figure S1).

The reactivity ratios for the copolymerizations were determined by the established Fineman-Ross formalism (as detailed in the Supporting Information).[40] For the monomer pair EO/glycidol the polymerization with cesium shows the reactivity ratios $r_{EO,Cs}$ = 0.42 ± 0.02 and $r_{G,Cs}$ = 2.34 ± 0.13. The slower reaction with potassium as a counterion leads to slightly more disparate reactivity ratios of $r_{EO,K}$ = 0.44 ± 0.02 and $r_{G,K}$ = 2.64 ± 0.14. The disparate reactivity ratios indicate a gradient copolymer structure. It should be noted, however, that chain transfer reactions after different reaction times cause the formation of a mixture of copolymers with varying composition due to the drifting molar ratio in the monomer feed. These chain transfers may only occur as long as glycidol is present in the monomer feed, as explained in section 'Consequences of the reaction kinetics for the copolymer structure'.

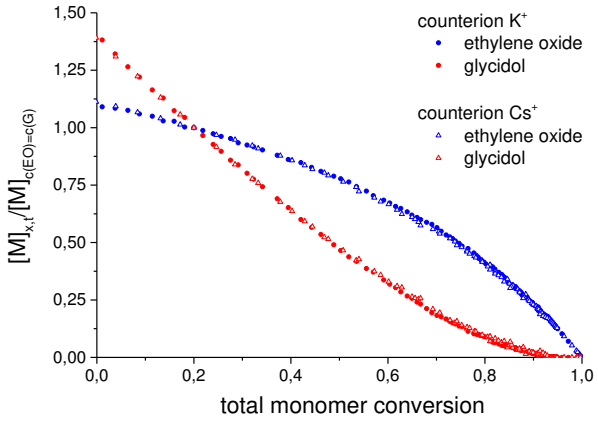

Figure 2. Comparison of the monomer conversion of ethylene oxide (blue) and glycidol (red) in dependence of the total monomer conversion and for different counterions.

Hb(PPO-co-PG). The NMR kinetic studies of the copolymerization of PO and glycidol were performed under the same conditions and with the same setup as the kinetic studies for EO/G. The integrals of the methine signals of glycidol (δ = 2.99 ppm, m) and propylene oxide (δ = 2.93 ppm, m) were followed for the calculation. Figure 3 shows a considerably faster decrease of the glycidol signal compared to the propylene oxide monomer signals. A concurrent increase of the signal of the polymer backbone can be observed. The single monomer conversion was calculated and plotted versus the total monomer conversion (Figure 4). The reactivity ratios determined for

the system PO/glycidol are $r_{PO,Cs}$ = 0.17 (± 0.02)/ $r_{G,Cs}$ = 4.70 (± 0.41) and $r_{PO,K}$ = 0.16 (± 0.01)/ $r_{G,K}$ = 4.86 (± 0.44). The polymerization with cesium as counterion proceeded slightly faster, and the potassium initiated copolymerization exhibited a slightly greater difference in the reactivity ratios. However, we emphasize that the kinetic data shows no significant difference in the polymers´ gradient structure for the different counterions. This monomer combination results in a pronounced gradient structure. Chain transfer reactions may only occur before a total conversion of 85% is reached, because the glycidol monomer has been consumed at this point.

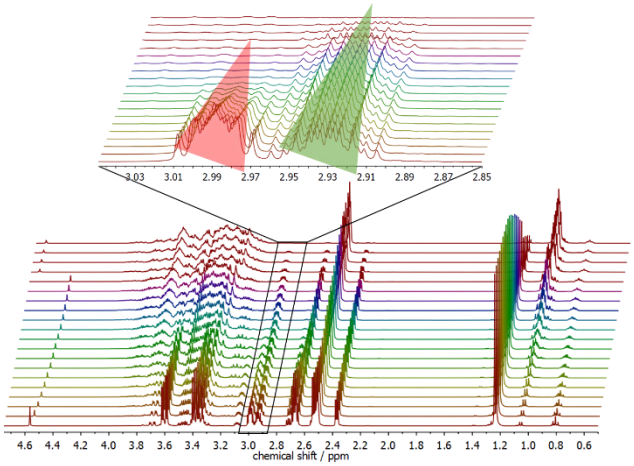

Figure 3. Online ^{1}H NMR copolymerization kinetics of propylene oxide and glycidol in DMSO-d_6. Bottom: Overlay of spectra of the online ^{1}H NMR kinetics study. Top: Zoom-in, showing the decrease of the monomer signals of glycidol (highlighted in red) and propylene oxide (highlighted in green).

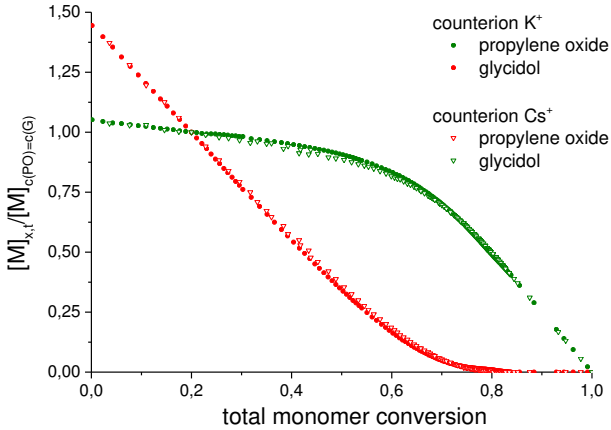

Figure 4. Comparison of the single monomer conversion of propylene oxide (green) and glycidol (red) in dependence of the total monomer conversion and for different counterions.

Hb(PBO-co-PG). The cesium alkoxide-initiated copolymerization of butylene oxide and glycidol had already been investigated in a preceding work.[36] The Fineman-Ross determination of the reactivity

ratios gave values of $r_{BO,Cs}$ = 0.19 (± 0.02)/ $r_{G,Cs}$ = 6.08 (± 0.23), revealing a strongly tapered structure with G being incorporated into the polymer considerably faster than BO.

Herein, we analyze this system initiated by a potassium alkoxide for comparison. Interestingly, for this monomer combination, the nature of the counterion shows a more significant influence. The polymerization with potassium was significantly slower than with cesium as a counterion. Nearly twice the reaction time was required with potassium to achieve full conversion (Figure S2). Reaction of the more reactive monomer glycidol was even more favored for the slower polymerization with the potassium counterion (Figure 5). This leads to reactivity ratios of $r_{BO,K}$ = 0.11 (± 0.01) and $r_{G,K}$ = 7.94 (± 0.67) for the potassium system, indicating an even more pronounced tapered microstructure. Chain transfer may occur before a total monomer conversion of 75% is reached.

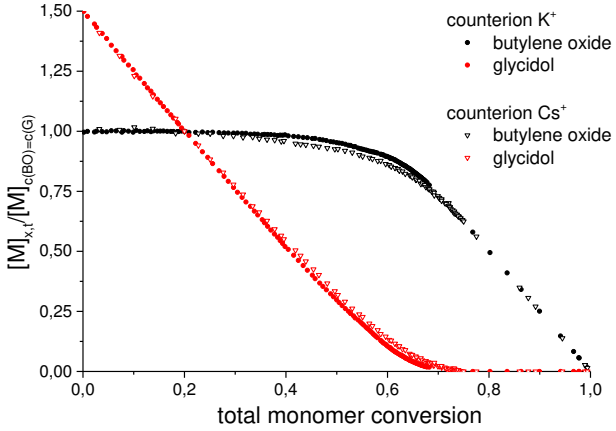

Figure 5. Comparison of the monomer conversion of butylene oxide (black) and glycidol (red) in dependence of the total monomer conversion and for different counterions.

Table 1. Reactivity ratios for the anionic copolymerization of glycidol with EO, PO and BO, respectively, with cesium or potassium as a counterion.

	glycidol + EO		**glycidol + PO**		**glycidol + BO**	
	r_G	**r_{EO}**	**r_G**	**r_{PO}**	**r_G**	**r_{BO}**
cesium	2.34 (±0.13)	0.42 (±0.02)	4.70 (±0.44)	0.17 (±0.02)	6.08 (±0.23)	0.19 (±0.02)
potassium	2.64 (±0.14)	0.44 (±0.02)	4.86 (±0.44)	0.16 (±0.01)	7.94 (±0.67)	0.11 (±0.01)

Comparison of the hyperbranched poly(alkylene oxide) copolymers. It is long known that in an anionic ring-opening polymerization substituted epoxides polymerize at considerably slower rates than ethylene oxide, both due to statistical reasons and higher electron density at the epoxide ring.[41–44] Under conventional AROP conditions, the nucleophilic attack on substituted alkylene oxides only takes place at the methylene group of the ring and not at the substituted carbon. The methine group does not react with alkoxide nucleophiles in general.[45–47] Thus, there is only one reactive site, whereas ethylene oxide contains two reactive methylene groups. Furthermore, the electron-releasing inductive effect of the alkyl side chain lowers the overall reactivity of the ring towards nucleophiles.

The decrease in reactivity with increasing alkyl chain length is reflected by the comparison of the three copolymerizations (Table 1). PO and BO are incorporated very late when a large fraction of glycidol is already consumed. In contrast, the system EO/glycidol shows a simultaneous decrease of the monomer signals. It is a surprising result that glycidol is still the more reactive component in this system. Glycidol exhibits similarly high reaction rates in all kinetic experiments. The differences in the gradients can be seen in Figure 6A. The monomer conversion of ethylene oxide, propylene oxide and butylene oxide was significantly slower than glycidol consumption, and the time required for full conversion increased with increasing alkyl chain length (Figure 6B).

The NMR kinetic data show similar results for potassium and cesium counterions. The only significant variation is the required time for complete monomer consumption with potassium.

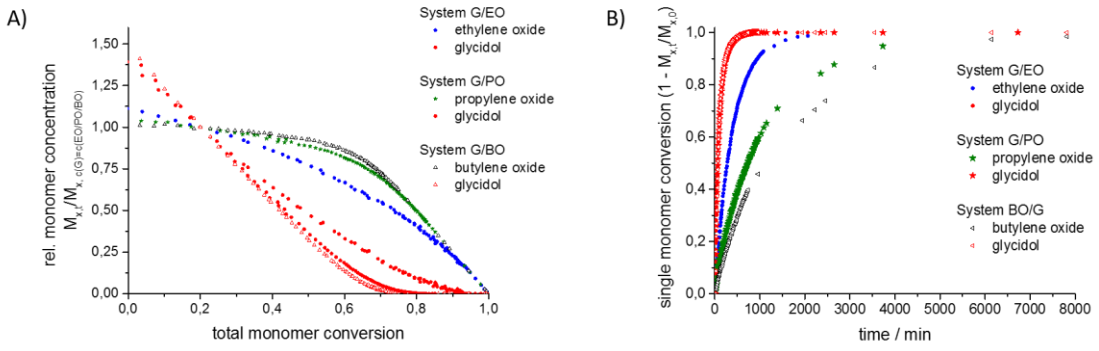

Figure 6. A) Plot of the normalized single monomer conversion versus the total monomer conversion of the systems ethylene oxide/glycidol (sphere), propylene oxide/glycidol (star) and butylene oxide/glycidol (triangle) with cesium counterion; B) Plot of the single monomer conversion versus the time.

We conclude that the statistical copolymerization of these three polyether systems leads to different copolymer topologies (Figure 7). Hyperbranched poly(ethylene oxide)-*co*-polyglycerol can be polymerized in a batch polymerization, however branches will be formed mainly in the

initial stages of the polymerization. Poly(propylene oxide)-*co*-polyglycerol exhibits a more pronounced gradient structure. Poly(butylene oxide)-*co*-polyglycerol possesses a hyperstar-like structure because the monomers react almost sequentially.

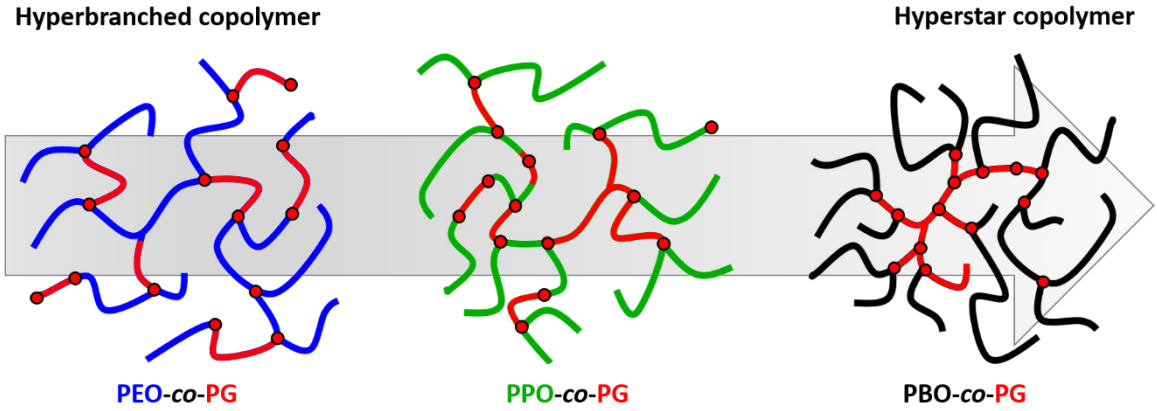

Figure 7. Visualization of the topologies of the different copolymers, based on the reactivity ratios determined.

Since all reactivity ratios have been determined, it is technically possible to generate all poly(alkylene oxide)-*co*-polyglycerol copolymers with branching points distributed homogeneously over the polymer structure. To this end, a reactor has to be charged with the less reactive epoxide monomer first and then glycidol would have to be added slowly at a specific rate determined by the reactivity ratios and concentration of monomers present. However, calculations have shown that for comonomers with greatly differing reactivity, such as BO and G, the more reactive monomer would have to be added at extremely low rates, leading to impracticably long reaction times.[30]

Consequences of the reaction kinetics for the copolymer structure. Contrary to (linear) living anionic copolymerizations that do not show transfer or termination steps, in which case the monomer consumption can be directly translated into a compositional profile of the resulting chains,[24–29] deriving structural information for a branched copolymer from the copolymerization kinetics is more complex.

The anionic (co)polymerization of glycidol does not proceed in a living fashion. Glycidol acts as an "inimer" because it contains both a polymerizable epoxide ring and an alcohol group. Thus, (co)polymerization of glycidol in batch involves chain transfer to this inimer and autoinitiation.[48] As a consequence, copolymers obtained from glycidol and a distinctly less reactive comonomer exhibit an inhomogeneous composition. The glycidol fraction in the monomer feed decreases during the copolymerization (Figure 8). The more disparate the reactivity ratios of the comonomers, the steeper the slope of the drift in the molar ratio of the monomer feed. Due to

the drift, chain transfer reactions at different total conversions lead to initiation of copolymers with varying initial comonomer ratio.

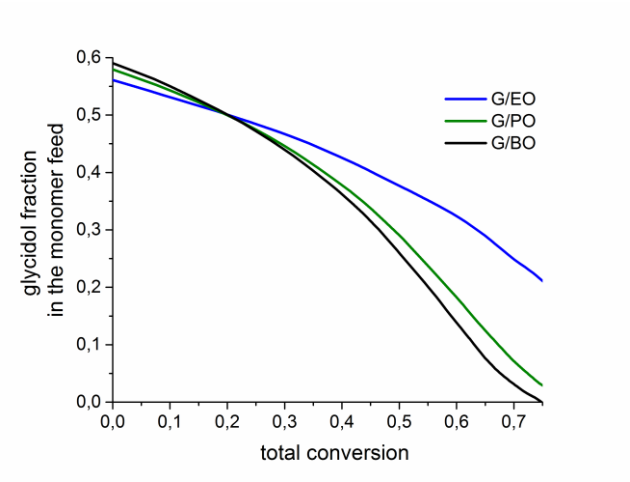

Figure 8. Decreasing glycidol fraction in the monomer feed with increasing total monomer conversion for the different potassium alkoxide-initiated copolymerizations.

In order to visualize this effect, a *hb*(PBO-*co*-PG) copolymer with overall glycidol content of 60% was separated by hydrodynamic volume into five fractions using preparative size-exclusion chromatography. Figure 9 shows the respective glycidol content of each fraction, determined by ^{1}H NMR, revealing a compositional drift from 55% to 62% glycidol with increasing molecular weight. This can be explained by the rapid decrease of the glycidol fraction in the monomer feed at the beginning of the copolymerization, while butylene oxide does not react significantly at first, but polymerizes without side reactions after glycidol is consumed completely. Therefore, chain transfer reactions occurring at different glycidol conversions result in different copolymer compositions and degrees of polymerization. On the one hand, a copolymer initiated at the beginning of the reaction contains a higher glycerol content than a copolymer started by a glycidol autoinitiation process later on, when a major fraction of glycidol is already consumed, however most BO is still present in the feed. On the other hand, delayed initiation leads to lowered molecular weight of the resulting polymer because the reaction time is shorter, provided that the deprotonation equilibrium among the hydroxyl groups is independent of the degree of polymerization.

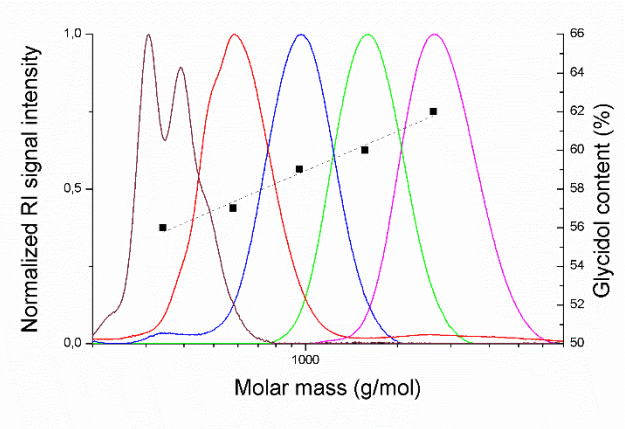

Figure 9. Shifting glycidol content of five fractions from the same *hb*(PBO-*co*-PG) copolymer in dependence of the molecular weight.

Additional information on the copolymers' microstructure can be obtained by relating the reactivity ratios determined from the ^{1}H NMR copolymerization kinetics to the degrees of branching of the resulting copolymers, determined from Inverse Gated (IG) ^{13}C NMR spectra. ^{1}H NMR spectra measured during the polymerization provide information regarding the monomer consumption during the copolymerization, but not on the respective propagation sites. Linear A+B copolymers commonly feature two types of active chain ends because either comomoner A or B can form the terminal unit. For the branched poly(alkylene oxide)-*co*-polyglycerol copolymers, however, there are more possible active chain ends than just terminal alkylene oxide and glycerol units. Due to the complex repeating pattern of branched polyglycerol, the polymerization of glycidol results in four different types of alkoxide moieties: primary alkoxides at terminal and 1,3-linked linear glycerol units as well as secondary alkoxides at terminal and 1,4-linked linear glycerol units. All of these end groups may participate in the polymerization because the deprotonation of the hydroxyl end groups resulting in intra- and intermolecular transfer is an extremely fast reaction.

Inverse Gated ^{13}C NMR spectroscopy allows for distinguishing the different repeating units and quantifying their relative amount in the copolymer. Thus, the degree of branching (DB) can be calculated according to Equation 1.[49]

$$DB_{\mathrm{PAO}-co-\mathrm{PG}} = \frac{2\,G_{\mathrm{Dendritic}}}{2\,G_{\mathrm{Dendritic}} + G_{1,3-\mathrm{Linear}} + G_{1,4-\mathrm{Linear}} + AO_{\mathrm{Linear}}} \quad (1)$$

Figure 10 shows the degrees of branching of poly(alkylene oxide)-polyglyerol copolymer samples, prepared by batch copolymerization, in dependence of the copolymer composition.[36–38] Our kinetic experiments revealed that glycidol is the more reactive monomer in each of these copolymerizations and that the alkylene oxides' reactivity decreases with increasing alkyl chain

length. In addition, the DB provides information about the chain end reactivity, since the DB depends on the ratio of propagation steps occurring at different types of active chain ends. Only propagation steps at the hydroxyl groups of linear glycerol units lead to branching, increasing the DB. Any other possible propagation steps result in linear segments, decreasing the DB. If all chain ends are of equal reactivity, branching occurs randomly according to Equation 2.[49]

$$DB_{\mathrm{AB/AB_2,ran.}} = 2\frac{r+1}{(r+2)^2}\text{, with } r = \frac{x_{\mathrm{AB}}}{x_{\mathrm{AB_2}}} \tag{2}$$

The dashed line in Figure 10 represents the theoretical DB values of a random AB/AB_2-system in dependence of the copolymer composition. It can be clearly seen that the DB values of the poly(ethylene oxide)-*co*-polyglycerol copolymers are close to the random values or slightly lower. This indicates an approximately equal reactivity of ethylene glycol and glycerol chain ends. The copolymerization of glycidol with substituted alkylene oxides leads to increased degrees of branching, corresponding to full reaction of the glycerol units. In contrast to EO units, terminal PO and BO units form secondary alkoxide chain ends after deprotonation, which are less reactive than primary alkoxides. Thus, propagation at primary glycerol alkoxide termini becomes more likely.

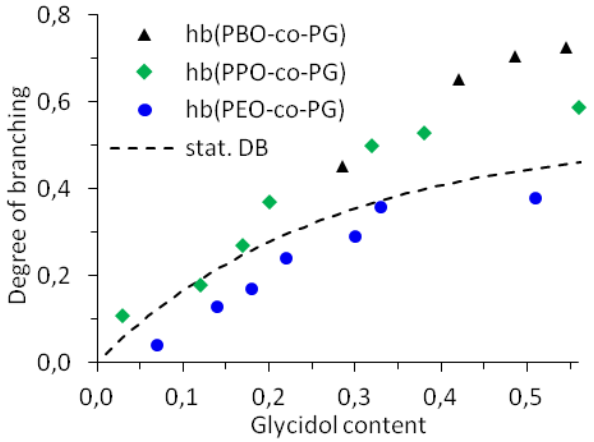

Figure 10. Degrees of branching of *hb*(PEO-*co*-PG) , *hb*(PPO-*co*-PG), *hb*(PBO-*co*-PG) copolymers with varying glycidol content. The dashed line represents the DB of an ideally random AB/AB_2 system with all end groups possessing the same reactivity.

Conclusion

The multibranching anionic copolymerizations of glycidol with EO, PO and BO were carried out in the NMR spectrometer and monitored *in situ* by ^{1}H NMR spectroscopy to elucidate the copolymerization kinetics. Following the single monomer consumption revealed high reactivity of glycidol and lower reactivity of the alkylene oxide comonomers. The reaction rate of the alkylene oxides decreases with increasing alkyl chain length. This trend is reflected in the reactivity ratios determined using the Fineman-Ross formalism (r_G/r_{EO} = 2.34/0.42, r_G/r_{PO} = 4.70/0.17, r_G/r_{BO} = 6.08/0.19). Variation of the counterion from cesium to potassium mainly resulted in the deceleration of the absolute polymerization rate for copolymerization of glycidol with ethylene oxide and propylene oxide, however without a significant effect on the reactivity ratios. The copolymerization of glycidol with butylene oxide is strongly retarded with the smaller counterion, also leading to a greater difference between the reactivity ratios (r_G/r_{BO} = 7.94/0.11). The reactivity ratios were related to the degrees of branching of the copolymers to clarify their topology. While the results imply a hyperbranched gradient structure for *hb*(PEO-*co*-PG) copolymers, *hb*(PPO-*co*-PG) and *hb*(PBO-*co*-PG) copolymers can be visualized as hyperstar-like materials, comprising a strongly branched, glycerol-rich core and mostly linear poly(alkylene oxide) arms. The occurrence of chain transfer reactions could be confirmed by investigating the molecular weight-dependent composition of a fractionated *hb*(PBO-*co*-PG) sample. As expected, lower molecular weight fractions, presumably resulting from delayed initiation by chain transfer, were found to contain lower glycerol content, due to the decrease of the glycidol fraction in the monomer feed during the copolymerization. In summary, the reactivity ratios determined by *in situ* ^{1}H NMR kinetics and the structural information derived from them provide a fundamental understanding on the three-dimensional structure of hyperbranched poly(alkylene oxide)s. These conveniently accessible complex polyether polyols allow polarity design, adjustment of the number of end groups, and further functionalization. Their tunable properties render them promising materials for diverse fields of application ranging from biomedicine to polyurethane cross-linking.

Acknowledgement

D.L acknowledges a fellowship via the Excellence Initiative (DFG/GSC 266) in the context of MAINZ “Materials Science in Mainz”. The authors thank Maria Golowin and Nadine Schenk for technical assistance.

References

(1) Flory, P. J. Molecular Size Distribution in Three Dimensional Polymers. VI. Branched Polymers Containing A—R—B_{f-1} Type Units. *J. Am. Chem. Soc.* **1952**, *74* (11), 2718–2723. DOI: 10.1021/ja01131a008.

(2) Irzhak, T. F.; Deberdeev, T. R.; Irzhak, V. I. Structural kinetics of the formation of hyperbranched polymers via condensation polymerization in the presence of the substitution effect. *Polym. Sci. Ser. B* **2015**, *57* (1), 55–60. DOI: 10.1134/S1560090415010066.

(3) Zhou, Z.; Jia, Z.; Yan, D. Kinetic analysis of AB_2 polycondensation in the presence of multifunctional cores with various reactivities. *Polymer* **2012**, *53* (15), 3386–3391. DOI: 10.1016/j.polymer.2012.05.032.

(4) Zhou, Z.; Jia, Z.; Yan, D. Kinetic analysis of co-polycondensation of AB_2 and AB type monomers in presence of multi-functional cores. *Polymer* **2010**, *51* (12), 2763–2768. DOI: 10.1016/j.polymer.2010.04.004.

(5) Konkolewicz, D.; Gray-Weale, A.; Perrier, S. The structure of randomly branched polymers synthesized by living radical methods. *Polym. Chem.* **2010**, *1* (7), 1067. DOI: 10.1039/C0PY00064G.

(6) Cheng, K.-C.; Su, Y.-Y.; Chuang, T.-H.; Guo, W.; Su, W.-F. Kinetic Model of Hyperbranched Polymers Formed by Self-Condensing Vinyl or Self-Condensing Ring-Opening Polymerization of AB Monomers Activated by Stimuli with Different Reactivities. *Macromolecules* **2010**, *43* (21), 8965–8970. DOI: 10.1021/ma101740r.

(7) Zhao, Z.-F.; Wang, H.-J.; Ba, X.-W. A statistical theory for self-condensing vinyl polymerization. *J. Chem. Phys.* **2009**, *131* (7), 74101. DOI: 10.1063/1.3207267.

(8) Galina, H.; Lechowicz, J. B.; Walczak, M. Model of Hyperbranched Polymerization Involving AB_2 Monomer and B_3 Core Molecules both Reacting with Substitution Effect. *Macromolecules* **2002**, *35* (8), 3261–3265. DOI: 10.1021/ma011722t.

(9) Galina, H.; Lechowicz, J. B.; Walczak, M. Kinetic Modeling of Hyperbranched Polymerization Involving an AB_2 Monomer Reacting with Substitution Effect. *Macromolecules* **2002**, *35* (8), 3253–3260. DOI: 10.1021/ma011603d.

(10) Cheng, K.-C.; Don, T.-M.; Guo, W.; Chuang, T.-H. Kinetic model of hyperbranched polymers formed by the polymerization of AB_2 monomer with a substitution effect. *Polymer* **2002**, *43* (23), 6315–6322. DOI: 10.1016/S0032-3861(02)00545-1.

(11) Cheng, K.-C.; Wang, L. Y. Kinetic Model of Hyperbranched Polymers Formed in Copolymerization of AB_2 Monomers and Multifunctional Core Molecules with Various Reactivities. *Macromolecules* **2002**, *35* (14), 5657–5664. DOI: 10.1021/ma0118062.

(12) Yan, D.; Müller, A. H. E.; Matyjaszewski, K. Molecular Parameters of Hyperbranched Polymers Made by Self-Condensing Vinyl Polymerization. 2. Degree of Branching. *Macromolecules* **1997**, *30* (23), 7024–7033. DOI: 10.1021/ma961919z.

(13) Müller, A. H. E.; Yan, D.; Wulkow, M. Molecular Parameters of Hyperbranched Polymers Made by Self-Condensing Vinyl Polymerization. 1. Molecular Weight Distribution. *Macromolecules* **1997**, *30* (23), 7015–7023. DOI: 10.1021/ma9619187.

(14) Liu, X.; Cool, L. R.; Lin, K.; Kasko, A. M.; Wesdemiotis, C. Tandem mass spectrometry and ion mobility mass spectrometry for the analysis of molecular sequence and architecture of hyperbranched glycopolymers. *Analyst* **2015**, *140* (4), 1182–1191. DOI: 10.1039/C4AN01599A.

(15) Wang, D.; Li, X.; Wang, W.-J.; Gong, X.; Li, B.-G.; Zhu, S. Kinetics and Modeling of Semi-Batch RAFT Copolymerization with Hyperbranching. *Macromolecules* **2012**, *45* (1), 28–38. DOI: 10.1021/ma202215s.

(16) Murakami, T.; Uchida, S.; Ishizu, K. Architecture of hyperbranched polymers consisting of a stearyl methacrylate sequence via a living radical copolymerization. *J. Colloid Interface Sci.* **2008**, *323* (2), 242–246. DOI: 10.1016/j.jcis.2008.04.014.

(17) Simon, P. F. W.; Müller, A. H. E. Kinetic Investigation of Self-Condensing Group Transfer Polymerization. *Macromolecules* **2004**, *37* (20), 7548–7558. DOI: 10.1021/ma0358834.

(18) Ishizu, K.; Shibuya, T.; Kawauchi, S. Kinetics on Formation of Hyperbranched Poly(ethyl methacrylate) via a Controlled Radical Mechanism of Photofunctional Inimer. *Macromolecules* **2003**, *36* (10), 3505–3510. DOI: 10.1021/ma021729q.

(19) Liu, Y.; Fan, Z. Novel hyperbranched polymers synthesized via A_3 + B(B') approach by radical addition-coupling polymerization. *J. Polym. Sci. Part A: Polym. Chem.* **2015**, *53* (7), 904–913. DOI: 10.1002/pola.27518.

(20) Quast, M. J.; Argall, A. D.; Hager, C. J.; Mueller, A. Synthesis and physical properties of highly branched perfluorinated polymers from AB and AB_2 monomers. *J. Polym. Sci. Part A: Polym. Chem.* **2015**, *53* (16), 1880–1894. DOI: 10.1002/pola.27639.

(21) Quast, M. J.; Mueller, A. Hyperbranched Polyfluorinated benzyl ether polymers: Mechanism, kinetics, and optimization. *J. Polym. Sci. Part A: Polym. Chem.* **2014**, *52* (7), 985–994. DOI: 10.1002/pola.27078.

(22) Reisch, A.; Komber, H.; Voit, B. Kinetic Analysis of Two Hyperbranched A_2 + B_3 Polycondensation Reactions by NMR Spectroscopy. *Macromolecules* **2007**, *40* (19), 6846–6858. DOI: 10.1021/ma070812g.

(23) Schmaljohann, D.; Komber, H.; Barratt, J. G.; Appelhans, D.; Voit, B. I. Kinetics of Nonideal Hyperbranched Polymerizations. 2. Kinetic Analysis of the Polycondensation of 3,5-Bis(trimethylsiloxy)benzoyl chloride Using NMR Spectroscopy †. *Macromolecules* **2003**, *36* (1), 97–108. DOI: 10.1021/ma020972m.

(24) Niederer, K.; Schüll, C.; Leibig, D.; Johann, T.; Frey, H. Catechol Acetonide Glycidyl Ether (CAGE): A Functional Epoxide Monomer for Linear and Hyperbranched Multi-Catechol Functional Polyether Architectures. *Macromolecules* **2016**, *49* (5), 1655–1665. DOI: 10.1021/acs.macromol.5b02441.

(25) Herzberger, J.; Kurzbach, D.; Werre, M.; Fischer, K.; Hinderberger, D.; Frey, H. Stimuli-Responsive Tertiary Amine Functional PEGs Based on *N*,*N* -Dialkylglycidylamines. *Macromolecules* **2014**, *47* (22), 7679–7690. DOI: 10.1021/ma501367b.

(26) Obermeier, B.; Frey, H. Poly(ethylene glycol-*co*-allyl glycidyl ether)s: a PEG-based modular synthetic platform for multiple bioconjugation. *Bioconjug. Chem.* **2011**, *22* (3), 436–444. DOI: 10.1021/bc1004747.

(27) Mangold, C.; Wurm, F.; Obermeier, B.; Frey, H. "Functional Poly(ethylene glycol)": PEG-Based Random Copolymers with 1,2-Diol Side Chains and Terminal Amino Functionality. *Macromolecules* **2010**, *43* (20), 8511–8518. DOI: 10.1021/ma1015352.

(28) Obermeier, B.; Wurm, F.; Frey, H. Amino Functional Poly(ethylene glycol) Copolymers via Protected Amino Glycidol. *Macromolecules* **2010**, *43* (5), 2244–2251. DOI: 10.1021/ma902245d.

(29) Schömer, M.; Frey, H. Water-Soluble "Poly(propylene oxide)" by Random Copolymerization of Propylene Oxide with a Protected Glycidol Monomer. *Macromolecules* **2012**, *45* (7), 3039–3046. DOI: 10.1021/ma300249c.

(30) Zhang, W.; Allgaier, J.; Zorn, R.; Willbold, S. Determination of the Compositional Profile for Tapered Copolymers of Ethylene Oxide and 1,2-Butylene Oxide by In-situ-NMR. *Macromolecules* **2013**, *46* (10), 3931–3938. DOI: 10.1021/ma400166n.

(31) Sandler, S. R.; Berg, F. R. Room temperature polymerization of glycidol. *J. Polym. Sci. A-1 Polym. Chem.* **1966**, *4* (5), 1253–1259. DOI: 10.1002/pol.1966.150040523.

(32) Son, S.; Shin, E.; Kim, B.-S. Redox-Degradable Biocompatible Hyperbranched Polyglycerols: Synthesis, Copolymerization Kinetics, Degradation, and Biocompatibility. *Macromolecules* **2015**, *48* (3), 600–609. DOI: 10.1021/ma502242v.

(33) Alkan, A.; Natalello, A.; Wagner, M.; Frey, H.; Wurm, F. R. Ferrocene-Containing Multifunctional Polyethers: Monomer Sequence Monitoring via Quantitative 13 C NMR Spectroscopy in Bulk. *Macromolecules* **2014**, *47* (7), 2242–2249. DOI: 10.1021/ma500323m.

(34) Wilms, D.; Stiriba, S.-E.; Frey, H. Hyperbranched polyglycerols: from the controlled synthesis of biocompatible polyether polyols to multipurpose applications. *Acc. Chem. Res.* **2010**, *43* (1), 129–141. DOI: 10.1021/ar900158p.

(35) Sunder, A.; Hanselmann, R.; Frey, H.; Mülhaupt, R. Controlled Synthesis of Hyperbranched Polyglycerols by Ring-Opening Multibranching Polymerization. *Macromolecules* **1999**, *32* (13), 4240–4246. DOI: 10.1021/ma990090w.

(36) Seiwert, J.; Leibig, D.; Kemmer-Jonas, U.; Bauer, M.; Perevyazko, I.; Preis, J.; Frey, H. Hyperbranched Polyols via Copolymerization of 1,2-Butylene Oxide and Glycidol: Comparison of Batch Synthesis and Slow Monomer Addition. *Macromolecules* **2016**, *49* (1), 38–47. DOI: 10.1021/acs.macromol.5b02402.

(37) Schömer, M.; Seiwert, J.; Frey, H. Hyperbranched Poly(propylene oxide): A Multifunctional Backbone-Thermoresponsive Polyether Polyol Copolymer. *ACS Macro Lett.* **2012**, *1* (7), 888–891. DOI: 10.1021/mz300256y.

(38) Perevyazko, I.; Seiwert, J.; Schömer, M.; Frey, H.; Schubert, U. S.; Pavlov, G. M. Hyperbranched Poly(ethylene glycol) Copolymers: Absolute Values of the Molar Mass, Properties in Dilute Solution, and Hydrodynamic Homology. *Macromolecules* **2015**, *48* (16), 5887–5898. DOI: 10.1021/acs.macromol.5b01020.

(39) Wilms, D.; Schömer, M.; Wurm, F.; Hermanns, M. I.; Kirkpatrick, C. J.; Frey, H. Hyperbranched PEG by random copolymerization of ethylene oxide and glycidol. *Macromol. Rapid Commun.* **2010**, *31* (20), 1811–1815. DOI: 10.1002/marc.201000329.

(40) Fineman, M.; Ross, S. D. Linear method for determining monomer reactivity ratios in copolymerization. *J. Polym. Sci.* **1950**, *5* (2), 259–262. DOI: 10.1002/pol.1950.120050210.

(41) Stolarzewicz, A.; Neugebauer, D. Influence of substituent on the polymerization of oxiranes by potassium hydride. *Macromol. Chem. Phys.* **1999**, *200* (11), 2467–2470. DOI: 10.1002/(SICI)1521-3935(19991101)200:11<2467:AID-MACP2467>3.3.CO;2-V.

(42) Heatley, F.; Yu, G.-e.; Booth, C.; Blease, T. G. Determination of reactivity ratios for the anionic copolymerization of ethylene oxide and propylene oxide in bulk. *European Polymer Journal* **1991**, *27* (7), 573–579. DOI: 10.1016/0014-3057(91)90138-E.

(43) Ponomarenko, V. A.; Khomutov, A. M.; Ilchenko, S. L.; Ignatenk, A. V. Influence of Substituted Groups on Reactivity of Monosubstituted Ethylene Oxide During Coordination-Anionic Copolymerization. *Vysokomol. Soedin. A* **1971**, *13*, 1556–1561.

(44) Ponomarenko, V. A.; Khomutov, A. M.; Ilchenko, S. L.; Ignatenk, A. V. Influence of Substituted Groups on Anionic Polymerization of Alpha-Oxides. *Vysokomol. Soedin. A* **1971**, *13*, 1546–1556.

(45) Chisholm, M. H.; Navarro-Llobet, D. NMR Assignments of Regioregular Poly(propylene oxide) at the Triad and Tetrad Level. *Macromolecules* **2002**, *35* (6), 2389–2392. DOI: 10.1021/ma0119934.

(46) Schilling, F. C.; Tonelli, A. E. Carbon-13 NMR determination of poly(propylene oxide) microstructure. *Macromolecules* **1986**, *19* (5), 1337–1343. DOI: 10.1021/ma00159a010.

(47) Oguni, N.; Lee, K.; Tani, H. Microstructure Analysis of Poly(propylene oxide) by ^{13}C Nuclear Magnetic Resonance Spectroscopy. *Macromolecules* **1972**, *5* (6), 819–820. DOI: 10.1021/ma60030a032.

(48) Walach, W.; Trzebicka, B.; Justynska, J.; Dworak, A. High molecular arborescent polyoxyethylene with hydroxyl containing shell. *Polymer* **2004**, *45* (6), 1755–1762. DOI: 10.1016/j.polymer.2004.01.033.

(49) Frey, H.; Hölter, D. Degree of branching in hyperbranched polymers. 3 Copolymerization of AB_m-monomers with AB and AB_n-monomers. *Acta Polym.* **1999**, *50* (2-3), 67–76. DOI: 10.1002/(SICI)1521-4044(19990201)50:2/3<67:AID-APOL67>3.0.CO;2-W.

Supporting Information

Calculation of the copolymerization parameters

Copolymerization:

$$P_1^- + M_1 \xrightarrow{k_{11}} P_1M_1^-$$

$$P_1^- + M_2 \xrightarrow{k_{12}} P_1M_2^-$$

$$P_2^- + M_1 \xrightarrow{k_{21}} P_2M_1^-$$

$$P_2^- + M_2 \xrightarrow{k_{22}} P_2M_2^-$$

P_1^-; P_2^-: active chain end

M_1; M_2: monomer

k: reactivity constant

Fineman-Ross equation: $x \cdot \frac{1-X}{X} = -\frac{x^2}{X} r_1 + r_2$ with $r_1 = \frac{k_{11}}{k_{12}}$ and $r_2 = \frac{k_{22}}{k_{21}}$

x: mole fraction of the stock

X: mole fraction of the polymer at certain mole fractions of the stock

r_1: reactivity ratio for monomer M_1

r_2: reactivity ratio for monomer M_2

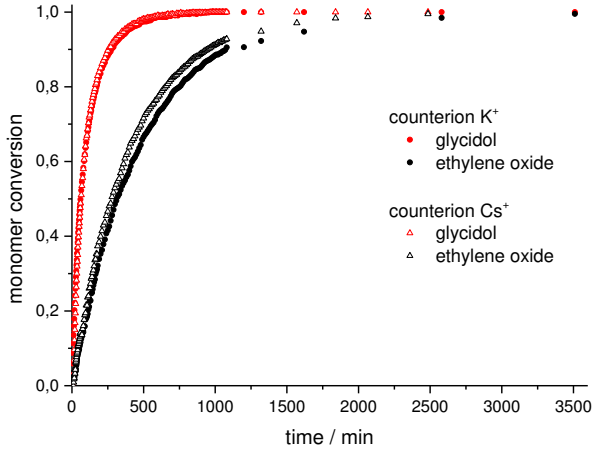

Figure S1. Plot of the single monomer conversion of glycidol (red) and ethylene oxide (black) versus the time.

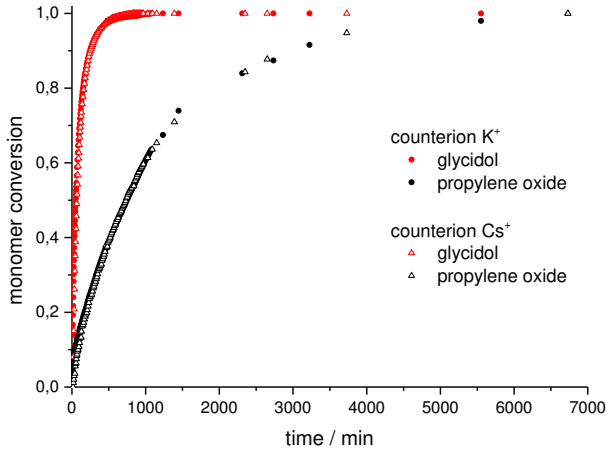

Figure S2. Plot of the single monomer conversion of glycidol (red) and propylene oxide (black) versus the time.

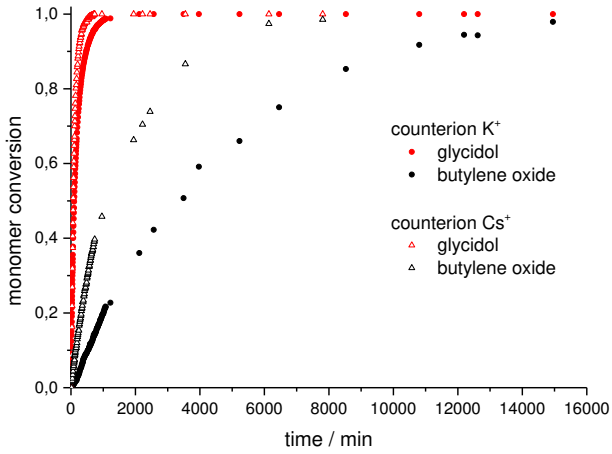

Figure S3. Plot of the single monomer conversion of glycidol (red) and butylene oxide (black) versus the time.

2.2 Hyperbranched Poly(ethylene glycol) Copolymers: Absolute Values of the Molar Mass, Properties in Dilute Solution and Hydrodynamic Homology

Igor Perevyazko[1,2,5], Jan Seiwert[3], Martina Schömer[3], Holger Frey[3,], Ulrich S. Schubert[1,2,*], Georges M. Pavlov[1,4,5,*]*

[1] Laboratory of Organic and Macromolecular Chemistry (IOMC), Friedrich Schiller University Jena, Humboldtstr. 10, 07743 Jena, Germany

[2] Jena Center for Soft Matter (JCSM), Friedrich Schiller University Jena, Philosophenweg 7, 07743 Jena, Germany

[3] Institute of Organic Chemistry, Johannes Gutenberg-University, Duesbergweg 10-14, 55128 Mainz, Germany

[4] Institute of Macromolecular Compounds, Russian Academy of Science, 199004 St. Petersburg, Russia

[5] Department of Molecular Biophysics and Polymer Physics, St. Petersburg State University, Ulyanovskaya ul. 1, 198504 St. Petersburg, Russia

Published in *Macromolecules* **2015**, *48*, 5887−5898.

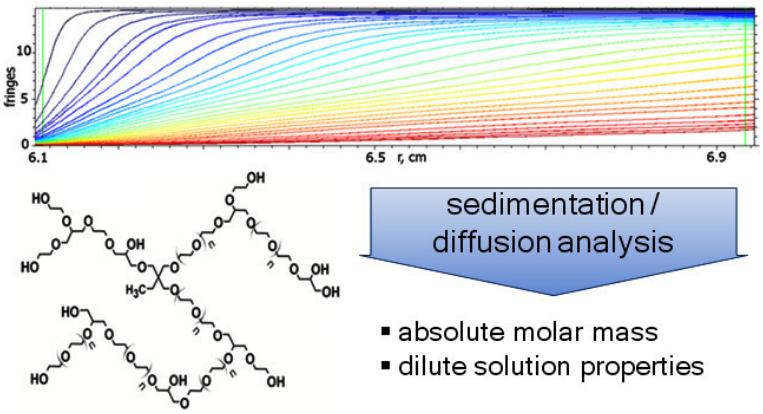

Abstract

Hyperbranched poly(ethylene glycol) copolymers were synthesized by random anionic ring-opening multibranching copolymerization of ethylene oxide with glycidol as a branching agent, leading to a poly(ethylene glycol) structure with glycerol branching points. Extending the available range of molar masses by novel synthesis strategies, a limited extent of control over the degree of polymerization was achieved by variation of the solvent in this copolymerization. Generally, absolute molar mass characterization of hyperbranched polymers still represents an unresolved challenge. A series of the hyperbranched poly(ethylene glycol)–*co*–(glycerol) copolymers (*hb*PEGs) of a wide range of molar masses ($1{,}400 < M < 1{,}700{,}000$ g mol^{-1}), degree of branching (DB) = 0.04-0.54 and moderate polydispersity ($M_w/M_n \approx (2.1 \pm 0.2)$) was studied, both in water and dimethylformamid by the methods of molecular hydrodynamics. Analytical ultracentrifugation, intrinsic viscosity, translational diffusion measurements and SEC were combined. Molar masses of *hb*PEGs were estimated from the comparison of the velocity sedimentation and translational diffusion coefficients, i.e. using Svedberg relationship. It was demonstrated that the use of linear PEG for the SEC calibration results in the significantly underestimated values of the molar masses of *hb*PEGs. The largest *hb*PEG samples exhibited a hydrodynamic radius of ≈ 14 nm in aqueous solution. The obtained Kuhn-Mark-Houwink-Sakurada scaling relations show linear trends in the entire range of molar masses. Detected scaling indexes virtually correspond to the homologous series characterized by a direct proportionality between the molar mass and volume of the macromolecules that make up this series. The effect of branching on the molecular dimensions and on the hydrodynamic characteristics is discussed, and the corresponding contraction factors have been estimated.

Introduction

Branched macromolecules with tree-like branching pattern play an important role in nature, where they perform a variety of essential functions, e.g., for energy storage and water retention. This class of polymers includes glycogen, amylopectin, dextran, glyco-protein complexes and others. Their synthetic analogues were first studied in a systematic manner in the seminal works of Paul Flory.[1] The first actual syntheses of perfectly branched macromolecules, eventually called “dendrimers”, were developed in the late 1970s and 1980s, capitalizing on both divergent and convergent construction approaches.[2-4] Dendrimers have attracted wide attention due to their unique branch-on-branch topology, compact structure and large number of end groups available for further modification. However, in recent years, motivated by the demanding multi-step

synthesis of dendrimers, the attention of researchers has turned to "one-pot" strategies, resulting in hyperbranched macromolecules that exhibit unique characteristics that are a consequence of their particular topology and high branching density.[5-12] However, hyperbranched polymers based on multifunctional AB_2 polycondensation show large heterogeneity both with respect to molar masses and branching.[8,13-15] An important strategy to overcome these drawbacks relies on the slow addition of reactive AB_2-monomers onto a core, permitting to reduce the dispersity and enabling a certain extent of control over molar mass.[16,17]

Despite the enormous advances in this area, absolute molar mass characterization for hyperbranched polymers is still an unresolved issue. Although several efforts have been reported in this direction and theoretical considerations have been published, in addition no suitable theory exists to describe the solution behavior of the different branched polymers.[18-25] In particular, it is still unclear whether hyperbranched polymers will follow the well-known scaling relationships between hydrodynamic characteristics ($P_i = K_{ij} P_j^b$, where P_i is one of the hydrodynamic characteristics $[\eta]$, D_0, s_0, k_s, f/f_{sph} and P_j is another hydrodynamic characteristic from this row or molar mass), and, as a consequence, whether they can be considered as fractal or self-similar structures. Furthermore, the conformation of these macromolecules in solution is still an open issue.

In this contribution, on the one hand we demonstrate that by variation of the solvent used for the synthesis a broad range of molar masses of the hyperbranched poly(ethylene glycol) copolymers becomes available. On the other hand we report the results of a study of a series of such non-fractionated hyperbranched poly(ethylene glycol)–*co*–poly(glycerol) copolymers ("hyperbranched PEG", *hb*PEG) copolymers with glycerol units as branching points, encompassing a wide range of molar masses. The materials were synthesized by the random anionic ring-opening copolymerization of ethylene oxide with glycidol as a branching agent, as introduced in a recent communication (Scheme 1).[26] Linear PEG is the gold-standard biomedical polymer because of its outstanding biocompatibility and solubility both in water as well as polar organic solvents.[27-29] Hyperbranched PEG copolymers combine these remarkable properties with a dendritic structure, which impedes or even prevents crystallization and provides multiple functional groups for further functionalization.[17, 30-33] Contrary to other strategies for the synthesis of branched PEG analogues,[34-44] *hb*PEG is obtained in a convenient one-step batch polymerization with full conversion, resulting in a purely aliphatic polyether structure (Scheme 1). The resulting *hb*PEGs exhibit high molar masses and moderate apparent dispersities in the range of 1.1 to 1.7, as determined by size-exclusion chromatography (SEC).[24] However, reliable results concerning absolute molar masses cannot be obtained by this relative method. We have therefore chosen to

investigate the copolymers by the methods of molecular hydrodynamics, in particular by analytical ultracentrifugation, intrinsic viscosity measurements, translation diffusion as well as by SEC measurements for comparison. We focus on the properties of dilute solutions of the hyperbranched PEG copolymers, aiming at the effect of branching on the molecular characteristics and the conformation of the macromolecules.

To the best of our knowledge, ultracentrifugation has hardly been employed for the study of hyperbranched polymers to date.[45] Here we introduce new synthetic strategies permitting to obtain *hb*PEG with different molar masses. In the ensuing sections we discuss the basic hydrodynamic data: (i) molar mass, (ii) scaling relationships, (iii) branching factors, and (iv) global conformation of the hyperbranched polyethers.

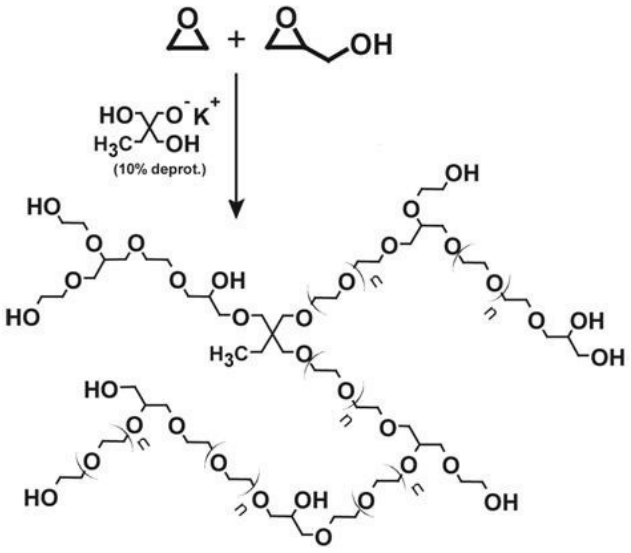

Scheme 1. Synthesis of hbPEG by random anionic ring-opening copolymerization of ethylene oxide and glycidol; the ratio of epoxide comonomers determines the degree of branching.

Experimental Part

Analytical Ultracentrifugation (AUC) and Translation Diffusion

Sedimentation velocity experiments were performed with a ProteomeLab XLI Protein Characterization System analytical ultracentrifuge (Beckman Coulter, Brea, CA), using conventional double-sector Epon or aluminum centerpieces of 12 mm optical path length and a four-hole rotor (AN-60Ti). Rotor speed was 40,000 to 60,000 rpm, depending on the sample. Cells were filled with 420 µL of sample solution and 440 µL of solvent (water or dimethylformamid (DMF)). Three concentrations of each sample in H_2O and in DMF were studied, covering a wide

concentration range ($3 \leq c_{max}/c_{min} \leq 7$). The parameter *c[□]* characterizing the degree of dilution was in the range $0.002 \leq c[\eta] \leq 0.038$, corresponding to a very high dilution state. This, in turn, allows for reliable extrapolation to concentration zero (*c:* polymer concentration in g cm^{-3}; [*η*]*:* intrinsic viscosity, measured in cm^3 g^{-1}). Before the run, the rotor was equilibrated for approximately 1 h at 20 °C in the centrifuge. Sedimentation profiles were obtained at the same temperature, using interference optics. For the analysis of the sedimentation velocity data, *ls-g*(s)* as well as *c(s)* with a Tikhonov–Phillips regularization procedure implemented into the Sedfit program were applied.[46] The *ls-g*(s)* model represents a least-square boundary analysis which describes sedimentation of non-diffusing species. The *c(s)* analysis is based on the numerical resolution of the Lamm equation assuming the same frictional ratio (f/f_{sph}) values for each sedimenting species. The velocity sedimentation coefficients (*s*) were extrapolated to zero concentration by linear approximation, following the relationship: $s^{-1} = s_0^{-1}(1+k_s c)$, where s_0 is the extrapolated value of the velocity sedimentation coefficient and k_s is the concentration sedimentation coefficient (Gralen coefficient).

The translation diffusion coefficients D_0 were estimated in water by the classical method of forming, in the analytical ultracentrifuge at low speed rotation (n = 3,000 rpm), a solution-solvent boundary using synthetic boundary cells.[47] The diffusion interferograms were processed by the maximal ordinate and area method.[48] The diffusion coefficient D_0 was calculated from the slope of the experimental dependence of the dispersion σ^2 (cm^2) of the diffusion boundary on time (Figure 1).

$$D = \left(\frac{\Delta\sigma^2}{2\Delta t}\right) \quad (1)$$

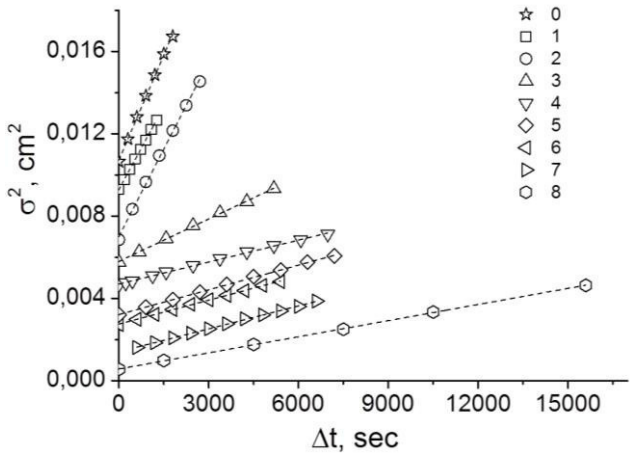

Figure 1. Dependence of the diffusion dispersion σ on the time t for the hyperbranched PEG copolymers in water. For other properties of the samples No. 0-8, see Table 1-3.

Viscosity Measurements

Viscosity measurements were conducted using an AMVn viscometer (Anton Paar, Graz, Austria), with a capillary/ball combination of the measuring system. The respective flow times for the solvent and polymer solutions, η_0 and t, were measured at 20 °C, with relative viscosities $\eta_r = t/t_0$ in the range of 1.2 to 2.5, which corresponds to dilute solutions. The extrapolation to zero concentration was achieved by using both the Huggins ($\frac{\eta_r - 1}{c} = [\eta] + k_H[\eta]^2 c + \cdots$, where k_H is the Huggins parameter, c – is the concentration) and the Kraemer equations ($\frac{\ln \eta_r}{c} = [\eta] + k_K[\eta]^2 c + \cdots$, where k_K is the Kramer parameter), and the average values were considered as the value of the intrinsic viscosity ($[\eta]$, $cm^3\ g^{-1}$).

Partial Specific Volume Determination

The density measurements were carried out in the density meter DMA 02 (Anton Paar, Graz, Austria) according to the procedure of Kratky *et al.*.[49]

NMR Spectroscopy

^1H NMR and ^{13}C NMR spectra were recorded at 400 MHz and 100 MHz, respectively, on a Bruker AMX400 apparatus and were referenced internally to residual signals of the deuterated solvent.

Size-exclusion Chromatography (SEC)

For SEC measurements in DMF (containing 0.25 g L^{-1} of lithium bromide as an additive), an Agilent 1100 series was used as an integrated instrument including a PSS HEMA column ($10^6/10^4/10^2$ Å porosity) and UV and RI detector. As the first step calibration was carried out with linear poly(ethylene glycol) standards provided by Polymer Standards Service (PSS). Due to the completely different hydrodynamic behavior of linear PEG standards compared to highly branched PEG copolymers, in this case, SEC is considered only as a qualitative method to obtain basic information regarding the differences between the synthesized samples according to their elution volume. For the quantitative estimates the columns were calibrated with the molar masses obtained from the sedimentation-diffusion analysis of the samples.

Materials

All reagents and solvents were used as received, if not otherwise mentioned. Ethylene oxide (EO) and glycidol were dried over calcium hydride (CaH_2) and distilled in vacuum directly prior to use. Tetrahydrofuran (THF) was purified by vacuum distillation over sodium/benzophenone.

Synthesis of the *hb*PEG Polymers

A two-necked glass flask equipped with a septum, teflon seal and a magnetic stirrer was connected to a vacuum line. 44 mg (0.33 mmol, 1.0 eq.) 1,1,1-tris(hydroxymethyl)propane (TMP) was mixed with 0.10 mL (0.10 mmol, 0.3 eq.) potassium *tert*-butoxide (1 M solution in THF) to deprotonate 10 % of the hydroxyl groups. 5 mL benzene was added to the resulting slurry, stirred for 30 min, and the flask was evacuated for at least 4 h to remove traces of water azeotropically as well as other volatiles. In contrast to previous syntheses,[24] different solvents were employed to increase or lower the molar mass of the resulting polymers. For the synthesis of *hb*PEG oligomers and low molar mass polymers, the deprotonated initiator was dissolved in 5 mL dry dimethyl sulfoxide (DMSO). High molar mass copolymers were obtained by using 20 mL dioxane or THF as an emulsifying solvent. In both cases a total amount of 100 mmol (300 eq) monomer was transferred to the reaction vessel, systematically varying the comonomer ratio to obtain a series of hyperbranched copolymers with different degree of branching (DB). Ethylene oxide (40 to 95 mmol) was transferred to an ampoule, dried over calcium hydride and subsequently transferred to the reaction flask in vacuum. The flask was sealed with a septum and glycidol (60 to 5 mmol) was introduced through the septum via cannula. The reaction mixture was then immediately heated to 80 °C and stirred for 18 h. After completion of the reaction, methanol was added and the solution was neutralized by filtration over an acidic cation exchange resin (DOWEX WX8). The resulting *hb*PEG polymers were precipitated in cold diethyl ether. In the case of the high molar mass polymers the products were dialyzed against methanol (MWCO 3,000 g mol^{-1}). All products were dried in vacuum overnight at 85 °C (yield 80 to 90%).

Caution: In very few cases the pressure evolving in the early stages of the reaction in the flask led to the spontaneous removal of the septum and release of ethylene oxide. Thus, the reaction has to be carried out in an appropriate fume hood, and the respective safety precautions should be taken. In general, the amount of EO used did not exceed 10 g per batch in a 250 mL flask to guarantee a safe reaction.

^{1}H NMR (DMSO-d_6, 400 MHz): δ (ppm) = 4.81 – 4.35 (m, br, OH); 4,10 – 3.06 (m, O-CH, O-CH_2); 1.36 – 1.18 (m, 2H, CH_3-CH_2 (TMP)); 0.89 – 0.68 (m, 3H, CH_3 (TMP)).

^{13}C NMR (DMSO-d_6, 100 MHz): δ (ppm) = 80.25 – 79.45 (m, $Linear_{G13}$ CH); 78.52 – 77.42 (m, $Dendritic_G$ CH); 73.22 – 72.10 (m,, 2 $Linear_{G14}$ CH_2); 72.04 – 69.62 (m, 2 $Dendritic_G$ CH_2, 2 $Linear_E$ CH_2, $Terminal_E$CH_2-CH_2-OH, $Terminal_G$ CH, $Terminal_G$ CH_2); 69.61 – 68.37 (m, $Linear_{G13}$ CH_2, $Linear_{G14}$ CH-OH); 63.39 – 62.96 ($Terminal_G$ CH_2-OH); 60.87 – 60.07 (m, $Terminal_E$ CH_2-OH, $Linear_{G13}$ CH_2-OH).

Results and Discussion

Synthesis and NMR/SEC Characterization

In the first communication on the polymerization of *hb*PEG, copolymers with apparent molar masses in the range of 23,000 to 50,000 g mol^{-1} were described, as determined by SEC calibrated with linear PEG standards, focusing on the control over the glycidol content and the degree of branching.[26] A detailed study of solvent effects in the current work made it possible to expand the synthetic strategy towards both higher and lower molar masses, as shown below. The degree of polymerization was found to be largely independent of the monomer ratio EO/glycidol. Unfortunately, the slow monomer addition strategy that was established for glycidol homopolymerization[29] was not applicable in this case, due to the low boiling point of EO. One-pot synthesis leads to an increased extent of autoinitiation processes, i.e., glycidolate formed by proton transfer during polymerization. This originates from the fast proton transfer from excess glycidol to a TMP anion. Hence, after separating low molecular byproducts from the polymer during workup, NMR studies revealed significant amounts of unreacted initiator.

Since the previously reported procedure for the synthesis of *hb*PEG always afforded (apparent) molar masses of 23,000 to 50,000 g mol^{-1} (SEC using PEG standards), both THF and dioxane have been explored as emulsifying agents for the copolymerization. *Hb*PEG samples with apparent molar masses up to 65,000 g mol^{-1}(SEC) and mostly narrow, monomodal molar mass distribution were obtained (Table 1). This is in analogy to the approach introduced by Brooks et al. who obtained narrowly distributed, high molar mass hyperbranched polyglycerol (*hb*PG) with apparent M_n (SEC) up to 700,000 g mol^{-1} using dioxane as a cosolvent.[50] The authors explained the unexpectedly high degree of polymerization with an accelerated proton transfer caused by the apolar medium and incomplete conversion of the initiator. Accordingly, for *hb*PEG as well as *hb*PG a small amount of a low molar mass fraction was obtained that could be removed from the

polymer by dialysis. In either case, neither the initiator nor the growing polymer is completely soluble in these solvents; i. e. the reaction can be viewed as an emulsion-like process. Surprisingly, although *hb*PEG 3 was prepared in the same manner, it exhibited a significantly lower molar mass of only 14,400 g mol^{-1} (SEC) and the broadest molecular weight distribution of all samples. Nevertheless, its solution properties were studied, despite the high dispersity of this sample, as no other polymers in the molar mass range between 3,000 to 20,000 g mol^{-1} (SEC) were obtained under the conditions explored.

In contrast, copolymerization of ethylene oxide and glycidol in DMSO was generally found to lead to the formation of oligomers and low molar mass polymers in the range of 500 to 3,000 g mol^{-1} (M_n, apparent molar mass, SEC; samples 0-2 in Table 1) with moderate polydispersities between 1.3 and 1.4 after purification by precipitation in diethyl ether. Due to the polar solvent, the initiator is dissolved completely, and presumably chain transfer from polymer to monomer occurs with higher frequency, since the anion solvation is better than in THF/dioxane. DMSO provides better complexation of the cation, and as a stronger Lewis base it polarizes the oxygen-hydrogen bond more strongly.

Determination of the degree of polymerization via ^{1}H NMR spectroscopy, as often used in the case of hyperbranched polyglycerol was not feasible, since full incorporation of the initiator into each macromolecule is a prerequisite for this characterization technique. Even complete conversion, however, would not permit characterization for a molar mass beyond a few thousand g mol^{-1}, as the initiator to monomer ratio is so low that the corresponding proton signal cannot be distinguished in the spectra. Characterization of the copolymers in this molar mass range by MALDI-ToF mass spectrometry is not possible either. However, both the ratio of incorporated monomers as well as the relative amounts of branched, linear and terminal units can be calculated from inverse gated ^{13}C NMR spectra, as described previously.[26] The signal splitting due to triad sequences allows for determining the relative amount of branched, linear and terminal units as well. From these, the degree of branching (*DB*) was calculated as defined by equation (2).[51]

$$DB_{\mathrm{AB/AB_2}} = \frac{2D}{2D+L_{co}} \qquad (2)$$

D summarizes all dendritic units, whereas L_{co} summarizes all linear units in the hyperbranched copolymers. *AB* represents a monomer unit containing two reactive sites, in this case ethylene oxide, and *AB$_2$* represents the branching unit glycidol as a latent *AB$_2$* monomer. Assuming equal reactivity of all *B*-groups and full conversion, the theoretical *DB* of an AB/AB$_2$ copolymer with the comonomer ratio *r* (x_{AB}/x_{AB2}; initial comonomer ratio) can be obtained from equation (3) for comparison, provided all B-groups possess reactivity (Figure 2).[51]

$$DB_{\mathrm{AB/AB_2,theo}} = 2\frac{r+1}{(r+2)^2}\text{, with } r = \frac{x_{\mathrm{AB}}}{x_{\mathrm{AB_2}}} \quad (3)$$

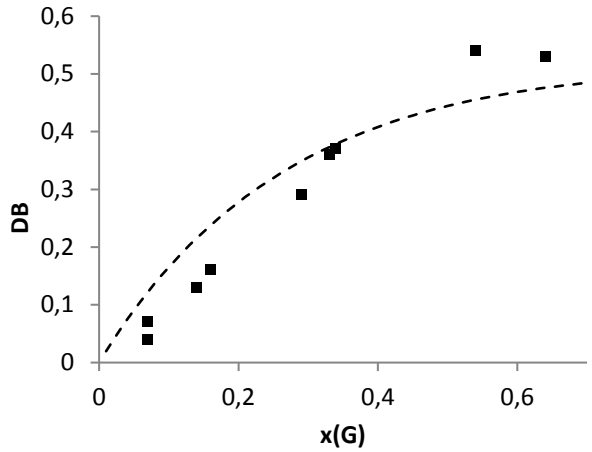

Figure 2. Experimentally determined degree of branching of *hb*PEG with varying monomer composition as function of the glycidol mole fraction. The dashed line represents theoretical values calculated from equation (3).

SEC and NMR data are given in Table 1**.** The SEC peak volume is included for the ensuing discussion. Summarizing the results, the lack of control over the molar mass for the copolymerization of ethylene oxide and glycidol in bulk has been overcome to a certain extent by modifying the existing reaction protocol. While still obtaining relatively moderate PDI values (Table 1), the use of polar aprotic solvent led to the formation of oligomers. On the other hand, carrying out the polymerization in cyclic ethers increased apparent molar masses (SEC) up to 65,000 g mol^{-1}.

Table 1. NMR and SEC characterization data for *hb*PEG with varying monomer composition, prepared in DMSO (samples 0 – 2) and THF/dioxane (samples 3 – 8).

№	G% (^{13}C)	DB (^{13}C)	M_n* g mol^{-1}	M_w/M_n*	M_n** g mol^{-1}	M_w/M_n**	peak volume cm^3
0	33	0.36	880	1.39	d	5.03	22.55
1	14	0.13	1,600	1.29	1,300	2.87	21.38
2	7	0.04	2,480	1.28	3,200	2.71	20.28
3	54	0.54	14,400	1.69	57,000	5.83	17.41
4	7	0.07	36,000	1.26	440,000	2.58	14.05
5	34	0.37	40,400	1.33	530,000	2.00	14.01
6	29	0.29	55,300	1.04	1,450,000	1.16	13.79
7	64	0.53	64,600	1.02	1,600,000	1.10	13.78
8	16	0.16	65,300	1.07	1,700,000	1.28	13.75

*apparent values of M_n and M_w/M_n obtained by calibration with linear PEG standards

** calculated based on the columns calibration with the molar masses obtained from AUC

Hydrodynamic Characterization

Discussion of Experimental Data that Generally do not Depend on Molar Mass:

Primary experimental data. First, we discuss those experimental data and their combinations that typically do not depend on the molar mass. Other data allow calculation of the molar mass of the substances dispersed in the solvent and evaluation of their hydrodynamic size and shape. Note that the former data are important for the characterization of polymers in solution and, as a rule, are used for the homologous series of linear polymers; moreover, these data are usually included in the summary tables in various polymer handbooks.[52] For branched polymer systems, the definition of "homologous" in its standard meaning cannot be applied due to the absence of uniform structural repeating units in the polymer. However, it seems worth testing how those values which are virtually constant for linear polymers will depend on the molar mass/composition for the particular case of hyperbranched poly(ethylene glycol)–*co*–polyglycerol copolymers.

Table 2. Intrinsic viscosity ([η], $cm^3 g^{-1}$), Huggins (k_H), Kraemer (k_K) parameters and values of partial specific volume (υ, $cm^3 g^{-1}$) for all hbPEG samples in water and DMF.

№	$[\eta]_{water}$	k_H	k_K	$[\eta]_{DMF}$	k_H	k_K	υ_{water}	υ_{DMF}
0	-	-	-	4.9	0.88	0.06	-	0.825
1	6.2	0.84	0.03	5.9	0.78	0.02	0.840	0.840
2	5.9	0.62	0.02	6.0	0.61	-0.04	0.817	0.853
3	6.5	1.79	0.53	6.9	1.23	0.26	0.787	0.792
4	7.3	2.03	0.50	6.8	2.33	0.44	0.829	0.857
5	5.7	2.40	0.52	6.3	1.14	0.22	0.802	0.813
6	5.6	2.05	0.50	5.7	1.76	0.35	0.772	0.810
7	5.5	1.59	0.42	6.5	0.77	0.03	0.769	0.760
8	7.9	1.78	0.32	7.1	1.65	0.33	0.813	0.857

Average values of the partial specific volume of *hb*PEG are $\upsilon = (0.804 \pm 0.03)$ $cm^3 g^{-1}$ and $\upsilon = (0.82 \pm 0.04)$ $cm^3 g^{-1}$ in H_2O and DMF, respectively. It should be noted that these values of the partial specific volume generally decrease somewhat with increasing glycerol fraction (Figure 2). This trend is more pronounced in DMF than in water. Consequently, for all corresponding calculations the individual values of υ were used.

Partial specific volume and refractive index increment. The partial specific volume υ ($cm^3 g^{-1}$) was calculated from the corresponding density increment measurements as $\Delta\rho/\Delta c = (1-\upsilon\rho_0)$, where ρ_0 is the density of the solvent, for all samples in water and DMF (values are given in Table 2).

The values of the refractive index increment were evaluated from the sedimentation velocity data as follows:

$$\frac{dn}{dc} = \left(\frac{J}{c}\right)\frac{\lambda}{kl} \qquad (4)$$

where (J/c) is the number of interference fringes, λ is the wavelength used (655 nm), l is the optical path length (12 mm) and k is a device constant.

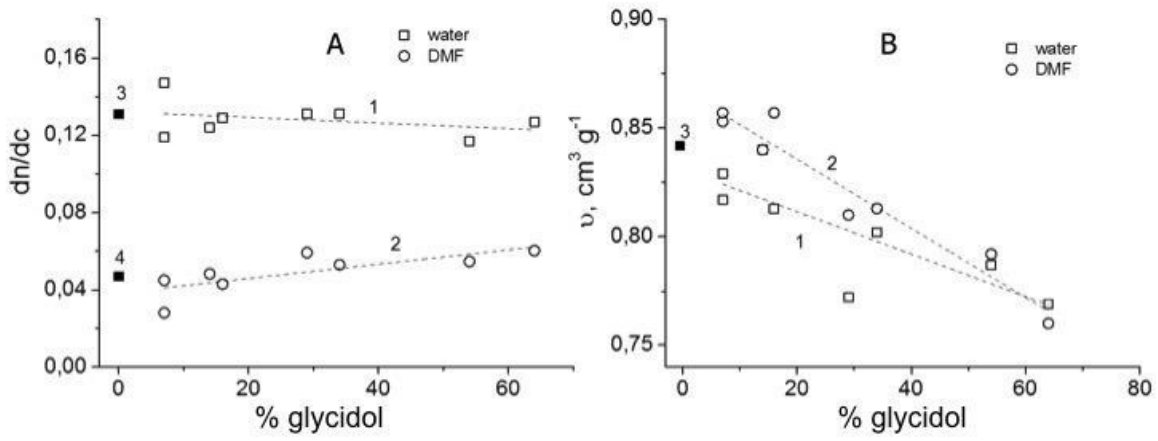

Figure 3. Correlation of the refractive index increment *dn/dc* (cm^3/g) and the partial specific volume υ (cm^3/g) on the glycidol content (%) in the *hb*PEG macromolecules. 1 – in water, 2 – in DMF, 3 – value for linear PEG in water and 4 – value for linear PEG in DMF (Polymer Handbook[52]).

In water, the values of the refractive index increment of *hb*PEG are virtually independent of the glycerol content for the high molar mass samples (M > 100,000 g mol^{-1}), and the average value of *dn/dc* is (0.126 ± 0.003) cm^3 g^{-1}. In DMF the *dn/dc* values increase slightly with increasing glycerol content (Figure 3) and the average values are lower in comparison to the aqueous solutions ($dn/dc^{ave} \approx 0.053$). This difference in *dn/dc* is mainly due to the difference in the refractive indices of the solvents ($n_{DMF} = 1.427$ and $n_{H2O} = 1.333$). The linear approximation for *dn/dc* dependence of glycidol content in DMF is characterized by a low coefficient of linear correlation and cannot be used to determine the proportion of glycerol in the copolymer. In contrast to that, the dependencies of the partial specific volume *vs*. glycidol content are more pronounced, have a palatable quality of the linear fit and in principle can be used for the evaluation of the glycidol content in copolymers. Following dependences of υ in both solvents: $\upsilon = 0.831 - 0.977\times10^{-3}$ G% (r = 0.8088) and $\upsilon = 0.867 + 1.590\times10^{-3}$G% (r = 0.9689) in water and DMF were obtained, respectively. The results obtained by densitometry indicate that the value of the partial specific volume may be used for the approximate estimation of the glycerol content in the samples and, thus, the degree of branching of the macromolecules.

Ratio of $k_s/[\eta]$. The dimensionless ratio $\gamma = k_s/[\eta]$, of the concentration dependence coefficient k_s (Gralen coefficient) on the intrinsic viscosity $[\eta]$,[53] depends on the particle/macromolecule asymmetry/conformation; the value for coils of linear macromolecules is ≈1.7 with the general tendency to decrease for more rigid macromolecules and to increase for compact, globular molecules.[53-55] The average values obtained for *hb*PEG samples are $\gamma = 2.9 \pm 0.5$ and 4 ± 2 for water and DMF solutions, respectively. Remarkably, these values are close to the theoretically predicted value for rigid spheres: $(k_s/[\eta])_{sph} = 2.75$.

Huggins and Kraemer parameters. The viscometric Huggins parameter (k_H) usually varies from 0.3 to 0.5 for linear polymers, and the Kraemer parameter (k_K) is usually negative. For the *hb*PEG copolymers of high molar mass (M > 100,000 g mol^{-1}), the k_H and k_K values fluctuate around the averages which are in H_2O: k_H^{av} = 1.9 ± 0.1, k_K^{av} = +(0.47 ± 0.03), and in DMF: k_H^{av} = 1.5 ± 0.2, k_K^{av} = +(0.27 ± 0.06). These values are typical for compact macromolecules in solution. For rigid spheres k_H^{sph} is 2.26.[56]

Hydrodynamic invariants. The intercorrelation between the basic hydrodynamic characteristics ([η], s_0, D_0, $(f/f_{sph})_0$) can be evaluated by calculating the hydrodynamic invariants A_0 ([g cm^2 s^{-2} K^{-1}mol$^{-1/3}$]) and β_s *([mol$^{-1/3}$])*, which remain virtually independent of molar mass for linear homologous series.[57, 58]

$$A_0 = (R[s][D]^2[\eta])^{\frac{1}{3}} \quad (5)$$

$$\beta_s = k_B^{-\frac{2}{3}}(N_A[s][D]^2 k_s)^{\frac{1}{3}} \quad (6)$$

where k_B is the Boltzmann constant, R is the gas constant, N_A is Avogadro's number, *[s]* is the intrinsic sedimentation coefficient ($[s] = \frac{s_0\eta_0}{(1-\upsilon\rho_0)}$), [D] = $D_0\eta_0/T$ – intrinsic diffusion coefficient, ρ_0 and η_0 are density and dynamic viscosity of the solvent, T - temperature in *K*

The average value of A_0 is 3.2 × 10^{-10} for linear flexible chain polymers and 3.8 × 10^{-10} for rigid chain molecules; the minimum theoretically predicted value for rigid spheres is 2.914 × 10^{-10}.[57] In the current case the average value of A_0 was calculated to be (2.35 ± 0.10)×10^{-10} and (2.5 ± 0.40)×10^{-10} for samples in water and DMF, respectively. Systematic observations on the hydrodynamic invariants for highly branched macromolecular systems have been published only for perfect dendrimers i.e., poly(amido amine) and poly(propylene imine) to date.[59-65] The overall average value obtained for different dendrimer generations with up to 128 end groups is A_0^{av} = (2.53 ± 0.05) × 10^{-10}, which correlates with the values obtained for *hb*PEG copolymers obtained in the current study. It should be noted that the values of A_0 for highly branched macromolecules are generally lower than the theoretical value for rigid spheres. At the same time, the obtained values of the sedimentation parameter β_s = (1.13 ± 0.06)×10^7 and (1.09 ± 0.10)×10^7 in water and DMF, respectively, are in the range known from the literature for linear chain polymers.[66]

Discussion: Basic Hydrodynamic Characteristics and Branching Factors of *hb*PEG: Molar Mass, Hydrodynamic Homology and Kuhn-Mark-Houwink-Sakurada Relationships

The basic hydrodynamic characteristics are s_0, D_0 and $[\eta]$. These values are related to the molar mass, size and shape of the dissolved species. The values of the molar mass were calculated based on the coefficients s_0 and D_0 using the Svedberg equation (5):

$$M_{sD} = \frac{s_0 RT}{D_0(1-\upsilon\rho_0)}; \quad (7)$$

alternatively it was based on s_0 and $(f/f_{sph})_0$ coefficients using a modified Svedberg equation:

$$M_{sf} = 9\pi\sqrt{2}N_A\left([s]\, f/f_{sph}\right)^{3/2}\sqrt{\upsilon} \quad (8)$$

In the following discussion, the average values of the molar masses will be used:

$$M_{av} = (M_{sD}^{H2O}+M_{sf}^{H2O}+M_{sf}^{DMF})/3 \quad (9)$$

The molar mass values, together with other hydrodynamic characteristics in H_2O, are summarized in Table 3; the data obtained in DMF are presented in the Supporting Information (Table 1 SI).

Table 3. Hydrodynamic characteristics, molar masses and hydrodynamic invariants of hyperbranched PEG copolymers in water at 20 °C.

№	G content %	s_0 S	k_s $cm^3\,g^{-1}$	$k_s/[\eta]$	$D\times10^7$ cm^2s^{-1}	$(f/f_{sph})_0$	$M_{av}^{*}\times10^{-3}$ g mol^{-1}	PDI**	$A_0\times10^{-10}$	$\beta\times10^7$
0	33	-	-		32.3		1.4	2.02	-	-
1	14	0.16	20	3.2	13.8	1.91	2.2	2.20	2.27	1.13
2	7	0.20	21	3.6	13.5	2.03	2.0	2.42	2.25	1.15
3	54	3.36	21	3.2	3.29	2.36	130	3.30	2.20	1.09
4	7	9.97	23	3.2	1.78	2.75	1,000	2.01	2.32	1.14
5	34	10.8	14	2.5	2.00	2.80	800	1.77	2.42	1.10
6	29	15.0	14	2.5	1.88	2.93	1,500	1.75	2.34	1.07
7	64	17.6	18	3.3	1.82	2.44	1,000	1.37	2.46	1.23
8	16	20.1	16	2.1	1.30	1.95	1,700	2.07	2.43	1.03

*****average values of the molar masses are obtained as: $M_{av} = (M_{sD}^{H2O}+M_{sf}^{H2O}+M_{sf}^{DMF})/3$ with the average relative error 23%

** calculated from the sedimentation velocity data

The absolute values of the molar masses evaluated from the sedimentation-diffusion analysis allow appropriate calibration of the SEC columns. Such SEC calibration provides the adequate values of the molar mass (compare data in Table 1 and 3).

Figure 4 compares differential distributions of the intrinsic sedimentation coefficients *[s]* of *hb*PEG in water and DMF. The two distributions are virtually identical. Notably, the distributions shift to higher values of the sedimentation coefficients with increasing molar mass. Moreover, the distributions in general are broad, which in turn reflects the high polydispersity/heterogeneity of the samples. In addition, it is obvious that at some point (sample 4) a second component in a higher molar mass region appears. In the following, the distribution becomes strictly bimodal (sample 5); afterwards the low molar mass component decreases (sample 6) and the distribution again becomes unimodal (sample 8). Since the samples are unfractionated, such a behavior is most probably related to inhomogeneous structures of the respective samples.

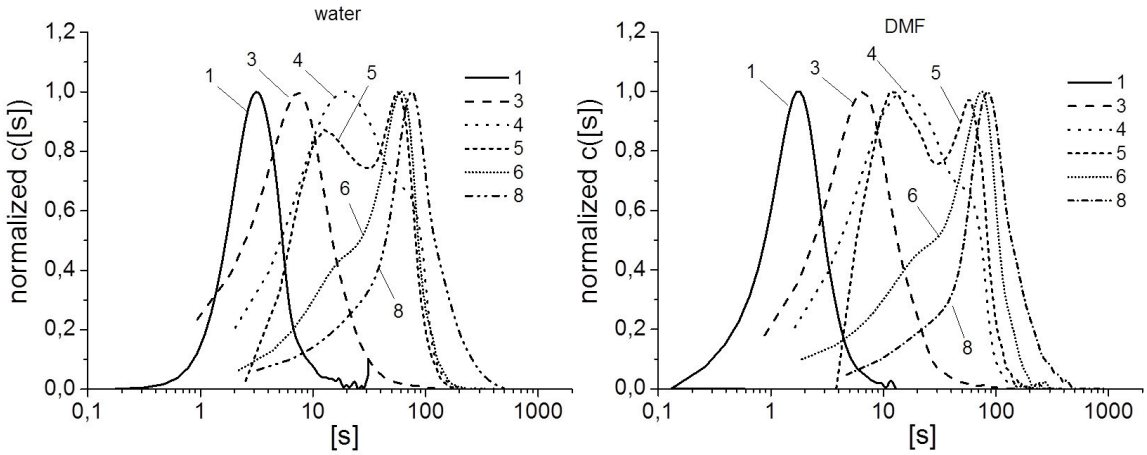

Figure 4. Semi-logarithmic plot of the differential distributions of intrinsic sedimentation coefficients of hyperbranched PEG copolymers in water, as obtained by the Sedfit software (c(s) analysis); left: samples in water, right: in DMF.

The SEC data (Figure 5) do not provide such a clear tendency towards the existence of several species in the solution. They show, however, the presence of a shoulder/wide tail for samples 4 and 5; moreover, a clear bimodal distribution was obtained for sample 3.

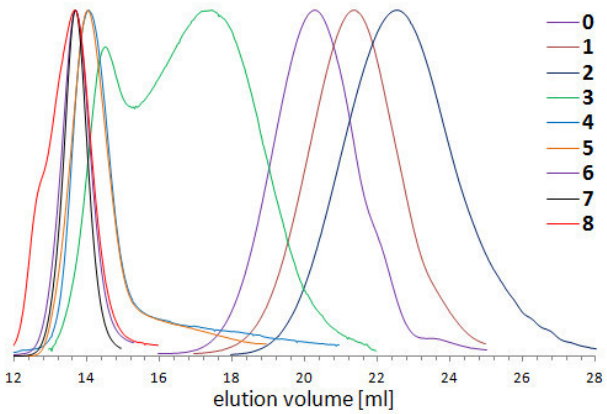

Figure 5. SEC traces (DMF, RI signal) of the hyperbranched PEG copolymers.

The polydispersity can also be evaluated from the sedimentation velocity data by transforming the initial distribution of sedimentation coefficients into the distribution by the molar masses. PDI can be then calculated based on the known relationships: $M_n = \frac{\sum_i N_i M_i}{N_i}$, $M_w = \frac{\sum_i N_i M_i^2}{\sum_i N_i M_i}$. The calculated values are listed in Table 3. The differences in the distributions obtained by analytical ultracentrifugation and SEC could be related to the fact that the AUC is more sensitive in the range of high molar mass, and SEC is more sensitive in the range of the low molar mass polymers. Detailed discussion regarding the analysis of differences in the distributions obtained by SEC on one side, and AUC on another one will be made in a future publication.

Comparison of the basic experimental characteristics s_0, D_0 and $[\eta]$ shows that the value of $[\eta]$ fluctuates around its average, while the values of s_0 increase by two and the D_0 values decrease by one order of magnitude when going from sample 1 to sample 8.

The *hb*PEG samples can be qualitatively assigned to the most probable conformation by comparing their hydrodynamic volumes with the corresponding molar masses.[67, 68] The $[\eta]M$ is the key value in interpreting the results of size exclusion chromatography of polymers (Benoit universal calibration).[69] It is proportional to the volume V occupied by the macromolecules in solution. In the first approximation, the slope of the $[\eta]M$ dependency on molar masses, in a double logarithmic scale, will be inversely proportional to the average intracoil density ($\sim \lg(1/\rho)$). The higher the curves are located along the ordinate, the lower will be the density of the polymer substance in the volume occupied by the polymer molecule. Figure 6 shows that the data obtained for *hb*PEG virtually coincide with the average dependence obtained for dendrimers, but also glycogen and globular proteins, where the slope is equal to 1. This means that the volume occupied by the macromolecules (V) is directly proportional to their molar mass: $V \sim M$ and,

consequently, the intrinsic viscosity values are virtually independent from M, since $[\eta] = 6^{3}/_{2}\Phi(\frac{<R_g^2>^{\frac{3}{2}}}{M})$, where Φ is the Flory hydrodynamic parameter and R_g is the radius of gyration.

Homology of linear macromolecules is provided by the constant chemical structure of the repeating units, and persistence of a structural parameter – linear density of the polymer chains M_L – can be defined as a *structural homology*. Homology of branched macromolecules, in particular hyperbranched copolymers, is more difficult to define and much more difficult to achieve and control. Here we propose the concept of *hydrodynamic homology*, which is based on the scaling relations linking the hydrodynamic characteristics of each other and/or the molar mass. The fulfillment of such relations would mean the macromolecules compared behave hydrodynamically similar to each other and would allow interpreting the experimental results based on a single hydrodynamic model. The *structural homology* – being the highest form of homology, automatically leads to *hydrodynamic homology*, whereas the latter does not necessarily grant the occurrence of the first one.

This result (Figure 6) also means that the shape and size of *hb*PEG macromolecules is not distorted significantly by certain "defects" in the structure of the copolymers. Note that computer modeling of the shape and size of randomly hyperbranched polymers in solution allows to conclude that random attachment of component parts produces a good model of regularly branched polymers, i.e. dendrimers.[18] It supports the conclusion that the size and shape of ideal dendrimers and dendrimer molecules of higher generations in solution, with few structural defects, are virtually indistinguishable.[70, 71] Thus, it follows from Figure 6 that glycogen as a hyperbranched biopolymer, perfectly branched dendrimers, the hyperbranched *hb*PEG studied in this contribution and globular proteins, despite their different chemical structures and fine topology, are *hydrodynamic homologues*. For these polymers direct proportionality between the volume occupied by such macromolecules in solution and their masses is observed. It is the main feature of these systems. As a consequence, the intrinsic viscosity is independent of the molar mass for such homologous series.

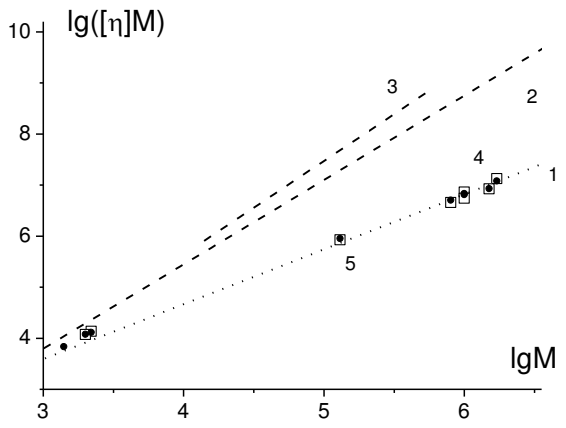

Figure 6. Dependence of the hydrodynamic volume [η]M on M, in a double-logarithmic plot. The dotted line 1: completely compact organization of the polymer species inside the occupied volume (similar to glycogen, dendrimers, globular proteins); dashed line 2 corresponds to the behavior of linear PEG (flexible linear macromolecules); the dashed line 3 describes the behavior of rigid linear macromolecules (polysaccharides schizophyllan[72] and xanthan[73]); 4 – points corresponding to the studied *hb*PEG macromolecules in H_2O, and 5 in DMF (see also Tables 2 and 3).

From Figure 6 it is possible to determine the scaling relation between the value of the intrinsic viscosity and molar mass: $[\eta] = K_\eta M^{b\eta}$. A similar scaling relation or Kuhn-Mark-Houwink-Sakurada (KMHS) relationship/plot can be set for other hydrodynamic characteristics. Double logarithmic KMHS scaling plots for samples in water are shown in Figure 7, (scaling plots in DMF are presented in Figure 3 SI; and the parameters of the KMHS relations are summarized in Table 4. In spite of the high heterogeneity of the studied *hb*PEGs (broad molar mass distributions, in some cases bimodal) all samples behave similarly and linear trends of KMHS relationships were obtained. A satisfactory correlation between the scaling indices b_i is observed within the error of their determination.

Table 4. Parameters of the KMHS relationships for *hb*PEG copolymers in water and DMF at 20 °C.

P_i-M*	$b_i \pm \Delta b_i$		K_i		r_i	
	water	**DMF**	**water**	**DMF**	**water**	**DMF**
s_0	0.69 ± 0.03	0.65 ± 0.03	9.34×10^{-4}	2.08×10^{-3}	0.9959	0.9944
[η]	0.01 ± 0.02	0.02 ± 0.01	5.67	4.70	0.1830	0.6333
D_0	-0.32 ± 0.02	-	159	-	0.9931	-
$(f/f_{sph})_0$	0.04 ± 0.02	0.01 ± 0.05	1.48	1.80	0.6454	0.0702

* The properties P_i of all the samples are related by: $\log P_i = \log K_i + b_i \log M$; r_i is the corresponding linear correlation coefficient. Taking into account experimental errors, it can be seen that the scaling indices b_i are related to each other in the characteristic ways of a hydrodynamic homologous series of polymers: $|b_{D0}| = (1 + b_{[\eta]})/3$; $|b_{D0}| + b_{s0} = 1$, $|b_{D0}| = b_{ff} + 0.333$.

All our sets of hydrodynamic data indicate that the friction elements considered (isolated macromolecules) are similar with respect to their hydrodynamic behavior to globular-like particles with virtually constant degree of asymmetry. This conclusion is supported by the values of the scaling indices obtained from the double-logarithmic plots of the hydrodynamic characteristics *vs.* molar mass. Thus, the macromolecules of the hyperbranched PEG copolymer follow the scaling relationships of the KMHS type, and the usual correlation between the scaling indices b_i is observed. In this approach, the series of the *hb*PEG copolymers may be considered as a hydrodynamically homologous series. Values of b_i as observed are characteristic of series of molecules/particles, which keep their form and asymmetry constant, going from low to high *M*. An example of a model that satisfies these conditions is a set of ellipsoids (spheroids) with a constant asymmetry. The simplest example of such a model is a series of hard spheres.

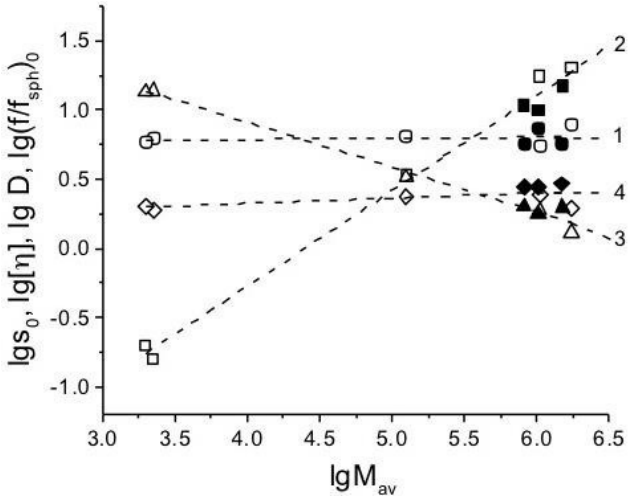

Figure 7. Dependencies of [η] (1), s_0 (2), D (3), and $(f/f_{sph})_0$ (4), in a double-logarithmic plot, on the average molar mass M_{av} of *hb*PEG in H_2O. The scaling indexes are summarized in Table 4. Filled symbols related to the samples with bimodal or highly broad molar mass distribution. It is evident that these data do not violate the general trend of the dependencies.

Comparison of the Retention Volume in SEC with Other Hydrodynamic Characteristics

In the ideal SEC (without adsorption contribution), molecules are separated according to their hydrodynamic volume. The well-known Benoit universal calibration curve connects the hydrodynamic volume, expressed as *[η]M*, with the retention volume V_R and can be used for molar mass estimation, however, the intrinsic viscosity must be known:

$$log[\eta]M = C_1 - C_2 V_R \quad (10)$$

where C_1 and C_2 are constants characterizing the columns and V_R is the retention volume.

Figure 6 aids in understanding the results obtained by SEC and the discrepancy between M_{sD} and M_{SEC}. In accordance with relation (10), each value of the retention volume corresponds to the hydrodynamic volume of macromolecules contained in a portion of eluent sorted from the column. Thus, any line parallel to the X-axis corresponds to a retention volume. Such a line parallel to the X-axis intercepts first line 2 corresponding to linear PEG at low *M* and then line 1 corresponding to *hb*PEG at higher *M*. The difference between M_{sD} and M_{SEC} increases with increasing molar mass and/or with decreasing V_R so far as the slope of line 1 is lower than that of line 2.

It has been shown previously that similar calibration curves can as well be applied for other hydrodynamic characteristics or their combinations and in the general case can be written as:

$$\log[f(< R >^2)] = C_i + C_{i+1} V_R \quad (11)$$

where f(<R>^{2}) is a function of the chain size and/or a combination of the experimental values which depend solely on the chain size, for instance, *[η]M,* $s_0[\eta]$, D_0, M/s_0, k_sM and C_{i+1} are the coefficients of different sign.[74] In Figure 8 the dependencies of $log(s_0[\eta])$, *D* and *[η]M* on V_{Ret} are shown; the parameters of the corresponding linear approximation procedures are listed in Table 2 SI. This kind of plot allows converting the macroscopic value of the retention volume to the nanoscale value of the hydrodynamic size of the macromolecules moving through the column.

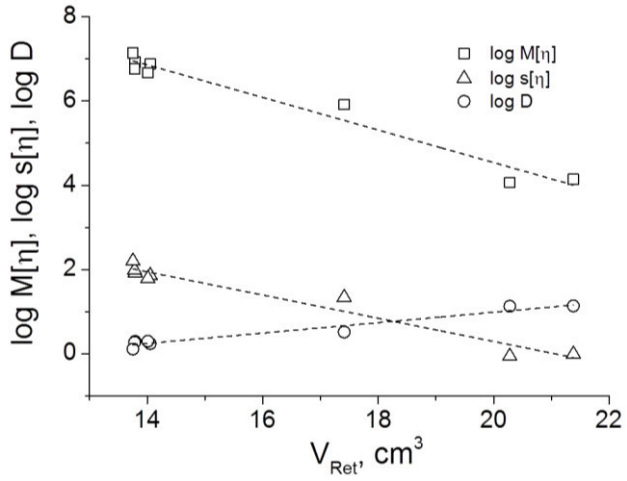

Figure 8. Universal calibration plots of log M[η], log s[η] and log D versus retention volume V_R in DMF. The scaling indexes are summarised in Table 2 SI.

Average Density of the Polymer in the Volume Occupied by Individual Macromolecules in Solution

The average density of the hyperbranched macromolecules in the volume occupied by them can be calculated based on the hydrodynamic characteristics for both branched and linear PEGs.[64] Using the equivalent sphere approximation, the following relationships is obtained:

$$\rho_{sD} = 3^4 2\pi^2 k_B^{-2}[s][D]^2;\ \rho_\eta = 2.5/[\eta] \quad (12)$$

The data for the calculations on linear PEG were taken from the literature and the corresponding densities were calculated according to the following equations:[52,74]

$$\rho_{sD} = P^3 k_B^{-2}(0.36)^{-1}[s][D]^2;\ \rho_\eta = \Phi/N_A 0.36[\eta] \quad (13, 14)$$

where *P* and *Φ* are the Flory hydrodynamic parameters. The dependency of the calculated average density values (in water) on molar mass is presented in Figure 9 in double logarithmic scale. For the hyperbranched molecules, at the highest molar mass the density of the polymer substance in the polymer coil is approximately 70 times higher than for the linear chains. Furthermore, for the hyperbranched chains the density is virtually independent on the molar mass, while for linear macromolecules it decreases with the molar mass. The average densities are ρ_η = (0.40 ± 0.02) and (0.41 ± 0.02) g cm^{-3} in water and DMF, respectively, and ρ_{sD} = (0.21 ± 0.01) and (0.3 ± 0.1) g cm^{-3} in water and DMF correspondingly. These values are comparable with or similar to those obtained for dendrimers based on poly(amido amine), poly(propylene imine) and perfectly branched dendrimers based on α-amino acids.[64,65,75]

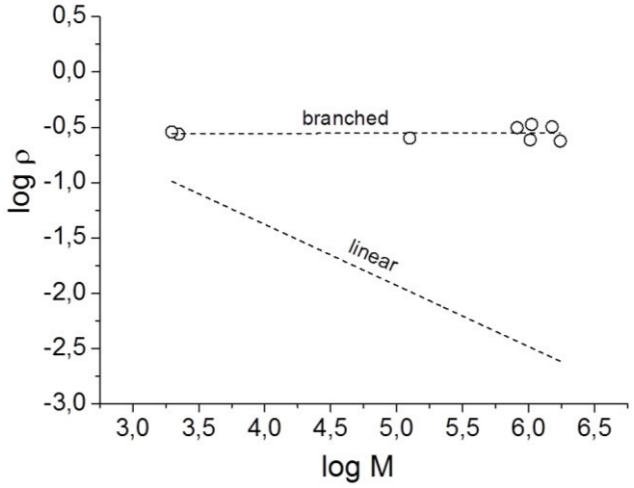

Figure 9. Dependence of the density of the polymer substance in the volume limited by the polymer coil (ρ) on the polymer mass (M) in double logarithmic scale, for linear and *hb*PEGs in water. The corresponding scaling relationships are the following: $\rho = 6.8\ M^{-0.55 \pm 0.01}$ and $\rho = 0.27\ M^{0.00 \pm 0.02}$ for linear PEG and hyperbranched PEG copolymers, respectively.

Sizes and Branching Factors of *hb*PEG

The degree of branching is an important parameter for the hydrodynamic volume of the macromolecule: the higher the degree of branching the smaller the size (as compared to linear macromolecules of the same molar mass). The effect of branching on the hydrodynamic volume of branched macromolecules can be characterized by the so-called shrinking or contraction factor, which is the ratio of the hydrodynamic characteristics and/or the square of the radius of gyration of the branched macromolecule and its linear analog of the same molar mass. These parameters were first introduced by Zimm and Stockmayer for the radius of gyration and then by Stockmayer and Fixman for the intrinsic viscosity. A similar relation can also be written for the translation friction coefficients g´ and h:[20,21]

$$g' = \frac{[\eta]_b}{[\eta]_{lin}};\ h = \frac{f_b^t}{f_{lin}^t} \qquad (15, 16)$$

The data on the intrinsic viscosity and translational friction coefficient (calculated from the corresponding diffusion coefficients) for linear PEGs can be taken from the literature ($[\eta] = 0.133\ M^{0.59}$, $D = 940\ M^{-0.53}$).[74] The size can directly be represented either by the hydrodynamic radius (R_D, R_s, and R_η) or by the mean-square radius of gyration (R_g). The molecular sizes were calulated using the following relationships:

$$R_D = \frac{k_B T}{6\pi\eta_0 D};\ R_S = \frac{3}{\sqrt{2}}\sqrt{[s]v};\ R_\eta = \left(\frac{3}{10\pi N_A}\right)^{\frac{1}{3}} (M[\eta])^{\frac{1}{3}} \quad (17, 18, 19)$$

The calculated values of the hydrodynamic radii for *hb*PEG in water and DMF are summarized in Table 3 SI. The hydrodynamic sizes increase with molar mass, reaching a maximum value of about 15 nm for the highest molar mass sample 8. The values of the contraction factors (*g'* and *h*) are summarized in Table 6. As expected, contraction factors decrease with increasing molar mass, reflecting higher segment density. The molar mass dependence of these parameters is presented in Figure 4 SI.

Table 6. Correlation parameters of the contraction factors g', h of the *hb*PEG with the molar masses and between them.

G_i-G_j*	$b_{ij} \pm \Delta b_{ij}$	$K_{ij} \pm \Delta K_{ij}$	r_{iJ}
g' – M	-(0.58 ± 0.02)	44 ± 3	0.9929
h – M	-(0.20 ± 0.01)	5.8 ± 0.5	0.9705
g' – h	2.75 ± 0.20	0.30 ± 0.04	0.9831

* The contraction factor G_i of all the samples are related by: $\lg G_i = \lg K_i + b_i \lg M$ or $\lg G_i = \lg K_{ij} + b_{ij} \lg G_j$, and r_{ij} is the corresponding linear correlation coefficient.

The relation between *g'* and *h* for branched macromolecules was firstly proposed by Stockmayer and Fixman based on the Kirkwood-Riseman theory. It was shown that *g'* could be evaluated from the following approximation:

$$g' \cong h^3 \quad (20)$$

which means that the differences in solvent draining between the linear and branched molecular chains, when included into their corresponding mean size, can describe both the frictional coefficient and the intrinsic viscosity.[25] The double logarithmic dependence *g' vs h* is presented in Figure 4 SI, and the corresponding relation was obtained as $g' = 0.30\ h^{2.75 \pm 0.20}$. In addition, some considerations regarding indirect estimation of the radius of gyration and evaluation of corresponding branching factor are presented in the supporting information.

Global Conformation of the *hb*PEG Macromolecules

The experimental data obtained for the series of *hb*PEG copolymers in solution can be summarized as follows: (i) the values of the intrinsic viscosity are small and almost independent of molar mass; (ii) the values of the sedimentation coefficients are high and strongly dependent on the molar mass of the samples, and (iii) the translational frictional coefficients are markedly dependent on the molar mass of the samples. In addition, higher Huggins parameter values and also higher values of the parameter $k_s/[\eta]$ are observed, as compared with the values characteristic for linear chains. All this suggests that the macromolecules studied are compact nano-objects, characterized by a high average density of the polymer material in the volume occupied by them. For instance, the average value of the intrinsic viscosity of the *hb*PEG copolymer samples are [η] = (6.3 ± 0.3) $cm^3\ g^{-1}$ in H_2O and [η] = 6.4 ± 0.4 in DMF, which is only 3 times higher than for the rigid sphere limit: $[\eta]_{sph}$ = 2.5 υ, which in our case will be $[\eta]_{sph} \approx 2.0\ cm^3\ g^{-1}$ in both solvents. The organization of the poly(ethylene glycol)–*co*–poly(glycerol)s can be described by a soft spheroid partially permeable for the solvent molecules. Modeling of the macromolecules in solution by rigid bodies, as performed earlier, nowadays is being replaced by the simulation of macromolecules by soft bodies.[76,77] Such mathematical modeling is implemented using a coarse-grained modeling concept.[78,79] The coarse-grained model (or "blob model") represents a macromolecule as a whole in the form of a soft body, the radius of which is equal to its radius of gyration and is allowed to fluctuate. Different soft-body models were considered for different types of polymers.[80,81] The direct application of a coarse-grained model and its straightforward comparison with the experimental results currently is not possible.

In general, the value of the intrinsic viscosity of the hyperbranched polymers may be represented as: $[\eta] = \nu(p, h, \varepsilon)\bar{\upsilon}$, where $\nu(p, h, \varepsilon)$ is a dimensionless coefficient depending on the asymmetry p of the soft body modeling of any macromolecule, on the thickness of the corona *h* accessible for the solvent molecules, and on the thermodynamic quality of the solvent (*ε*). A significant part of the energy loss due to friction of any macromolecule in solution is contributed by the external layers. Some attempts to obtain a theoretical expression for the intrinsic viscosity of the soft sphere depending on the thickness of the layer available for the solvent molecules may be found in literature.[82,83] However, the present state of theory does not allow for the interpretation of experimental data on the intrinsic viscosity of soft macromolecules.

The influence of draining effects on the value of the intrinsic viscosity of spheres has been demonstrated by the Debye−Bueche theory for a model of a rigid sphere permeable for the solvent molecules.[84] The value of *[η]* for the uniformly permeable sphere was found to be 3.6

times higher than that for the impermeable one. The solution behavior of the *hb*PEG macromolecules can be described by soft spheroids with some asymmetry and with partial draining by the solvent molecules. Separating the contributions to the small value of *[η]* due to the draining effect on one side and to molecular asymmetry on the other side is currently not possible. The main result obtained in this study on the *hb*PEG copolymers is to establish a scaling relation, which is typical for a series of the macromolecules characterized by direct proportionality between molar mass and volume of the macromolecules/species. (The simplest case of such series is a series of rigid spheres.) This allows us to consider the studied set of *hb*PEG copolymers as a hydrodynamically homologous series.

Conclusions

To the best of our knowledge, this study represents the first combined approach of analytical ultracentrifugation, intrinsic viscosity, translational diffusion measurements and SEC to a long-standing challenge, i.e., absolute molar mass determination of hyperbranched polymers. The one-step synthesis of hyperbranched poly(ethylene glycol)–*co*–poly(glycerol)s (*hb*PEG) copolymers based on random anionic ring-opening copolymerization of ethylene oxide with a minor fraction of glycidol as a branching agent has been further developed to generate a variety of molar masses. Biocompatible, material with multiple hydroxyl functionalities are obtained by this strategy. A series of copolymers with moderate polydispersity (M_w/M_n ≈2.1) was obtained, with varying glycerol content (7 to 64 mol%, DB = 0.04 to 0.54) and molar masses from 1,400 to 1,700,000 g mol^{-1}, depending on the solvent employed for the synthesis. The randomly branched structure of the copolymers was confirmed by ^{1}H and ^{13}C NMR spectroscopy. Absolute molar mass characterization still represents a major challenge for hyperbranched polymers in general. This study aims at this issue using molecular hydrodynamic methods in dilute solution, showing that the isolated macromolecules follow the scaling relationships with scaling indices characteristic of particles with constant asymmetry. Remarkably, the intrinsic viscosity of the *hb*PEG polymers virtually does not depend on molar mass ($[\eta] \sim M^{\approx 0}$), on another hand the sedimentation velocity coefficients strongly depend on molar mass ($s_0 \sim M^{0.69}$). The solution behavior of the *hb*PEG macromolecules can be qualitatively described by soft spheroids with some degree of draining and unknown asymmetry. Based on their hydrodynamic behavior and based on average coil density, the *hb*PEG macromolecules in solution can be viewed to some extent as a dendrimer or globular-like systems. Furthermore, the value of the partial specific volume of the copolymer molecules correlates with the content of glycerol component, which confirms the degree of

branching (DB) and may be used to estimate the DB. The retention volumes of the samples in SEC analysis correlate reasonably with other experimental hydrodynamic values characterizing the size of the macromolecules. Hydrodynamic radii of up to 16.5 nm in aqueous solution suggest that the hyperbranched PEGs prepared in dioxane might be the largest synthetic hyperbranched structures reported to date.

Acknowledgments

The authors are grateful to the Thuringia Ministry for Education, Science, and Culture (grant #B514-09051, NanoConSens) and to the Carl-Zeiss Stiftung (Strukturantrag JCSM) for financial support. We thank Prof. Dr. Dieter Schubert for helpful comments on the manuscript.

References

1. Flory, P. J. *J. Am. Chem. Soc.* **1941,** *63*, 3083-3090.
2. Tomalia, D. A.; Naylor, A. M.; Goddard, W. A. *Angew. Chem. Int. Ed.* **1990,** *29*, 138-175.
3. de Brabander-van den Berg, E. M. M.; Meijer, E. W. *Angew. Chem. Int. Ed.* **1993,** *32*, 1308-1311.
4. Newkome, G. R.; Moorefield, C. N.; Vogtle, F., *Dendritic Molecules: Concepts, Syntheses, Perspectives*. Wiley-VCH, Weinheim: **1996**.
5. Carlmark, A.; Hawker, C.; Hult, A.; Malkoch, M. *Chem. Soc. Rev.* **2009,** *38*, 352-362.
6. Gao, C.; Yan, D. *Prog. Polym. Sci.* **2004,** *29*, 183-275.
7. Inoue, K. *Prog. Polym. Sci.* **2000,** *25*, 453-571.
8. Segawa, Y.; Higashihara, T.; Ueda, M. *Polymer Chemistry* **2013,** *4*, 1746-1759.
9. Voit, B. I.; Lederer, A. *Chem. Rev.* **2009,** *109*, 5924-5973.
10. Dong, R.; Zhou, Y.; Zhu, X. *Acc. Chem. Res.* **2014**.
11. Knop, K.; Pavlov, G. M.; Rudolph, T.; Martin, K.; Pretzel, D.; Jahn, B. O.; Scharf, D. H.; Brakhage, A. A.; Makarov, V.; Mollmann, U.; Schacher, F. H.; Schubert, U. S. *Soft Matter* **2013,** *9*, 715-726.
12. Sunder, A.; Heinemann, J.; Frey, H. *Chem. Eur. J.* **2000,** *6*, 2499-2506.
13. Wei, Z.; Hao, X.; Kambouris, P. A.; Gan, Z.; Hughes, T. C. *Polymer* **2012,** *53*, 1429-1436.
14. Konkolewicz, D.; Monteiro, M. J.; Perrier, S. B. *Macromolecules* **2011,** *44*, 7067-7087.

15. Hult, A.; Johansson, M.; Malmström, E., Hyperbranched Polymers. In *Branched Polymers II*, Roovers, J., Ed. Springer Berlin Heidelberg: **1999**; Vol. 143, 1-34.
16. Schüll, C.; Rabbel, H.; Schmid, F.; Frey, H. *Macromolecules* **2013,** *46*, 5823-5830.
17. Sunder, A.; Hanselmann, R.; Frey, H.; Mülhaupt, R. *Macromolecules* **1999,** *32*, 4240-4246.
18. Konkolewicz, D.; Gilbert, R. G.; Gray-Weale, A. *Phys. Rev. Lett.* **2007,** *98*, 238301.
19. Konkolewicz, D.; Perrier, S.; Stapleton, D.; Gray-Weale, A. *J. Polym. Sci. Part B Polym. Phys.* **2011,** *49*, 1525-1538.
20. Zimm, B. H.; Stockmayer, W. H. *The Journal of Chemical Physics* **1949,** *17*, 1301-1314.
21. Stockmayer, W. H.; Fixman, M. *Ann. N. Y. Acad. Sci.* **1953,** *57*, 334-352.
22. Kurata, M.; Fukatsu, M. *J. Chem. Phys.* **1964,** *41*, 2934-2944.
23. Kurata, M.; Abe, M.; Iwama, M.; Matsushima, M. *Polym J* **1972,** *3*, 729-738.
24. Li, L.; Lu, Y.; An, L.; Wu, C. *J. Chem. Phys.* **2013,** *138*, -.
25. Burchard, W., Solution Properties of Branched Macromolecules. In *Branched Polymers II*, Roovers, J., Ed. Springer Berlin Heidelberg: **1999**; Vol. 143, 113-194.
26. Wilms, D.; Schömer, M.; Wurm, F.; Hermanns, M. I.; Kirkpatrick, C. J.; Frey, H. *Macromol. Rapid Commun.* **2010,** *31*, 1811-1815.
27. Zalipsky, S.; Harris, J. M., *Poly(ethylene glycol)*. American Chemical Society: **1997**; Vol. 680, 508.
28. Knop, K.; Hoogenboom, R.; Fischer, D.; Schubert, U. S. *Angew. Chem. Int. Ed.* **2010,** *49*, 6288-6308.
29. Dingels, C.; Schömer, M.; Frey, H. *Chem. unserer Zeit* **2011,** *45*, 338-349.
30. Kainthan, R. K.; Janzen, J.; Levin, E.; Devine, D. V.; Brooks, D. E. *Biomacromolecules* **2006,** *7*, 703-709.
31. Wilms, D.; Stiriba, S.-E.; Frey, H. *Acc. Chem. Res.* **2009,** *43*, 129-141.
32. Schömer, M.; Frey, H. *Macromol. Chem. Phys.* **2011,** *212*, 2478-2486.
33. Lee, S.-I.; SchѴðmer, M.; Peng, H.; Page, K. A.; Wilms, D.; Frey, H.; Soles, C. L.; Yoon, D. Y. *Chem. Mater.* **2011,** *23*, 2685-2688.
34. Hawker, C. J.; Chu, F.; Pomery, P. J.; Hill, D. J. T. *Macromolecules* **1996,** *29*, 3831-3838.
35. Dimitrov, P.; Hasan, E.; Rangelov, S.; Trzebicka, B.; Dworak, A.; Tsvetanov, C. B. *Polymer* **2002,** *43*, 7171-7178.
36. Feng, X.-S.; Taton, D.; Chaikof, E. L.; Gnanou, Y. *J. Am. Chem. Soc.* **2005,** *127*, 10956-10966.
37. Feng, X.; Taton, D.; Chaikof, E. L.; Gnanou, Y. *Macromolecules* **2009,** *42*, 7292-7298.
38. Pang, Y.; Liu, J.; Wu, J.; Li, G.; Wang, R.; Su, Y.; He, P.; Zhu, X.; Yan, D.; Zhu, B. *Bioconj. Chem.* **2010,** *21*, 2093-2102.

39. Cao, H.; Dong, Y.; O'Rorke, S.; Wang, W.; Pandit, A. *Nanotechnology* **2011,** *22*, 065604.
40. Walach, W.; Trzebicka, B.; Justynska, J.; Dworak, A. *Polymer* **2004,** *45*, 1755-1762.
41. Lapienis, G.; Penczek, S. *Macromolecules* **2000,** *33*, 6630-6632.
42. Lapienis, G.; Penczek, S. *J. Polym. Sci. A Polym. Chem.* **2004,** *42*, 1576-1598.
43. Unal, S.; Lin, Q.; Mourey, T. H.; Long, T. E. *Macromolecules* **2005,** *38*, 3246-3254.
44. Schömer, M.; Schüll, C.; Frey, H. *J. Polym. Sci. A Polym. Chem.* **2013,** *51*, 995-1019.
45. Filippov, A.; Amirova, A. I.; Kirila, T.; Belyaeva, E. V.; Sheremetyeva, N. A.; Muzafarov, A. M. *Polym. Int.* **2015,** *64*, 780-786.
46. Schuck, P. *Biophys. J.* **2000,** *78*, 1606-19.
47. Maechtle, W.; Boerger, L., *Analytical Ultracentrifugation of Polymers and Nanoparticles*. Springer Berlin / Heidelberg: **2006**.
48. Tsvetkov, V. N., *Rigid Chain Polymers*. Plenum Press: New York, **1989**.
49. Kratky, O.; Leopold, H.; Stabinger, H., The determination of the partial specific volume of proteins by the mechanical oscillator technique. In *Methods Enzymol.*, Academic Press: **1973**; Vol. Volume 27, 98-110.
50. Kainthan, R. K.; Muliawan, E. B.; Hatzikiriakos, S. G.; Brooks, D. E. *Macromolecules* **2006,** *39*, 7708-7717.
51. Frey, H.; Hölter, D. *Acta Polym.* **1999,** *50*, 67-76.
52. Brandrup, J.; Immergut, E. H.; Grulke, E. A., *Polymer handbook, 4th edition*. Wiley: New York, 1999.
53. Rowe, A. J. *Biopolymers* **1977,** *16*, 2595-2611.
54. Pyun, C. W.; Fixman, M. *J. Chem. Phys.* **1964,** *41*, 937-944.
55. Wales, M.; Van Holde, K. E. *J. Polym. Sci.* **1954,** *14*, 81-86.
56. Morawetz, H., *Macromolecules in Solution*. Second ed.; Wiley: New York, **1975**.
57. Tsvetkov, V. N.; Lavrenko, P. N.; Bushin, S. V. *J. Polym. Sci. Pol. Chem.* **1984,** *22*, 3447-3486.
58. Pavlov, G. M.; Perevyazko, I. Y.; Okatova, O. V.; Schubert, U. S. *Methods* **2011,** *54*, 124-135.
59. Pavlov, G. M.; Korneeva, E. V.; Nepogod'ev, S. A.; Jumel, K.; Harding, S. E. *Polymer Sci. Ser. A* **1998,** *40*, 1282.
60. Pavlov, G.; Korneeva, E.; Jumel, K.; Harding, S.; Meijer, E. W.; Peerlings, H. W. I.; Stoddart, J. F.; Nepogodiev, S. *Carbohydr. Polym.* **1999,** *38*, 195-202.
61. Pavlov, G. M.; Korneeva, E. V.; Roy, R.; Michailova, N. A.; Ortega, P. C.; Perez, M. A. *Prog. Colloid Polym. Sci.* **1999,** *113*, 150-157.

62. Pavlov, G. M.; Korneeva, E. V.; Michailova, N. A.; Roy, R.; Cejas Ortega, P.; Alamino Perez, M.; . *Vysokomolekul. soedin Ser.A* **1999,** *41*, 1810-1815.
63. Pavlov, G. M.; Errington, N.; Harding, S. E.; Korneeva, E. V.; Roy, R. *Polymer Sci. Ser. A* **2001,** *43*, 118.
64. Pavlov, G. M.; Errington, N.; Harding, S. E.; Korneeva, E. V.; Roy, R. *Polymer* **2001,** *42*, 3671-3678.
65. Pavlov, G. M.; Korneeva, E. V.; Meijer, E. W. *Colloid Polym. Sci.* **2002,** *280*, 416-423.
66. Pavlov, G.; Frenkel, S. *Prog. Colloid Polym. Sci.* **1995,** *99*, 101-108.
67. Pavlov, G. M. *Eur. Phys. J. E* **2007,** *22*, 171-80.
68. Pavlov, G., Hydrodynamics of Macromolecules: Conformation Zoning for General Macromolecules. In *Encyclopedia of Biophysics*, Roberts, G. K., Ed. Springer Berlin Heidelberg: **2013**; 1014-1024.
69. Grubisic, Z.; Rempp, P.; Benoit, H. *J. Polym. Sci., Polym. Lett.* **1967,** *5*, 753-759.
70. Mikhailov, I. V.; Darinskii, A. A. *Polymer Sci. Ser. A* **2014,** *56*, 534-544.
71. Bessonov, V.; Balabaev, N.; Mazo, M., Influence of Branch Defect on Shape and Size of Dendrimers. In *5th International Symposium "Molecular mobility and order in polymer systems"* St.Petersburg, Russia, **2005**.
72. Yanaki, T.; Norisuye, T.; Fujita, H. *Macromolecules* **1980,** *13*, 1462-1466.
73. Sato, T.; Norisuye, T.; Fujita, H. *Macromolecules* **1984,** *17*, 2696-2700.
74. Pavlov, G. M.; Korneeva, E. V.; Panarin, E. F. *J. Appl. Polym. Sci.* **1992,** *46*, 2059-2061.
75. Vlasov, G. P.; Pavlov, G. M.; Bayanova, N. V.; Korneeva, E. V.; Ebel, C.; Khodorkovskii, M. A.; Artamonova, T. O. *Dokl. Phys. Chem.* **2004,** *399*, 290-292.
76. Murat, M.; Kremer, K. *J. Chem. Phys.* **1998,** *108*, 4340-4348.
77. Sheiko, S.; Möller, M., Hyperbranched Macromolecules: Soft Particles with Adjustable Shape and Persistent Motion Capability. In *Dendrimers III*, Vögtle, F., Ed. Springer Berlin Heidelberg: **2001**; Vol. 212, 137-175.
78. D'Adamo, G.; Pelissetto, A.; Pierleoni, C. *Soft Matter* **2012,** *8*, 5151-5167.
79. Zhang, G.; Daoulas, K. C.; Kremer, K. *Macromol. Chem. Phys.* **2013,** *214*, 214-224.
80. Vettorel, T.; Besold, G.; Kremer, K. *Soft Matter* **2010,** *6*, 2282-2292.
81. Eurich, F.; Karatchentsev, A.; Baschnagel, J.; Dieterich, W.; Maass, P. *J. Chem. Phys.* **2007,** *127*, 134905.
82. Ohshima, H. *Langmuir* **2008,** *24*, 6453-6461.
83. Mendoza, C. I. *J. Chem. Phys.* **2011,** *135*, 054904.
84. Debye, P.; Bueche, A. M. *J. Chem. Phys.* **1948,** *16*, 573-579.

Supporting Information

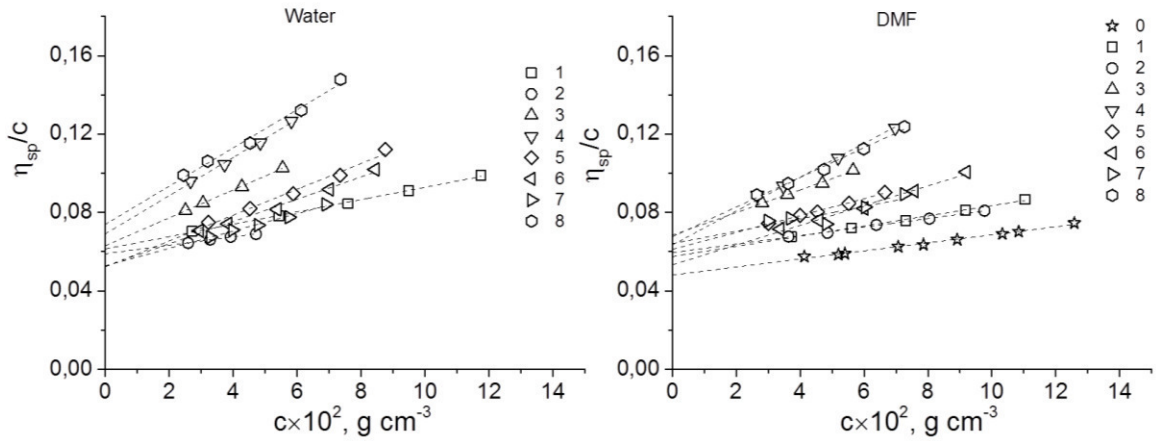

Figure 1 SI. Concentration dependencies of the reduced viscosities η_{sp}/c of *hb*PEG samples in water (left) and DMF (right). The corresponding values of the intrinsic viscosities and Huggins parameters are presented in Table 1.

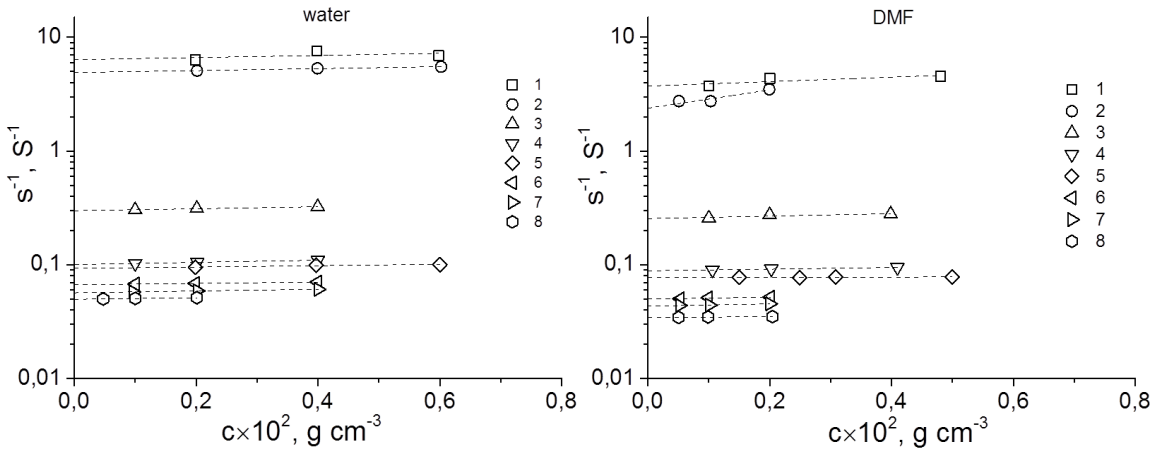

Figure 2 SI. Concentration dependence of the sedimentation coefficients of hyperbranched PEG copolymers, in a semi-logarithmic plot, in water (left) and DMF (right).

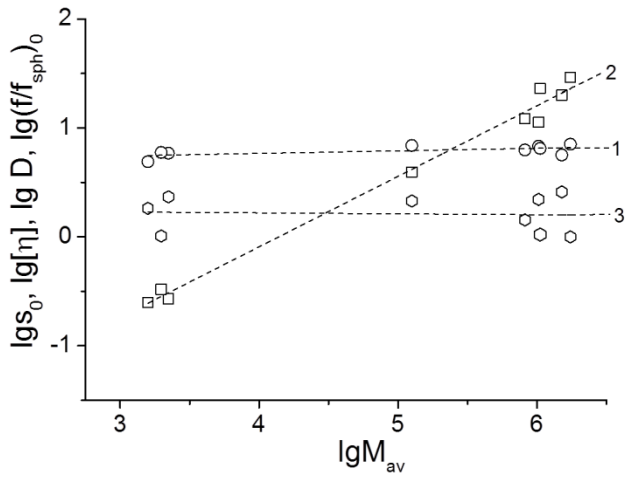

Figure 3 SI. Dependencies of *s*, *[η]* and *(f/f$_{sph}$)$_0$* in a double-logarithmic plot, on the molar mass *M* for the *hb*PEG samples in DMF. The scaling indexes are summarized in Table 4.

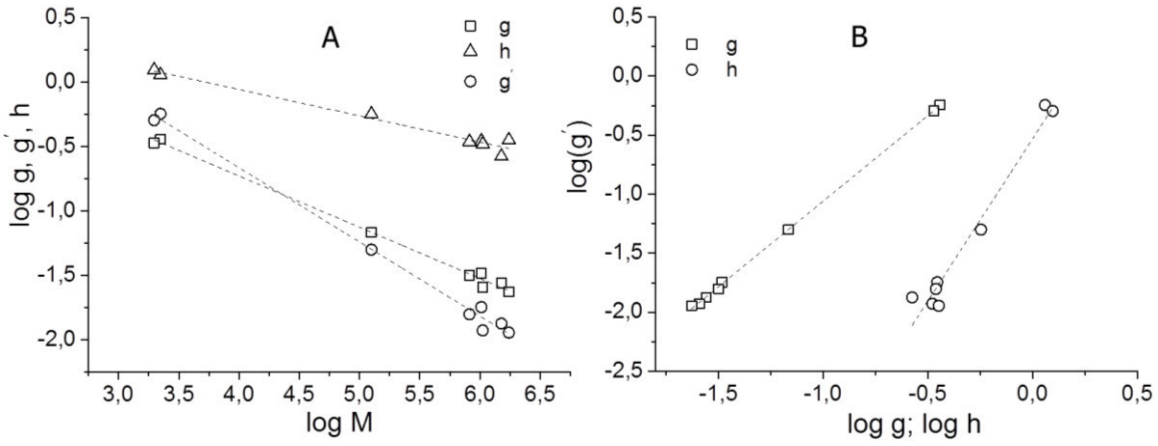

Figure 4 SI. A – double logarithmic dependence of the contraction factors g, g' and h on the molar mass. B – viscosity contraction factor as a function of geometric contraction factor g and h for the hyperbranched copolymers. The corresponding values of the equations are listed in Table 4 SI.

Table 1 SI. Hydrodynamic characteristics, molar mass and hydrodynamic invariants of *hb*PEG in DMF at 20 °C

№	G content	S_0	k_s	$k_s/[\eta]$	$(f/f_{sph})_0$	$M_{sf}\times10^{-3}$	$M_{av}\times10^{-3}$	A_0	β
	%	S	$cm^3\,g^{-1}$			$g\,mol^{-1}$	$g\,mol^{-1}$	$\times10^{-10}$	$\times10^{7}$
0	33	0.25	(200)	(56.3)	1.83	1.6	1.4	3.68	4.75
1	14	0.27	50	8.5	2.33	3.1	2.2	2.58	1.79
2	7	0.33	(47)	(38.3)	1.02	1.7	2.0	3.14	3.57
3	54	3.93	26	3.8	2.14	109	130	1.98	1.03
4	7	11.3	18	2.6	2.21	890	1,000	2.07	0.96
5	34	13.0	3	0.5	1.43	410	800	2.16	0.57
6	29	20.0	20	3.5	2.59	1,870	1,500	2.78	1.42
7	64	23.1	22	3.4	1.05	440	1,000	2.39	1.21
8	16	29.1	10	1.4	1.00	1,100	1,700	2.94	1.11

Table 2 SI. Correlation of hydrodynamic characteristics to their retention volumes for the *hb*PEG (Figure 7).

characteristic	C_i	C_{i+1}	r_i
M[η]	12.27	-0.386	0.9823
s_0[η]	5.80	-0.275	0.9770
D_0	-1.48	0.124	0.9751

Table 3 SI. Hydrodynamic (R_D and R_s), viscosimetric (R_η) and radii of gyration (R_g) in nm for the hyperbranched PEG copolymers in water and DMF.

№	R_D	R_η	R_s	R_g^{av}	R_D	R_η	R_s	R_g^{av}
	water				DMF			
0								
1	1.6	1.2	1.2	1	1.3	1.2	1.3	1
2	1.6	1.2	1.7	1.2	1.1	1.2	1.5	1
3	6.5	4.9	4.7	4.2	7.0	5.0	4.4	4,2
4	12.3	9.8	9.3	8.1	12.8	9.5	9.0	8,1
5	10.7	8.4	9.1	7.3	11.1	8.7	8.5	7,3
6	11.4	9.1	9.6	7.7	8.9	9.1	10.5	7,4
7	11.8	9.6	10.3	8.3	11.7	10.2	9.9	8,2
8	16.5	13.6	12.6	11	12.3	13.1	14.5	10.3

Radius of Gyration

The estimation of the radii of gyration may be done through the well known relation $\langle r_g^2 \rangle = 0.6r^2$ (Table 3 SI). The Rg estimations in this case should be considered only as tentative. Furthermore, the Flory parameter Φ may be then formally calculated for the rigid sphere model to make the relationships similar to corresponding relationships regarding the linear macromolecules. The corresponding value is $\Phi = 9.23\times10^{23}$ mol^{-1}, while for the linear PEGs the value of $\Phi = 2.87\times10^{23}$ mol^{-1}.[1] It must be noted that the Flory-Fox parameter could be different depending on the degree of branching.[2] Based on the estimated Rg values the corresponding branching factor has been obtained.

$$g = \frac{R_{g,b}^2}{R_{g,lin}^2};$$

Moreover, a quantitative relationship between g and g' can be established as follows: $g' \approx g^b$.[3] (Figure 4 SI) For hyperbranched topologies, a wide spread of b values in the range of $2 < b < 0.26$ was postulated for different polymers.[4-6] Surprisingly, b was found to be equal to 1.51 ± 0.02. This value correlates well with the theoretically predicted value for branched polymers by Stockmayer (b = 1.5).[7]

Table 4 SI. Correlation parameters of the contraction factors, g and g' of the *hb*PEG.

G_i-G_j*	$b_{ij} \pm \Delta b_{ij}$	$K_{ij} \pm \Delta K_{ij}$	r_{ij}
g – M	-(0.39 ± 0.01)	5.95 ± 0.50	0.9970
g' – g	1.51 ± 0.02	3.1 ± 0.5	0.9998

References

1. Freire, J., Conformational Properties of Branched Polymers: Theory and Simulations. In *Branched Polymers II*, Roovers, J., Ed. Springer Berlin Heidelberg: **1999**; Vol. 143, 35-112.
2. Tande, B. M.; Wagner, N. J.; Mackay, M. E.; Hawker, C. J.; Jeong, M. *Macromolecules* **2001**, *34*, 8580-8585.
3. Burchard, W., Solution Properties of Branched Macromolecules. In *Branched Polymers II*, Roovers, J., Ed. Springer Berlin Heidelberg: **1999**; Vol. 143, 113-194.
4. Ioan, C. E.; Aberle, T.; Burchard, W. *Macromolecules* **1999**, *32*, 7444-7453.
5. Ioan, C. E.; Aberle, T.; Burchard, W. *Macromolecules* **2001**, *34*, 3765-3771.
6. De Luca, E.; Richards, R. W. *J. Polym. Sci. Part B Polym. Phys.* **2003**, *41*, 1339-1351.
7. Stockmayer, W. H.; Fixman, M. *Ann. N. Y. Acad. Sci.* **1953**, *57*, 334-352.

2.3 Controlling the Molar Mass of Hyperbranched Poly(ethylene oxide) Copolymers via Polymerization under Slow Monomer Addition Conditions

Jan Seiwert[1,‡], Jürgen Vitz[2,3,‡], Tobias Majdanski[2,3,‡], Tobias Kaiser[1], Ulrich S. Schubert[2,3,4], Holger Frey[1,]*

[1] Institute of Organic Chemistry, Organic and Macromolecular Chemistry, Duesbergweg 10-14, Johannes Gutenberg University Mainz, 55128 Mainz, Germany

[2] Laboratory of Organic and Macromolecular Chemistry (IOMC), Humboldtstr. 10, Friedrich Schiller University Jena, 07743 Jena, Germany

[3] Jena Center for Soft Matter (JCSM), Philosophenweg 7, Friedrich Schiller University Jena, 07743 Jena, Germany

[4] Dutch Polymer Institute (DPI), P.O. Box 902, 5600 AX Eindhoven, the Netherlands

[‡] These authors contributed equally to this work.

In preparation.

The data shown in this chapter represent preliminary results as this project is still in progress.

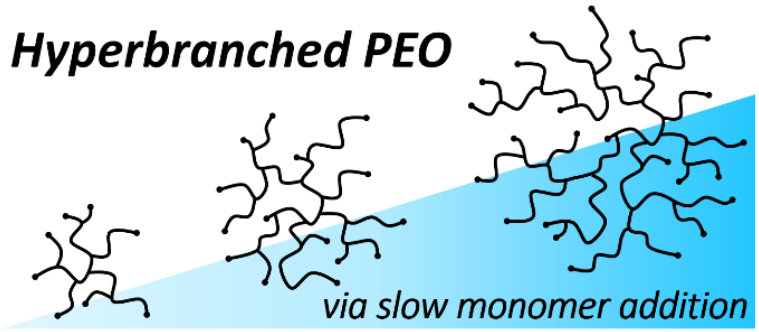

Abstract

Hyperbranched poly(ethylene oxide) (*hb*PEO) copolymers with adjustable molar mass have been prepared using a slow monomer addition (SMA) procedure. Realizing a SMA procedure was the key to achieving control of the degrees of polymerization. The challenge of continuously adding low-boiling ethylene oxide and high-boiling glycidol to a partially deprotonated trimethylolpropane (TMP) core at 100 °C was solved by employing a customized, automated reactor setup. The setup comprised pressure resistant autoclaves and burettes, and customized mass flow controllers for the simultaneous addition of both liquid and gaseous monomers. An integrated automation and control unit was employed to ensure controlled copolymerization. By variation of the monomer to initiator ratio, three *hb*PEO copolymers exhibiting molar masses ranging from 3500 to 6800 g mol^{-1} and comparable glycidol ratios of 24% to 33% (determined by ^{1}H NMR spectroscopy) were obtained. SEC characterization based on linear PEO standards yielded lower apparent molar masses in the range of 3000 to 4100 g mol^{-1} and narrow to moderate dispersities (M_w/M_n = 1.2 to 1.5). Medium degrees of branching ranging from 0.41 to 0.54 were determined by inverse gated ^{13}C NMR spectroscopy.

Introduction

Due to its excellent solubility in aqueous media and its low toxicity, poly(ethylene oxide) (PEO) has become the gold standard polymer for pharmaceutical applications and a wide-spread additive in cosmetic and food products as well.[1,2] The prevalent production process for PEO relies on the anionic ring-opening polymerization (AROP) of ethylene oxide. The ethylene oxide monomer, however, is a carcinogenic, mutagenic, toxic and extremely flammable substance. Its low boiling point of 11 °C complicates safe processing, particularly at elevated temperatures.

As a consequence, EO polymerization on larger scales is commonly carried out in semibatch procedures under slow addition of the monomer to avoid uncontrolled pressure build-up, explosive decomposition and runaway reactions.[3,4] The required equipment capable of continuous addition of EO at elevated pressure over the course of the polymerization can hardly be found in university laboratories. However, Schubert and coworkers have presented an automated semibatch reactor setup for the synthesis of well-defined PEO on the multigram scale recently.[5] Using common laboratory glassware, the semibatch approach can only be realized safely, if EO is processed under ambient pressure and strong cooling in the liquid state.[6] Although the slow addition of EO is an important safety precaution for the preparation of PEO on larger

scales, it is not a necessary prerequisite for a controlled polymerization from a mechanistic point of view. Provided that appropriate reaction conditions are applied, the anionic ring-opening polymerization of EO proceeds in a living manner, independent of whether the reaction is conducted in a semibatch procedure or in a batch procedure. A large variety of well-defined linear PEO polymers and copolymers have been prepared by simple batch reactions on the lab scale.[2,7]

In contrast, slow monomer addition is a mandatory measure for multibranching glycidol polymerization with control of the degree of polymerization. Due to a different polymerization mechanism of glycidol from the polymerization mechanism of EO, batch procedures for the multibranching polymerization of glycidol do not enable control of the degree of polymerization.[8–12] The mechanism of the anionic ring-opening multibranching polymerization is shown in Scheme 1. Glycidol acts as an inimer, comprising both a polymerizable epoxide ring and a hydroxyl moiety capable of initiating the growth of a new polyether chain. Chain transfer reactions occur due to a fast proton exchange equilibrium between different hydroxyl and alkoxide moieties, particularly if the monomer concentration is high. Polymerization under slow monomer addition (SMA) conditions is essential for obtaining well-defined hyperbranched polyglycerol (co)polymers.[13–21] SMA allows keeping the monomer concentration low during the entire course of the polymerization. This has a profound influence on polymerization kinetics, and side reactions involving two monomer molecules are reduced. Since hyperbranched polymers feature advantages over their linear counterparts, such as a compact three-dimensional structure and large amounts of functional end groups,[22,23] our group recently introduced hyperbranched analogues of widely used linear poly(alkylene oxide)s.[20,24,25] These materials can be obtained by anionic ring-opening copolymerization of EO, propylene oxide PO or 1,2-butylene oxide with glycidol in batch procedures without control over the degree of polymerization. To date, the low boiling points of EO and PO (34 °C) in combination with the high reaction temperatures required for the polymerization of glycidol have prevented slow monomer copolymerization procedures for PO/glycidol and EO/glycidol. Only limited variation of the molar masses has been achieved for hyperbranched PEO (*hb*PEO) by employing different solvents for the copolymerization of EO and glycidol to date.[26]

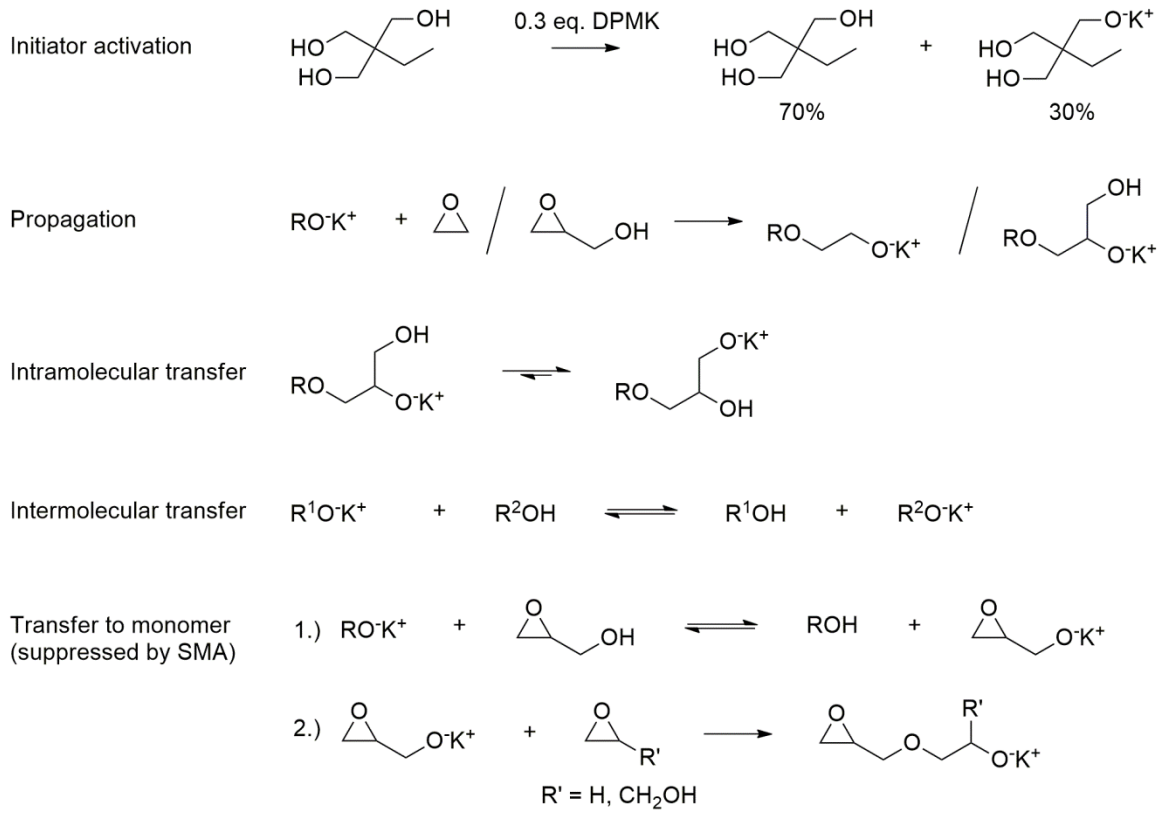

Scheme 1. Mechanism of the anionic ring-opening multibranching copolymerization of EO and glycidol, showing intramolecular transfer as a key step to obtain branching.

In the current work we present a slow monomer addition procedure for the controlled anionic multibranching copolymerization of ethylene oxide and glycidol, resulting in well-defined *hb*PEO copolymers with adjustable molar mass. To realize slow monomer addition for the low-boiling EO (b_p = 11 °C) and to ensure a safe polymerization under the evolving EO pressure, we rely on an automated reactor setup of Schubert and coworkers. The data shown herein represent preliminary results, as this project is still in progress at present and other molecular weights will be prepared.

Experimental Part

Materials

All reagents and solvents were purchased from Sigma Aldrich or Linde. Purification of ethylene oxide (EO) was performed in the closed autoclave system under inert conditions: EO (99.9%) was condensed from the lecture bottle into the dry glass autoclave, dried over sodium and subsequently transferred to the pressure burette via distillation. Glycidol (96%) and 1-methyl-2-pyrrolidone (NMP, 99.0%) were purified by distillation over calcium hydride before use. Diphenylmethyl potassium (DPMK) solution in THF was prepared following an established procedure.[27] The exact concentration was determined by titration prior to use. Trimethylolpropane (TMP) was dried in high vacuum for 4 hours at 60 °C before use.

Instrumentation

Reactor setup: Figure 1 shows a schematic illustration of the experimental setup comprising two autoclaves, two pressure burettes, two mass flow controllers, a cryostat and an automation and control unit. Polymerizations were carried out in two BüchiGlasUster (Uster, Switzerland) small scale PicoClave glass autoclaves (200 and 300 mL, pressure resistant up to 6 bar and 10 bar, respectively). The autoclaves are equipped with a stainless steel cover, fast action closure, pressure gauge, different valves, a rupture disc and a polycarbonate safety shield. They were dried under vacuum for 24 hours and flushed with argon prior to use.

The pressure burettes consist of a cylindrical glass tube, equipped with a heating/cooling jacket, inside a stainless steel frame. They are pressure resistant up to 12 bar. Both autoclaves and burettes are equipped with PT100 temperature sensors as well as a signal to mA converters (GE UNIK 5000, PRelectronics 9113B2 and 9116B), displays (PRelectronics 4501) as well as power supply and control (PRelectronics 9410, 9420). Two Bronkhorst mini CORI-FLOW (M12V14I-PGD-22-K-S, Bronkhorst High-Tech B.V., Ruurlo, Netherlands) mass flow controllers were used (flow rate ranging from 0.1 to 200 g h^{-1}, flow rate accuracy: ±0.2%). Temperature was adjusted using a Huber Unistat 390w chiller, enabling a temperature range of -90 °C to 200 °C (Huber Kältemaschinenbau GmbH, Offenburg, Germany). A Siemens Simatic S7-1200 was employed for the automation and control system (Siemens AG, Munich, Germany), equipped with the following modules: CPU 1212C, 2x SM 1231 AI, CM 1241 RS232, CM 1243-5 Profibus-DP, CSM 1277 Network switch, SM 1207 power supply.

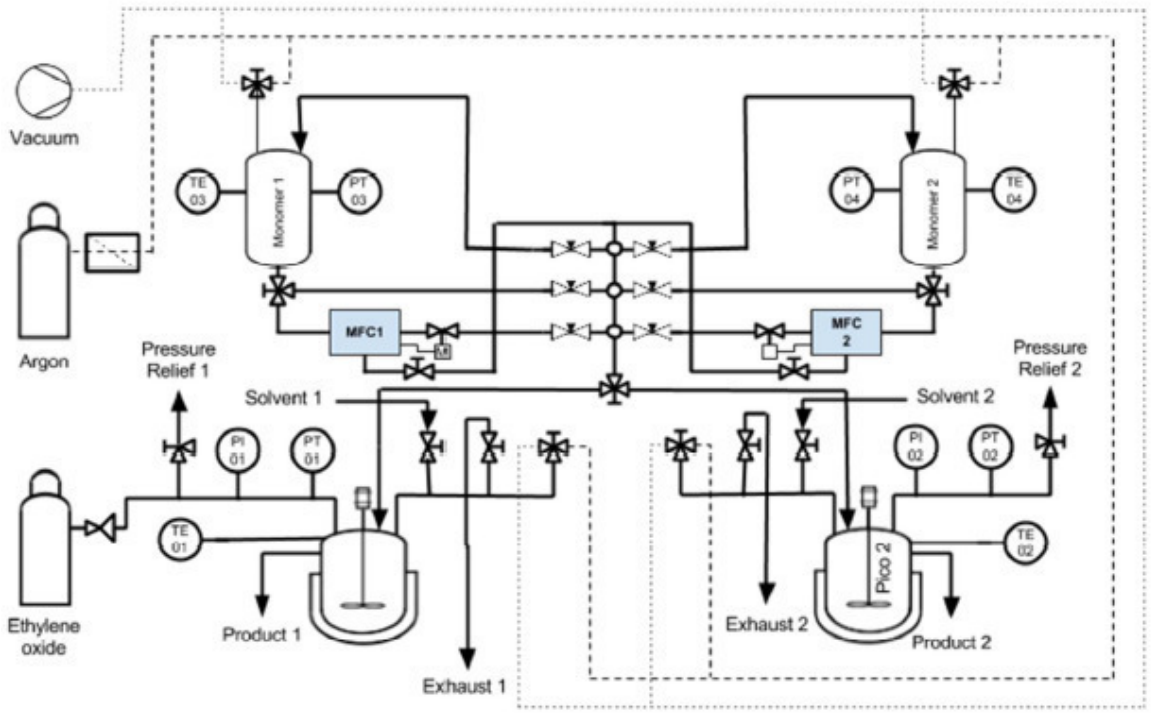

Figure 1. Piping and instrumentation diagram (P&ID) showing the reactor setup.[5] (Reproduced by permission of The Royal Society of Chemistry)

NMR spectroscopy: ^{1}H and inverse gated ^{13}C NMR spectra were recorded on a *Bruker* Advance III HD 400 (5 mm BBFO-SmartProbe with z-gradient and ATM) at 400 MHz and 100 MHz, respectively. The residual signals of the deuterated solvent were utilized as an internal reference.

Size-exclusion chromatography: SEC measurements in DMF (containing 0.25 g L^{-1} of lithium bromide) were performed using an integrated Agilent 1100 series instrument, equipped with a PSS HEMA column combination ($10^6/10^4/10^2$ Å porosity), UV and RI detector. Calibration is based on linear poly(ethylene oxide) standards (Polymer Standards Service).

Synthesis

Initiator preparation: The procedure was carried out inside the glove box under inert gas atmosphere. In a glass flask with a screw cap and tube connection, 268 mg (2 mmol, 1 eq.) TMP was dissolved in 120 mL NMP. The initiator was partially deprotonated by addition of 136 mg (0.66 mmol, 0.3 eq.) DPMK. The flask was sealed and removed from the glove box. The solution was homogenized by ultrasonication and transferred to the autoclave via a tube under reduced pressure. For the synthesis of *hb*PEO_{69}, an initiator solution with double concentration was used.

Copolymerization of EO and glycidol: Glycidol was mixed with an equal volume of NMP in a pressure-resistant glass flask with a screw cap and tube connection. The flask was connected to one of the mass flow controllers. The other mass flow controller was connected to a pressure burette containing EO. After heating the initiator solution to 100 °C and applying excess argon pressure of 1 bar (0.5 bar for *hb*PEO_{69}), the slow addition of the glycidol/NMP mixture and EO at a respective rate of 0.5 g h^{-1} was started. The amount of monomers added was adjusted via the automated control unit according to the desired molecular weight. After addition was completed, the autoclave was kept at 100 °C for one hour and then cooled to room temperature. Excess pressure was released through a washing bottle containing a concentrated potassium hydroxide solution in isopropyl alcohol, to eliminate residual EO. The polymerization was terminated using acetic acid. The reaction mixture was transferred to a flask and solvents were removed by distillation in vacuum. The crude polymers were purified by twofold precipitation in cold diethyl ether and subsequent dialysis in MeOH (MWCO = 1 kDa) to yield *hb*PEO as a brown, viscous oil.

^{1}H NMR (DMSO-d_6, 400 MHz): δ (ppm) = 4.76 – 4.35 (m, br, OH); 3.90 – 3.15 (m, O-CH, O-CH_2); 1.36 – 1.18 (m, 2H, CH_3-CH_2 (TMP)); 0.87 – 0.75 (m, 3H, CH_3 (TMP)).

^{13}C NMR (DMSO-d_6, 100 MHz): δ (ppm) = 80.25 – 79.45 (m, CH $G_{1,3\text{-Linear}}$); 78.52 – 77.42 (m, CH $G_{\text{Dendritic}}$); 73.22 – 72.10 (m, 2 CH_2 $G_{1,4\text{-Linear}}$); 72.04 – 69.62 (m, 2 CH_2 $G_{\text{Dendritic}}$, 2 CH_2 EO_{Linear}, *C*H_2-CH_2-OH EO_{Terminal}, CH G_{Terminal}, CH_2 G_{Terminal}); 69.61 – 68.37 (m, CH_2 $G_{1,3\text{-Linear}}$, CH-OH $G_{1,4\text{-Linear}}$); 63.39 – 62.96 (CH_2-OH G_{Terminal}); 60.87 – 60.07 (m, CH_2-OH EO_{Terminal}, CH_2-OH $G_{1,3\text{-Linear}}$).

Results and Discussion

The anionic ring-opening multibranching copolymerization of ethylene oxide (EO) with glycidol under slow monomer conditions was realized in analogy to the established procedure for synthesizing hyperbranched polyglycerol. However, a key issue in this context is the low boiling point (11°C) of EO in combination with the reaction temperature of 100°C required for the multibranching copolymerization. Both monomers were added continuously to a potassium alkoxide core in 1-methyl-2-pyrrolidone at 100 °C and 0.5 to 1 bar argon pressure. Due to the high reaction temperature and the low boiling point of EO, ensuring a safe and controlled execution of the addition and copolymerization of these two comonomers presented a particular challenge. While homopolymerization of glycidol is usually conducted using common laboratory glassware, the copolymerization with EO requires special equipment comprising pressure resistant autoclaves and burettes, and customized mass flow controllers for the simultaneous addition of

both a liquid glycidol/NMP mixture and gaseous EO. The slow monomer addition was enabled via an automated control unit, which allowed dosing the specified amounts of comonomers at a constant rate of 0.5 g h^{-1}.

By varying the duration of the addition process and, thereby, the initial molar ratio of added epoxide monomers to initiator, three different *hb*PEO copolymers with target molar masses of 2700, 5200 and 6700 g mol^{-1} were synthesized. SEC and NMR characterization data of the copolymers are summarized in Table 1.

Table 1. NMR and SEC characterization data of the *hb*PEO copolymers.

Sample[a]	M_n[b] (g mol^{-1})	M_n[c] (g mol^{-1})	$Đ$[c]	$X_{n,EO}$[b,e]	$X_{n,G}$[b,e]	*G%* theo.	*G%*[b]	*G%*[d]	*DB*[d]
hbPEO_{69}	3500	3000	1.23	52	17	23	24	31	0.41
hbPEO_{98}	5200	3600	1.37	68	30	23	31	40	0.48
hbPEO_{127}	6800	4100	1.54	85	42	27	33	41	0.54

[a] Terminology: indices denote the overall degree of polymeriziaton, determined from ^{1}H NMR spectroscopy, [b] determined from ^{1}H NMR spectroscopy, [c] determined from SEC (DMF, linear PEO standard), [d] determined from inverse gated ^{13}C NMR spectroscopy, [e] number of the respective repeating unit per polymer, rounded to integer.

The SEC traces of the copolymers are shifted to lower elution volumes (Figure 2) with increasing targeted molar mass, confirming successful variation of the molar mass. Oligomeric side products, which can be seen in the elugrams of the crude polymers (Figure 2, left), were removed by precipitating the copolymers in diethyl ether and subsequent dialysis in MeOH (MWCO = 1000 g mol^{-1}), resulting in mostly monomodal molecular weight distributions (Figure 2, right). SEC calibration based on linear PEO standards yields apparent molar masses ranging from 3000 to 4100 g mol^{-1} and narrow to moderate dispersities in the range of 1.23 to 1.54. While the average molar mass of 3000 g mol^{-1} determined for *hb*PEO_{69} is in good agreement with the targeted molar mass, the values determined for the larger copolymers deviate significantly from theory. This can be ascribed to the increasing difference in the hydrodynamic volume of a hyperbranched polymer and the corresponding linear standard material of the same molar mass with increasing degree of polymerization, as it was demonstrated in previous work by Perevyazko et al..[26]

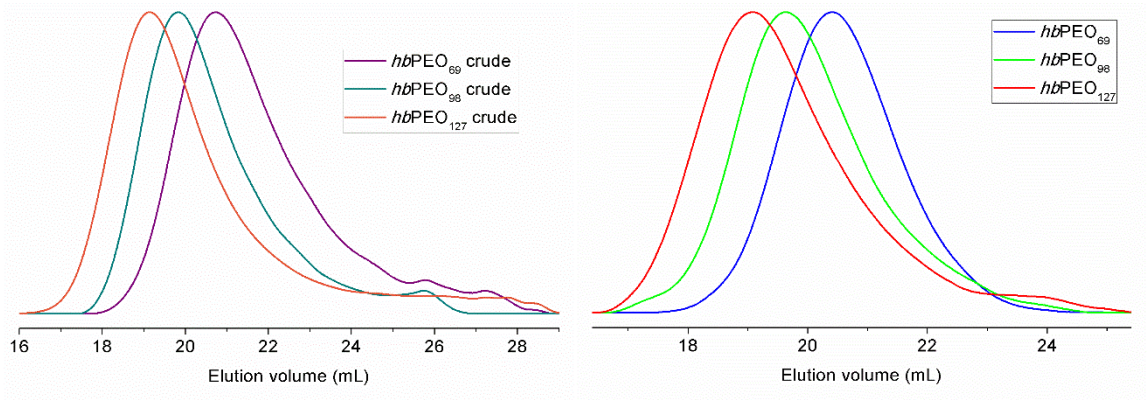

Figure 2. SEC elugrams (DMF) of three *hb*PEO copolymers with different molar masses before (left) and after (right) removal of oligomeric side products.

^{1}H NMR spectroscopy in DMSO-d_6 (Figure 3) provides information about the molar mass and the composition of the *hb*PEO copolymers. Using the methyl signal of the TMP core at 0.8 ppm as a reference, the number average (X_n) of glycerol (G) and EO repeating units per polymer can be determined from the hydroxyl signal (4.4 to 4.8 ppm) and the polyether backbone signal (3.2 to 3.9 ppm), according to equation 1 and 2.

$$X_{n,G} = I(\mathrm{OH}) - 3 \tag{1}$$

$$X_{n,EO} = \frac{I(\mathrm{backbone}) - 5 \cdot n_G - 6}{4} \tag{2}$$

The normalized overlay of the spectra of the three samples in Figure 3 clearly demonstrates the differences in the degree of polymerization. The intensity of the backbone and hydroxyl signal increases with increasing target molar mass. The average molar mass of the copolymers can be calculated from the number of repeating units as follows:

$$M_n(hb\mathrm{PEO}) = M(\mathrm{TMP}) + 74.1\ {}^{\mathrm{g}}/_{\mathrm{mol}}\ X_{n,G} + 44.1\ {}^{\mathrm{g}}/_{\mathrm{mol}}\ X_{n,EO} \tag{3}$$

Average molar masses determined from ^{1}H NMR spectroscopy range from 3500 to 6800 g mol^{-1}. The values match the targeted molar masses well. Only the molar mass determined for *hb*PEO$_{69}$ is 800 g mol^{-1} higher than the targeted value (cf. Table 1). This can be ascribed to the removal of oligomeric products by dialysis prior to the NMR characterization. All *hb*PEO samples were purified using a membrane with molecular weight cut-off (MWCO) at 1000 g mol^{-1}. Since the targeted molar mass of *hb*PEO$_{69}$ is closest to the MWCO, a larger fraction of the polymer was removed during dialysis, resulting in a shifted molar mass average. The determination of absolute molar mass values by analytical ultracentrifugation and on-line viscometry is currently in progress.

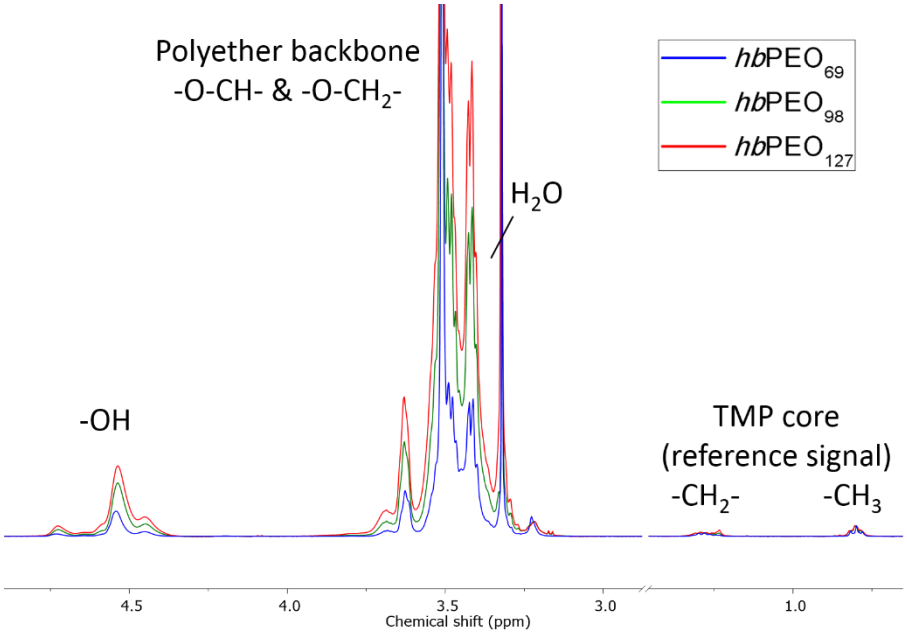

Figure 3. ^{1}H NMR spectra (DMSO-*d*$_6$, 400 MHz) of three *hb*PEO copolymers with different molar masses, normalized on the methyl signal of the trimethylolpropane (TMP) core.

From the numbers of repeating units determined by ^{1}H NMR spectroscopy based on the TMP core molecule as a reference, the copolymer composition of the *hb*PEO samples was calculated according to equation 4.

$$G\ \text{content} = \frac{X_{n,G}}{X_{n,G} + X_{n,EO}} \tag{4}$$

For comparison, the copolymer composition was also determined from inverse gated (IG) ^{13}C NMR spectroscopy as described in previous work (equation 5).[24] Using this approach, integration over hydroxyl proton signals and the overlay of the polyether backbone signals with the water signal were eliminated as potential sources of error. This method, however, suffers from a worse signal to noise ratio than determination of the composition based on ^{1}H-NMR spectra.

$$G\ \text{content} = \frac{I(G_{Dendritic}) + I(G_{1,3Linear}) + I(G_{1,4Linear}) + I(G_{Terminal})}{I(G_{Dendritic}) + I(G_{1,3Linear}) + I(G_{1,4Linear}) + I(G_{Terminal}) + I(EO_{Linear}) + I(EO_{Terminal})} \tag{5}$$

IG ^{13}C NMR spectroscopy yields higher glycidol contents than ^{1}H NMR spectroscopy with a deviation of 7% to 9% (cf. Table 1). Further investigation will be necessary to identify the reason for this deviation. The glycidol content in the monomer feed of the samples *hb*PEO$_{69}$ and *hb*PEO$_{98}$ was 23%. The monomer feed of sample *hb*PEO$_{127}$ contained 27% glycidol. Samples *hb*PEO$_{98}$ and *hb*PEO$_{127}$ were prepared applying an argon pressure of 1 bar to improve EO solvation and reaction rate. Due to the evaporation of EO at 100°C, the pressure in the autoclave further increased to 1.2 - 1.3 bar during the reaction. As a consequence, EO also condensed in the tubing connection

and was therefore not converted completely. Thus, the glycidol content incorporated into the resulting copolymers was found to be 6 and 8% (IG ^{13}C NMR: 14 and 17%) higher than the glycidol content in the monomer feed. To avoid EO condensation, the ensuing synthesis of *hb*PEO$_{69}$ was performed at a lower pressure of 0.5 bar. The glycidol content incorporated into this copolymer matches the monomer feed ratio well. Only a slight deviation of 1% (IG ^{13}C NMR: 8%) was found.

The degree of branching (DB) is a key parameter for describing the structure of a hyperbranched polymer. It can assume values between 0 (linear) and 1 (fully branched). The DB of *hb*PEO can be determined from IG ^{13}C NMR spectroscopy as described in the literature.[24,28] Figure 4 shows the DB values, calculated according to equation 6, in dependence of the glycidol content.

$$DB = \frac{2\, I(G_{Dendritic})}{2\, I(G_{Dendritic}) + I(G_{1,3Linear}) + I(G_{1,4Linear}) + I(EO_{Linear})} \quad (6)$$

The calculated DB values in the range of 0.41 to 0.54 confirm the synthesis of branched polymers with medium degree of branching. They are close to the theoretical values for an ideal AB/AB$_2$ copolymerization by slow monomer addition (Figure 6, dashed line).[13] The slightly higher DB value of *hb*PEO$_{127}$ (red) might be a statistical deviation. As expected from theory, the DB values determined herein are higher than the DB values of *hb*PEO copolymers with comparable composition obtained by batch copolymerization.[26,28] Further experiments concerning systematic variation of the copolymer composition will help to elucidate the general branching behavior of *hb*PEO copolymers prepared via slow monomer addition.

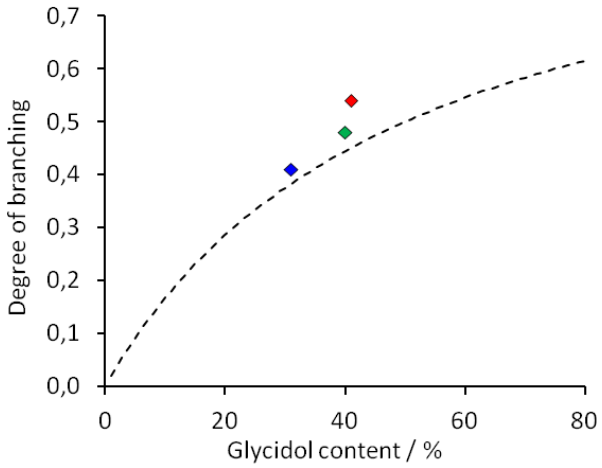

Figure 4. Degrees of branching of *hb*PEO$_{69}$ (blue), *hb*PEO$_{98}$ (green) and *hb*PEO$_{127}$ (red) as a function of the glycidol content (determined from IG ^{13}C NMR spectroscopy). The dashed line represents theoretical values for a random AB/AB$_2$ copolymerization by slow monomer addition.[13]

Conclusion

In summary, three *hb*PEO copolymers with different molar masses were synthesized by anionic ring-opening copolymerization of ethylene oxide and glycidol. Achieving control of the degree of polymerization presented a key challenge for the multibranching copolymerization of glycidol and EO. This challenge was mastered by employing a slow monomer addition protocol instead of the batch copolymerization procedure established previously. Molar masses were varied systematically in a range of 3500 to 6800 g mol^{-1} (determined by ^{1}H NMR spectroscopy), surpassing the molar mass range accessible by batch copolymerization. The technical requirements for a safe and controlled continuous addition of EO and glycidol were met by conducting the reaction in an autoclave system setup including customized mass flow controllers. Glycidol incorporation in the copolymers was found to be slightly higher than the glycidol fraction in the monomer feed due to condensation of EO in the tubing connections which resulted in incomplete EO conversion. Medium degrees of branching in the range of 0.41 to 0.54 were determined from IG ^{13}C NMR spectroscopy. Further studies with regard to absolute molar mass determination, enhancement of the accessible molar mass range, variation of the copolymer composition, and establishing structure-property relationships are in progress. The synthetic strategy presented herein provides access to amorphous, multifunctional, hyperbranched, mainly PEO-based materials with adjustable number of end groups and molar mass. The procedure can be modified in various ways to increase the number and type of functional groups: First, it opens up synthetic pathways towards heterofunctional, hyperbranched PEOs by terpolymerization with glycidol and another functional epoxide monomer. Second, it enables the controlled introduction of a single functionality at the focal point of the branched structure by employing a functional core molecule. Third, linear-hyperbranched block and graft copolymer architectures with a PEO-based hyperbranched blocks become accessible by initiating the polymerization from a hydroxyl-functionalized linear polymer.

Acknowledgement

The authors thank Alexander Meier for technical assistance.

References

1. Dingels, C.; Schömer, M.; Frey, H. *Chem. Unserer Zeit* **2011**, *45*, 338–349.
2. Herzberger, J.; Niederer, K.; Pohlit, H.; Seiwert, J.; Worm, M.; Wurm, F. R.; Frey, H. *Chem. Rev.* **2016**, *116*, 2170–2243.
3. Gustin, J.-L. *IChemE Symposium Series* **2000**, *147*, 251–263.
4. Salzano, E.; Di Serio, M.; Santacesaria, E. *Proc. Safety prog.* **2007**, *26*, 304–311.
5. Vitz, J.; Majdanski, T. C.; Meier, A.; Lutz, P. J.; Schubert, U. S. *Polym. Chem.* **2016**.
6. Sandler, S. R.; Karo, W. Polyoxyalkylation of Hydroxy Compounds. *Polymer Synthesis*; Elsevier, **1996**; 152–182.
7. Brocas, A.-L.; Mantzaridis, C.; Tunc, D.; Carlotti, S. *Progress in Polymer Science* **2013**, *38*, 845–873.
8. Sandler, S. R.; Berg, F. R. *J. Polym. Sci. A Polym. Chem.* **1966**, *4*, 1253–1259.
9. Tsuruta, T.; Inoue, S.; Koenuma, H. *Makromol. Chem.* **1968**, *112*, 58–65.
10. Vandenberg, E. J. *J. Polym. Sci. Polym. Chem. Ed.* **1985**, *23*, 915–949.
11. Tokar, R.; Kubisa, P.; Penczek, S.; Dworak, A. *Macromolecules* **1994**, *27*, 320–322.
12. Dworak, A.; Walach, W.; Trzebicka, B. *Macromol. Chem. Phys.* **1995**, *196*, 1963–1970.
13. Sunder, A.; Türk, H.; Haag, R.; Frey, H. *Macromolecules* **2000**, *33*, 7682–7692.
14. Tonhauser, C.; Schüll, C.; Dingels, C.; Frey, H. *ACS Macro Lett.* **2012**, *1*, 1094–1097.
15. Shenoi, R. A.; Narayanannair, J. K.; Hamilton, J. L.; Lai, B. F.; Horte, S.; Kainthan, R. K.; Varghese, J. P.; Rajeev, K. G.; Manoharan, M.; Kizhakkedathu, J. N. *J. Am. Chem. Soc.* **2012**, *134*, 14945–14957.
16. Schüll, C.; Gieshoff, T.; Frey, H. *Polym. Chem.* **2013**, *4*, 4730.
17. Shenoi, R. A.; Chafeeva, I.; Lai, B. F. L.; Horte, S.; Kizhakkedathu, J. N. *J. Polym. Sci. A Polym. Chem.* **2015**, *53*, 2104–2115.
18. Son, S.; Shin, E.; Kim, B.-S. *Macromolecules* **2015**, *48*, 600–609.
19. Alkan, A.; Klein, R.; Shylin, S. I.; Kemmer-Jonas, U.; Frey, H.; Wurm, F. R. *Polym. Chem.* **2015**, *6*, 7112–7118.
20. Seiwert, J.; Leibig, D.; Kemmer-Jonas, U.; Bauer, M.; Perevyazko, I.; Preis, J.; Frey, H. *Macromolecules* **2016**, *49*, 38–47.
21. Niederer, K.; Schüll, C.; Leibig, D.; Johann, T.; Frey, H. *Macromolecules* **2016**, *49*, 1655–1665.
22. Voit, B. I.; Lederer, A. *Chem. Rev.* **2009**, *109*, 5924–5973.
23. Yan, D.; Gao, C.; Frey, H. *Hyperbranched Polymers: Synthesis, Properties, and Applications*; Wiley series on polymer engineering and technology; Wiley: Hoboken, 2011.

24. Wilms, D.; Schömer, M.; Wurm, F.; Hermanns, M. I.; Kirkpatrick, C. J.; Frey, H. *Macromol. Rapid Commun.* **2010**, *31*, 1811–1815.
25. Schömer, M.; Seiwert, J.; Frey, H. *ACS Macro Lett.* **2012**, *1*, 888–891.
26. Perevyazko, I.; Seiwert, J.; Schömer, M.; Frey, H.; Schubert, U. S.; Pavlov, G. M. *Macromolecules* **2015**, *48*, 5887–5898.
27. Normant, H.; Angelo, B. *Bull. Soc. Chim. Fr.* **1960**, *2*, 354–359.
28. Frey, H.; Hölter, D. *Acta Polym.* **1999**, *50*, 67–76.

2.4 Hyperbranched Polyols via Copolymerization of 1,2-Butylene Oxide and Glycidol: Comparison of Batch Synthesis and Slow Monomer Addition

Jan Seiwert[1], Daniel Leibig[1,2], Ulrike Kemmer-Jonas[1], Marius Bauer[1], Igor Perevyazko[3], Jasmin Preis[4], Holger Frey[1,2,]*

[1] Institute of Organic Chemistry, Johannes Gutenberg-University, Duesbergweg 10-14, 55128 Mainz, Germany

[2] Graduate School Materials Science in Mainz, Staudinger Weg 9, 55128 Mainz, Germany

[3] Department of Molecular Biophysics and Polymer Physics, St. Petersburg State University, Universitetskaya nab. 7/9, 199034, Saint Petersburg, Russia

[4] PSS Polymer Standards Service GmbH, In der Dalheimer Wiese 5, 55120 Mainz, Germany

Published in *Macromolecules* **2016**, *49*, 38-47.

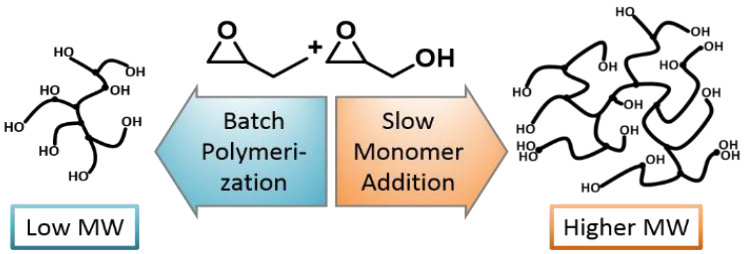

Abstract

Hyperbranched poly(butylene oxide) polyols have been synthesized by multibranching anionic ring-opening copolymerization of 1,2-butylene oxide and glycidol. Systematic variation of the composition from 24 to 74% glycidol content resulted in a series of moderately distributed copolymers (Đ = 1.41 to 1.65, SEC), albeit with limited molecular weights in the solvent-free batch process in the range of 900 to 1300 g mol^{-1} (apparent M_n determined by SEC). In situ monitoring of the copolymerization kinetics by ^{1}H NMR showed a pronounced compositional drift with respect to the monomer feed, indicating a strongly tapered microstructure caused by the higher reactivity of glycidol. In the case of slow monomer addition considerably higher apparent molecular weights up to 8500 g mol^{-1} were obtained (SEC). By alteration of the comonomer ratio, aqueous solubility of the hyperbranched copolymers could be tailored, resulting in well-defined cloud points between 20 and 84 °C. Glass transition temperatures between -60 and -29 °C were observed for the resulting polyether polyols. High degrees of branching (DB) between 0.45 and 0.77 were calculated from inverse gated (IG) ^{13}C NMR. On-line viscosimetry and analytical ultracentrifugation (AUC) were employed to study hydrodynamic properties and to establish a universal calibration curve for the determination of absolute molecular weights. This resulted in M_w values between 2100 and 35000 g mol^{-1} that were generally 2-3 times higher than the apparent values determined by SEC with linear PEG standards.

Introduction

Since their commercialization in the 1950s, poly(alkylene oxide)s have become important materials for an immense variety of consumer products and industrial applications.[1] Both improving synthetic strategies, exploring and tailoring of polymer architectures and the resulting materials properties have been in the focus of research in this area. Among the alkylene oxide monomers, ethylene oxide and propylene oxide are the starting materials for the majority of polyether syntheses. Besides these two monomers, 1,2-butylene oxide (BO) is the third alkylene oxide monomer that is commercially available on an industrial scale. With the advent of advanced polymerization methods to overcome the low reactivity of the BO monomer and to suppress chain transfer reactions, materials based on poly(butylene oxide) (PBO) are now gaining increasing attention.[2–7] PBOs are used as hydrophobic, oil-soluble polyether materials.[8] Amphiphilic copolymers consisting of PBO and a hydrophilic block have found application as non-ionic surfactants.[9] Linear and cyclic copolymer architectures with PBO and poly(ethylene oxide) (PEO)

have been studied in detail, particularly by Booth and coworkers.[10] Carlotti et al. synthesized PBO-based amphiphilic structures containing multiple hydroxyl groups, obtained in two steps by monomer-activated copolymerization of BO with ethoxyethyl glycidyl ether or *tert*-butyl glycidyl ether and subsequent deprotection.[11] The surfactant properties of the resulting linear PG-*b*-PBO copolymers, however, were not explored.

Hyperbranched polymers have been attracting significant attention for more than two decades because they combine dendrimer-like structural features with facile accessibility.[12,13] They possess a high number of functional end groups and a compact structure, resulting in low viscosity both in bulk and in solution. Generally, crystallization is impeded by branching in this class of polymers, leading to amorphous structures. Synthetic methods that provide control over molecular weights and molecular weight distributions of hyperbranched polymers are an important target in this area.[14–20]

Glycidol is an established branching comonomer for anionic and cationic multibranching polyether synthesis.[15,21–25] Anionic polymerization using slow monomer addition (SMA) gives access to well-defined hyperbranched polyglycerols with a broad range of accessible molecular weights and rather narrow molecular weight distributions.[26] This technique has been successfully employed for the homopolymerization of glycidol and also for copolymerization with several glycidyl ethers. Via these comonomers, functional groups for 'click' coupling reactions, biodegradable cleavage sites, and redox-responsive ferrocene moieties were introduced into the hyperbranched polyether structure in recent years.[27–33]

To the best of our knowledge, hyperbranched poly(alkylene oxide) copolymers have not been synthesized using a slow monomer addition protocol to date, which is mainly due to the low boiling point of the relevant alkylene oxide monomers (bp_{EO} = 11 °C, bp_{PO} = 34 °C, bp_{BO} = 63 °C) and high temperatures required to polymerize glycidol at a reasonable rate. Taton and coworkers prepared well-defined oligomeric PG-*co*-PPO branching segments using a sequential procedure to generate dendrimer-like PEO structures.[34] Tsvetanov et al. obtained high molecular weight PG-*co*-PEO copolymers by bubbling gaseous EO through a solution of glycidol and a calcium amide-alkoxide initiator.[35] This method, however, permits limited glycidol incorporation of 3% at maximum. Recently, our group introduced a convenient one-step batch polymerization strategy for the anionic copolymerization of glycidol with EO and PO, respectively, allowing for systematic variation of the composition.[36–38] In this way, narrowly to moderately distributed hyperbranched polyethers containing PEO or poly(propylene glycol) (PPO) segments became accessible. Such

hyperbranched polyether polyols have found application as initiators for the synthesis of multiarm star polymers and as a scaffold for further end group modification.[39,40]

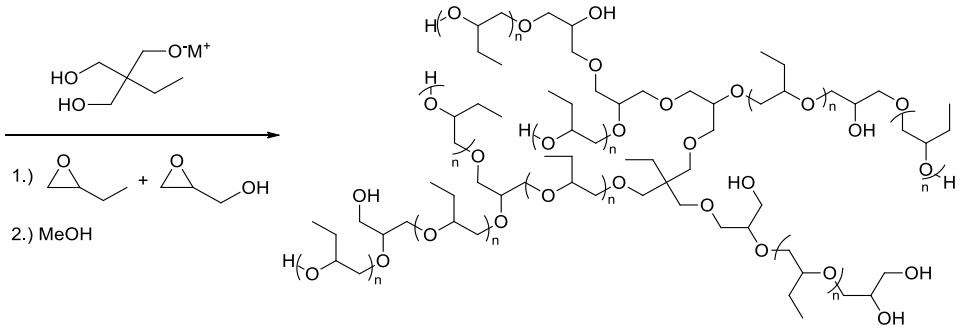

Scheme 1: Synthesis of hyperbranched copolymers from butylene oxide and glycidol.

In this work, we describe the first synthesis of hyperbranched PBO copolymers by random anionic copolymerization of butylene oxide with glycidol as a branching unit, both by batch polymerization and slow monomer addition procedures (Scheme 1). This allowed us to systematically vary both copolymer composition and molecular weight. For the batch process, detailed *in situ* investigations of the kinetics regarding the reaction rate of both comonomers have been carried out. In addition, we aim at characterization of absolute molecular weights of the novel hyperbranched polyethers by a combination of ultracentrifugation, viscosimetry and coupled SEC techniques.

Experimental Part

The instrumentation employed for characterization is described in the Supporting Information.

Materials

All solvents and reagents were purchased from Acros Organics or Sigma Aldrich and used as received, if not mentioned otherwise. 1,2-Butylene oxide (99%) and glycidol (96%) were dried over calcium hydride (CaH_2) and distilled in vacuum directly prior to use. Tetrahydropyran (THP) was freshly distilled from sodium prior to use.

Synthesis

Batch Copolymerization. In a 250 mL Schlenk flask equipped with a magnetic stirrer, 89 mg (0.66 mmol, 1.00 eq.) 1,1,1-tris(hydroxymethyl)propane (TMP) and 37 mg (0.22 mmol, 0.33 eq.) cesium hydroxide monohydrate were dissolved in 3 mL methanol, and 5 mL benzene were added. The reaction vessel was evacuated for at least 5 h to remove methanol and traces of water azeotropically. After cooling to -78 °C a combined amount of 100 mmol (150 eq) butylene oxide (BO) and glycidol (G) was syringed into the flask and the reaction mixture was then immediately heated to 120 °C and stirred for 48 h. Due to the pressure evolving in the early stages of the polymerization, the flask was secured against spontaneous removal of the septum and the release of gaseous BO. Excess methanol was added to terminate the reaction and the solution was neutralized by filtration over acidic cation exchange resin (DOWEX WX8). After removal of the solvent, the resulting pale brown oil was precipitated in a mixture of cold diethyl ether and petroleum ether (ratio depending on comonomer composition). All products were dried in vacuum over night at 85°C (yield 80 - 90%).

For *in situ* ^{1}H NMR kinetics, the dried initiator was dissolved in 0.5 mL DMSO-d_6 and placed in a NMR tube equipped with a Teflon stopcock. The solution was frozen, and G and BO were added under cooling. Immediately after melting, mixing and heating to 60 °C, the first ^{1}H NMR spectrum was measured. Spectra were recorded with 16 scans. The intervals between two measurements were 5 min within the first 2 hours, 10 min during the next 6 hours and extended afterwards.

Copolymerization under SMA (Slow Monomer Addition) Conditions. After drying in vacuum, the deprotonated initiator was dissolved in 1 mL THP and heated to 90 °C. A combined amount of 50 mmol G and BO diluted with an equal volume of THP was added to the reaction flask over the course of 3 days via a syringe pump. Termination was performed in analogy to the bulk polymerizations, and the resulting polymers were subsequently precipitated in methanol or dialyzed against methanol (MWCO 1000 g mol^{-1}).

^{1}H NMR (DMSO-d_6, 400 MHz): δ (ppm) = 4.55 – 4.33 (m, br, OH); 4.08 – 3.02 (m, O-CH, O-CH_2); 1.56 – 1.12 (m, CH_3-CH_2 (BO & TMP)); 0.87 (t, CH_3 (BO); 0.79 (t, CH_3 (TMP)).

^{13}C NMR (DMSO-d_6, 100 MHz): δ (ppm) = 80.6 – 79.0 (CH $G_{1,3\text{-Linear}}$, CH BO_{Linear}); 78.8 – 77.4 (CH $G_{Dendritic}$); 75.8 – 75.0 (CH_2 $BO_{Terminal}$); 74.6 – 73.6 (CH_2 BO_{Linear}) 73.2 – 72.1 (2 CH_2 $G_{1,4\text{-Linear}}$); 72.0 – 69.9 (2 CH_2 $G_{Dendritic}$, CH $G_{Terminal}$, CH $G_{Terminal}$, CH_2 $BO_{Terminal}$); 69.9 – 68.3 (CH_2 $G_{1,3\text{-Linear}}$, CH-OH $G_{1,4\text{-Linear}}$); 63.5 – 62.8 (CH_2-OH $G_{Terminal}$); 61.4 – 60.6 (CH_2-OH $G_{1,3\text{-Linear}}$).

Results and Discussion

A. Copolymer Synthesis and Characterization

Two different strategies have been employed for the ring-opening anionic copolymerization of butylene oxide (BO) and glycidol (G). The batch polymerization procedure is based on a modified protocol for the multibranching copolymerization of PO and G reported recently.[38] The lower reactivity of BO leads to low polymerization rates, thus long reaction times, and high reaction temperatures above the boiling point of BO (bp_{BO} = 63 °C) are required to obtain high conversion. The rise of pressure in the sealed flask due to the evaporation of the BO monomer in the early stages of the reaction accelerates the polymerization. It should be emphasized that the batch copolymerization does not require the use of a solvent. The monomer mixture was added to partially deprotonated TMP as an established trifunctional initiator in vacuum, heated to 120 °C for two days, and subsequently the polymerization was terminated by adding methanol (Scheme 1). Scheme 2 demonstrates the reaction mechanism of the copolymerization. Fast intra- and intermolecular proton transfer among the partially deprotonated hydroxyl groups leads to a branched polymer structure. Cesium hydroxide was used as a base because the soft Cs cation leads to weak coordination to the alkoxide, increasing the reactivity of the chain ends.

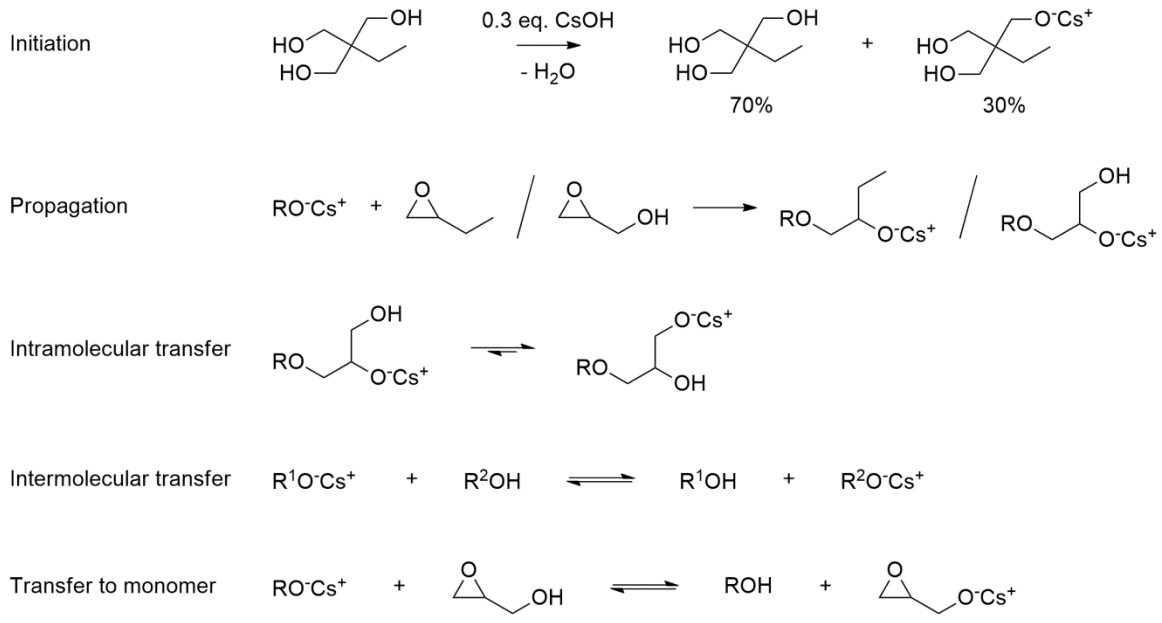

Scheme 2: Mechanism of the anionic ring-opening copolymerization of butylene oxide and glycidol.

^{1}H NMR spectra of the reaction mixture after two days revealed 97 to 99% monomer conversion calculated from the residual epoxide signals. As illustrated in Figure 1 and Equation 1, the polymer

composition after purification was determined by comparing the ethyl proton signals to the protons of the polymer backbone.

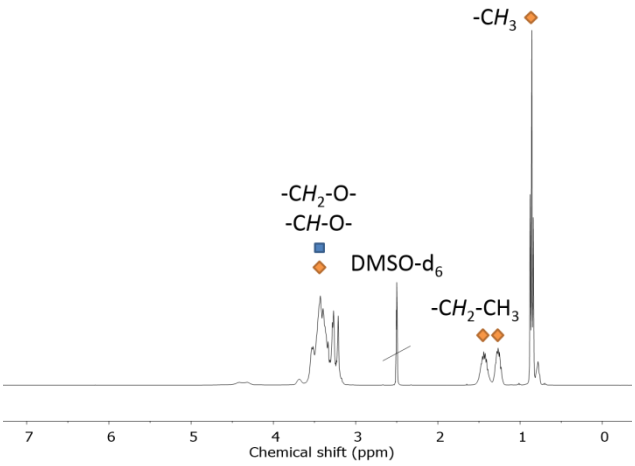

Figure 1. Calculation of the copolymer composition from BO signals (yellow diamonds) and G signals (blue squares) in the ^{1}H NMR spectra (400 MHz, DMSO-d_6).

$$[G] = \frac{3\,(I_{\text{Backbone}} - I_{\text{Methyl}})}{3\,I_{\text{Backbone}} + 2\,I_{\text{Methyl}}} \quad (1)$$

A small deviation of the copolymer composition compared to the molar fractions in the monomer feed was observed. This is a consequence of the incomplete BO conversion and the formation of a small amount of oligomeric side products. However, it was possible to obtain a series of copolymers with similar molecular weights and systematic variation of the BO/G ratio (see Table 1). Furthermore, the absence of unsaturated proton signals in the ^{1}H NMR spectra proves that no allylic alcohols are formed by proton abstraction at the methylene group during the copolymerization of BO and glycidol. This common side reaction for the anionic polymerization of substituted epoxides under harsh conditions might be prevented by the high concentration of OH groups present in the multibranching copolymerization.[2]

Calculation of the degree of polymerization DP_n of these samples from NMR is not feasible, because the batch copolymerization procedure leads to an unknown fraction of polymers that do not contain the TMP core molecule. This is supported by the presence of unreacted TMP that could be separated from the copolymers after precipitation. These findings can be explained by the addition of large amounts of glycidol at the beginning of the batch reaction, acting as a chain transfer agent as seen in Scheme 2. After proton transfer from glycidol to the deprotonated TMP, glycidolate autoinitiation can take place, initiating new polymer chains. This explains that the degree of polymerization was found to be independent of the monomer/initiator ratio.

Table 1. Characterization data of *hb*(PBO-*co*-PG) copolymers prepared via batch copolymerization.

№	Sample name[a]	G% Theo	G% (^{1}H)	DB% (IG ^{13}C)	M_n / g · mol^{-1} (SEC)	Đ (SEC)	T_g / °C (DSC)	LCST / °C
1	*hb*($PBO_{0.76}$-*co*-$PG_{0.24}$)	20	24	45	1280	1.65	-59	-
2	*hb*($PBO_{0.71}$-*co*-$PG_{0.29}$)	30	29	65	1160	1.42	-55	-
3	*hb*($PBO_{0.58}$-*co*-$PG_{0.42}$)	40	42	71	940	1.56	-48	20
4	*hb*($PBO_{0.51}$-*co*-$PG_{0.49}$)	45	49	73	1150	1.46	-40	32
5	*hb*($PBO_{0.46}$-*co*-$PG_{0.54}$)	50	54	63	1290	1.42	-39	49
6	*hb*($PBO_{0.40}$-*co*-$PG_{0.60}$)	55	60	59	930	1.55	-35	84
7	*hb*($PBO_{0.34}$-*co*-$PG_{0.66}$)	60	66	60	1130	1.41	-32	-
8	*hb*($PBO_{0.26}$-*co*-$PG_{0.74}$)	70	74	54	890	1.64	-29	-

[a]Nomenclature: Samples 1-8 are named according to the content of BO and the content of G in the copolymers, as calculated from the ^{1}H NMR spectra.

SEC (calibrated with linear PEG standards) revealed rather low apparent molecular weights in the range of 900 to 1300 g mol^{-1} and mostly monomodal, moderate distributions with Đ ranging in the range of 1.41 to 1.65. The molecular weight limiting chain transfer reaction was observed for hyperbranched polyethylene oxide and polypropylene oxide copolymers before.[37,38] There are, however, clearly no signs of chain transfer by proton abstraction at the α-methylene group of the BO monomer, which is commonly observed during anionic homopolymerization of 1,2-butylene oxide.[41] In this case, unsaturated chain ends would be found in the NMR spectra, which is not the case.

In order to study the structure formation of *hb*(PBO-*co*-PG) in a detailed manner, the kinetics of the batch copolymerization was monitored *in-situ*, carrying out the polymerization directly in an NMR tube. The consumption of BO and G during the copolymerization was investigated by *in situ* ^{1}H NMR spectroscopy (Figure 2). For technical reasons, the reaction temperature had to be lowered to 60 °C, and deuterated dimethyl sulfoxide (DMSO-d_6) was added as a solvent. The *in situ* ^{1}H NMR spectra reveal different incorporation rates for both comonomers (Figure 3A); i.e., glycidol is consumed considerably faster than butylene oxide. Full glycidol conversion was reached within 16 hours, at which point there is still about 60% unreacted BO left. The conversion of BO was complete only after five days.

Since both the molar fraction of the monomer feed and the copolymer composition are known at all times from the NMR data (Figure 3B), apparent copolymerization parameters r_G and r_{BO} could be determined using a Fineman-Ross plot (Figure S2, Supporting Information).[42,43] The calculated values $r_G = 6.1$ and $r_{BO} = 0.19$ reflect the considerably higher reactivity of the G monomer, indicating a distinct gradient microstructure with a PG-rich, strongly branched core and a PBO-rich corona with little branched, dangling PBO chains. It must be noted that reactivity of all propagating glycerol chain ends has to be regarded as uniform in the simplified model of the Fineman-Ross formalism. Interestingly the reactivity ratios are in good agreement with previous studies of the copolymerization kinetics of the system ethylene oxide/butylene oxide, which also unveiled a strongly tapered microstructure.[44]

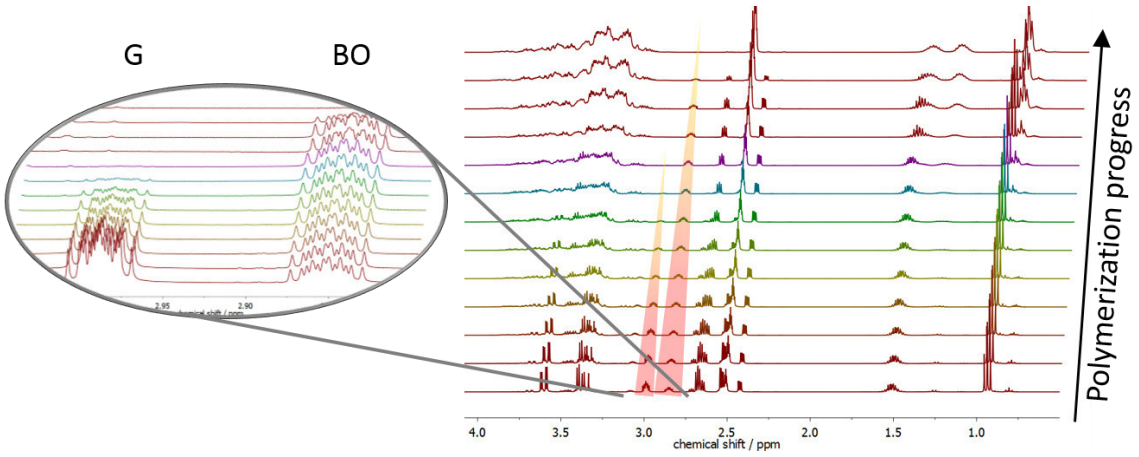

Figure 2. *In situ* ^{1}H NMR spectra of the batch copolymerization of BO and G at 60 °C in DMSO-d_6, revealing a decrease of the epoxide methine signal intensities over time (BO: 2.85 ppm, G: 2.99 ppm).

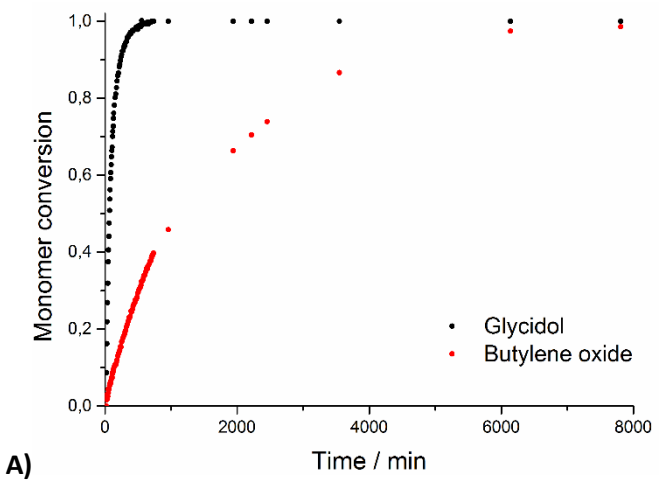

Figure 3. Batch copolymerization kinetic data: A) glycidol and 1,2-butylene oxide consumption over time, B) Relative residual monomer concentration and BO content in the copolymer versus total monomer conversion.

Slow addition of glycidol is commonly employed for the controlled synthesis of the hyperbranched polyglycerol homopolymer.[26] Aiming on the one hand at elevated molecular weight *hb*(PBO-*co*-PG) copolymers and on the other hand at a comparison of the methods, a second series of copolymers was synthesized employing a slow monomer addition protocol (Table 2). Under these reaction conditions, monomer concentrations are kept low during the entire course of the polymerization. Consequently, polymer-monomer reactions are statistically favored over monomer-monomer reactions, and chain transfer to the glycidol inimer is almost completely suppressed. Due to the increasing bulk viscosity of the polymers with increasing molecular weight, SMA syntheses had to be performed in solution. Since diglyme and N-methylpyrolidone (NMP), which are well-established solvents for the synthesis of other polyglycerol-based copolymers, were found to be unsuitable for the copolymerization of BO and G, tetrahydropyran (THP) was

chosen as an appropriate solvent.[26,33] Furthermore, the reaction temperature was lowered to 88 °C, the boiling point of THP. As a consequence, BO conversion was reduced compared to the batch polymerizations, which was ascribed to leakage of the volatile monomer through the rubber septum at first. By adding the monomer via a long cannula through a reflux condenser, overall conversion was increased from 64-65% to 75-78%. NMR spectra of the reaction mixture revealed residual unreacted BO, even after extending reaction times from three to five days. Employing this procedure, the accessible molecular weight range could be increased considerably and molecular weights can be controlled to a certain extent, as can be seen in Figure 4. Low molecular weight samples 9 and 10 have also been synthesized deliberately to obtain materials for comparison with the polymers obtained by batch polymerization.

Again, apparent molecular weights were determined by SEC using linear PEG standards. The average molar mass of the *hb*(PBO-*co*-PG) copolymers prepared by the slow monomer addition strategy can also be calculated from ^{1}H NMR by comparison with the signals of the initiator core, as it is known from other examples of glycidol copolymers.[27–33] The methyl signal of the TMP core provides a reference for integration. This signal, however, diminishes with increasing degree of polymerization, rendering this method less exact for higher molecular weight copolymers. Furthermore, on-line viscosimetry and analytical ultracentrifugation characterization were employed to obtain absolute molar mass averages for the hyperbranched copolymers, which were compared with the apparent values from SEC characterization. The results are discussed in the section below.

Table 2. Characterization data of *hb*(PBO-*co*-PG) copolymers prepared by the slow monomer addition procedure (SMA).

№	Sample name[a]	G% Theo	G% (^{1}H)	DB% (IG ^{13}C)	M_n / g · mol^{-1} theo	M_n / g · mol^{-1} (NMR)	M_n / g · mol^{-1} (SEC)	Đ (SEC)	T_g / °C (DSC)	LCST / °C
9	*hb*(PBO_7-*co*-PG_3)	20	29	57	3000	820	850	1.29	-49	23
10	*hb*(PBO_8-*co*-PG_6)	35	39	67	3000	1110	1170	1.49	-37	34
11[b]	*hb*(PBO_8-*co*-PG_{29})	50	77	66	6000	2800	2940	1.30	-37	-
12[b]	*hb*(PBO_{17}-*co*-PG_{66})	50	78	70	11000	6300	4250	1.49	-33	-
13	*hb*(PBO_{36}-*co*-PG_{64})	50	64	77	6000	7500	7830	1.65	-36	-
14	*hb*(PBO_{57}-*co*-PG_{120})	50	67	59	11000	13200	8460	1.58	-30	-

[a] Nomenclature: Samples 9-14 are named according to the number of comonomer units *hb*(PBO_x-*co*-PG_y), where x is the absolute number of BO units and y the absolute number of G units, calculated from ^{1}H NMR spectra. [b] Polymers prepared without reflux condenser.

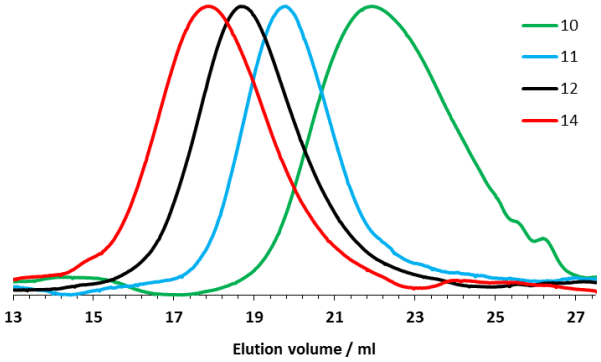

Figure 4. SEC traces (DMF, RI signal) of the hyperbranched *hb*(PBO-*co*-PG) copolymers; samples 10, 11, 12, and 14 (Table 2) prepared by slow monomer addition.

In order to study the influence of the slow monomer addition on composition and DB, kinetic studies were also important in this case. However, since *in situ* ^{1}H NMR kinetic studies are not feasible for the copolymerization under slow monomer addition conditions, NMR samples were taken during polymerization using the conventional setup. In this manner, it was possible to monitor composition of the growing copolymers in the course of the reaction (Figure 5). It is a striking observation that in contrast to the copolymerization in batch (Figure 3B), there is no compositional drift. Except for the very beginning of the reaction, the monomers are incorporated at a constant ratio of 75% glycidol and 25% butylene oxide, when added in a 1:1 feed ratio. Although residual unreacted BO monomer can be found in the reaction mixture, its accumulation appears to have no visible effect on the copolymer composition due to its very low reactivity. Allgaier and coworkers calculated for the copolymerization of BO with ethylene oxide that extremely slow monomer addition over a period of more than a month would be required to avoid accumulation of the BO monomer in the reaction mixture.[44] The exact microstructure of the copolymers cannot be elucidated, because there are multiple reactive chain ends per polymer molecule. Each monomer may react with alkoxide termini belonging to the two different linear G units as well as terminal BO or G units. However, significant deviations in the aqueous solubility of polymers prepared by batch polymerization and SMA, respectively, were found, which indicate that the SMA protocol leads to a less pronounced gradient structure. The findings are discussed in detail in the corresponding section.

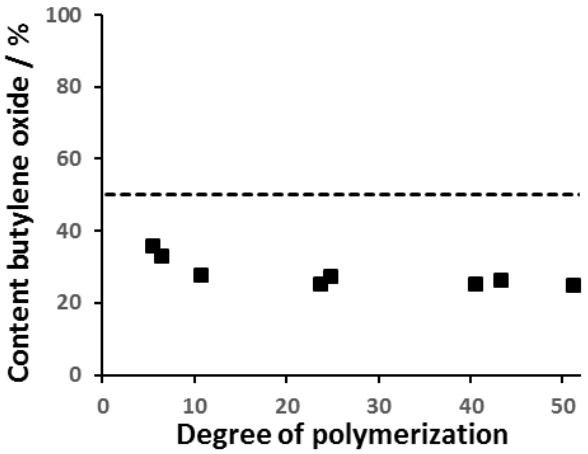

Figure 5. Copolymer composition over the course of a copolymerization under slow monomer addition conditions. The dashed line represents the mole fraction in the monomer feed.

B. Determination of Absolute Molecular Weights and Intrinsic Viscosities

Determining absolute molecular weight averages and molecular weight distribution is a key issue in the comprehensive characterization of hyperbranched polymers. Nevertheless, most works published in this area to date rely solely on conventional SEC calibrated with linear polymer standards, neglecting that significant deviations arise from the different hydrodynamic volumes of hyperbranched polymers and those of linear SEC standards.[37] In addition, interaction of the multiple functional end groups with the SEC columns can also lead to erroneous results.

We studied the two series of hyperbranched copolymers formed in batch and by SMA, respectively, by on-line viscosimetry and analytical ultracentrifugation to obtain absolute molar mass values. On-line viscosimetry is a hyphenated liquid chromatography coupling technique, combining a viscometer and a refractive index detector (RI). The intrinsic viscosity of the copolymers is measured, and subsequently the absolute molar mass distribution is determined based on a universal calibration curve. This method is independent of the polymer type or architecture of the calibration standards.

All *hb*(PBO-*co*-PG) copolymers exhibited low intrinsic viscosities [η] in DMF, which were in the range of 3.2 to 6.3 mL g^{-1}, as summarized in Table S1. These results are typical for hyperbranched polymers due to their compact, three-dimensional structure. The values are in good agreement with reported [η] values of hyperbranched polyglycerol and hyperbranched poly(ethylene glycol)-*co*-polyglycerol copolymers.[37,45] As a general trend, [η] of *hb*(PBO-*co*-PG) obtained by batch polymerization shows a slight increase with increasing glycidol fraction (see Figure S3). This can be ascribed to a more expanded polymer conformation due to the increasingly favorable interactions between the polar solvent and the increasingly polar copolymers due to the additional hydroxyl groups.

Measurements of the intrinsic viscosity of *hb*(PBO-*co*-PG) in DMF using the samples obtained by the SMA protocol yielded a scaling relationship between [η] and the molar mass. Perfectly branched dendrimers do not show a straight linear dependence between intrinsic viscosity and molecular weight: the corresponding scaling Kuhn-Mark-Houwink-Sakurada plot ($[\eta] = KM^{\alpha}$) passes through a maximum.[46,47] A similar behavior was also observed for several hyperbranched structures.[48–50] As illustrated in Figure 6, the hyperbranched PBO copolymers prepared by the SMA protocol exhibit a change in the slope from 0.33 ($[\eta] = 0.265\ M^{0.33\pm0.03}$) to $\alpha \approx 0$, which reflects a transition to a highly compact state. This was shown to be a direct consequence of the change in the ratio of mass to volume for different degrees of polymerization. The samples prepared by batch polymerization, due to the very short molar mass range, do not show any dependence on

the molar mass. However, in spite of the differences between the samples obtained by SMA and batch procedure, the entire viscosity data in DMF can be considered in a single dependence, yielding the exponent value of 0.15 ([η] = 1.300 $M^{0.15\pm0.04}$), which corresponds to a highly compact structure of the series of *hb*(PBO-*co*-PG) copolymers as well.

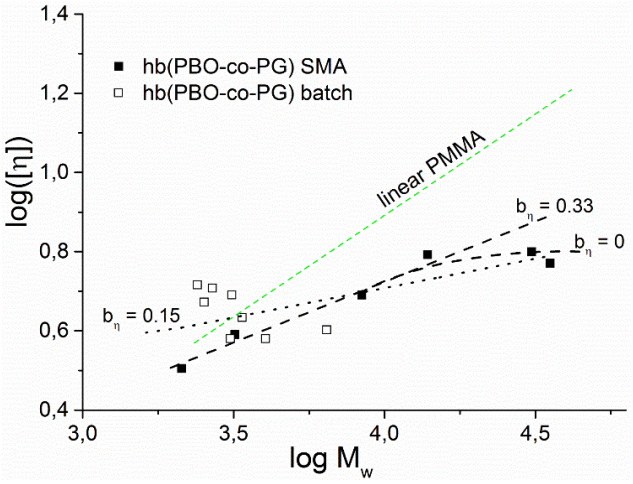

Figure 6. Double logarithmic dependence of intrinsic viscosity [η] on the molar mass M_w in DMF at 70 °C: ■ - samples synthesized using SMA procedure, □ – samples obtained by batch procedure. Dotted line – linear extrapolation through all data points (SMA+batch).

Based on the intrinsic viscosities, universal SEC calibration becomes feasible. Hence, absolute molecular weight averages could be determined (Table S1). When compared with the apparent molecular weights obtained from conventional SEC, up to three times higher values were found. The M_w values of the batch copolymers are in the range of 2400 to 6440 g mol^{-1}. The molecular weight of the copolymers prepared in the batch procedure decreases with increasing glycidol content, presumably because higher glycidol content leads to increased chain transfer to the monomer during polymerization. This correlation is not reflected in the conventional SEC results. The values obtained from universal calibration confirm that for *hb*(PBO-*co*-PG) copolymers prepared by the SMA procedure molecular weights can be tailored in a wide range from 2130 to 35400 g mol^{-1}. Again, the viscosimetry results reveal an underestimation of M_w by SEC. However, Table 3 shows that - with one exception - both methods yield consistent results. Sample *hb*(PBO_{36}-*co*-PG_{64}) showed a larger M_w value than *hb*(PBO_{57}-*co*-PG_{120}) according to the viscosimetry data, contrasting SEC results. In this case, the molecular weight distribution of the former appears to be significantly broader than estimated by SEC.

For comparison, *hb*(PBO-*co*-PG) samples 8, 12, 13, and 14 with glycidol content around 75% and varying degree of polymerization were also studied in aqueous solution by the methods of molecular hydrodynamics, particularly regarding sedimentation velocity and intrinsic viscosity. The measured values of the intrinsic viscosity in water are similar to those obtained in DMF and do not show any dependence on molecular weight (Table 3). Furthermore, Figure 7 illustrates the differential distributions of the sedimentation coefficients. The distributions are generally rather broad and shift to higher sedimentation coefficients with increasing molar mass.

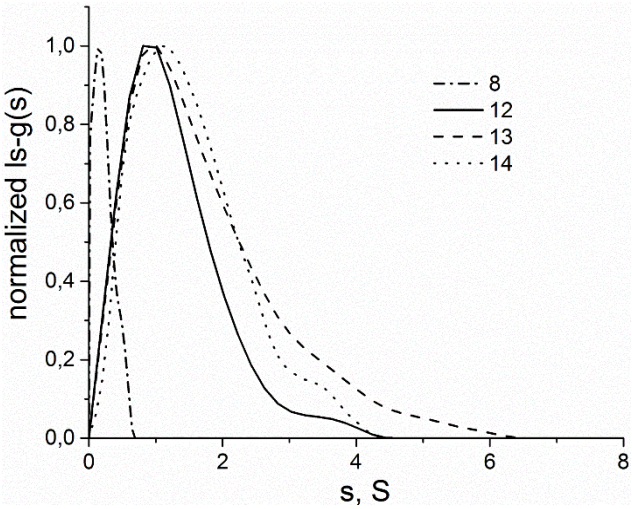

Figure 7. Normalized distributions of the sedimentation coefficients for *hb*(PBO-*co*-PG) copolymers № 8, 12, 13, 14 in water at 25 °C obtained by Sedfit.

The molar masses were calculated based on the modified Svedberg equation using the estimated values of the sedimentation coefficient (s_0) and frictional ratio $(f/f_{sph})_0$:

$$M_{sf} = 9\pi\sqrt{2}N_A\left([s]\, f/f_{sph}\right)^{3/2}\sqrt{\upsilon} \qquad (2)$$

where $[s]$ is the intrinsic sedimentation coefficient ($[s] = \frac{s_0\eta_0}{(1-\upsilon\rho_0)}$ where ρ_0 and η_0 are the density and dynamic viscosity of the solvent) and υ is the partial specific volume. The molar mass values, together with other hydrodynamic characteristics are summarized in Table 1. The molecular weights determined by analytical ultracentrifugation are in good agreement with the results of the on-line viscosimetry measurements. This confirms the accurate molecular weight characterization.

Table 3. Hydrodynamic characteristics of selected hyperbranched copolymers in water at 25 °C and comparison of molecular weight characterization data from AUC, on-line viscosimetry and conventional SEC.

Sample name	s_0 / S (AUC)	$(f/f_{sph})_0$	$[\eta]_{aq}$ / $cm^3 \cdot g^{-1}$	M_{sf} / $g \cdot mol^{-1}$ (AUC)	M_w / $g \cdot mol^{-1}$ (Visco)	M_w / $g \cdot mol^{-1}$ (SEC)
hb($PBO_{0.26}$-*co*-$PG_{0.74}$)	0.34	1.1	5.2	2100	2400	1450
hb(PBO_{17}-*co*-PG_{66})	1.20	1.1	4.7	14000	13900	6300
hb(PBO_{36}-*co*-PG_{64})	2.14	1.1	5.4	32300	35400	12900
hb(PBO_{57}-*co*-PG_{120})	1.55	1.1	4.7	20000	30700	13300

Information on the polymer conformation in aqueous solution can be obtained from comparing the hydrodynamic characteristics (s and [η]) with the corresponding molar masses. In addition to the already established [η]-M dependence, a scaling relationship between the sedimentation coefficient and molar mass was obtained: $s = 0.002 \times M^{0.672 \pm 0.005}$ (Figure S4). Thus, the conformation of the *hb*(PBO-*co*-PG) polymer chains can be described as a compact, spherical-like structure (an ellipsoid) with a constant asymmetry. This result agrees well with the previously published study on hyperbranched poly(ethylene glycol)–*co*–poly(glycerol) copolymers.[37] Furthermore, the series of *hb*(PBO-*co*-PG) copolymers could be considered as hydrodynamic homologues i.e. the macromolecules behave hydrodynamically similar to each other.

C. Degree of Branching (DB)

Besides exact molecular weight determination, determination of the degree of branching (DB) is crucial in order to understand the actual structure of a hyperbranched polymer. When copolymerizing glycidol and BO, fast inter- and intramolecular proton transfer between different alkoxide chain ends leads to branching of the polymer (Scheme 2). The formation of a hyperbranched structure is proven by a characteristic splitting of the polyether backbone signals in the ^{13}C NMR spectra (Figure S4). The peaks in the range of 60 to 80 ppm can be assigned to dendritic, linear and terminal units. The peak assignment of the differently linked BO and G units was confirmed by HSQC (Figure S5) and HMBC NMR (Figure S6). Using inverse gated ^{13}C NMR, the degree of branching (DB) of the copolymers was determined according to the definition for AB/AB_2 systems (Equation 3).[51] The calculated values are summarized in Table 1 and Table 2 above.

$$DB_{\mathrm{AB/AB_2}} = \frac{2D}{2D+\sum L} \quad (3)$$

AB represents a monomer unit containing two reactive sites, in this case butylene oxide, that can only be incorporated as a linear or terminal unit, and AB_2 stands for the branching unit glycidol. Surprisingly high DB values in the range of 0.45 and 0.73 for copolymerization in batch (Figure S7) and in the range of 0.57 and 0.77 for copolymerization under slow monomer addition conditions (Figure S8) were found. These values are significantly higher than the theoretical DB for a random AB/AB_2 copolymerization. Presumably, lowered reactivity of BO termini leads to increased growth at the remaining linear and terminal glycerol units. This assumption is supported by the high number of terminal BO units that can be found in the IG ^{13}C NMR spectra (Figure S4). As a result of the saturation of the glycerol units, copolymers with medium glycidol fraction show the highest experimental DB values. The DB values of copolymers containing mainly polyglycerol are closer to the theoretical values because the small BO content has less influence on the polymer structure. The high degrees of branching and the resulting compact structure of the copolymers may explain the exceptionally low b_η parameter of 0.15 observed in the viscometric measurements.

D. Physical Properties of *hb*(PBO-*co*-PG) Copolymers in Bulk and Solution

Thermal analysis of the *hb*(PBO-*co*-PG) copolymers by differential scanning calorimetry confirmed the expected amorphous structure for all samples and a linear correlation between the comonomer ratio and the glass transition temperature (T_g) of the polymers prepared by batch copolymerization (Figure 8). The T_g increases gradually with increasing glycidol content, reflecting the decrease in flexibility and the increased number of hydroxyl groups and resulting hydrogen bond interactions. The T_g can be readily adjusted from -59 to -29 °C via alteration of the composition. This findings resemble the features of both hyperbranched polypropylene oxide copolymers and the corresponding PPO multiarm star polymers.[38,52] Copolymers synthesized via SMA exhibit more spread, but generally similar glass transition temperatures (Figure S9). This is tentatively explained by the influence of various polymerization parameters (monomer addition rate, initiator concentration, conversion, molecular weight) on the microstructure.

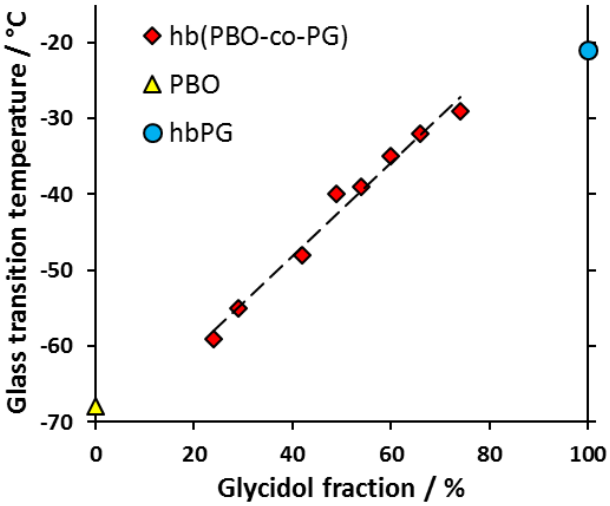

Figure 8. Glass transition temperatures (T_g) of the *hb*(PBO-*co*-PG) copolymers obtained in the batch process, with varying composition. T_g of linear PBO and *hb*PG for comparison.[26,53]

Copolymers consisting of glycidol and propylene oxide as well as other hydrophobic comonomers are known to show thermoresponsive behavior and lower critical solution temperatures (LCST) in aqueous solution.[33,38,54,55] The aqueous solubility of *hb*(PBO-*co*-PG) and its dependence on temperature and comonomer ratio was investigated by turbidimetry. Due to the opposite polarities of the hydrophilic glycerol segments and the hydrophobic BO units, the solubility of the copolymers varies greatly with composition. Copolymers with G fraction ≥ 66% (polymerized in batch) were water-soluble at all temperatures. An amount of G in the range between 42% and 60% resulted in thermoresponsive behavior. Aqueous solutions of these copolymers exhibit reversible demixing above a lower critical solution temperature (Figure 9A). Except for sample 6 (60% G), which exhibits a broad transition close to the boiling point of water, all thermoresponsive copolymers show well-defined cloud points. For this intermediate range of compositions the LCST depends strongly on the comonomer ratio and can be tailored in a wide temperature range from 20 to 84 °C (Figure 9B). G contents of 29% and below resulted in hydrophobic materials that are not soluble in water at any temperature.

*Hb*PBO polymers obtained by the SMA procedure with comparable molecular weights exhibit clearly increased aqueous solubility in comparison to copolymers obtained in the batch procedure. For instance, sample *hb*(PBO_7-*co*-PG_3) with 29% G exhibits a cloud point temperature of 23 °C, whereas the corresponding sample *hb*($PBO_{0.71}$-*co*-$PG_{0.29}$) with the same fraction of 29% G is completely insoluble in aqueous media. The LCST of this sample is even slightly above the cloud point of *hb*($PBO_{0.58}$-*co*-$PG_{0.42}$) with 42% G. A similar shift can be seen between *hb*(PBO_8-*co*-PG_6), 39% G, and *hb*($PBO_{0.51}$-*co*-$PG_{0.49}$) (FigureB). These deviations can be attributed to a less

pronounced gradient microstructure, resulting from the SMA procedure, with more hydrophilic glycerol units situated at the periphery of the polymer.

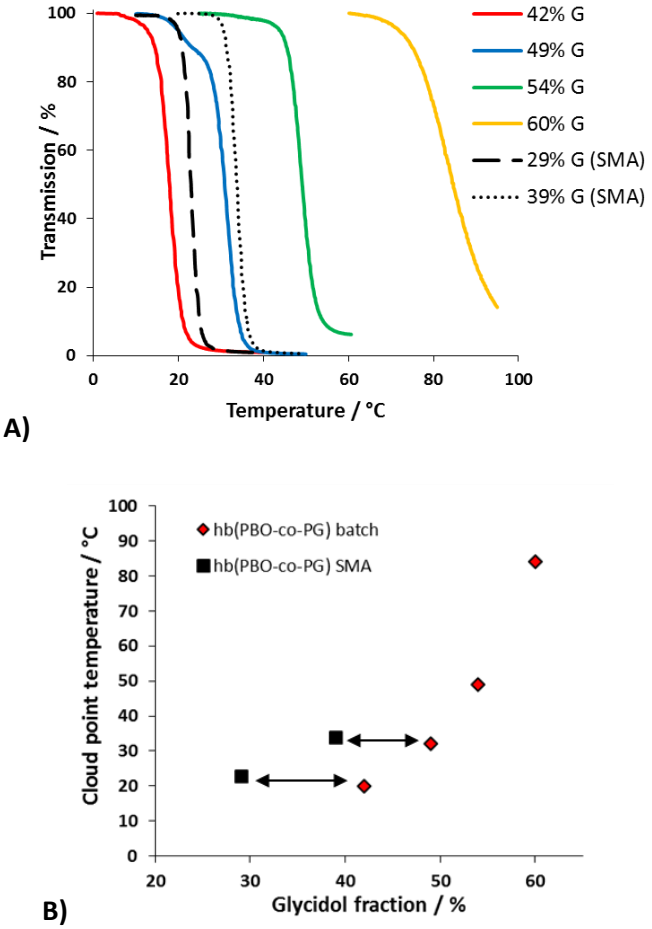

Figure 9. A) Intensity of transmitted laser light versus temperature for *hb*(PBO-*co*-PG) copolymers of various compositions at a concentration of 5 mg mL^{-1} in aqueous solution, B) Comparison of the effect of the glycidol fraction on the cloud point temperatures of copolymers prepared by batch procedure and SMA.

Conclusion

Hyperbranched, multi-hydroxyfunctional polyethers based on the copolymerization of the apolar epoxide monomer 1,2-butylene oxide with glycidol have been introduced. The ring-opening multibranching copolymerization of the AB/AB_2 type has been studied in a detailed manner, including *in-situ* NMR kinetics and absolute molecular weight determination On the one hand, batch polymerization without solvent was employed in order to vary the copolymer composition systematically. On the other hand, slow monomer addition of mixtures of both comonomers enabled variation of the molecular weight up to 35000 g mol^{-1}. The copolymerization kinetics of

the two synthetic approaches was compared by NMR spectroscopy, revealing significant differences concerning the incorporation of the comonomers, which are also reflected in the aqueous solubility and cloud points of the resulting materials.

Beyond standard SEC and NMR characterization, absolute molar mass determination - an important challenge in the characterization of hyperbranched polymers - was carried out comprehensively, relying on both on-line viscosimetry and analytical ultracentrifugation, resulting in a universal calibration curve for SEC characterization of the hyperbranched polyols. Both methods yielded consistent molecular weight values that were up to three times higher than the apparent values determined by SEC calibrated with linear PEG standards. The calculated hydrodynamic scaling relationships prove the globular and compact shape of the hyperbranched poly(butylene oxide) copolymers, which is a consequence of the surprisingly high degrees of branching up to 0.77, determined by Inverse Gated ^{13}C NMR. The high DB values are tentatively explained by the low reactivity of terminal butylene oxide units.

Combination of the apolar butylene oxide monomer and glycidol with its opposite polarity enables tailoring the materials' physical properties, such as glass transition temperatures (T_g) and hydrophilicity, which translates to lower critical solution temperatures (LCST) in a wide temperature range that can be tuned by the copolymer composition. With their large number of hydroxyl groups, these *hb*(PBO-*co*-PG) copolymers open up possibilities for further chemical functionalization or crosslinking, rendering *hb*(PBO-*co*-PG) a stimuli-responsive building block for e.g., hydrogels, surface modification and polyurethane foams. Despite the limited molecular weights obtained, the solvent-free batch polymerization procedure based on the industrially available butylene oxide monomer may be readily adapted to larger scales.

Acknowledgement

The authors thank Luka Decker for technical assistance.

References

1. a) Bailey, F. E.; Koleske, J. V. *Alkylene oxides and their polymers*; Surfactant science series Vol. 35; Dekker: New York, **1991**; b) Herzberger, J.; Niederer, K.; Pohlit, H.; Seiwert, J.; Worm, M.; Wurm, F. R.; Frey, H. *Chem. Rev.* **2016**, *116*, 2170−2243.
2. Allgaier, J.; Willbold, S.; Chang, T. *Macromolecules* **2007**, *40*, 518–525.
3. Liu, Y.; Wei, W.; Xiong, H. *Polym. Chem.* **2015**, *6*, 583–590.
4. Misaka, H.; Tamura, E.; Makiguchi, K.; Kamoshida, K.; Sakai, R.; Satoh, T.; Kakuchi, T. *J. Polym. Sci. A Polym. Chem.* **2012**, *50*, 1941–1952.
5. Isono, T.; Kamoshida, K.; Satoh, Y.; Takaoka, T.; Sato, S.-I.; Satoh, T.; Kakuchi, T. *Macromolecules* **2013**, *46*, 3841–3849.
6. Zhao, J.; Alamri, H.; Hadjichristidis, N. *Chem. Commun.* **2013**, *49*, 7079–7081.
7. Zhao, J.; Pahovnik, D.; Gnanou, Y.; Hadjichristidis, N. *Macromolecules* **2014**, *47*, 3814–3822.
8. Greaves, M.; Zaugg-Hoozemans, E.; Khelidj, N.; Voorst, R.; Meertens, R. *Lubr. Sci.* **2012**, *24*, 251–262.
9. Nace, V. M. *Nonionic surfactants: Polyoxyalkylene block copolymers*; Surfactant science series v. 60; M. Dekker: New York, **1996**.
10. Booth, C.; Attwood, D. *Macromol. Rapid Commun.* **2000**, *21*, 501–527.
11. Gervais, M.; Brocas, A.-L.; Cendejas, G.; Deffieux, A.; Carlotti, S. *Macromolecules* **2010**, *43*, 1778–1784.
12. Voit, B. I.; Lederer, A. *Chem. Rev.* **2009**, *109*, 5924–5973.
13. Zheng, Y.; Li, S.; Weng, Z.; Gao, C. *Chem. Soc. Rev.* **2015**, *44*, 4091–4130.
14. Fréchet, J. M.; Henmi, M.; Gitsov, I.; Aoshima, S.; Leduc, M. R.; Grubbs, R. B. *Science* **1995**, *269*, 1080–1083.
15. Tokar, R.; Kubisa, P.; Penczek, S.; Dworak, A. *Macromolecules* **1994**, *27*, 320–322.
16. Bernal, D. P.; Bedrossian, L.; Collins, K.; Fossum, E. *Macromolecules* **2003**, *36*, 333–338.
17. Miyakoshi, R.; Yokoyama, A.; Yokozawa, T. *J. Polym. Sci. A Polym. Chem.* **2008**, *46*, 753–765.
18. Ohta, Y.; Fujii, S.; Yokoyama, A.; Furuyama, T.; Uchiyama, M.; Yokozawa, T. *Angew. Chem. Int. Ed.* **2009**, *48*, 5942–5945.
19. Min, K.; Gao, H. *J. Am. Chem. Soc.* **2012**, *134*, 15680–15683.
20. Shi, Y.; Graff, R. W.; Cao, X.; Wang, X.; Gao, H. *Angew. Chem. Int. Ed.* **2015**, *54*, 7631–7635.
21. Calderón, M.; Quadir, M. A.; Sharma, S. K.; Haag, R. *Adv. Mater.* **2010**, *22*, 190–218.
22. Wilms, D.; Stiriba, S.-E.; Frey, H. *Acc. Chem. Res.* **2010**, *43*, 129–141.
23. Royappa, A. T.; Dalal, N.; Giese, M. W. *J. Appl. Polym. Sci.* **2001**, *82*, 2290–2299.

24. Klein, R.; Übel, F.; Frey, H. *Macromol. Rapid. Commun.* **2015**, *36*, 1822–1828.
25. Christ, E.-M.; Hobernik, D.; Bros, M.; Wagner, M.; Frey, H. *Biomacromolecules* **2015**, *16*, 3297–3307.
26. Sunder, A.; Hanselmann, R.; Frey, H.; Mülhaupt, R. *Macromolecules* **1999**, *32*, 4240–4246.
27. Sunder, A.; Türk, H.; Haag, R.; Frey, H. *Macromolecules* **2000**, *33*, 7682–7692.
28. Schüll, C.; Gieshoff, T.; Frey, H. *Polym. Chem.* **2013**, *4*, 4730.
29. Tonhauser, C.; Schüll, C.; Dingels, C.; Frey, H. *ACS Macro Lett.* **2012**, *1*, 1094–1097.
30. Shenoi, R. A.; Narayanannair, J. K.; Hamilton, J. L.; Lai, Benjamin F L; Horte, S.; Kainthan, R. K.; Varghese, J. P.; Rajeev, K. G.; Manoharan, M.; Kizhakkedathu, J. N. *J. Am. Chem. Soc.* **2012**, *134*, 14945–14957.
31. Shenoi, R. A.; Chafeeva, I.; Lai, Benjamin F. L.; Horte, S.; Kizhakkedathu, J. N. *J. Polym. Sci. A Polym. Chem.* **2015**, *53*, 2104–2115.
32. Son, S.; Shin, E.; Kim, B.-S. *Macromolecules* **2015**, *48*, 600–609.
33. Alkan, A.; Klein, R.; Shylin, S. I.; Kemmer-Jonas, U.; Frey, H.; Wurm, F. R. *Polym. Chem.* **2015**, *6*, 7112-7118.
34. Feng, X.; Taton, D.; Chaikof, E. L.; Gnanou, Y. *Macromolecules* **2009**, *42*, 7292–7298.
35. Dimitrov, P.; Hasan, E.; Rangelov, S.; Trzebicka, B.; Dworak, A.; Tsvetanov, C. *Polymer* **2002**, *43*, 7171–7178.
36. Wilms, D.; Schömer, M.; Wurm, F.; Hermanns, M. I.; Kirkpatrick, C. J.; Frey, H. *Macromol. Rapid Commun.* **2010**, *31*, 1811–1815.
37. Perevyazko, I.; Seiwert, J.; Schömer, M.; Frey, H.; Schubert, U. S.; Pavlov, G. M. *Macromolecules* **2015**, *48*, 5887–5898.
38. Schömer, M.; Seiwert, J.; Frey, H. *ACS Macro Lett.* **2012**, *1*, 888–891.
39. Schömer, M.; Frey, H. *Macromol. Chem. Phys.* **2011**, *212*, 2478–2486.
40. Hilf, J.; Schulze, P.; Seiwert, J.; Frey, H. *Macromol. Rapid Commun.* **2014**, *35*, 198–203.
41. Gagnon, S. D. Propylene Oxide and Higher 1,2-Epoxide Polymers. *Encyclopedia of Polymer Science and Technology*; John Wiley & Sons, Inc: Hoboken, NJ, USA, **2002**.
42. Fineman, M.; Ross, S. D. *J. Polym. Sci.* **1950**, *5* (2), 259–262.
43. Natalello, A.; Werre, M.; Alkan, A.; Frey, H. *Macromolecules* **2013**, *46*, 8467–8471.
44. Zhang, W.; Allgaier, J.; Zorn, R.; Willbold, S. *Macromolecules* **2013**, *46*, 3931–3938.
45. Imran ul-haq, M.; Lai, Benjamin F. L.; Chapanian, R.; Kizhakkedathu, J. N. *Biomaterials* **2012**, *33*, 9135–9147.
46. Mourey, T. H.; Turner, S. R.; Rubinstein, M.; Fréchet, J. M. J.; Hawker, C. J.; Wooley, K. L. *Macromolecules* **1992**, *25*, 2401–2406.

47. Fréchet, J. M. J. *Science* **1994**, *263*, 1710–1715.
48. Hobson, L. J. *Chem. Commun.* **1997,** *21*, 2067–2068.
49. Lederer, A.; Voigt, D.; Clausnitzer, C.; Voit, B. *J. Chrom. A* **2002**, *976*, 171–179.
50. Boye, S.; Komber, H.; Friedel, P.; Lederer, A. *Polymer* **2010**, *51*, 4110–4120.
51. Frey, H.; Hölter, D. *Acta Polym.* **1999**, *50*, 67–76.
52. Sunder, A.; Mülhaupt, R.; Frey, H. *Macromolecules* **2000**, *33*, 309–314.
53. Lai, J.; Trick, G. S. *J. Polym. Sci. A-1 Polym. Chem.* **1970**, *8*, 2339–2350.
54. Schömer, M.; Frey, H. *Macromolecules* **2012**, *45*, 3039–3046.
55. Xia, Y.; Wang, Y.; Wang, Y.; Wang, D.; Deng, H.; Zhuang, Y.; Yan, D.; Zhu, B.; Zhu, X. *Macromol. Chem. Phys.* **2011**, *212*, 1056–1062.

Supporting Information

Instrumentation

NMR spectroscopy. ^{1}H NMR and ^{13}C NMR spectra were recorded at 400 MHz and 100 MHz, respectively, on a Bruker AMX400 and are referenced internally to residual signals of the deuterated solvent.

Size-exclusion chromatography. For SEC measurements in DMF (containing 0.25 g L^{-1} of lithium bromide as an additive), an Agilent 1100 series was used as an integrated instrument including a PSS HEMA column ($10^6/10^4/10^2$ Å porosity) and UV and RI detector. Calibration was achieved with poly(ethylene glycol) standards provided by Polymer Standards Service (PSS).

Differential scanning calorimetry. DSC measurements were performed using a PerkinElmer 8500 thermal analysis system and a Perkin-Elmer CLN2 thermal analysis controller in the temperature range from -90 to +20 °C at a heating rate of 10 K min^{-1}.

Turbidimetry. Cloud points were determined using a Jasco V-630 photospectrometer with a Jasco ETC-717 Peltier element, and observed by optical transmittance of a light beam (λ = 670 nm) through a 1 cm sample quartz cell. The intensity of the transmitted light was recorded *versus* the temperature of the sample cell. The heating/cooling rate was 1 K min^{-1}, and values were recorded in 1 K steps. The polymers were solved in deionized water at a concentration of 5 mg mL^{-1}.

Analytical ultracentrifugation. Sedimentation velocity experiments were performed with a ProteomeLab XLI Protein Characterization System analytical ultracentrifuge (Beckman Coulter, Brea, CA), using conventional double-sector Epon or aluminum centerpieces of 12 mm optical path length and a four-hole rotor (AN-60Ti). Rotor speed was 60,000 rpm, cells were filled with 420 µL of sample solution and 440 µL of solvent (water). Three concentrations of each sample were studied, covering a wide concentration range. The parameter $c[\eta]$ characterizing the degree of dilution was in the range $0.00047 \leq c[\eta] \leq 0.0216$, which translates to a very high dilution state, which in turn allows for reliable extrapolation to concentration zero. Here c is the polymer concentration in g cm^{-3} and $[\eta]$ is the intrinsic viscosity, measured in $cm^3\,g^{-1}$. Before the run, the rotor was equilibrated for approximately 1 h at 25 °C in the centrifuge. Sedimentation profiles were obtained by interference optics at the same temperature. Sedfit software was employed for the analysis of the sedimentation velocity data. *ls-g*(s)* as well as *c(s)* with a Tikhonov–Phillips regularization procedure implemented into the Sedfit program were applied.[1] The *ls-g*(s)* model represents the least-square boundary analysis, which describes sedimentation of non-diffusing

species. *c(s)* analysis based on the numerical resolution of the Lamm equation assuming the same frictional ratio (f/f_{sph}) values for each *s* value. The reciprocal velocity sedimentation coefficients were extrapolated to zero concentration in the linear approximation, following the relationship: $s^{-1} = s_0^{-1}(1+k_s c)$, when s_0 is the extrapolated value of the velocity sedimentation coefficient and k_s is the concentration sedimentation coefficient (Gralen coefficient).

Viscosity measurements. Viscosity measurements were conducted using an AMVn viscometer (Anton Paar, Graz, Austria), with capillary/ball combination of the measuring system. The respective flow times for the solvent and polymer solutions, η_0 and t, were measured at 25 °C, with relative viscosities $\eta_r = t/t_0$ in the range of 1.2 – 2.5, which corresponds to dilute solutions. The extrapolation to zero concentration was achieved by using both the Huggins and the Kraemer equations, and the average values were considered as the value of the intrinsic viscosity.

Partial specific volume determination. The density measurements were carried out in the density meter DMA 02 (Anton Paar, Graz, Austria) according to the procedure of Kratky et al..[2] The partial specific volume was found to be $\upsilon = 0.821\ cm^3g^{-1}$.

On-line viscometry. On-line viscometry measurements were performed at Polymer Standards Service GmbH using a PSS GRAM column (30/100/1000 Å porosity) equipped with a SECcurity GPC1260 Refractive Index RI detector and a SECcurity on-line viscometer DVD1260. DMF containing 5 g L^{-1} LiBr was used as a solvent. Samples and solvent were weighed in precisely to obtain exactly known sample concentrations of about 20 mg mL^{-1}. After eight hours, 100 µL solution were injected. The flow rate was 1 mL min^{-1}, and the temperature 70 °C. For each sample, the average over three injects was calculated. The universal calibration was based on poly(methyl methacrylate) standards.

Calculation of the Copolymerization Parameters

Copolymerization:

$$P_1^- + M_1 \xrightarrow{k_{11}} P_1M_1^-$$

$$P_1^- + M_2 \xrightarrow{k_{12}} P_1M_2^-$$

$$P_2^- + M_1 \xrightarrow{k_{21}} P_2M_1^-$$

$$P_2^- + M_2 \xrightarrow{k_{22}} P_2M_2^-$$

P_1^-; P_2^-: active chain end

M_1; M_2: monomer

k: reactivity constant

Fineman-Ross equation: $x \cdot \frac{1-X}{X} = -\frac{x^2}{X} r_1 + r_2$ with $r_1 = \frac{k_{11}}{k_{12}}$ and $r_2 = \frac{k_{22}}{k_{21}}$

x: mole fraction of the stock

X: mole fraction of the polymer at certain mole fractions of the stock

r_1: reactivity ratio for monomer M_1

r_2: reactivity ratio for monomer M_2

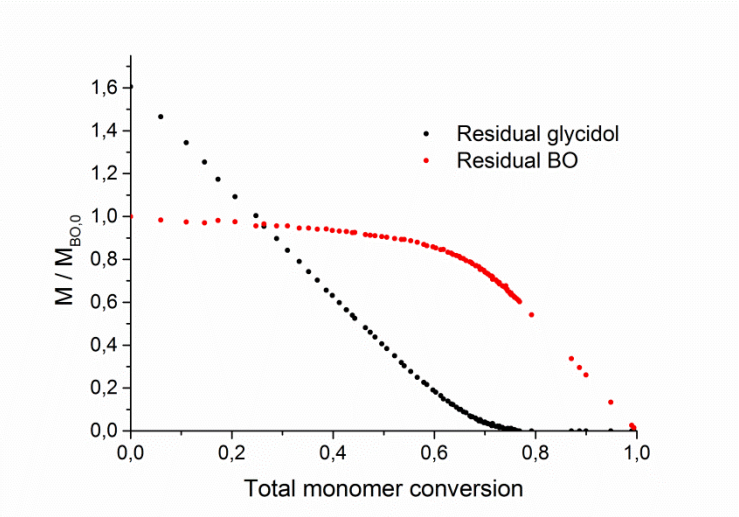

Figure S1. Normalized monomer concentration plotted versus total conversion for BO and G

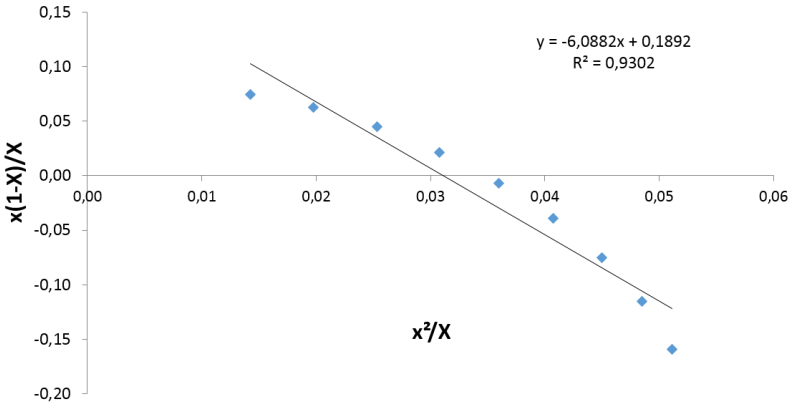

Figure S2. Fineman-Ross plot for the calculation of the copolymerization parameters

On-line Viscometry

Table S1. Characterization data from SEC and on-line viscometry in DMF

№	Sample name	M_w / g · mol^{-1} (SEC)	M_w / g · mol^{-1} (Visco)[a]	$[\eta]_{DMF}$ / cm^3 · g^{-1} (Visco)
1	hb(PBO$_{0.76}$-*co*-PG$_{0.24}$)	2110	6440	4.0
2	*hb*(PBO$_{0.71}$-*co*-PG$_{0.29}$)	1640	4040	3.8
3	*hb*(PBO$_{0.58}$-*co*-PG$_{0.42}$)	1460	3090	3.8
4	*hb*(PBO$_{0.51}$-*co*-PG$_{0.49}$)	1680	3380	4.3
5	*hb*(PBO$_{0.46}$-*co*-PG$_{0.54}$)	1830	3120	4.9
6	*hb*(PBO$_{0.40}$-*co*-PG$_{0.60}$)	1430	2530	4.7
7	*hb*(PBO$_{0.34}$-*co*-PG$_{0.66}$)	1600	2690	5.1
8	*hb*(PBO$_{0.26}$-*co*-PG$_{0.74}$)	1450	2400	5.2
9	*hb*(PBO$_7$-*co*-PG$_3$)	1100	2130	3.2
10	*hb*(PBO$_8$-*co*-PG$_6$)	1750	3190	3.9
11	*hb*(PBO$_8$-*co*-PG$_{29}$)	3820	8420	4.9
12	*hb*(PBO$_{17}$-*co*-PG$_{66}$)	6300	13900	6.2
13	*hb*(PBO$_{36}$-*co*-PG$_{64}$)	12900	35400	5.9
14	*hb*(PBO$_{57}$-*co*-PG$_{120}$)	13300	30700	6.3

[a]The weight-average molecular weights (M_w) are given because M_W is less susceptible to detector noise and hence can be calculated with better accuracy.

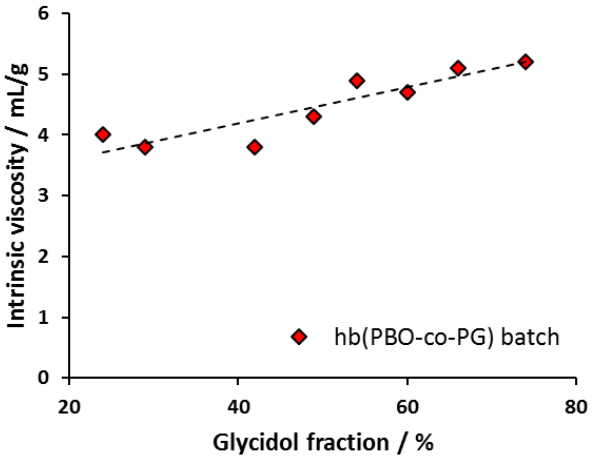

Figure S3. Dependence of the intrinsic viscosity of the copolymers obtained by batch polymerization on the glycidol fraction

Hydrodynamic Characterization

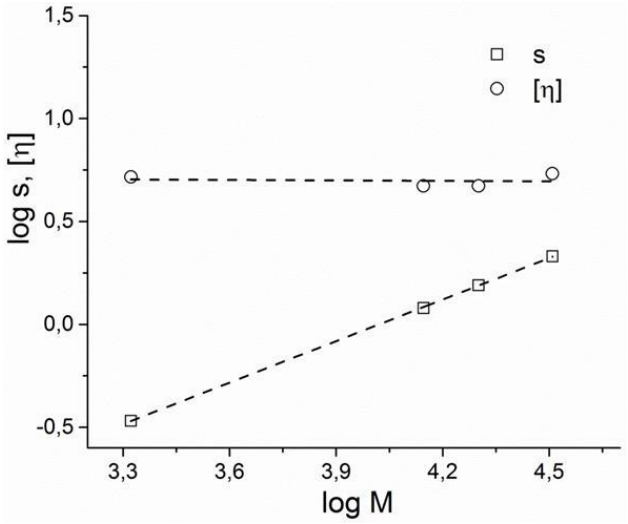

Figure S4. Double logarithmic dependence of the sedimentation coefficient (s) and intrinsic viscosity ([η]) on the molar mass (M) for the hyperbranched polymers in water at 25 °C. The resulting scaling relationships are: $s = 0.002\ M^{0.672\pm0.005}$ and $[\eta] = 5.36\ M^{0.01\pm0.05}$.

Determination of the Degree of Branching

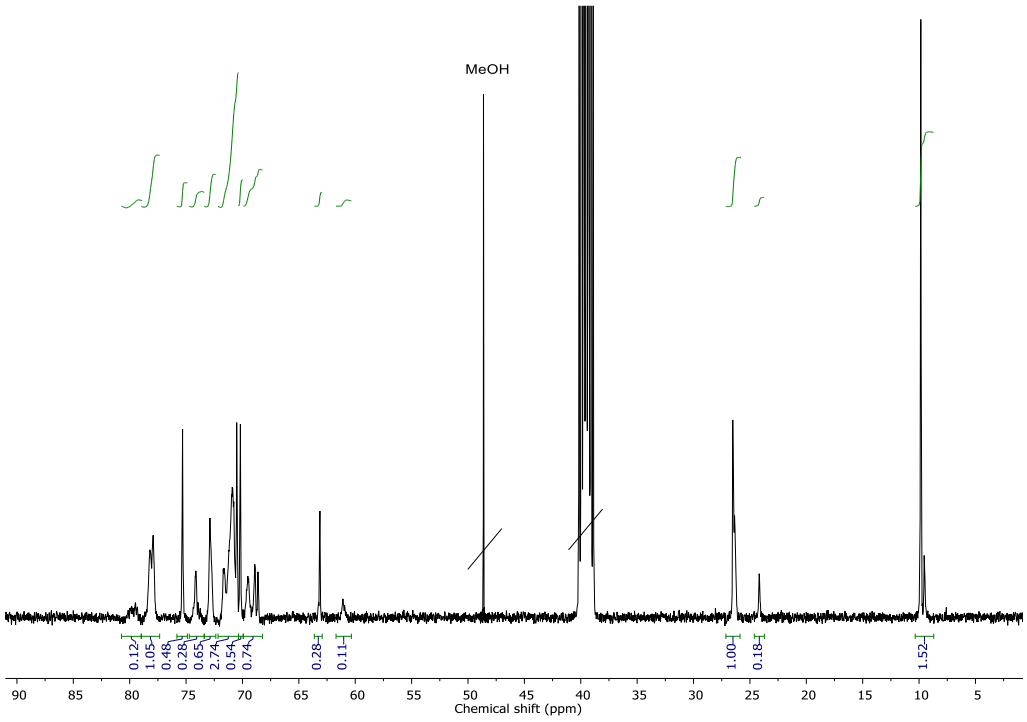

Figure S5. Inverse gated ^{13}C NMR spectrum of *hb*(PBO_{36}-*co*-PG_{64}) (100 MHz, DMSO-d_6)

Partial overlap and the noise level inherent to inverse gated ^{13}C NMR may cause errors when integrating the signals of the different repeating units.

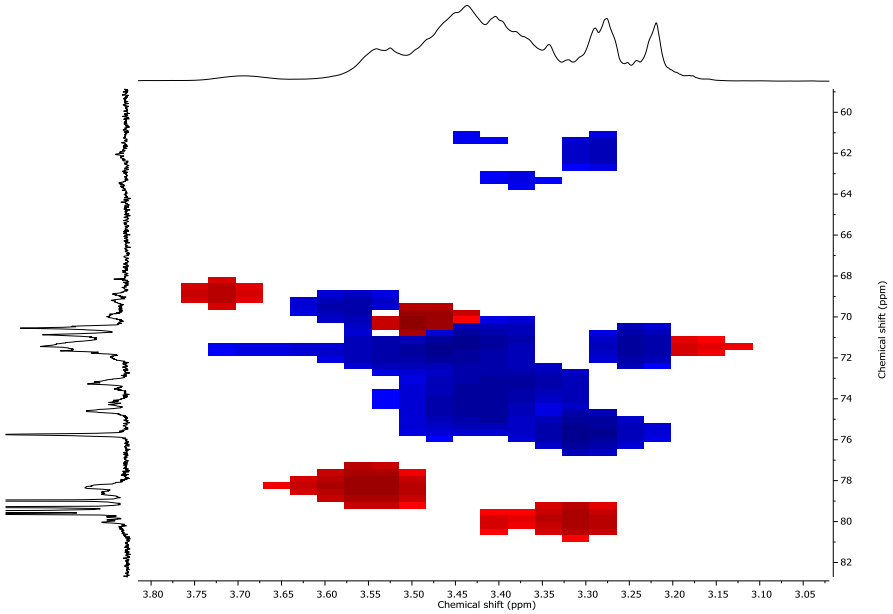

Figure S6. HSQC spectrum of *hb*(PBO_8-*co*-PG_6) (400/100 MHz, DMSO-d_6 + $CDCl_3$). ^1H- and ^{13}C NMR spectra can be found on the horizontal and vertical axis, respectively. Phase correlation is given by correlation of cross peaks (red: methyl, methine, blue: methylene).

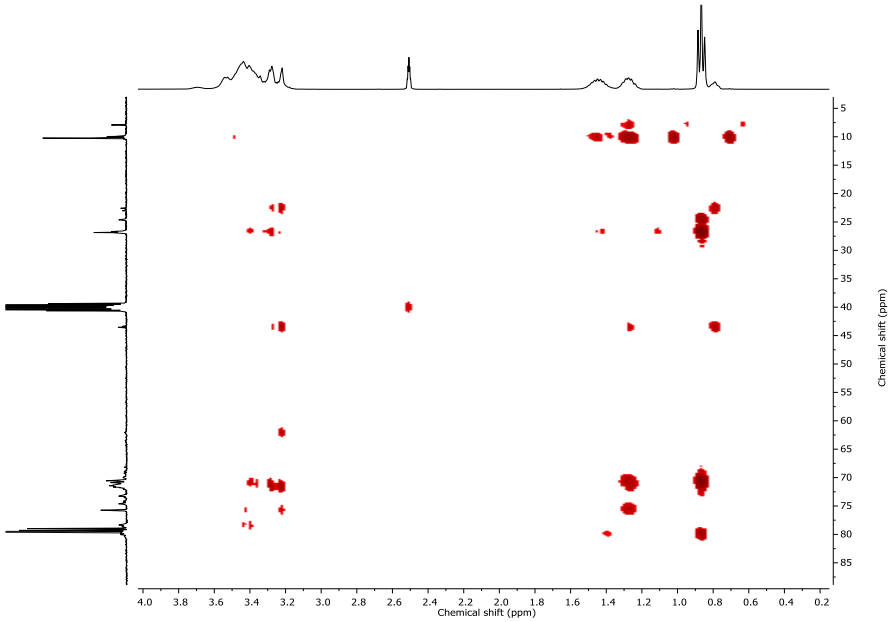

Figure S7. HMBC spectrum of *hb*(PBO_8-*co*-PG_6) (400/100 MHz, DMSO-d_6+$CDCl_3$). ^1H- and ^{13}C NMR spectra can be found on the horizontal and vertical axis, respectively.

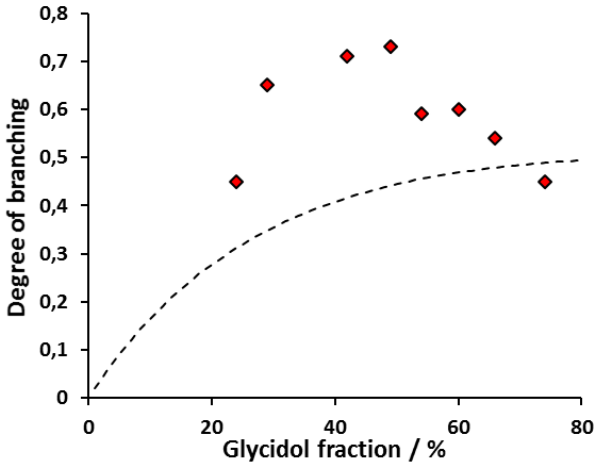

Figure S8. Calculated degrees of branching of *hb*(PBO-*co*-PG) with varying monomer composition prepared by batch polymerization as a function of the glycidol molar fraction. The dashed line represents theoretical values for a random AB/AB_2 copolymerization in batch.[3]

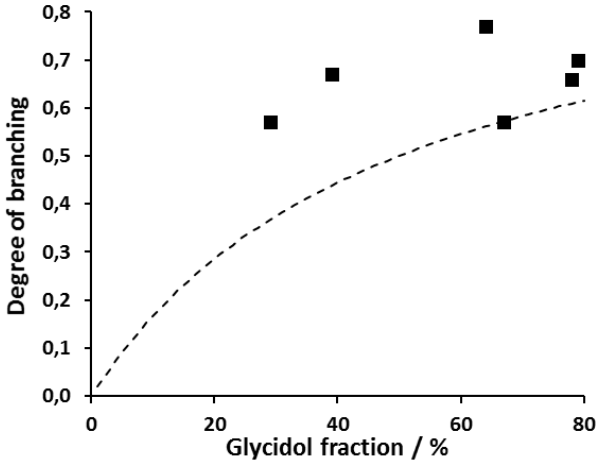

Figure S9. Calculated degrees of branching of *hb*(PBO-*co*-PG) with varying monomer composition prepared by slow monomer addition as a function of the glycidol molar fraction. The dashed line represents theoretical values for a random AB/AB_2 copolymerization by slow monomer addition.[4]

Thermal Properties

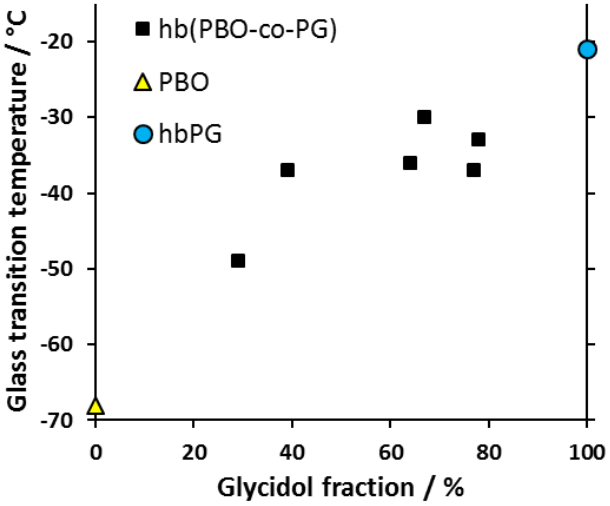

Figure S10. Glass transition temperatures (T_g) of the *hb*(PBO-*co*-PG) copolymers with varying composition, prepared by SMA procedure. T_g of linear PBO and *hb*PG for comparison.[5,6]

References

1. Schuck, P. *Biophys. J.* **2000**, *78*, 1606–1619.
2. Kratky, O.; Leopold, H.; Stabinger, H. [5] The determination of the partial specific volume of proteins by the mechanical oscillator technique. *Part D: Enzyme Structure*; Methods in Enzymology; Elsevier, **1973**; 98–110.
3. Frey, H.; Hölter, D. *Acta Polym.* **1999**, *50*, 67–76.
4. Sunder, A.; Türk, H.; Haag, R.; Frey, H. *Macromolecules* **2000**, *33*, 7682–7692.
5. Lai, J.; Trick, G. S. *J. Polym. Sci. A-1 Polym. Chem.* **1970**, *8*, 2339–2350.
6. Sunder, A.; Hanselmann, R.; Frey, H.; Mülhaupt, R. *Macromolecules* **1999**, *32*, 4240–4246.

3

HYPERBRANCHED POLY(ALKYLENE OXIDE)S AS MACROINITIATORS FOR MULTIARM STAR COPOLYMERS

3.1 Controlled Synthesis of Multi-Arm Star Polyether-Polycarbonate Polyols Based on Propylene Oxide and CO_2

*Jeannette Hilf[1,2], Patricia Schulze,[1] Jan Seiwert[1] and Holger Frey[1,2,]**

[1] Institute of Organic Chemistry, Johannes Gutenberg-University, Duesbergweg 10-14, 55128 Mainz, Germany

[2] Graduate School Materials Science in Mainz, Staudinger Weg 9, 55128 Mainz, Germany

Published in *Macromolecular Rapid Communications* **2014**, *35*, 198–203.

This chapter originates from a collaboration with Dr. Jeannette Hilf and was also presented in her PhD thesis.

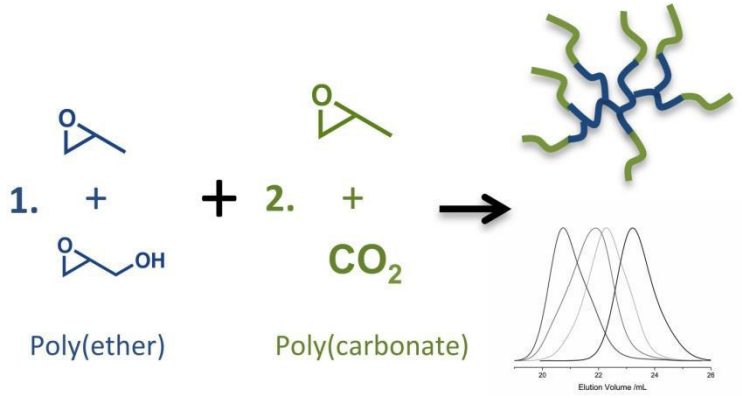

Abstract

Multiarm star copolymers based on a hyperbranched poly(propylene oxide) polyether-polyol (*hb*PPO) as a core and poly(propylene carbonate) (PPC) arms have been synthesized in two steps from propylene oxide (PO), a small amount of glycidol and CO_2. The PPC arms were prepared via carbon dioxide (CO_2)/propylene oxide copolymerization, using *hb*PPO as a multifunctional macroinitiator and the (R,R)-(salcy)-CoOBzF_5 catalyst. Star copolymers with 14 and 28 PPC arms, respectively, and controlled molecular weights in the range of 2700-8800 g/mol have been prepared (M_w/M_n =1.23-1.61). Thermal analysis revealed lowered glass transition temperatures in the range of -8 to 10°C for the poly(propylene carbonate) star polymers compared to linear PPC, which is due to the influence of the flexible polyether core. Successful conversion of the terminal hydroxyl groups with phenylisocyanate demonstrates the potential of the polycarbonate polyols for polyurethane synthesis.

Introduction

Carbon dioxide (CO_2), an industrial waste product, is a potentially interesting C1 feedstock, as it is nontoxic, renewable, abundant and inexpensive. The growing recent interest of organic and bio-organic chemists in CO_2 has led to the development of a variety of synthetic reactions using carbon dioxide directly as a raw material, especially in the field of polymer chemistry. [1–7] Since the seminal discovery of the copolymerization of CO_2 and epoxide monomers by Inoue et al in 1969,[8,9] numerous works on different heterogeneous and homogeneous catalyst systems have been reported, and mostly propylene oxide and cyclohexene oxide have been polymerized to poly(propylene carbonate) (PPC) and poly(cyclohexene carbonate) (PCHO).[10–16] The commercialization of PPC has recently reached a modest volume of approximately 1000 t/year and is gaining increasing attention.[5] The main reason for the interest in PPC is its smooth biological degradation characteristics.[5] Current challenges for PPC include the diversification of its properties, especially with respect to broadening the scope of applications beyond the use as a thermoplastic material. Mostly linear poly(propylene carbonate) homopolymers have been studied to date.[13,17–19] Only few works aimed at the synthesis of block copolymers or branched PPC architectures. Since it is well-known that in the synthesis of PPC molecular weights can be controlled, using various catalyst systems in an immortal polymerization, and in elegant works Lee et al. demonstrated the general feasibility of linear PPC block copolymers[8,9,14,20–23], tailoring of

macromolecular parameters such as molecular weight, polydispersity, and chain-ends for PPC-based complex polymer structures is emerging as a current focus of research.

Here we present a rapid two-step approach to flexible multiarm star polymers with PPC arms. In multiarm star polymers a large number of linear arms is connected to a central branched core. Such materials show unusual mechanical, rheological, and biomedical properties that differ from the corresponding linear polymers.[24–28] Furthermore they are particularly interesting because of their large number of functional end groups compared to linear polymers of similar molecular weight as well as their improved solubility profile.[24,29,30] To date, multifunctional polycarbonate polymer architectures have been exclusively prepared by the ring-opening polymerization of six-membered cyclic carbonate monomers.[31,32,33] Aliphatic polycarbonate polyols have already been suggested for a wide range of potential applications.[34–38] The additional free hydroxyl groups in polycarbonate polyols provide sites for the attachment of dyes, flame retardants, bioactive molecules, or cross-linking of materials. In addition, polycarbonate polyols have been introduced for the manufacture of polyurethanes for high-performance coating applications.[39] However, the respective cyclic carbonate monomers have to be prepared in multistep reactions, which represents a drawback for actual application.

In this work we describe a synthetic route for flexible multiarm star block copolymers, using a hyperbranched poly(propylene oxide) copolymer with glycerol branching points[40] as a multifunctional initiator for the controlled catalytic copolymerization of carbon dioxide with propylene oxide (Scheme 1).

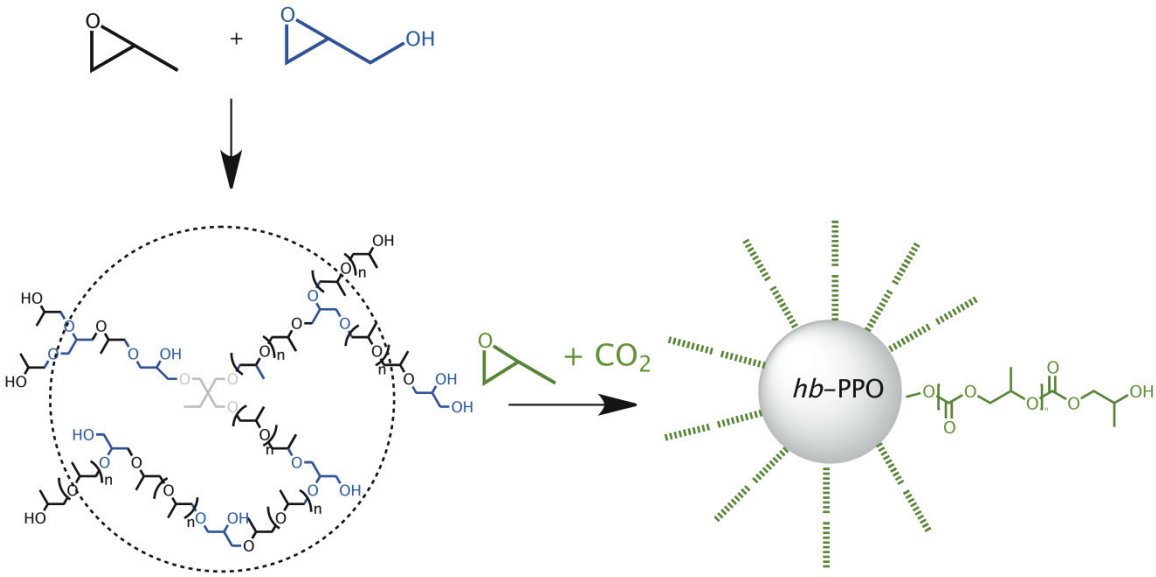

Scheme 1: Two-step synthesis of hyperbranched PPC multiarm star copolymers from PO and CO_2 with *hb*(PG-*co*-PPO) core (left); branching points are generated from glycidol in the first step.

This approach results in PPC multiarm star copolymers with flexible polyether core. The resulting multifunctional PPC copolymers have been investigated with respect to molecular weight control, PPC chain length per arm, thermal properties as well as the possibility to use the terminal hydroxyl groups for derivatization reactions with isocyanates.

Experimental Section

Instrumentation as well as synthesis and characterization of the hyperbranched PPO core structures[40] and the preparation of the catalyst employed for the PO/CO_2 copolymerization are described in the Supporting Information.

Synthesis of *hb*-PG-*co*-PPO/PPC Star Copolymers (Table 1, Sample 3)

A 100 mL Roth autoclave was dried under vacuum at 40 °C. (R,R)-(salcy)-CoOBzF_5 (11.7 mg, 0.0143 mmol), the cocatalyst (PPN)Cl (8.2 mg, 0.014 mmol), PO (1.9 mL, 26 mmol) and dried 200 mg *hb*-$PG_{0.17}$-*co*-$PPO_{0.83}$ (Table 1, sample 1) were placed in a glass tube with a Teflon stir bar inside the autoclave. The autoclave was pressurized at 50 bar CO_2 and was left to stir at 30 °C for 18 h. The reactor was vented; the polymerization mixture was dissolved in chloroform (5 mL), quenched with 5% HCl solution in methanol (0.2 mL) and then precipitated in ice-cold pentane. The polymer (sample 3) was fractionated by preparative SEC, collected and dried *in vacuo*. Yield 95 %.

^{1}H NMR ($CDCl_3$-*d*$_1$, 300 MHz): δ (ppm) = 5.00 (methane CH backbone), 4.19 (methylene CH_2), 3.55 (hyperbranched core), 1.33 (CH_3) and 1.18 (CH_3 core).

Transformation with Phenylisocyanate.

150 mg *hb*($PG_{0.39}$-*co*-$PPO_{0.61}$)-*g*-PPC_{38} and 2mL phenylisocyanate were mixed and stirred under Argon for 4 h. The solution was precipitated once in methanol and twice in pentane to remove the excess of phenylisocyanate. The resulting product was dried at 60°C in vacuum for 24 h. Yield 90 %.

^{1}H NMR ($CDCl_3$-*d*$_1$, 300 MHz): δ (ppm) = 7.40-7.08 (aromatic protons and $CDCl_3$-*d*$_1$), 5.00 (methane CH backbone), 4.19 (methylene CH_2), 3.55 (hyperbranched core), 1.33 (CH_3) and 1.18 (CH_3 core).

Results and Discussion

Multifunctional, hyperbranched PPO copolymers with varied glycerol content and consequently varied number of glycerol branching points and end groups[40] have been used to synthesize PPC multiarm star copolymers. The polyether-polyol samples were prepared by one-pot synthesis via random copolymerization of propylene oxide and glycidol (anionic ring-opening multibranching polymerization), using partially deprotonated trimethylolpropane as a trifunctional initiator according to a recently published procedure.[40]As listed in Table 1, two different hyperbranched PPO copolymers, namely *hb*($PG_{0.17}$-*co*-$PPO_{0.83}$) and *hb*($PG_{0.39}$-*co*-$PPO_{0.61}$) (listed as samples **1** and **5** in Table 1) have been prepared and used as multifunctional initiators, containing 17 and 39 mol% glycerol units, respectively. The fraction of glycerol units incorporated in the polymer was calculated by referencing to the methyl group of the initiator (0.78 ppm) and comparing this value with the integral of the methyl group of the propylene oxide units (0.99-1.05 ppm) and the methylene and methine groups of the polymer backbone (3.1-3.9 ppm). In addition, the total number of glycidol units of each macromolecule corresponds to the total number of hydroxyl groups (4.4-4.7 ppm) minus the number of hydroxyl groups introduced by the initiator moiety (assuming that the core is fully incorporated into all polymer molecules of the distribution). In the case of a trimethylolpropane core, n(OH) core equals a value of 3. The other five protons of each glycerol unit as well as three propylene oxide protons generate a broad resonance between 3.1 and 3.8 ppm. Hence, the ratio between propylene oxide and glycerol repeat units can be directly calculated. For sample 1 and 5 the average number of hydroxyl groups was determined to be 14 and 28, respectively. Depending on the amount of hydroxyl functionalities, the number of arms can be varied in the *grafting-from* strategy applied. Characterization data for the core molecules can be found in the Supporting Information.

In a solvent-free synthesis procedure, different poly(propylene carbonate) arm lengths were obtained by varying the PO/CO_2 monomer to hydroxyl group concentration of the multifunctional macroinitiator (Figure 1). The synthesis of the copolymers was achieved via a *grafting-from* approach, performing the copolymerization of propylene oxide (PO) and carbon dioxide (CO_2) in the presence of the multifunctional polyether as a macro-transfer agent, i.e., as a multifunctional initiator. It is imperative for the approach described in this work that the hyperbranched PPO macroinitiator is soluble in propylene oxide under pressure. In a series of solubility experiments it was established that the macroinitiator forms a homogeneous solution in the PO/CO_2 monomer mixture. Due to the solubility of the hyperbranched PPO macroinitiator in neat propylene oxide no additional solvent was used. All PO/CO_2 polymerizations were carried out under identical

reaction conditions, i.e., argon atmosphere, room temperature and 50 bar CO_2 pressure with a (R,R)-(salcy)$CoBzF_5$ catalyst and bis(triphenylphosphine(iminium cloride) (PPNCl) as a cocatalyst for 2 hours. The catalyst and cocatalyst were efficiently removed from the final product via precipitation in cold pentane (0°C). The resulting star polymers have been characterized by NMR- and IR-spectroscopy, size exclusion chromatography (SEC) and differential scanning calorimetry (DSC). All data are summarized in Table 1.

Table 1. Characterization data of all copolymer samples prepared.

#	Sample[a]	M_n (g/mol)[b]	M_n (g/mol) (NMR)	PDI[b]	# PPC Arms[c]	DB[d]	T_g (°C)[e]
1	*hb* ($PG_{0.17}$-*co*-$PPO_{0.83}$)	1800	4300	1.45	-	0.28	-59
2	*hb*($PG_{0.17}$-*co*-$PPO_{0.83}$)-*g*-PPC_9	2700	17 100	1.23	14	0.28	-8
3	*hb*($PG_{0.17}$-*co*-$PPO_{0.83}$)-*g*-PPC_{19}	5800	31 400	1.41	14	0.28	2
4	*hb*($PG_{0.17}$-*co*-$PPO_{0.83}$)-*g*-PPC_{27}	8800	42 800	1.38	14	0.28	7
5	*hb*($PG_{0.39}$-*co*-$PPO_{0.61}$)	1400	3500	1.61	-	0.55	- 48
6	*hb*($PG_{0.39}$-*co*-$PPO_{0.61}$)-g-PPC_{22}	3500	66 300	1.62	28	0.55	-5
7	*hb*($PG_{0.39}$-*co*-$PPO_{0.61}$)-g-PPC_{38}	5300	112 000	1.53	28	0.55	1
8	*hb*($PG_{0.39}$-*co*-$PPO_{0.61}$)-g-PPC_{46}	6800	134 800	1.58	28	0.55	10

Reaction conditions: 50 bar CO_2, 2h, RT; [a)]block lengths determined by ^{1}H NMR spectroscopy, [b)]SEC calibrated with PEG standards in DMF at 40 °C, [c)] determined by ^{1}H NMR spectroscopy [d)]Degree of branching of the polyether core determined by Inverse-Gated ^{13}C NMR spectroscopy [e)]Glass transition obtained from DSC.

In Figure 1 the ^{1}H NMR spectrum of *hb*($PG_{0.17}$-*co*-$PPO_{0.83}$)-*g*-PPC_{27} (Table 1, sample 4) in $CDCl_3$ is shown as a typical example for the multiarm star copolymers. In this case, the average degree of polymerization of each PPC-arm is 27. In addition to the hyperbranched PPO core signal (3.50 and 1.12 ppm), the typical resonances for poly(propylene carbonate) can be discerned (5.00, 4.19 and 1.33 ppm). The average PPC side chain length and also the molecular weight were determined by comparison of the integration values of the PPC chain end-group resonances (4.86 ppm) with the poly(propylene carbonate) methine resonances (5.00 ppm). The number of PPC chains attached can be calculated as described below. Detailed characterization of the hyperbranched core molecules was performed as described in the Supporting Information. From these studies the number of protons in the macroinitiator-core is known. With this information the number of PPC end groups can be determined, and thus the number of PPC side chains can be calculated. For the

star copolymers prepared in this study, the number of PPC side chains is in good agreement with the number of hydroxyl groups from the macro initiator. ^{13}C NMR spectroscopy also confirmed the structure of the copolymers and the typical carbonate resonance of the PPC arms at δ = 154.26 ppm can clearly be detected. Furthermore the typical signals of the polyether core molecules are clearly visible at δ = 77.16, 65.68 and 17.35 ppm (Figure S6).

In addition to the NMR data, the incorporation of CO_2 into the polymer was confirmed by IR spectroscopy (Figure S5). Only one carbonate band at around 1740 cm^{-1} was detected, which can be assigned to the C=O group of the linear carbonate. No bands for a cyclic carbonate, which appear at around 1790 cm^{-1}, were observed in the IR (or NMR) spectra of the non-purified copolymers.

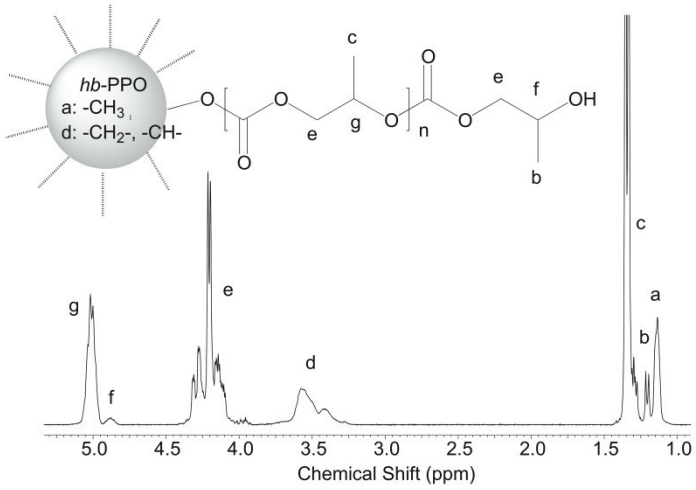

Figure 1. ^{1}H NMR spectrum of *hb*-($PG_{0.17}$-*co*-$PPO_{0.83}$)-*g*-PPC_{27} (Table 1, sample 4) (300 MHz, $CDCl_3$).

Size exclusion chromatography (SEC) revealed apparent molecular weights between 2700 and 8800 g/mol, monomodal distributions and low to moderate PDI values between 1.23-1.61. The molecular weights (M_n) of all synthesized copolymers were significantly higher than for the starting core copolymers, and the molecular weight distributions were monomodal, indicating complete conversion of the *hb*-PPO-*co*-PG core molecule (Figure 2). In general, a strong deviation of the molecular weights determined by SEC and the calculated values based on the NMR results was observed (Table 1). The underestimation of M_n is particularly noticeable for samples 6-8 with the highest DB of the core molecule and can be ascribed to the highly branched architecture. It is well-known that the hydrodynamic radius, which determines the elution volume of the polymer, does not increase linearly with the increase in mass.[41,42] Generally star-shaped or hyperbranched copolymers show lower hydrodynamic volume in solution compared to linear analogues of similar

molar mass. This explains why the most significant underestimation of molecular weight is found for the higher branched systems with the longest side chains.

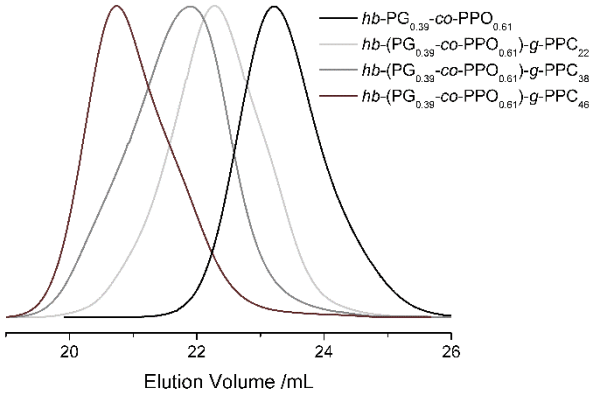

Figure 2. SEC results for some of the (PG-*co*-PO)-*g*-PPC star copolymers in chloroform (samples 5-8, Table 1).

Thermal and Solution Properties

The thermal behavior of the PPC multiarm copolymers has been studied by differential scanning calorimetry (DSC). No melting points were detected, as expected due to the atatic nature of the PPC chains and the hyperbranched core. For all samples no separate glass transition temperatures for the *hb*PPO or PPC homopolymer constituents were detected. These results lend additional support to the conclusion, that *hb*PPO/PPC star copolymers without homopolymer contaminants were obtained, as also confirmed by the SEC data. In general, the glass transition temperatures of the star copolymer structures are in the range of -8°C to 10°C and increase with increasing degree of polymerization of the PPC chains attached. However, compared to the linear PPC homopolymer (T_g around 40°C) the glass transition temperatures are still considerably lowered for the star copolymers, which is attributed to the flexibilizing effect of the polyether core. On the other hand, polymerization of poly(propylene carbonate) onto the hyperbranched core molecule leads to an increase of the T_g by about 50 °C compared to the highly flexible polyether core polymers. With increasing degree of polymerization of the PPC block from 9 to 46 units the glass transition temperature increases from -8°C to 7 °C and from -5°C to 10°C, respectively, which demonstrates the increasing impact of the PPC chains with their length. No significant difference can be found for the different types of stars, and also no significant effect of the number of PPC arms on T_g is visible. In summary, rather flexible polycarbonate-polyols can be realized by employing the mobile polyether core structure.

The intrinsic viscosity of samples 1-4 was determined using a Ubbelohde viscometer at 25°C in chloroform (for details see Supporting Information). The lowest intrinsic viscosity (5.9 cm^3/g) was obtained for the hyperbranched core molecules (sample 1), which agrees with expectation, since it is a hyperbranched structure with low molecular weight. The star copolymers revealed values from 9.1 (sample 2) and 11.6 (sample 3) to 12.6 cm^3/g (sample 4). Depending on the degree of polymerization of the PPC side chains the intrinsic viscosity increased, which again is in agreement with expectation. However the overall intrinsic viscosities are low in comparison to linear PPC[44] and reflect the star shaped structure of the synthesized copolymers.

Functionalization

Polycarbonate polyols with 2-3 hydroxyl end groups have been introduced as components for polyurethane elastomers, foams and coatings, in analogy to the polyether polyols that are highly established in these fields. Polycarbonate polyols are prepared by reacting polyol components such as 1,4-butanediol, 1,6-hexanedediol or 2-methyl-1,8-octanediol with an organic carbonate, such as dimethylcarbonate. However, most of these polyols available at present are solids at room temperature. Therefore additional solvents or heating is required in order to form polyurethanes. Therefore, non-crystalline and flexible polycarbonate polyols are desirable. Compared to linear polyether-polycarbonate polyols, the number of hydroxyl groups is strongly increased for the star shaped polycarbonate polyols reported in this work, and as shown above they are not crystalline. The hyperbranched polyether core provides flexibility, and the amorphous PPC arms prevent crystallization.

For a proof of principle study, phenylisocyanate has been used as a model compound for the reaction with the newly synthesized star shaped polyols to form urethanes. To this end, the polymers were mixed with an excess of phenylisocyanate and stirred for 4 hours. Subsequently the polymers were precipitated in cold pentane and dried in high vacuum to remove the excess of isocyanate. Figure S10 shows the ^{1}H NMR spectrum of *hb* ($PG_{0.17}$-*co*-$PPO_{0.83}$)-*g*-PPC_{19} (Table 1, sample 3) in $CDCl_3$ after reaction with phenylisocyanate. The aromatic signals of the phenyl group can clearly be seen in the region from 7.45 to 7.00 ppm, and the integral fits with the number of PPC side chains. SEC confirmed transformation of the hydroxyl end groups (Figure S9), evident from a strong UV-signal. Thus, these hyperbranched polyether-polycarbonate stars are promising polyols for polyurethane formation. Further work in this area is in progress.

Conclusions

To the best of our knowledge, this work is the first account of the combination of anionic multibranching polymerization and the immortal polymerization of epoxides and CO_2. Multiarm star shaped poly(propylene carbonate) polyols have been synthesized directly from CO_2 and propylene oxide, based on a flexible, hyperbranched poly(propylene oxide) core. Importantly, this core molecule is fully soluble in liquid PO, which is a crucial precondition for the solvent-free synthesis strategy described. The average degree of polymerization of the poly(propylene carbonate) arms is adjustable by the monomer/initiator ratio. For the full structure elucidation of the resulting polymers SEC, NMR spectroscopy, DSC and FT-IR spectroscopy have been employed. A systematically varied series of polycarbonate stars with apparent molecular weights between 1400-8800 g/mol was obtained. The polydispersity was moderate for all materials, and the polydispersity index was in the range of 1.23 to 1.62 for all polymers. The materials exhibited low viscosity in solution, as is typical for multiarm star polymers. It should be emphasized that a solvent-free procedure was used for the PPC star polymer synthesis, which renders the approach interesting for large scale.

Depending on the degree of polymerization of the PPC arms the glass transitions decreased in comparison to the linear poly(propylene carbonate). Notably, the post-polymerization functionalization of the hydroxyl end groups with phenylisocyanate was shown to be highly efficient and occured without observable backbone degradation, enabling the potential use of the multifunctional PPC polymers as flexible, non-crystalline polycarbonate polyols for polyurethanes.

Acknowledgment

J. H. is grateful for support through the Excellence Initiative (DFG/GSC 266) in the context of the graduate school of excellence “MAINZ” (Materials Science in Mainz) and financial support by a fellowship from the Fonds der Chemischen Industrie (FCI). Furthermore we thank Pascal Guckes and Maria Müller for technical assistance.

References

1. Coates, G. W.; Moore, D. R. *Angew. Chem. Int. Ed.* **2004**, *43*, 6618–6639.
2. Cheng, M.; Lobkovsky, E. B.; Coates, G. W. *J. Am. Chem. Soc.* **1998**, *120*, 11018–11019.
3. Darensbourg, D. Rieger, B.; Künkel, A.; Coates, G. W.; Reichardt, R.; Dinjus, E.; Zevaco, T. A., Eds.; Springer Berlin / Heidelberg, **2012**; Vol. 245, 1–27.
4. Klaus, S.; Lehenmeier, M. W.; Anderson, C. E.; Rieger, B. *Coord. Chem. Rev.* **2011**, *255*, 1460–1479.
5. Rieger, B.; Künkel, A.; Coates, G. W. *Synthetic Biodegradable Polymers*; Rieger, B.; Künkel, A.; Coates, G. W., Eds.; 1st ed.; Springer Berlin / Heidelberg: Berlin, **2012**.
6. Kember, M. R.; Buchard, A.; Williams, C. K. *Chem. Commun.* **2011**, *47*, 141–163.
7. Darensbourg, D. J. *Chem. Rev.* **2007**, *107*, 2388–2410.
8. Inoue, S.; Koinuma, H.; Tsuruta, T. *Makromol. Chem.***1969**, *130*, 210–220.
9. Inoue, S. *J. Macromol. Sci.: Part A - Chem.***1979**, *13*, 651–664.
10. Dean, R. K.; Dawe, L. N.; Kozak, C. M. *Inorg. Chem.***2012**, *51*, 9095–9103.
11. Kim, J. G.; Cowman, C. D.; LaPointe, A. M.; Wiesner, U.; Coates, G. W. *Macromolecules* **2011**, *44*, 1110–1113.
12. Kember, M. R.; Copley, J.; Buchard, A.; Williams, C. K. *Poly. Chem.* **2012**, *3*, 1196–1201.
13. Cyriac, A.; Lee, S. H.; Varghese, J. K.; Park, J. H.; Jeon, J. Y.; Kim, S. J.; Lee, B. Y. *Green Chem.* **2011**, *13*, 3469–3475.
14. Seong, J. E.; Na, S. J.; Cyriac, A.; Kim, B.-W.; Lee, B. Y. *Macromolecules* **2009**, *43*, 903–908.
15. Luinstra, G. A. *Polym. Rev.* **2008**, *48*, 192–219.
16. Korashvili, R.; Nörnberg, B.; Bornholdt, N.; Borchardt, E.; Luinstra, G. A. *Chem. Ing. Tec.* **2013**, *85*, 437–446.
17. Rokicki, A.; Kuran, W. *Makromol. Chem.***1979**, *180*, 2153–2161.
18. Li, H. C.; Niu, Y. S. *Polymer Journal* **2011**, *43*, 121–125.
19. Ree, M.; Bae, J. Y.; Jung, J. H.; Shin, T. J.; Hwang, Y. T.; Chang, T. *Polym. Eng. Sci.* **2000**, *40*, 1542–1552.
20. Cyriac, A.; Lee, S. H.; Lee, B. Y. *Polym. Chem.* **2011**, *2*, 950–956.
21. Lee, S. H.; Cyriac, A.; Jeon, J. Y.; Lee, B. Y. *Clean Tec.* **2011**, *17*, 244–249.
22. Cyriac, A.; Lee, S. H.; Varghese, J. K.; Park, E. S.; Park, J. H.; Lee, B. Y. *Macromolecules* **2010**, *43*, 7398–7401.
23. Inoue, S. *J. Polym. Sci. Part A: Polym. Chem.* **2000**, *38*, 2861–2871.
24. Inoue, K. *Prog. Polym. Sci.* **2000**, *25*, 453–571.
25. Gottschalk, C.; Wolf, F.; Frey, H. *Macromol. Chem. Phys.* **2007**, *208*, 1657–1665.

26. Choi, Y. K.; Bae, Y. H.; Kim, S. W. *Macromolecules* **1998**, *31*, 8766–8774.
27. a) Li, Y.; Kissel, T. *Polymer* **1998**, *39*, 4421–4427; b) A. Sunder, R. Mülhaupt, H. Frey, *Macromolecules* **2000**, *33*, 309; c) S. Maier, A. Sunder, H. Frey, R. Mülhaupt, *Macromol. Rapid. Commun.* **2000**, *21,* 226.
28. Su, W.; Luo, X.; Wang, H.; Li, L.; Feng, J.; Zhang, X.-Z.; Zhuo, R. *Macromol. Rapid Commun.* **2011**, *32*, 390–396.
29. Voit, B. I.; Lederer, A. *Chem. Rev.* **2009**, *109*, 5924–5973.
30. Schömer, M.; Frey, H. *Macromol. Chem. Phys.* **2011**, *212*, 2478–2486.
31. Parzuchowski, P. G.; Jaroch, M.; Tryznowski, M.; Rokicki, G. *Macromolecules* **2008**, *41*, 3859–3865.
32. Tryznowski, M.; Tomczyk, K.; Fraś, Z.; Gregorowicz, J.; Rokicki, G.; Wawrzyńska, E.; Parzuchowski, P. G. *Macromolecules* **2012**, *45*, 6819–6829.
33. Liu, C.; Jiang, Z.; Decatur, J.; Xie, W.; Gross, R. A. *Macromolecules* **2011**, *44*, 1471–1479.
34. Pokharkar, V. B.; Sivaram, S. *J. Control. Rel.* **1996**, *41*, 157–162.
35. Liu, B.; Zhang, M.; Yu, A.; Chen, L. *Gongcheng* **2004**, *20*, 76–79.
36. Chen, T.; Bai, Y.; Sun, R. *J. Appl. Polym. Sci.* **1998**, *67*, 569–575.
37. Hinz, W.; Dexheimer, E. M.; Broge, J.; Neff, R. A.; Smiecinski, T. M. A Method of forming a polyethercarbonate polyol **2006**, WO 2006/103214 A1.
38. Toshihide, K.; Yasunori, T.; Takashi, N.; Koichiro, N. Process for producing highly functional polycarbonate polyol **2003**, JP2003246852.
39. Schollenberger, C. S.; Stewart, F. D. *Angew. Makromol. Chem.* **1973**, *29*, 413–430.
40. Schömer, M.; Seiwert, J.; Frey, H. *ACS Macro Letters* **2012**, *1*, 888–891.
41. Schmidt, M.; Burchard, W.; Ford, N. C. *Macromolecules* **1978**, *11*, 452–454.
42. Schmidt, M.; Burchard, W. *Macromolecules* **1978**, *11*, 460–465.
43. Cohen, C. T.; Chu, T.; Coates, G. W. *J. Am. Chem. Soc.* **2005**, *127*, 10869–10878.
44. Kuran, W.; Listoś, T. *Macromol. Chem. Phys.* **1994**, *195*, 1011–1015.

Supporting Information

Materials and Instrumentation

Propylene oxide (PO, 98%, Aldrich) was distilled over CaH_2 under reduced pressure prior to use. Carbon dioxide (>99.99%) was used as received. All other reagents were used as received.

*NMR experiments***.** ^{1}H and ^{13}C NMR spectra were recorded on a Bruker AC 300 spectrometer, operated at 300 and 75.4 MHz and the chemical shifts are given in parts per million (ppm).

*Gel permeation Chromatography***.** Size exclusion chromatography (SEC) measurements were carried out in $CHCl_3$ on an instrument consisting of a Waters 717 plus auto sampler, a TSP Spectra Series P 100 pump, a set of three PSS SDV columns (104/500/50 Å), RI- and UV-detectors (absorption wavelength: 254 nm or 500 nm). All SEC diagrams show the RI detector signal, unless otherwise stated, and the molecular weights refer to linear polystyrene (PS) standards provided by Polymer Standards Service (PSS).

*Differential Scanning Calorimetry***.** DSC curves were recorded with a Perkin-Elmer DSC 7 CLN2 in the temperature range from – 100 to 150 °C at heating rates of 10 K min^{-1} under nitrogen.

IR-Spectroscopy. FT-IR spectra were recorded on a Thermo Scientific iS10 FT-IR spectrometer, equipped with a diamond ATR unit.

Ubbelohde Viscometer. Viscosity measurements to determine the intrinsic viscosity were performed with a LAUDA S5 and LAUDA PVS 1 Ubbelohde viscometer, equipped with a Metrohm liquid dosing unit. An 0c capillary with k=0.003 and 290 mm length was used. All measurement were performed at 25 °C. For each sample four different concentration were measured. For each concentration, after a relaxation period of 10 s, five flow times were measured. The mean values of the five measurements were used to calculate the reduced viscosity. The intrinsic viscosity was then obtained by plotting the reduced viscosity against concentration and extrapolating against c=0.

$$[\eta] = \lim_{c \to 0} \eta_{red}$$

Synthesis

Synthesis of Hyperbranched PPO-*co*-PG copolymers

(as described by Schömer et al.[1])

Typical procedure for the preparation of hyperbranched random copolymers of proyplene oxide and glycidol: An exemplary synthetic protocol is described for hb$PPO_{0.80}$-co-$PG_{0.20}$: A two-necked flask equipped with a septum, teflon seal and a magnetic stirrer was connected to a vacuum line. 45 mg (0.33 mmol) of 1,1,1-tris(hydroxymethyl)propane (TMP) was deprotonated with 0.3 eq. potassium tert-butoxide in methanol and dried azeotropically with benzene to remove the methanol together with formed tert-butanol and other volatiles. 2.32 g (40 mmol) propylene oxide (PO) was transferred to an ampoule and subsequently to the reaction flask in vacuo.

The flask was sealed and 740 mg (10 mmol) freshly distilled glycidol was introduced through the septum via cannula. The reaction mixture was then immediately heated to 120°C and stirred for 18 h. After addition of an excess of methanol to quench the polymerization, the solution of the copolymer was precipitated in a mixture of hexanes and isopropanol to afford the hyperbranched $PPO_{0.80}$-co-$PG_{0.20}$ in ca. 80-90% yield.

Synthesis of (R,R)-(salcy)-$CoOBzF_5$.

(R,R)-(salcy)$CoOBzF_5$ was prepared as described by Coates et. al.[43] Recrystallized (R,R)-(salcy)-Co^{II} and pentafluorobenzoic acid (0.42 g, 2 mmol) were added to a 50 mL round-bottom flask charged with a Teflon stir bar. Toluene (20 mL) was added to the reaction mixture, and it was stirred open to air at 22 °C for 12 h. The solvent was removed by rotary evaporation at 22 °C, and the solid was suspended in 200 mL of pentane and filtered. The dark green material was dried *in vacuo* and collected in quantitative yield (1.5 g).

^{1}H NMR (DMSO-d_6, 500 MHz): δ 1.30 (s, 18H), 1.59 (m, 2H), 1.74 (s, 18H), 1.90 (m, 2H), 2.00 (m, 2H), 3.07 (m, 2H), 3.60 (m, 2H), 7.44 (d, 4J) 2.5 Hz, 2H), 7.47 (d, 4J) 3.0 Hz, 2H), 7.81 (s, 2H).

Characterization

Characterization Data for the *hb*(PPO-*co*-PG) Copolymer Macroinitiators

Figure S1 shows the ^{1}H NMR spectrum of a typical PPO-*co*-PG copolymer. Both the initiator core and the hydroxyl protons are clearly visible. The fraction of glycerol units incorporated into the polymer was calculated by referencing to the methyl group of the initiator (0.78 ppm) and comparing this value with the integral of the methyl group of the propylene oxide units (0.99-1.05 ppm) and the methylene and methine groups of the polymer backbone (3.1-3.9 ppm). In addition, the total number of glycidol units of each macromolecule corresponds to the total number of hydroxyl groups (4.4-4.7 ppm) minus the number of hydroxyl groups introduced by the initiator moiety (assuming that the core is fully incorporated into all chains of the polymer distribution). In the case of a trimethylolpropane core, n(OH) core equals a value of 3. The other five protons of each glycerol unit as well as three propylene oxide protons generate a broad resonance between 3.1 and 3.8 ppm. Hence, the ratio of propylene oxide and glycerol repeat units can be directly calculated.

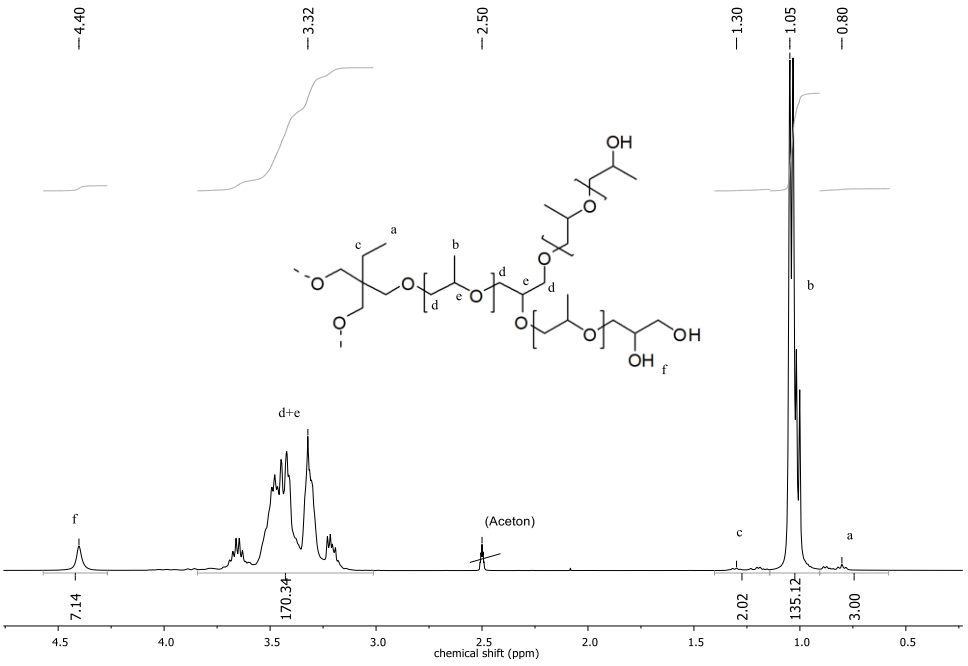

Figure S1. ^{1}H NMR spectrum of a typical hyperbranched PPO-*co*-PG copolymer.

$$\#PO = \frac{I_{Methyl}}{3}$$

$$\#G = \frac{I_{Backbone} - 3 \times \#PO}{5}$$

$$\#G = n(OH)_{total} - n(OH)_{core}$$

Both equations for the calculation of the number of glycidol units are in good agreement. These values become incorrect if the core is not fully incorporated into the polymer and/or if the intensity of the hydroxyl groups is very low (e.g., at low glycidol feed ratios).

$$DP_n = \#G + \#PO$$

$$\%G = \frac{\#G}{DP_n}$$

The overall degree of polymerization (DP_n) is the sum of both comonomers, and the glycidol content is calculated by dividing the number of G units by the DP_n. All values are rounded to integer.

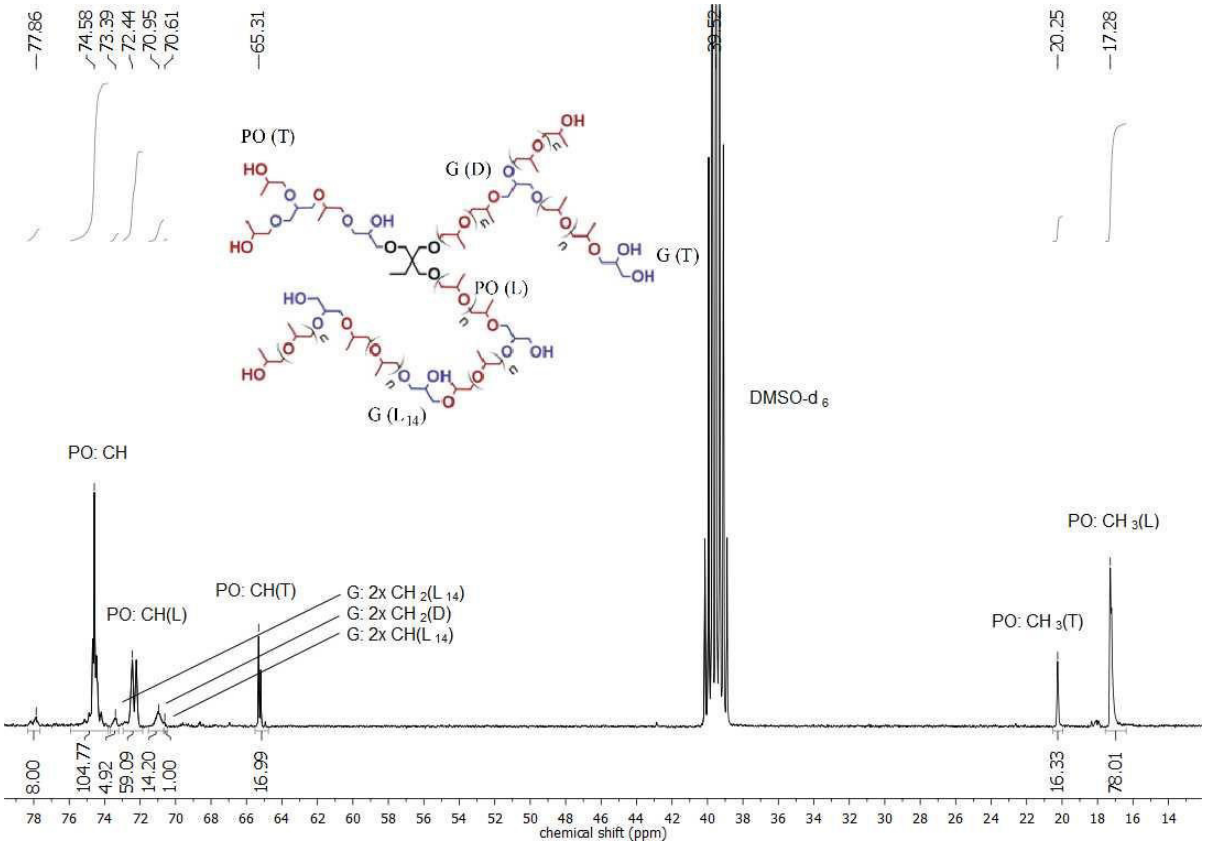

Figure S2. ^{13}C NMR spectrum of a typical PPO-*co*-PG copolymer.[1]

The degree of branching DB was calculated using the equation introduced by Hölter and Frey for random copolymerization of AB/AB_2 systems.[1]

$$DB_{AB/AB_2} = \frac{2D}{2D + L_{co}}$$

Figure S3 shows typical SEC traces of hb-PPO-*co*-PGs, measured in DMF with linear PEG standards.

Figure S3. SEC Results for hyperbranched core molecules

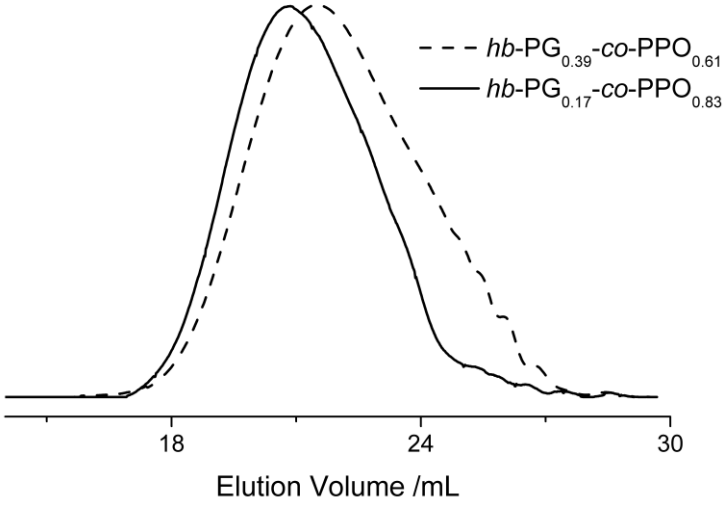

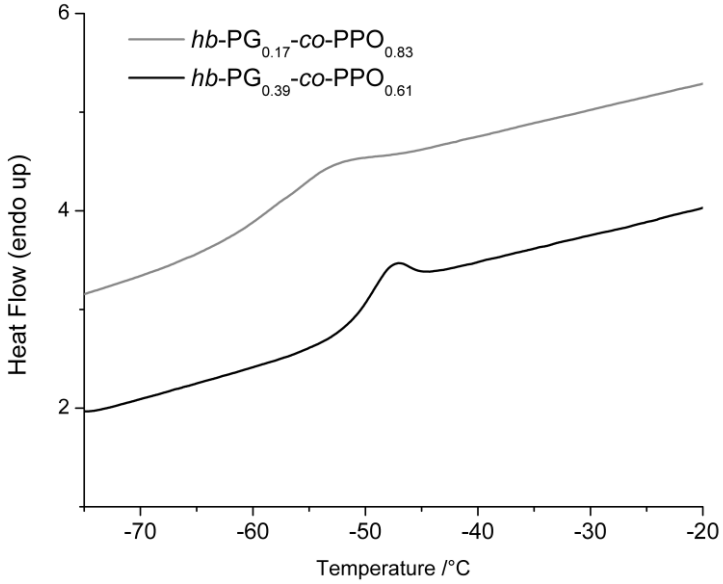

Figure S4. DSC Results for the hyperbranched core molecules.

Characterization Data for (PPO-*co*-PG)-*g*-PPC Star Copolymers

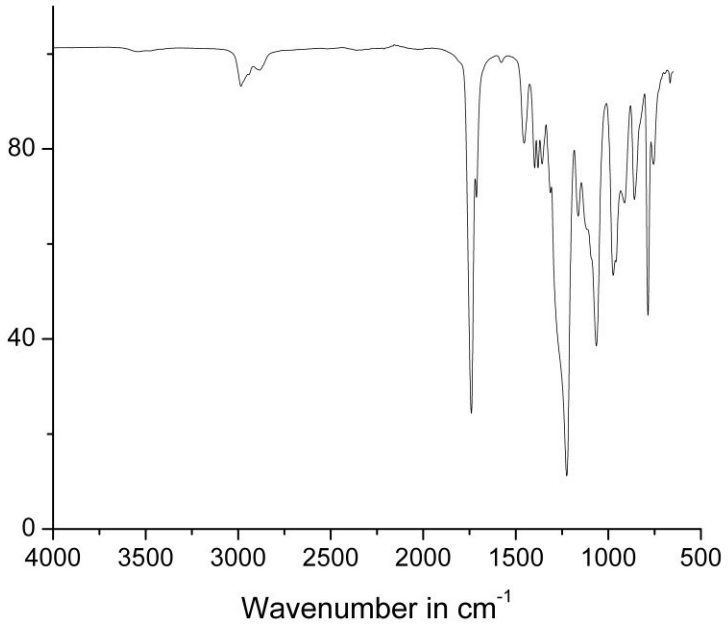

Figure S5. FT-IR spectrum of a typical (PPO-*co*-PG)-*g*-PPC star copolymer.

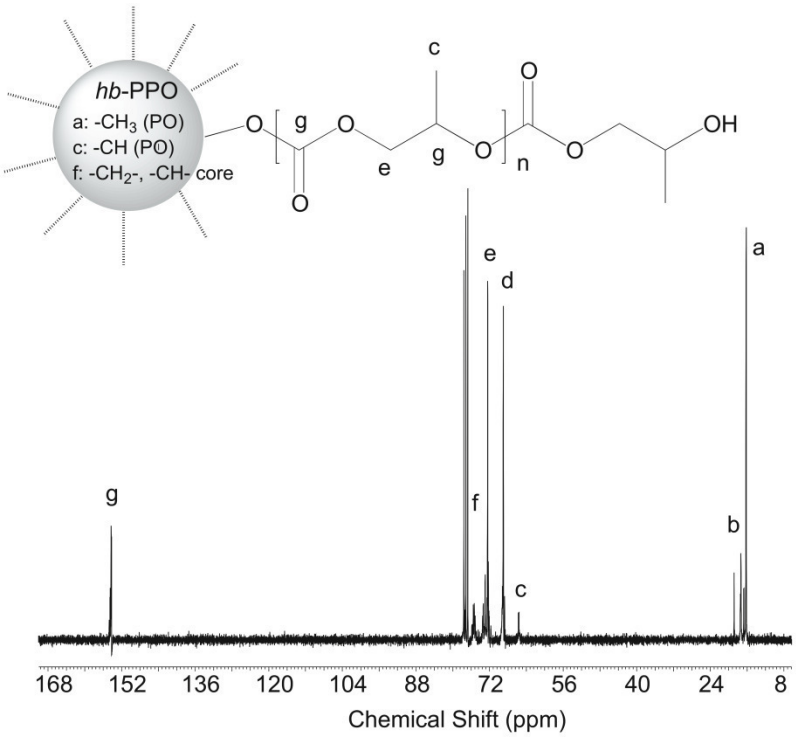

Figure S6. ^{13}C NMR spectrum of *hb*-($PG_{0.17}$-*co*-$PPO_{0.83}$)-*g*-PPC_{19} (Table 1, sample 3).

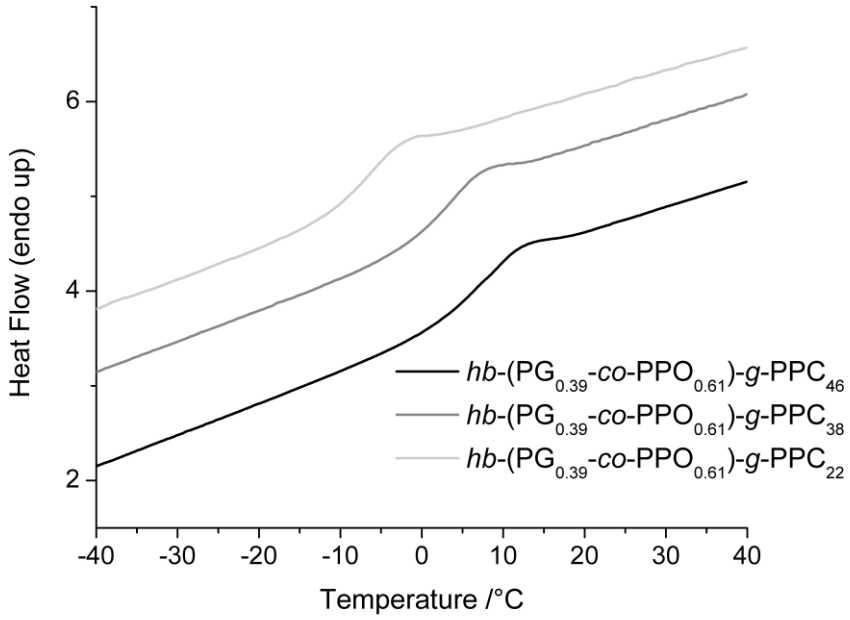

Figure S8. DSC results for the (PPO-*co*-PG)-*g*-PPC star copolymers.

Figure S9. SEC results before and after functionalization with phenylisocyanate.

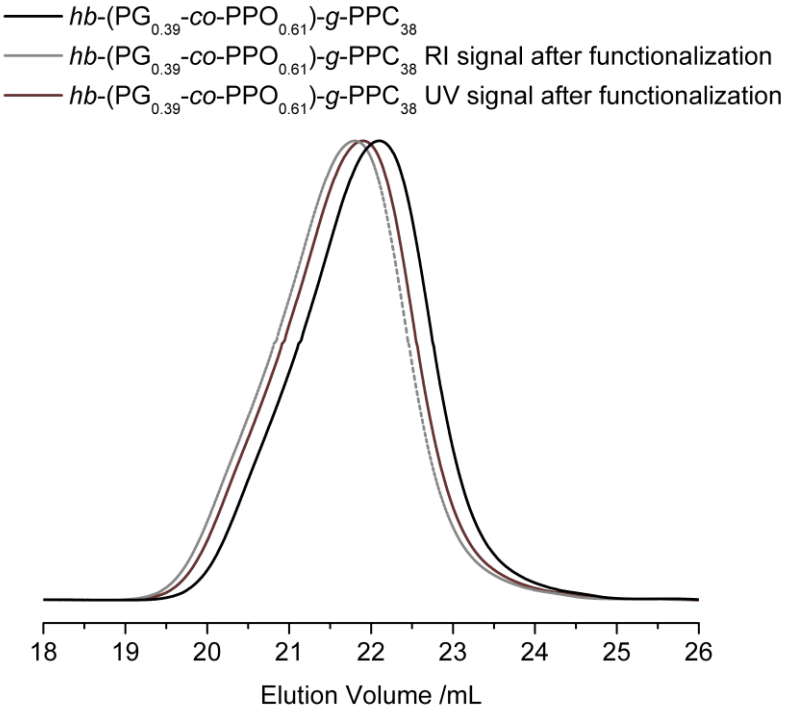

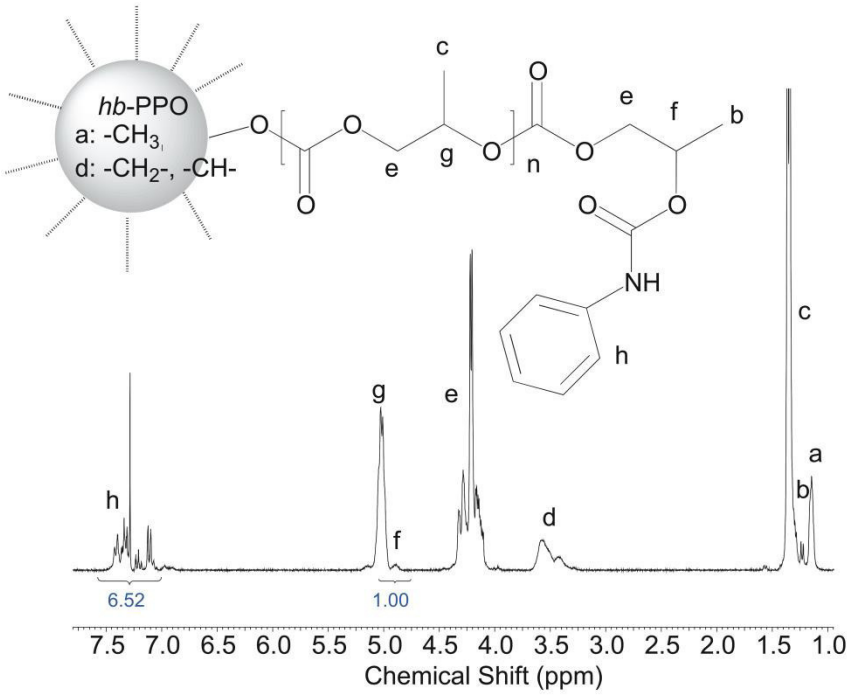

Figure S10. ^{1}H NMR spectrum of *hb*($PG_{0.17}$-*co*-$PPO_{0.83}$)-*g*-PPC_{19} (Table 1, sample 3) after reaction with phenylisocyanate in $CDCl_3$.

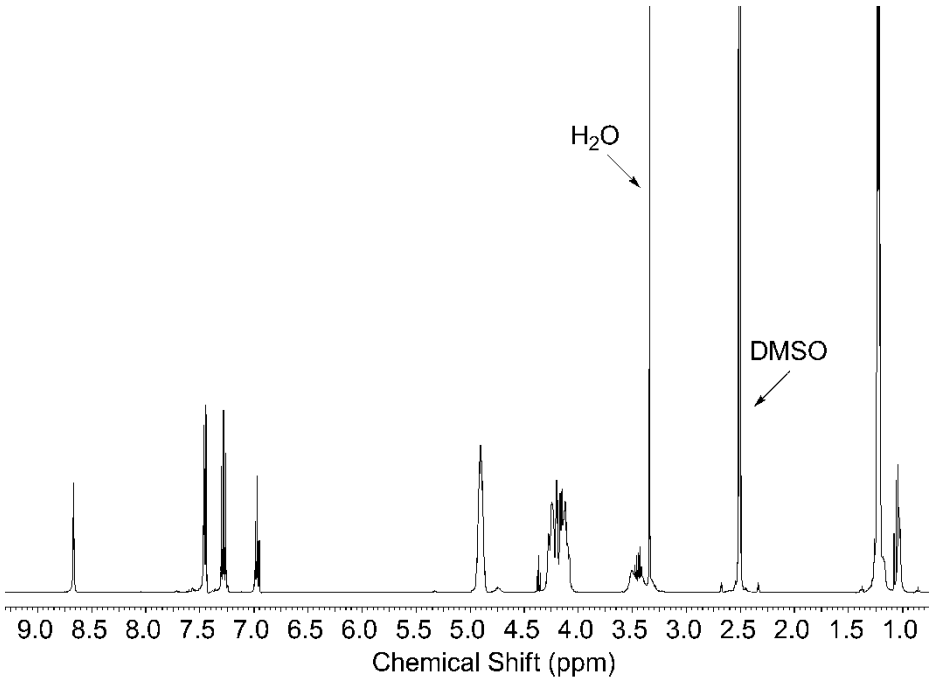

Figure S10. ^{1}H NMR spectrum of *hb*($PG_{0.17}$-*co*-$PPO_{0.83}$)-*g*-PPC_{19} (Table 1, sample 3) after reaction with phenylisocyanate in DMSO.

Determination of the intrinsic viscosity in chloroform at 25 °C

***hb*(PG$_{0.17}$-*co*-PPO$_{0.83}$) (sample 1):**

#	Concentration (g/cm^3)	Reduced Viscosity (cm^3/g)
1	0.0554	5.6776
2	0.0523	5.6782
3	0.0496	5.5844
4	0.0471	5.4530
	Intrinsic Viscosity	***5.8847 cm^3/g***

hb(PG$_{0.17}$-*co*-PPO$_{0.83}$)-*g*-PPC$_9$(sample 2):

#	Concentration (g/cm^3)	Reduced Viscosity (cm^3/g)
1	0.0441	12.3249
2	0.0416	12.1737
3	0.0394	12.0034
4	0.0375	11.8464
	Intrinsic Viscosity	***9.0658 cm^3/g***

hb(PG$_{0.17}$-*co*-PPO$_{0.83}$)-*g*-PPC$_{19}$ (sample 3):

#	Concentration (g/cm^3)	Reduced Viscosity (cm^3/g)
1	0.0783	17.4745
2	0.0718	17.0068
3	0.0664	16.6044
4	0.0618	16.2729
	Intrinsic Viscosity	***11. 6199 cm^3/g***

hb($PG_{0.17}$-*co*-$PPO_{0.83}$)-*g*-PPC_{27} (sample 4):

#	Concentration (g/cm^3)	Reduced Viscosity (cm^3/g)
1	0.0535	17.6031
2	0.0505	17.3698
3	0.0478	17.1377
4	0.0433	16.6439
	Intrinsic Viscosity	***12.5777 cm^3/g***

hb($PG_{0.39}$-*co*-$PPO_{0.61}$) (sample 5, hyperbranched polyether):

#	Concentration (g/cm^3)	Reduced Viscosity (cm^3/g)
1	0.1034	6.7147
2	0.0976	6.6653
3	0.0925	6.5750
4	0.0837	6.3701
	Intrinsic Viscosity	***4.9413 cm^3/g***

References

1. M. Schömer, J. Seiwert, H. Frey, *ACS Macro Lett.* **2012**, *1*, 888-891.

3.2 Multiarm Star Polyether-Polycarbonates Based on Hyperbranched Polyether Polyols, Carbon Dioxide and Tailored Epoxides

Markus Scharfenberg[1,‡], Jan Seiwert[1,‡], Maximilian Scherger[1], Jasmin Preis[2], Holger Frey [1,]*

[1] Institute of Organic Chemistry, Organic and Macromolecular Chemistry, Duesbergweg 10-14, Johannes Gutenberg-University Mainz, 55128 Mainz, Germany

[2] PSS Polymer Standards Service GmbH, In der Dalheimer Wiese 5, 55120 Mainz, Germany

[‡] Markus Scharfenberg and Jan Seiwert contributed equally to this work.

Submitted.

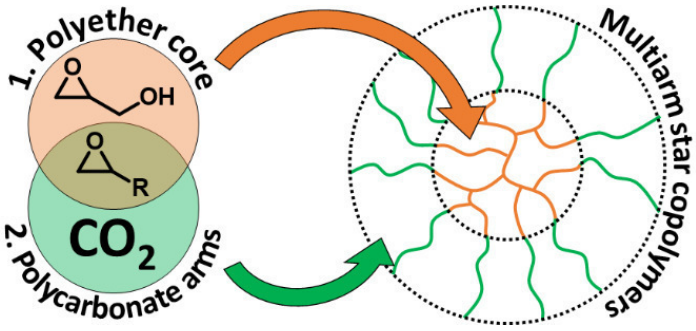

Abstract

Multiarm star copolymers, consisting of hyperbranched poly(ethylene oxide) (*hb*PEO) or poly(butylene oxide) (*hb*PBO), respectively as a core, and linear aliphatic polycarbonate arms generated from carbon dioxide (CO_2) and epoxides, were synthesized via a "core-first" approach in two steps. First, hyperbranched polyether polyols were prepared by anionic copolymerization of ethylene oxide or 1,2-butylene oxide with 8 - 35% glycidol. Second, multiple arms were grown via immortal copolymerization of CO_2 with propylene oxide or 1,2-butylene oxide using the polyether polyols as macroinitiators and (*R,R*)-(salcy)-CoCl as catalyst in a solvent-free procedure. Molecular weights up to 812 000 g·mol^{-1} were obtained for the resulting multiarm polycarbonates. Comparing the synthesis of different multiarm star polycarbonates, a combination of a highly reactive macroinitiator with a less reactive monomer was found to be most suitable to obtain well-defined structures containing 25 – 88 mol% polycarbonate. The multiarm star copolymers were investigated with respect to their thermal properties, intrinsic viscosity, and their ability to encapsulate hydrophilic guest molecules. Glass transition temperatures in the range of -41 °C to +25 °C were observed by varying the amount of polycarbonate.

Introduction

Carbon dioxide (CO_2) is a non-toxic, sustainable and renewable C_1 building block for chemicals that is available inexpensively in almost unlimited quantities. However, its thermodynamic stability and low reactivity impede the use of CO_2. Since the discovery of the immortal copolymerization of carbon dioxide with epoxide monomers by Inoue *et al.*, CO_2 can also be used as a feedstock for aliphatic polycarbonates.[1,2] Currently, the industrial production of these polymers has a modest volume of 1 000 tons per year, albeit with an increasing trend.[3] Mostly propylene oxide and cyclohexene oxide are used as comonomers together with CO_2 for the immortal polymerization with CO_2, resulting in biodegradable materials.[3,4] However, the resulting linear poly(propylene carbonate) and poly(cyclohexene carbonate) polymers exhibit glass transition temperatures (T_g) above room temperature, which are limiting for some areas of application, such as flexible polyols for polyurethanes.[4] Besides the addition of flexible side chains, the introduction of branching points into the polycarbonate backbone can be used as a synthetic tool to decrease the T_g and to obtain unusual rheological and mechanical properties.[5-13]

Except for a single example of branched polycarbonate oligomers based on carbon dioxide and glycidol, only hyperbranched aliphatic polycarbonates prepared by the ring-opening of cyclic six membered carbonates are known to date.[14–18] They have been tested successfully with regards to their properties for controlled release of drugs.[17] However, the synthesis of these cyclic carbonate monomers requires multiple steps, presenting a drawback for scale-up and eventual application.

Branched and linear polymers can be combined in multiarm star copolymers with a branched core and linear arms. Due to the unique architecture, these materials can feature both polymer and colloidal properties,[19] and a large amounts of functional end groups. Multiarm star copolymers can be obtained by "arm-first" or "core-first" strategies.[20–24] In the "arm-first" approach, prefabricated linear polymers are either attached to a hyperbranched core or interconnected via cross-linking of one end group. "Core-first" approaches rely on multifunctional, branched macroinitiators to graft linear arms. Hyperbranched polyether polyols have been employed as suitable macroinitiators for various types of arms as they tolerate most polymerization techniques.[25–27] Recently, our group introduced hyperbranched poly(alkylene oxide)s based on the anionic ring-opening copolymerization of glycidol with ethylene oxide, propylene oxide, and 1,2-butylene oxide, respectively. The one-step synthetic procedures provide access to hyperbranched polyether polyols with adjustable branching, solubility and number of hydroxyl end groups.[28–31] Using the hydrophilic hyperbranched poly(ethylene oxide) as a core, multiarm star copolymers with hydrophobic polylactide arms were prepared. Such polymers are inverse unimolecular micelles and can be used for the encapsulation of hydrophilic guest molecules.[12]

In contrast, all star-shaped aliphatic polycarbonates synthesized from CO_2 and epoxides known to date are purely hydrophobic materials. Furthermore, star-shaped polycarbonates with low numbers of arms (3, 4 and 6) exhibit glass transition temperatures above room temperature, comparable to those of linear poly(propylene oxide) (PPC).[32,33] Multiarm star polycarbonates have been hardly studied. In a first communication, our group reported multiarm star copolymers based on a hyperbranched poly(propylene oxide) (*hb*PPO) core and PPC arms. In that work, the star copolymers had to be fractionated to characterize the properties of the pure star-shaped copolymer separate from polycarbonate homopolymer side product.[5]

In the current work, the core-first synthesis of amphiphilic star-shaped polyether polycarbonates from hyperbranched poly(ethylene oxide) (*hb*PEO) cores and poly(butylene carbonate) (PBC) arms is introduced. We present a systematic comparison of two kinds of cores (*hb*PEO and *hb*PBO) and two epoxide monomers (propylene oxide and butylene oxide) for the copolymerization with CO_2 with regard to controlled synthesis of the resulting multiarm star copolymers. The star copolymers

have been investigated with respect to their thermal properties, intrinsic viscosity, and their ability to encapsulate hydrophilic guest molecules. Both low and high molecular weight star copolymers in the range of 3 800 to 812 000 g·mol^{-1} were synthesized.

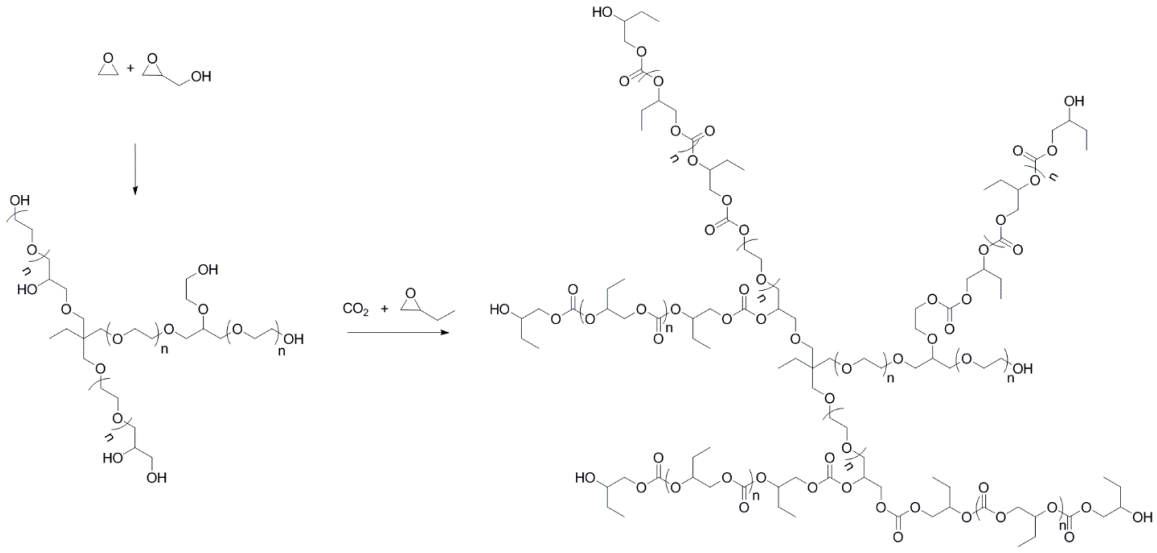

Figure 1. Synthetic scheme for the *hb*(PG-*co*-PEO)-*g*-PBC star copolymers from BO and CO_2 with *hb*(PG-*co*-PEO) core.

Experimental Section

Materials, instrumentation and further synthetic procedures are described in the Supporting Information.

Synthesis of Polyether-Polycarbonate Star Copolymers

A typical polymerization was performed as follows for both types of core as well as for both epoxides. A 100 mL Roth autoclave was dried under vacuum at 50 °C. *hb*PG_9-*co*-PEO_{16} (190 mg) dried in high vacuum for 2 d, BO (1.5 mL, 17 mmol), (R,R)-(salcy)-CoCl (9.1 mg, 0.014 mmol) and [PPN]Cl (8.4 mg, 0.014mmol) were combined with a stir bar inside the autoclave. The mixture was stirred under 50 bar and 30 °C for 3 d. The crude product was dissolved in 5 mL acetone and quenched with 1.0 mL 5% HCl solution in methanol. Subsequently, the solution was precipitated in cold methanol. The solid product was dried in vacuum for 24 h; yield 75%. Dichloromethane

was used as a solvent for samples prepared from cores with a molecular weight of 389.000 g·mol^{-1}. Purification was carried out by dialysis in CH_2Cl_2 (MWCO = 1000 Da).

hb(PG-*co*-PEO)-*g*-PBC (samples 1 - 6): ^{1}H NMR (CD_3CN-d_3, 400 MHz): δ (ppm) = 4.87 – 4.76 (CH PBC backbone), 4.38 – 3.92 (CH_2 PBC backbone), 3.79 – 3.40 (polyether core), 3.01 (OH PBC) 1.74 – 1.55 (CH_2), 1.53 – 1.32 (CH_2 terminal unit), 1.09 – 0.83 (CH_3).^{13}C NMR (CD_3CN-d_3, 100 MHz): δ (ppm) = 155.88 – 155.38 (-O-CO-O-), 77.90 – 77.65 (CH PBC backbone), 72.41 (CH_2 terminal PBC backbone), 71.79 – 70.06 (polyether core), 69.44 – 68.15 (CH_2 PBC backbone), 26.97 (CH_2 terminal unit), 24.26 (CH_2), 10.13 – 9.69 (CH_3).

hb(PG-*co*-PEO)-*g*-PPC (sample 7): ^{1}H NMR (CD_3CN-d_1, 400 MHz): δ (ppm) = 5.30 – 4.69 (CH PPC backbone), 4.32 – 3.88 (CH_2 PBC backbone), 3.74 – 3.42 (polyether core), 1.33 – 1.18 (CH_3), 1.12 – 1.07 (CH_3 terminal group).

hb(PG-*co*-PBO)-*g*-PPC (sample 8): ^{1}H NMR (CD_3CN-d_3, 400 MHz): δ (ppm) = 5.02 – 4.89 (CH PPC backbone), 4.77 – 4.63 (CH PPC backbone terminal unit), 4.30 – 4.04 (CH_2 PPC backbone), 4.02 – 3.88 (CH_2 PPC backbone terminal unit), 3.77 – 3.19 (polyether core), 3.02 (OH PPC) 1.78 – 1.38 (CH_2 polyether core), 1.36 – 1.14 (CH_3 PPC), 1.14 – 1.06 (CH_3 PPC terminal unit), 0.99 – 0.81 (CH_3 polyether core).

hb(PG-*co*-PBO)-*g*-PBC (sample 9): ^{1}H NMR (CD_3CN-d_3, 400 MHz): δ (ppm) = 4.88 – 4.75 (CH PBC backbone), 4.75 – 4.63 (CH PBC backbone terminal unit), 3.40 – 3.86 (CH_2 PBC backbone), 3.77 – 3.18 (polyether core), 2.98 (OH PBC) 1.75 – 1.56 (CH_2 PBC), 1.56 – 1.25 (CH_2 polyether core), 0.99 – 0.79 (CH_3 PBC and polyether core).

Results and Discussion

A. Synthesis and Characterization of Polycarbonate-Polyether Multiarm Stars

Controlled synthesis of well-defined multiarm star architectures exclusively based on simple epoxide monomers and carbon dioxide was investigated. Four series of multiarm star polymers were targeted by grafting two types of polycarbonate arms from two different multifunctional hyperbranched polyether polyol cores. Control over the star architecture was achieved by using the immortal polymerization of CO_2 with tailored epoxides with the polyether polyols acting as transfer agents, i.e., as multifunctional initiators.[34,35]

Hydrophilic hyperbranched poly(ethylene oxide) (*hb*PEO) and hydrophobic hyperbranched poly(1,2-butylene oxide) (*hb*PBO) copolymers with molecular weights ranging from 800 to 389 000 g mol^{-1} (determined by on-line viscometry) and moderate dispersities (Đ = 2.0 to 3.4) were employed as initiators, respectively. Both kinds of copolymers were synthesized via anionic ring-opening multibranching copolymerization of the respective alkylene oxide monomer with glycidol as a branching unit, according to procedures reported recently.[30,31] Both polyether polyols were well soluble in propylene oxide and 1,2-butylene oxide. Variation of the glycidol content yielded polyols with different degrees of branching and different hydroxyl functionality. It should be noted that *hb*PEO polyols with low glycidol content mainly feature primary hydroxyl moieties from terminal ethylene oxide units, whereas *hb*PBO polyols mostly contain secondary hydroxyl groups from terminal butylene oxide units.[36] The different repeating units of the hyperbranched polyether polyols can be determined from inverse gated ^{13}C NMR spectroscopy (Supp. Inf., Table S 1).[28,31]

Propylene oxide and 1,2-butylene oxide were used as comonomers for the immortal polymerization with CO_2 to study the influence of the comonomer and its reactivity on the success of the grafting of the polycarbonate arms. It is known that 1,2-butylene oxide reacts significantly slower than propylene oxide during anionic homopolymerization.[37–39] Differences in reactivity can also be observed for the catalytic copolymerization with CO_2. It has to be emphasized that based on the low glass transition, amorphous nature and flexibility of the hyperbranched polyether polyols the polymerizations were performed in bulk, with the epoxide monomers being good solvents for both the hyperbranched polyether polyol and the multiarm star polymers formed. Only for the reaction using a *hb*PEO core with very high molecular weight of 389.000 g·mol^{-1}, dichloromethane had to be added as a solvent. (*R,R*)-(salcy)-CoCl as catalyst and bis(triphenylphosphine(iminium chloride) as cocatalyst were used. All multiarm star polymers were precipitated in ice-cold methanol. The insolubility in methanol demonstrates the transformation of the hydrophilic *hb*PEO cores to hydrophobic products, or more precise, to an amphiphilic star-like structure with a hydrophilic core and a hydrophobic shell.

By changing the ratio of initiator and monomer, different polycarbonate arm lengths were targeted. Furthermore, the glycidol content of the cores was varied, resulting in different initiator to monomer ratios, which is due to their different number of hydroxyl groups. SEC, DSC and ^{1}H NMR spectroscopy characterization data as well as the calculated composition of the multiarm star copolymers are summarized in Table 1.

Table 1. Overview of the characterization data for all multiarm star copolymers.

#	Sample name[a)]	M_n / g mol^{-1} (SEC)[b)]	Đ (SEC)[b)]	M_n / g mol^{-1} (^{1}H NMR)[a)]	Unit ratio[c)d)]	T_g / °C[e)]
1	*hb*(PG$_9$-*co*-PEO$_{16}$)-*g*-PBC$_{168}$	8 800	1.69	20 800	7.40	4
2	*hb*(PG$_9$-*co*-PEO$_{16}$)-*g*-PBC$_{92}$	6500	1.55	12 000	4.05	1
3	*hb*(PG$_4$-*co*-PEO$_{15}$)-*g*-PBC$_{50}$	10 600	1.37	6 800	2.99	-2
4	*hb*(PG$_5$-*co*-PEO$_{10}$)-*g*-PBC$_{25}$	3 300	1.64	3 800	2.02	-11
5	*hb*(PG$_5$-*co*-PEO$_{57}$)-*g*-PBC$_{20}$	3 900	1.62	5 300	0.33	-41
6	*hb*(PG$_{1250}$-*co*-PEO$_{6750}$)-*g*-PBC$_{3640}$	68 800	1.13	812 000	0.46	-40
7	*hb*(PG$_4$-*co*-PEO$_{45}$)-*g*-PPC$_{349}$	21 100	1.55	38 000	7.53	21
8	*hb*(PG$_4$-*co*-PBO$_{10}$)-*g*-PPC$_{146}$	8 900	1.90	16 000	10.98	25
9	*hb*(PG$_4$-*co*-PBO$_{10}$)-*g*-PBC$_{66}$	5 200	2.32	8 700	4.93	-12

[a)] Terminology: Indices represent the absolute number of the respective repeating unit (rounded to integer), determined by ^{1}H NMR spectroscopy and on-line viscometry with universal calibration, [b)] determined by SEC in DMF calibrated with a PEO standard, [c)] determined by ^{1}H NMR spectroscopy, [d)] ratio between polycarbonate and polyether repeating units, polyether units are normalized to 1 [e)] determined by DSC.

The formation of cyclic carbonates, a typical side reaction in the polymerization of CO_2 with epoxides, occurred just in a very small amount, when using butylene oxide. In the case of propylene oxide, no cyclic carbonates were formed. The small amount of this side product was confirmed by FT-IR spectra of the crude products (Figure S 1-4, Supporting Information). Besides the band at 1740 cm^{-1} that can be clearly assigned to the linear polycarbonate backbone, a small signal at 1804 cm^{-1} occurred when using BO as a monomer. This signal results from a small amount of cyclic carbonate byproduct. These impurities were conveniently removed by precipitation in methanol, as demonstrated by FT-IR and other characterization techniques.

In addition to the FT-IR analysis the samples were also characterized by ^{1}H NMR, ^{13}C NMR and 2D NMR spectroscopy (correlation spectroscopy (COSY), hetero single quantum coherence (HSQC) and heteronuclear multiple bond correlation (HMBC)) with regard to their composition and their structure. Figure 2 shows a typical ^{1}H NMR spectrum of *hb*(PG$_9$-*co*-PEO$_{16}$)-*g*-PBC$_{92}$ (Table 1, sample 2). Beside the *hb*PEO backbone signal (3.79 – 3.40 ppm) the signals of aliphatic 1,2-poly(butylene carbonate) are visible at 4.87 – 4.76 ppm (methine backbone), 4.38 – 3.92 ppm (methylene backbone), 1.74 – 1.55 ppm (methylene side chain) and 1.09 – 0.83 ppm (methyl side chain). Furthermore, the methylene group in the side chain (1.53 – 1.32 ppm) and the hydroxyl group

(3.01 ppm) of the terminal carbonate unit are recognizable. Capitalizing on the signals of the terminal units and the known absolute molecular weight of the hyperbranched core polymers, determined by on-line viscometry, the number and chain length of the polycarbonate arms were calculated. An overview of the calculated data is given in Table 1.

The ^{13}C NMR spectrum of *hb*(PG$_9$-*co*-PEO$_{16}$)-*g*-PBC$_{92}$ (Table 1, sample 2) is shown in Figure 3. Signal h (155.88 – 155.38 ppm), signal g (77.90 – 77.65 ppm), signal d (69.44 – 68.15 ppm), signal b (24.26 ppm) and signal a (10.13 – 9.69 ppm) can be assigned to the poly(butylene carbonate) chains. The signal 71.79 – 70.06 ppm results from the hyperbranched polyether core. Similar to the ^{1}H NMR spectra, resonances of the terminal carbonate unit are visible in the ^{13}C NMR spectra. Signal f (72.41 ppm) and signal c (26.97 ppm) can be clearly distinguished from other signals, whereas the methine group signal of the terminal unit overlaps with the polyether signal.

The 2D NMR spectra of *hb*(PG$_9$-*co*-PEO$_{16}$)-*g*-PBC$_{92}$ (Table 1, sample 2) and the NMR spectra of further multiarm star copolymers with different core and epoxide combinations (*hb*(PG$_4$-*co*-PEO$_{45}$)-*g*-PPC$_{349}$, *hb*(PG$_4$-*co*-PBO$_{10}$)-*g*-PPC$_{146}$, *hb*(PG$_4$-*co*-PBO$_{10}$)-*g*-PBC$_{66}$) are listed in the Supporting Information (Figure S 5-10).

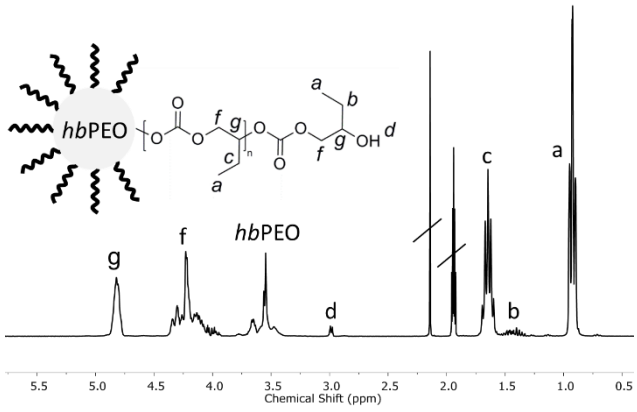

Figure 2. ^{1}H NMR spectrum of *hb*(PG$_9$-*co*-PEO$_{16}$)-*g*-PBC$_{92}$ (Table 1, sample 2) (300 MHz, CD$_3$CN).

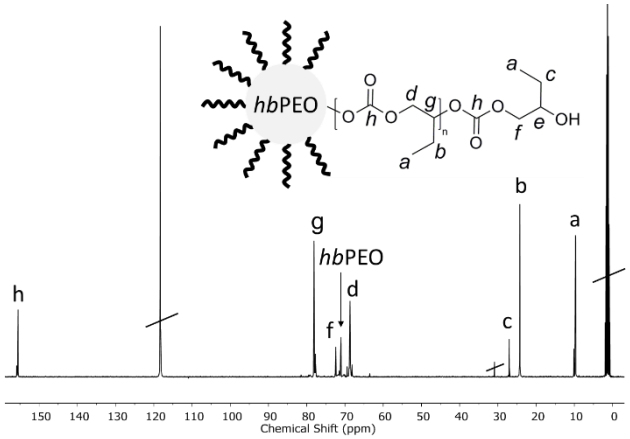

Figure 3. ^{13}C NMR spectrum of *hb*(PG$_9$-*co*-PEO$_{16}$)-*g*-PBC$_{92}$ (Table 1, sample 2) (100 MHz, CD_3CN).

Size exclusion chromatography (SEC, *lin*PEO standards) yielded molecular weights between 3 300 g·mol^{-1} and 68 800 g·mol^{-1} with Đ ($\bar{M}_w/\bar{M}_n$) values between 1.13 and 2.32. All polyether polycarbonate star copolymer samples exhibit a lower elution volume than the macromolecular initiator, corresponding to a higher molecular weight.

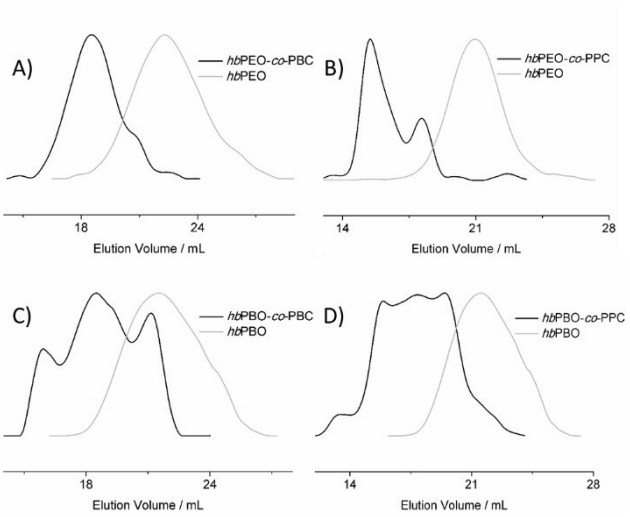

Figure 4. SEC results of A) *hb*(PG$_9$-*co*-PEO$_{16}$)-*g*-PBC$_{92}$ (Table 1, sample 2), B) *hb*(PG$_4$-*co*-PEO$_{45}$)-*g*-PPC$_{349}$ (Table 1, sample 7), C) *hb*(PG$_4$-*co*-PBO$_{10}$)-*g*-PBC$_{66}$ (Table 1, sample 9) and D) *hb*(PG$_4$-*co*-PBO$_{10}$)-*g*-PPC$_{146}$ (Table 1, sample 8) and their macroinitiators in DMF.

Figure 4 A shows the distribution of *hb*(PG$_9$-*co*-PEO$_{16}$)-*g*-PBC$_{92}$ (Table 1, sample 2). It is monomodal, apart from a small shoulder at lower molecular weights. The elugrams of other *hb*PEO-*g*-PBC samples are listed in the Supporting Information (Figure S 12) and exhibit comparable distributions. In contrast, grafting poly(propylene carbonate) arms from *hb*PEO cores generally results in bimodal distributions (Figure 4 B). Using *hb*PBO as macroinitiator leads to

polymodal distributions independently of whether poly(propylene carbonate) or poly(butylene carbonate) are grafted from it (Figure 4 C and D).

To elucidate, if the polycarbonate chains formed are attached to the hyperbranched polyether polyol core, DOSY NMR spectra were measured. Figure 5 reveals only one signal with low diffusion coefficient, corresponding to the ^{1}H NMR signals of both the polyether as well as the polycarbonate for *hb*(PG$_9$-*co*-PEO$_{16}$)-*g*-PBC$_{92}$ (Table 1, sample 2). The formation of a significant amount of polycarbonate homopolymer and unreacted polyether core can thus be excluded and successful grafting can be confirmed. However, DOSY NMR spectroscopy cannot distinguish star copolymers and polycarbonate homopolymer with the same diffusion coefficient. Furthermore, the DOSY NMR data do not explain the existing lower molecular weight shoulder found in the SEC traces. The DOSY NMR spectra of further multiarm star copolymers with different core and polycarbonate arms (*hb*(PG$_4$-*co*-PEO$_{45}$)-*g*-PPC$_{349}$, *hb*(PG$_4$-*co*-PBO$_{10}$)-*g*-PPC$_{146}$, *hb*(PG$_4$-*co*-PBO$_{10}$)-*g*-PBC$_{66}$) are listed in the Supporting Information (Figure S 13-15). For *hb*(PG$_4$-*co*-PBO$_{10}$)-*g*-PPC$_{146}$ the mass fraction of the PPC arms is too high to permit resolution of the polyether signals. The other spectra are comparable to Figure 5.

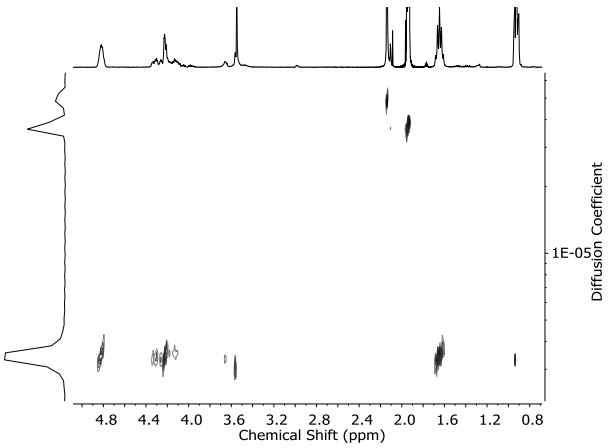

Figure 5. DOSY spectrum of *hb*(PG$_9$-*co*-PEO$_{16}$)-*g*-PBC$_{92}$ (Table 1, sample 2) (CD$_3$CN, 400 MHz).

Preparative size exclusion chromatography was used to shed light on the molecular weight-dependent composition of the different copolymers. The respective samples were dissolved in $CHCl_3$ and fractionated depending on their hydrodynamic volume. For the discussion, fractions are labeled in ascending order with decreasing molecular weight according to SEC. These fractions were analyzed by ^{1}H NMR spectroscopy and SEC individually. The NMR and SEC results of *hb*(PG$_9$-*co*-PEO$_{16}$)-*g*-PBC$_{92}$ are shown exemplarily in Figure 6 and Figure 7. The ^{1}H NMR spectra in Figure 6 show that polyether structures (signal 3.79 – 3.40 ppm) are present in each fraction. The ratio of core and polycarbonate chains is the same in the first eleven fractions. Larger polyether polyol

cores contain more hydroxyl groups and more polycarbonate chains can be grafted from them. However, the polyether to polycarbonate ratio exhibits a decreasing gradient from the lower molecular weight fractions 12 to fraction 18. This is a hint at the formation of short polycarbonate homopolymer. It can deduced from comparing SEC (Figure 7) and NMR spectroscopy data (Figure 6) that the small shoulder in the monomodal distribution of *hb*(PG_9-*co*-PEO_{16})-*g*-PBC_{92} (Table 1, sample 2) is non-grafted, bimodal homopolymer. It is known that the catalyst (R,R)-(salcy)-CoCl is able to copolymerize carbon dioxide and epoxides without macroinitiator, resulting in bimodal distributions.[40] Characterization of fractionated samples was also performed for *hb*(PG_4-*co*-PEO_{45})-*g*-PPC_{349}, *hb*(PG_4-*co*-PBO_{10})-*g*-PPC_{146} and *hb*(PG_4-*co*-PBO_{10})-*g*-PBC_{66}) (Figure S 17-22). In analogy to *hb*(PG_9-*co*-PEO_{16})-*g*-PBC_{92} (Table 1, sample 2), modes corresponding to lower molecular weight polycarbonate homopolymers are found at higher elution volume. All data show that the amount of non-grafted homopolycarbonate is higher when using PO instead of BO. PO is more reactive than BO in the immortal polymerization, rendering the formation of PPC homopolymer more likely. In addition, the characterization data demonstrate that *hb*PEO is a better initiator than *hb*PBO. The molecular weight distribution of the grafted polymers is much narrower with the polyfunctional *hb*PEO macroinitiator than with *hb*PBO, independently of whether PO or BO was used for polycarbonate synthesis. In line with these observations, the amount of PBC homopolymer using *hb*PEO as an initiator is very low compared to the other three combinations. Therefore, it can be concluded that the copolymerization of BO and CO_2 with *hb*PEO as a polyfunctional macroinitiator represents the best combination to provide the targeted well-defined multiarm star polyether-polycarbonate polyols.

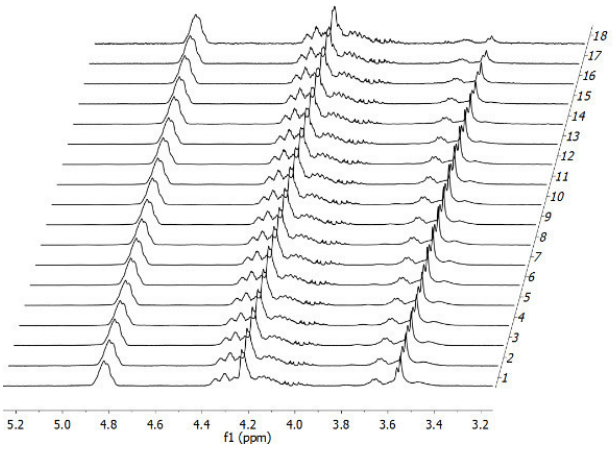

Figure 6. ^{1}H NMR spectra of *hb*(PG_9-*co*-PEO_{16})-*g*-PBC_{92} (Table 1, sample 2) after separation with a preparative SEC. (300 MHz, CD_3CN), demonstrating similar composition of all fractions of the material.

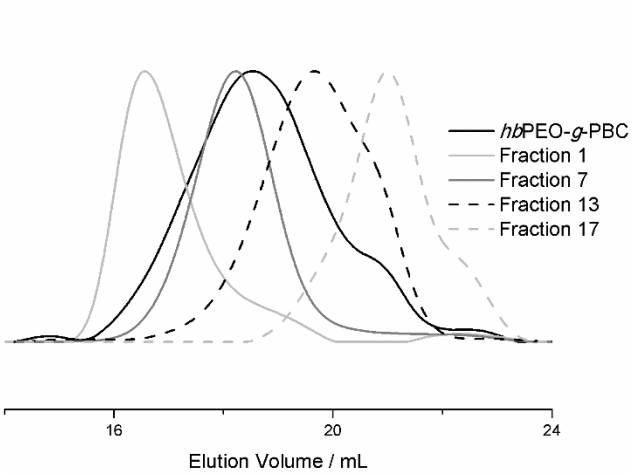

Figure 7. SEC results for some fraction of *hb*(PG_9-*co*-PEO_{16})-*g*-PBC_{92} (Table 1, sample 2) star polymers in DMF.

Capitalizing on the polyether polycarbonate combination yielding the most defined star copolymers, *hb*PEO and butylene oxide were used to create a high molecular weight multi-arm star polymer with a molecular weight average of 812 000 g·mol^{-1}. This material is based on *hb*PEO macro initiator with a molecular weight of 389 000 g·mol^{-1}. Due to the poor solubility of *hb(*PG_{1250}-*co*-PEO_{6750}) in butylene oxide, the grafting of PBC arms was carried out in dichloromethane as a solvent.

B. Properties of the Multiarm Stars

In a proof of principle study, the thus obtained amphiphilic *hb*(PG_{1250}-*co*-PEO_{6750})-*g*-PBC_{3640} core-shell multiarm star polymer was used as a container to incorporate Congo red. This hydrophilic dye is not soluble in organic solvents such as dichloromethane (Figure 7, left vial). In the presence of *hb*(PG_{1250}-*co*-PEO_{6750})-*g*-PBC_{3640}, however, it was possible to colorize a CH_2Cl_2 solution (Figure 8). This was achieved following a protocol by Chen *et al.*.[41] Congo red was dissolved in water and the amphiphilic star copolymer in CH_2Cl_2. Both solutions were mixed thoroughly by ultrasonication for 30 min. Strikingly, the red color spreads from the aqueous into the methylene chloride layer (Figure 7, right vial). The same treatment has no effect on the distribution of Congo red if the two layers are mixed without adding the star copolymer first (Figure 7, left vial). Thus, this experiment demonstrates successful uptake of the hydrophilic dye Congo red inside the hydrophilic *hb*PEO core and its shielding with the help of the hydrophobic PBC shell. More detailed studies to confirm the encapsulation and to quantify the amount of encapsulated dye are still in progress. Since

mixing by ultrasonication might cause polymer degradation during the mixing process, dye uptake under milder mixing conditions will be explored in further experiments.

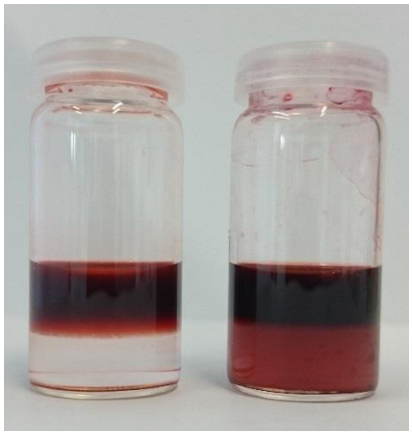

Figure 8. Illustration of the incorporation of hydrophilic Congo red into the amphiphilic *hb*(PG_{1250}-*co*-PEO_{6750})-*g*-PBC_{3640} star copolymer (bottom layer: methylene chloride; upper layer: water). Picture taken 12 h after mixing (ultrasonication, 30 min) of the samples, without (left vial) and with (right vial) addition of star copolymer to the organic layer.

The thermal behavior of the multiarm star polymers was studied by differential scanning calorimetry (DSC). The DSC results are listed in Table 1. As expected, the polymers reveal no melting point due to the amorphous nature of both the hyperbranched polyether core and the polycarbonate chains prepared from racemic PO and BO. Poly(butylene carbonate) homopolymer shows a glass transition temperature (T_g) around 8 °C, whereas hyperbranched poly(ethylene oxide) exhibits a T_g around - 60 °C. Hyperbranched poly(ethylene oxide) is known to exhibit a melting point only if a small amount of glycerol units is incorporated.[28] The T_g of hyperbranched poly(ethylene oxide) is largely independent of the degree of branching.[28] A blend of *hb*PEO and PBC exhibits two distinct glass transitions, because these polymers are immiscible (Figure 9, top). The synthesized multiarm star copolymers, however, exhibit merely a single T_g between the values of the homopolymers due to coupling of the different polymers. Figure 9 shows the DSC curves of different *hb*PEO-*g*-PBC copolymers, revealing increasing glass transitions with increasing content of polycarbonate units. As expected, a higher polycarbonate fraction results in a higher T_g. A clear shift from -41 °C to 4 °C is visible. The other three multiarm star combinations also exhibit single T_gs between those of the homopolymers. The stars comprising PPC arms showed values ranging from 21 °C (*hb*(PG_4-*co*-PEO_{45})-*g*-PPC_{349}) (Table 1, sample 7) to 25 °C (*hb*(PG_4-*co*-PBO_{10})-*g*-PPC_{146}) because of their high amount of polycarbonate. Furthermore, the DSC data clearly reveal that the T_g is independent of the molecular weight of the multiarm stars, but depend on the amount of the polycarbonate arms. *hb*(PG_5-*co*-PEO_{57})-*g*-PBC_{20} and *hb*(PG_{1250}-*co*-PEO_{6750})-*g*-PBC_{3640} (Table 1,

sample 5 and 6) have significantly different molecular weights, but their ratio of polycarbonate to polyether unit and their glass transition temperatures are nearly the same. Their cores have also similar T_gs (Table S 1).

Comparable results had been found previously for hyperbranched poly(propylene oxide) grafted with poly(propylene carbonate).[5] In contrast to the preceding work the current findings reveal a more pronounced effect of the amount of polycarbonate. As a consequence, it was possible to tune the T_g in a broader temperature range from -41 °C to 25 °C, reflecting the flexibility of the respective polycarbonate polyols.

Viscometry experiments are still in progress at this time.

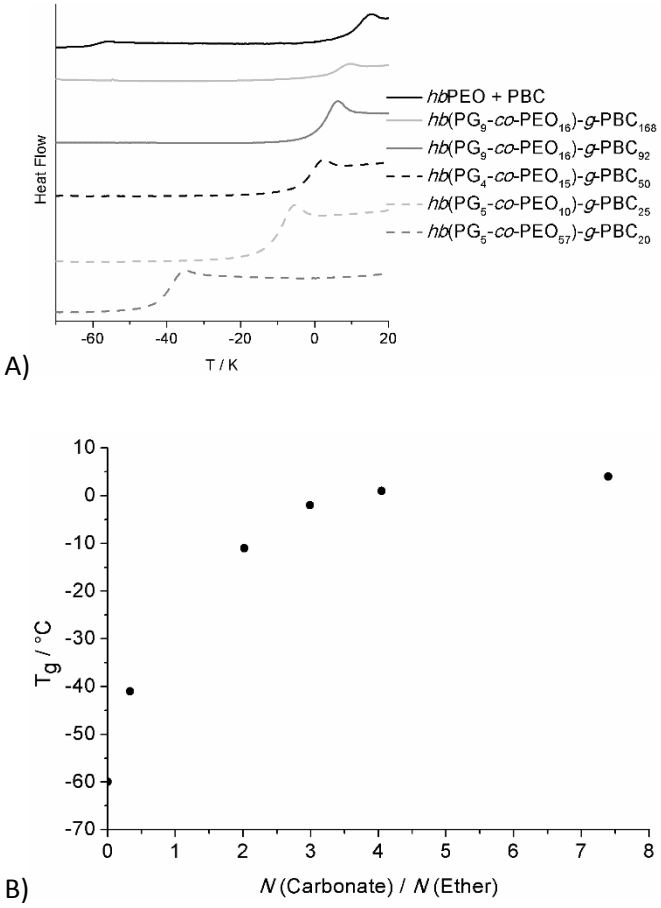

Figure 9. a) DSC results of the series of *hb*(PG-*co*-PEO)-*g*-PBC copolymers with decreasing PBC amount from top to bottom. The top curve resulting from a mixture of both homopolymers. Temperature range from -70 to +20 °C at heating rates of 10 K min^{-1}; b) Glass transition temperatures of the series of *hb*(PG-*co*-PEO)-*g*-PBC copolymers plotted versus monomer unit ratio *N*(Carbonate) / *N*(Ether).

Conclusion

Flexible multiarm stars based on hyperbranched polyether polyol core and linear aliphatic polycarbonate arms of varied degree of polymerization were synthesized in a two-step *core-first* approach. First, hyperbranched polyether polyols were prepared by anionic ring-opening copolymerization of glycidol with EO or BO, thereby varying the nature of the end groups from primary hydroxyls to secondary hydroxyl groups. In the second step, the resulting *hb*PEO and *hb*PBO polyols were employed as macro initiators for the immortal copolymerization of carbon dioxide with propylene oxide and butylene oxide, respectively. The star architecture was confirmed by IR spectroscopy, ^{1}H, ^{13}C and 2D NMR spectroscopy, SEC and DSC. The influence of both macroinitiators (*hb*PEO and *hb*PBO) and the two different epoxide monomers employed for the immortal copolymerization on the formation of multiarm star copolymers was investigated systematically. The molecular weight distributions were found to be much narrower when using *hb*PEO instead of *hb*PBO as initiators, independently of whether PO or BO was used for the grafting of the polycarbonate arms. Furthermore, a larger amount of polycarbonate homopolymer is formed in the case of *hb*PBO. These findings demonstrate the significant difference in the reactivity of the almost exclusively primary hydroxyl groups of *hb*PEO and the mainly secondary hydroxyl groups of *hb*PBO. Comparing the copolymerization of PO and BO with CO_2, it becomes obvious that butylene oxide is more suitable for the preparation of well-defined multiarm star polymers, because of the lower amount of homopolymer formed. A series of multiarm star polymers based on *hb*PEO and PBC were prepared with molecular weights ranging from 3 800 to 20 800 g mol^{-1} and with moderate Đ between 1.4 and 1.7. Depending on the ratio of polyether units and polycarbonate units, the glass transition temperature as well as the intrinsic viscosity can be tuned in a broad range between the values of the respective homopolymers.

Furthermore, an amphiphilic high-molecular *hb*PEO-*g*-PBC star copolymer (812 000 g mol^{-1}) was prepared. This multiarm star polymer was used in a proof of principle study as a container to incorporate a hydrophilic dye, to shield it from external influences and thus solubilize it in dichloromethane. The multiarm star copolymers presented herein are obtained from very simple epoxide monomers and CO_2. This renders them conveniently available materials with potential applications as inverse unimolecular micelles with a degradable shell and as highly flexible, biodegradable cross-linkers for polyurethanes. Viscometry experiments are still in progress at this time.

Acknowledgement

M. Scharfenberg is grateful for the financial support through the Max Planck Graduate Center (MPGC) with the Johannes Gutenberg University. The authors thank Pia Winterwerber and Maria Golowin for technical assistance.

References

(1) Inoue, S.; Koinuma, H.; Tsuruta, T. Copolymerization of Carbon Dioxide and Epoxide with Organometallic Compounds. *Macromol. Chem. Phys.* **1969**, *130*, 210–220.

(2) Inoue, S. Copolymerization of Carbon Dioxide and Epoxide: Functionality of the Copolymer. *J. Macromol. Sci., Pure Appl. Chem.* **1979**, *13* (5), 651–664. DOI: 10.1080/00222337908056679.

(3) Rieger, B.; Amann, M. *Synthetic biodegradable polymers*; Advances in polymer science 245; Springer: Berlin, 2012.

(4) Welle, A.; Kröger, M.; Döring, M.; Niederer, K.; Pindel, E.; Chronakis, I. S. Electrospun aliphatic polycarbonates as tailored tissue scaffold materials. *Biomaterials* **2007**, *28* (13), 2211–2219. DOI: 10.1016/j.biomaterials.2007.01.024.

(5) Hilf, J.; Schulze, P.; Seiwert, J.; Frey, H. Controlled Synthesis of Multi-Arm Star Polyether-Polycarbonate Polyols Based on Propylene Oxide and CO 2. *Macromol. Rapid Commun.* **2014**, *35* (2), 198–203. DOI: 10.1002/marc.201300663.

(6) Nakamura, M.; Tominaga, Y. Utilization of carbon dioxide for polymer electrolytes [II]: Synthesis of alternating copolymers with glycidyl ethers as novel ion-conductive polymers. *Electrochim. Acta* **2011**, *57*, 36–39. DOI: 10.1016/j.electacta.2011.03.003.

(7) Zhang, X.-H.; Wei, R.-J.; Zhang, Y.; Du, B.-Y.; Fan, Z.-Q. Carbon Dioxide/Epoxide Copolymerization via a Nanosized Zinc–Cobalt(III) Double Metal Cyanide Complex: Substituent Effects of Epoxides on Polycarbonate Selectivity, Regioselectivity and Glass Transition Temperatures. *Macromolecules* **2015**, *48* (3), 536–544. DOI: 10.1021/ma5023742.

(8) Geschwind, J.; Frey, H. Poly(1,2-glycerol carbonate): A Fundamental Polymer Structure Synthesized from CO 2 and Glycidyl Ethers. *Macromolecules* **2013**, *46* (9), 3280–3287. DOI: 10.1021/ma400090m.

(9) Ceroni, P.; Bergamini, G.; Marchioni, F.; Balzani, V. Luminescence as a tool to investigate dendrimer properties. *Prog. Polym. Sci.* **2005**, *30* (3-4), 453–473. DOI: 10.1016/j.progpolymsci.2005.01.003.

(10) Choi, Y. K.; Bae, Y. H.; Kim, S. W. Star-Shaped Poly(ether−ester) Block Copolymers: Synthesis, Characterization, and Their Physical Properties. *Macromolecules* **1998**, *31* (25), 8766–8774. DOI: 10.1021/ma981069i.

(11) Gottschalk, C.; Wolf, F.; Frey, H. Multi-Arm Star Poly(L-lactide) with Hyperbranched Polyglycerol Core. *Macromol. Chem. Phys.* **2007**, *208* (15), 1657–1665. DOI: 10.1002/macp.200700168.

(12) Schömer, M.; Frey, H. Organobase-Catalyzed Synthesis of Multiarm Star Polylactide With Hyperbranched Poly(ethylene glycol) as the Core. *Macromol. Chem. Phys.* **2011**, *212* (22), 2478–2486. DOI: 10.1002/macp.201100386.

(13) Voit, B. I.; Lederer, A. Hyperbranched and Highly Branched Polymer Architectures - Synthetic Strategies and Major Characterization Aspects. *Chem. Rev.* **2009**, *109*, 5924–5973.

(14) Motokucho, S.; Sudo, A.; Sanda, F.; Endo, T. Reaction of carbon dioxide with glycidol: The synthesis of a novel hyperbranched oligomer with a carbonate main chain with a hydroxyl terminal. *J. Polym. Sci. A Polym. Chem.* **2004**, *42* (10), 2506–2511. DOI: 10.1002/pola.20081.

(15) Liu, C.; Jiang, Z.; Decatur, J.; Xie, W.; Gross, R. A. Chain Growth and Branch Structure Formation during Lipase-Catalyzed Synthesis of Aliphatic Polycarbonate Polyols. *Macromolecules* **2011**, *44* (6), 1471–1479. DOI: 10.1021/ma102899c.

(16) Parzuchowski, P. G.; Jaroch, M.; Tryznowski, M.; Rokicki, G. Synthesis of New Glycerol-Based Hyperbranched Polycarbonates. *Macromolecules* **2008**, *41* (11), 3859–3865. DOI: 10.1021/ma8000912.

(17) Su, W.; Luo, X.-h.; Wang, H.-f.; Li, L.; Feng, J.; Zhang, X.-Z.; Zhuo, R.-x. Hyperbranched polycarbonate-based multimolecular micelle with enhanced stability and loading efficiency. *Macromol. Rapid Commun.* **2011**, *32* (4), 390–396. DOI: 10.1002/marc.201000600.

(18) Tryznowski, M.; Tomczyk, K.; Fraś, Z.; Gregorowicz, J.; Rokicki, G.; Wawrzyńska, E.; Parzuchowski, P. G. Aliphatic Hyperbranched Polycarbonates: Synthesis, Characterization, and Solubility in Supercritical Carbon Dioxide. *Macromolecules* **2012**, *45* (17), 6819–6829. DOI: 10.1021/ma3011153.

(19) Vlassopoulos, D.; Fytas, G.; Pakula, T.; Roovers, J. Multiarm star polymers dynamics. *J. Phys. Condens. Matter* **2001,** No. 13, R855-R876.

(20) Blencowe, A.; Tan, J. F.; Goh, T. K.; Qiao, G. G. Core cross-linked star polymers via controlled radical polymerisation. *Polymer* **2009**, *50* (1), 5–32. DOI: 10.1016/j.polymer.2008.09.049.

(21) Charleux, B.; Faust, R. *Synthesis of Branched Polymers by Cationic Polymerization*; Advances in polymer science; Springer Berlin Heidelberg, 1999.

(22) Gao, H. Development of star polymers as unimolecular containers for nanomaterials. *Macromol. Rapid Commun.* **2012**, *33* (9), 722–734. DOI: 10.1002/marc.201200005.

(23) Lapienis, G. Star-shaped polymers having PEO arms. *Prog. Polym. Sci.* **2009**, *34* (9), 852–892. DOI: 10.1016/j.progpolymsci.2009.04.006.

(24) Taton, D.; Gnanou, Y.; Matmour, R.; Angot, S.; Hou, S.; Francis, R.; Lepoittevin, B.; Moinard, D.; Babin, J. Controlled polymerizations as tools for the design of star-like and dendrimer-like polymers. *Polym. Int.* **2006**, *55* (10), 1138–1145. DOI: 10.1002/pi.2014.

(25) Cameron, D. J. A.; Shaver, M. P. Aliphatic polyester polymer stars: synthesis, properties and applications in biomedicine and nanotechnology. *Chem. Soc. Rev.* **2011**, *40* (3), 1761–1776. DOI: 10.1039/c0cs00091d.

(26) Wilms, D.; Stiriba, S.-E.; Frey, H. Hyperbranched polyglycerols: from the controlled synthesis of biocompatible polyether polyols to multipurpose applications. *Acc. Chem. Res.* **2010**, *43* (1), 129–141. DOI: 10.1021/ar900158p.

(27) Yan, D.; Zhou, Y.; Hou, J. Supramolecular Self-Assembly of Macroscopic Tubes. *Science* **2004**, *303* (65-67).

(28) Wilms, D.; Schömer, M.; Wurm, F.; Hermanns, M. I.; Kirkpatrick, C. J.; Frey, H. Hyperbranched PEG by random copolymerization of ethylene oxide and glycidol. *Macromol. Rapid Commun.* **2010**, *31* (20), 1811–1815. DOI: 10.1002/marc.201000329.

(29) Schömer, M.; Seiwert, J.; Frey, H. Hyperbranched Poly(propylene oxide): A Multifunctional Backbone-Thermoresponsive Polyether Polyol Copolymer. *ACS Macro Lett.* **2012**, *1* (7), 888–891. DOI: 10.1021/mz300256y.

(30) Perevyazko, I.; Seiwert, J.; Schömer, M.; Frey, H.; Schubert, U. S.; Pavlov, G. M. Hyperbranched Poly(ethylene glycol) Copolymers: Absolute Values of the Molar Mass, Properties in Dilute

Solution, and Hydrodynamic Homology. *Macromolecules* **2015**, *48* (16), 5887–5898. DOI: 10.1021/acs.macromol.5b01020.

(31) Seiwert, J.; Leibig, D.; Kemmer-Jonas, U.; Bauer, M.; Perevyazko, I.; Preis, J.; Frey, H. Hyperbranched Polyols via Copolymerization of 1,2-Butylene Oxide and Glycidol: Comparison of Batch Synthesis and Slow Monomer Addition. *Macromolecules* **2016**, *49* (1), 38–47. DOI: 10.1021/acs.macromol.5b02402.

(32) Spoljaric, S.; Seppälä, J. One-pot, mouldable, thermoplastic resins from poly(propylene carbonate) and poly(caprolactone triol). *RSC Adv.* **2016**, *6* (41), 34977–34986. DOI: 10.1039/c6ra07191k.

(33) Sugimoto, H.; Goto, H.; Honda, S.; Yamada, R.; Manabe, Y.; Handa, S. Synthesis of four- and six-armed star-shaped polycarbonates by immortal alternating copolymerization of CO 2 and propylene oxide. *Polym. Chem.* **2016.** DOI: 10.1039/c6py00558f.

(34) Cyriac, A.; Lee, S. H.; Varghese, J. K.; Park, E. S.; Park, J. H.; Lee, B. Y. Immortal CO 2 /Propylene Oxide Copolymerization: Precise Control of Molecular Weight and Architecture of Various Block Copolymers. *Macromolecules* **2010**, *43* (18), 7398–7401. DOI: 10.1021/ma101259k.

(35) Trott, G.; Saini, P. K.; Williams, C. K. Catalysts for CO2/epoxide ring-opening copolymerization. *Philos. Trans. R. Soc. London, Ser. A* **2016**, *374* (2061). DOI: 10.1098/rsta.2015.0085.

(36) Leibig, D.; Seiwert, J.; Liermann, J.; Frey, H. **2016**, *submitted*.

(37) Ponomarenko, V. A.; Khomutov, A. M.; Ilchenko, S. L.; Ignatenk, A. V. Influence of Substituted Groups on Anionic Polymerization of Alpha-Oxides. *Vysokomol. Soedin. A* **1971**, *13*, 1546–1556.

(38) Ponomarenko, V. A.; Khomutov, A. M.; Ilchenko, S. L.; Ignatenk, A. V.; Khomutov, N. M. Influence of Substituted Groups on Reactivity of Monosubstituted Ethylene Oxide During Coordination-Anionic Copolymerization. *Vysokomol. Soedin. A* **1971**, *13*, 1551–1561.

(39) Stolarzewicz, A.; Neugebauer, D. Influence of substituent on the polymerization of oxiranes by potassium hydride. *Macromol. Chem. Phys.* **1999**, *200*, 2647.

(40) Cohen, C. T.; Chu, T.; Coates, G. W. Cobalt Catalysts for the Alternating Copolymerization of Propylene Oxide and Carbon Dioxide: Combining High Activity and Selectivity. *J. Am. Chem. Soc.* **2005**, *127* (31), 10869–10878. DOI: 10.1021/ja051744l.

(41) Chen, Y.; Shen, Z.; Frey, H.; Pérez-Prieto, J.; Stiriba, S.-E. Synergistic assembly of hyperbranched polyethylenimine and fatty acids leading to unusual supramolecular nanocapsules. *Chem. Commun.* **2005,** No. 6, 755–757. DOI: 10.1039/b414046j.

(42) Ford, D. D.; Nielsen, Lars P C; Zuend, S. J.; Musgrave, C. B.; Jacobsen, E. N. Mechanistic basis for high stereoselectivity and broad substrate scope in the (salen)Co(III)-catalyzed hydrolytic kinetic resolution. *J. Am. Chem. Soc.* **2013**, *135* (41), 15595–15608. DOI: 10.1021/ja408027p.

Supporting Information

Materials

$TsOH \cdot H_2O$ was dried using benzene. Propylene oxide (PO, 98%, Aldrich), 1,2-butylene oxide (BO, 99%, Aldrich) and glycidol (96%, Aldrich) were distilled over CaH_2 under reduced pressure prior to use. Carbon dioxide (>99.99%) and all other solvents and reagents were used as received.

Instrumentation

*NMR experiments***.** ^{1}H and ^{13}C NMR spectra were recorded on a Bruker AC 300 and a Bruker 400 spectrometer, operated at 300, 400, 75,4 and 100 MHz respectively, at 21 °C and the chemical shifts are given in parts per million (ppm). All spectra are referenced to residual solvent signal.

Size Exclusion Chromatography. For size exclusion chromatography (SEC) measurements in DMF (containing 0.25 g/L of lithium bromide as an additive) an Agilent 1100 Series was used as an integrated instrument, including a PSS HEMA column ($10^6/10^5/10^4$ g mol^{-1}) and a RI detector. Calibration was carried out using poly(ethylene oxide) standards provided by Polymer Standards Service.

*Preparative Size Exclusion Chromatography***.** For preparative size exclusion chromatography measurements in $CHCl_3$, a LC-91XX Next Series Recycling Preparative HPLC Anlage by *Japan Analytical Industry Co. Ltd.*, equipped with a Jaigel-2H column (upper exclusion limit $5 \cdot 10^4$ g mol^{-1}) and a UV and RI detector, was used. Sample fractionation was performed at 25 °C and a flow rate of 3.5 mL min^{-1}.

Differential Scanning Calorimetry. Differential Scanning Calorimetry (DSC) curves were recorded with a Perkin-Elmer DSC 7 CLN2 in the temperature range from -70 to +20 °C at heating rates of 10 K min^{-1} under nitrogen.

IR-Spectroscopy. FT-IR spectra were recorded using a Thermo Scientific iS10 FT-IR spectrometer, equipped with a diamond ATR unit.

On-line Viscometry. On-line viscometry measurements were performed using a PPS GRAM column (30/100/1000 Å porosity) with a SECcurity GPC1260 Refractive Index RI detector as well as a SECcurtity on-line viscometer DVD1260. As solvent DMF with 5 g·mol^{-1}LiBr was used. Samples with a concentration of 20 mg·mL^{-1} and a volume of 100 µL were measured after 8 h at 70 °C. Each

sample was measured three times and the average of the data obtained was calculated. As a universal standard, well-defined PMMA samples were used.

Synthesis of (R,R)-(salcy)-CoCl

(R,R)-(salcy)-CoCl was prepared as described by Ford *et al*.[42] A flame dried 250 mL flask was charged with (salen)Co(II) (1 g, 1.65 mmol) and 87 mL CH_2Cl_2. To this red suspension $TsOH \cdot H_2O$ (0.33 g, 1.735 mmol) was added. The mixture was stirred for 1.5 h until it became a dark green solution. This solution was washed three times with 30 mL brine, dried over Na_2SO_4 and concentrated in vacuum. The dark solid was suspended in cold pentane, filtered over Celite® and washed with cold pentane. The (salen)Co(III)Cl complex was obtained as a dark green solid and was stored under inner gas atmosphere. (360 mg, 30% yield).

Synthesis of *hb*PEO and *hb*PBO Copolymers

General procedure:[30] In a Schlenk flask equipped with a septum and a magnetic stirrer, 44 mg (0.33 mmol, 1.0 eq.) trimethylolpropane (TMP) and 17 mg (0.10 mmol, 0.3 eq.) CsOH monohydrate were dissolved in MeOH. The partly deprotonated initiator salt was isolated by azeotropic removal of MeOH with benzene and subsequent drying in high vacuum overnight.

The dried initiator salt was dissolved in 1 mL dimethyl sulfoxide. The flask was immersed in liquid nitrogen and glycidol was added via a syringe. Ethylene oxide was added via distillation (amount of monomers combined: 100 mmol, 300 eq.). The flask was sealed under vacuum and heated to 80 °C for 18 h. MeOH was added to terminate the reaction and the solution was neutralized by filtration over DOWEX WX8 resin. After removal of the solvents in vacuum and the removal of formed oligomers by precipitation in cold diethyl ether, the polymer was isolated as a brown oil and dried in vacuum at 85 °C for 24 h. Yield 80-90%.

For the synthesis of high molecular weight *hb*PEO, the initiator salt was dissolved in 10 mL dioxane instead of DMSO. The resulting copolymer was purified by dialysis (MWCO = 3500 Da).

Caution: In very few cases the pressure evolving in the early stages of the reaction in the flask may lead to the spontaneous removal of the septum and release of ethylene oxide. Thus, the reaction has to be carried out in an appropriate fume hood, and the respective safety precautions should be taken. In general, the amount of EO used did not exceed 5 g per batch in a 250 mL flask to guarantee a safe reaction.

^{1}H NMR (DMSO-d_6, 400 MHz): δ (ppm) = 4.81 – 4.35 (m, br, OH); 4,10 – 3.06 (m, O-CH, O-CH_2); 1.36 – 1.18 (m, 2H, CH_3-CH_2 (TMP)); 0.89 – 0.68 (m, 3H, CH_3 (TMP)).

^{13}C NMR (DMSO-d_6, 100 MHz): δ (ppm) = 80.25 – 79.45 (m, CH $G_{1,3\text{-Linear}}$); 78.52 – 77.42 (m, CH $G_{\text{Dendritic}}$); 73.22 – 72.10 (m, 2 CH_2 $G_{1,4\text{-Linear}}$); 72.04 – 69.62 (m, 2 CH_2 $G_{\text{Dendritic}}$, 2 CH_2 EO_{Linear}, *C*H_2-CH_2-OH EO_{Terminal}, CH G_{Terminal}, CH_2 G_{Terminal}); 69.61 – 68.37 (m, CH_2 $G_{1,3\text{-Linear}}$, CH-OH $G_{1,4\text{-Linear}}$); 63.39 – 62.96 (CH_2-OH G_{Terminal}); 60.87 – 60.07 (m, CH_2-OH EO_{Terminal}, CH_2-OH $G_{1,3\text{-Linear}}$).

Copolymers based on glycidol and BO were obtained by changing the reaction conditions to solvent-free copolymerization at 120 °C for 2 days.[31] Both comonomers were added via a syringe before polymerization (amount of monomers combined: 50 mmol, 150 eq.). The resulting copolymers were precipitated in a cold mixture of diethyl ether and hexane.

^{1}H NMR (DMSO-d_6, 400 MHz): δ (ppm) = 4.55 – 4.33 (m, br, OH); 4.08 – 3.02 (m, O-CH, O-CH_2); 1.56 – 1.12 (m, CH_3-CH_2 (BO & TMP)); 0.87 (t, CH_3 (BO); 0.79 (t, CH_3 (TMP)).

^{13}C NMR (DMSO-d_6, 100 MHz): δ (ppm) = 80.6 – 79.0 (CH $G_{1,3\text{-Linear}}$, CH BO_{Linear}); 78.8 – 77.4 (CH $G_{\text{Dendritic}}$); 75.8 – 75.0 (CH_2 BO_{Terminal}); 74.6 – 73.6 (CH_2 BO_{Linear}) 73.2 – 72.1 (2 CH_2 $G_{1,4\text{-Linear}}$); 72.0 – 69.9 (2 CH_2 $G_{\text{Dendritic}}$, CH G_{Terminal}, CH G_{Terminal}, CH_2 BO_{Terminal}); 69.9 – 68.3 (CH_2 $G_{1,3\text{-Linear}}$, CH-OH $G_{1,4\text{-Linear}}$); 63.5 – 62.8 (C*H*$_2$-OH G_{Terminal}); 61.4 – 60.6 (C*H*$_2$-OH $G_{1,3\text{-Linear}}$).

Table S 1. Overview of the characterization data for all hyperbranched polyether polyols.

Sample name[a)c)]	**M_n / g mol^{-1} (Visco)**[a)]	**PDI (Visco)**[a)]	**M_n / g mol^{-1} (SEC)**[b)]	**PDI (SEC)**[b)]	**[G] %**[c)]	**T_g / [°C]**[d)]
hb(PG_5-*co*-PEO_{57})	3000	2.12	2 500	1.58	8	-56
hb(PG_4-*co*-PEO_{45})[e)]	n.d.	n.d.	2 300	1.35	9	-62
hb(PG_4-*co*-PEO_{15})	980	2.03	1 900	1.31	21	-62
hb(PG_5-*co*-PEO_{10})	800	2.00	1 600	1.33	30	-64
hb(PG_9-*co*-PEO_{16})	1400	2.16	1 100	1.51	35	-61
hb(PG_{1250}-*co*-PEO_{6750})	389 000	2.81	53 000	1.18	16	-60
hb(PG_4-*co*-PBO_{10})	1100	3.40	1 100	1.69	29	-53

Terminology: Indices represent the absolute number of the respective repeating unit (rounded to integer), [a)] determined by on-line viscometry with universal calibration [b)] determined by SEC in DMF calibrated with a PEO standard, [c)] determined by inverse gated ^{13}C NMR spectroscopy, [d)] determined by DSC, [e)] no on-line viscometry data available; M_n approximated from SEC and the on-line viscometry data of the other samples. n.d. = not determined

Investigation of the Weight-depending Composition

To investigate the weight depending composition of the synthesized multiarm star polymers 300 mg polymer were dissolved in 3 mL $CHCl_3$ and then fractionated by preparative SEC. The solvent was removed under reduced pressure, and the fractionated polymers were investigated by ^{1}H NMR spectroscopy and SEC.

Dye Inclusion

2.8 mg Congo red were dissolved in 1 mL water. 20 mg *hb*(PG_{1250}-*co*-PEO_{6750})-*g*-PBC_{3640} was dissolved in 1 mL dichloromethane (DCM). The two solutions were mixed thoroughly by ultrasonication for 30 min. Subsequently, the mixture was allowed to demix overnight to ensure complete phase separation. For comparison, the same procedure was carried out using a blank DCM solution without polymer added.

Additional Characterization Data

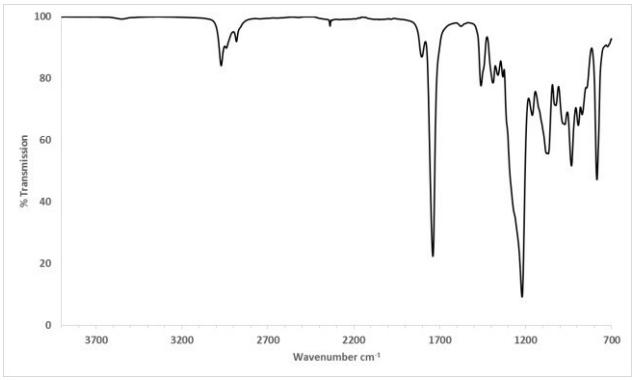

Figure S 1. FT-IR spectrum of *hb*(PG_9-*co*-PEO_{16})-*g*-PBC_{92} (Table 1, sample 2).

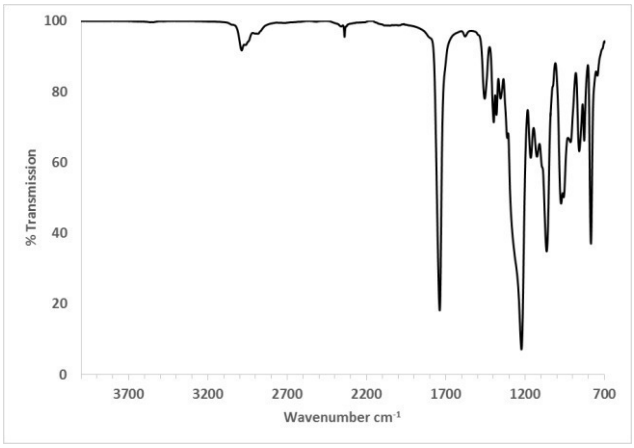

Figure S 2. FT-IR spectrum of *hb*(PG$_4$-*co*-PEO$_{45}$)-*g*-PPC$_{349}$ (Table 1, sample 7).

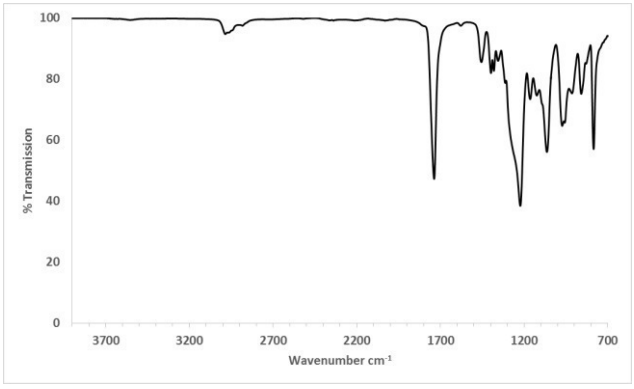

Figure S 3. FT-IR spectrum of *hb*(PG$_4$-*co*-PBO$_{10}$)-*g*-PPC$_{146}$ (Table 1, sample 8).

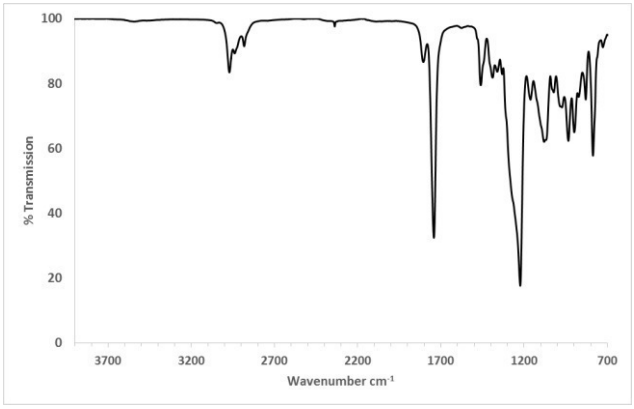

Figure S 4. FT-IR spectrum of *hb*(PG$_4$-*co*-PBO$_{10}$)-*g*-PBC$_{66}$ (Table 1, sample 9).

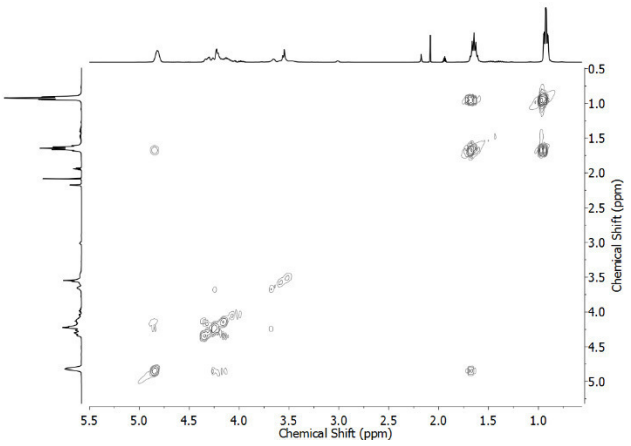

Figure S 5. COSY spectrum of *hb*(PG$_9$-*co*-PEO$_{16}$)-*g*-PBC$_{92}$ (Table 1, sample 2) (400 MHz, CD_3CN).

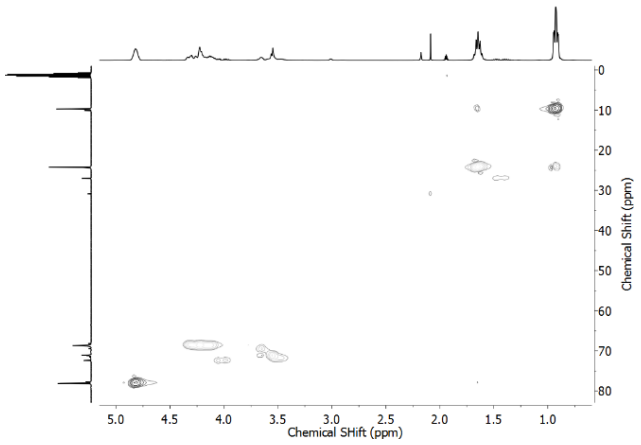

Figure S 6. HSQC spectrum of *hb*(PG$_9$-*co*-PEO$_{16}$)-*g*-PBC$_{92}$ (Table 1, sample 2) (400 MHz, CD_3CN).

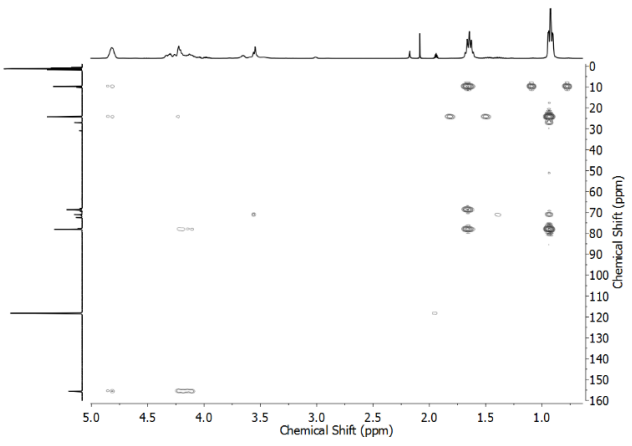

Figure S 7. HMBC spectrum of *hb*(PG$_9$-*co*-PEO$_{16}$)-*g*-PBC$_{92}$ (Table 1, sample 2) (400 MHz, CD_3CN).

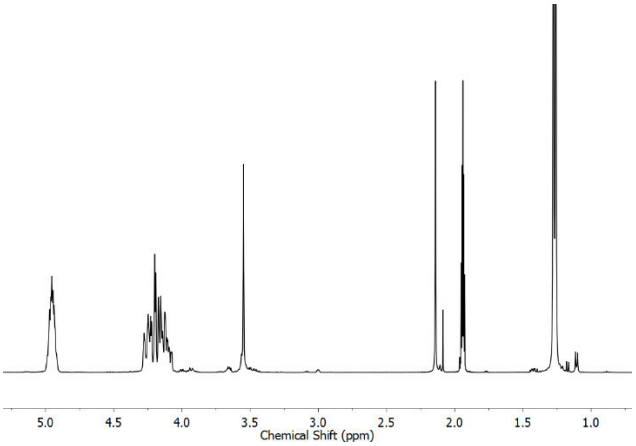

Figure S 8. ^{1}H NMR spectrum of *hb*(PG$_4$-*co*-PEO$_{45}$)-*g*-PPC$_{349}$ (Table 1, sample 7) (400 MHz, CD3CN).

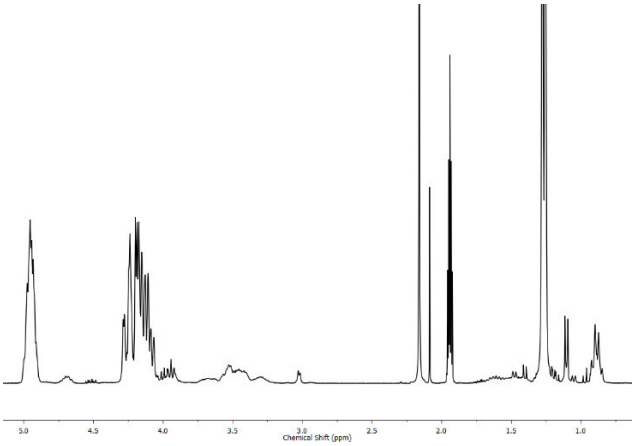

Figure S 9. ^{1}H NMR spectrum of *hb*(PG$_4$-*co*-PBO$_{10}$)-*g*-PPC$_{146}$ (Table 1, sample 8) (300 MHz, CD3CN).

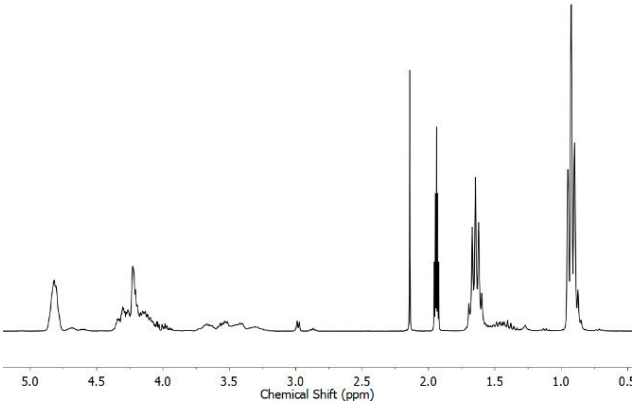

Figure S 10. ^{1}H NMR spectrum of *hb*(PG$_4$-*co*-PBO$_{10}$)-*g*-PBC$_{66}$ (Table 1, sample 9) (300 MHz, CD3CN).

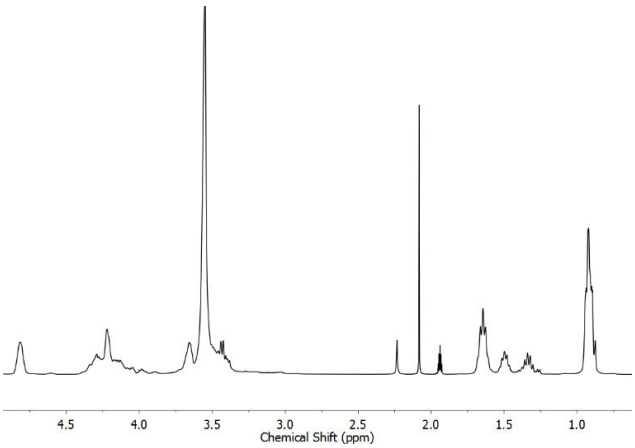

Figure S 11. 1H NMR spectrum of *hb*(PG_{1250}-*co*-PEO_{6750})-*g*-PBC_{3640} (Table 1, sample 6) (400 MHz, CD3CN).

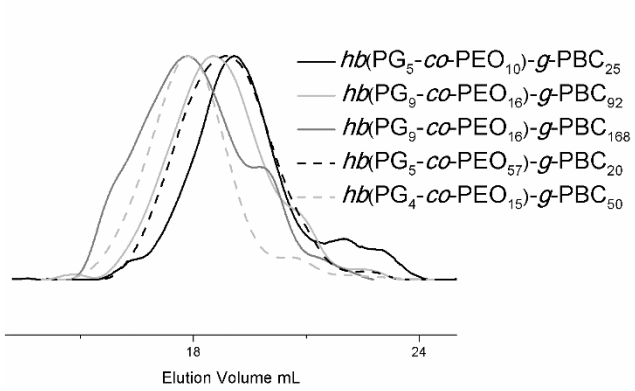

Figure S 12. SEC results of all *hb*PEO-*g*-PBC samples in DMF.

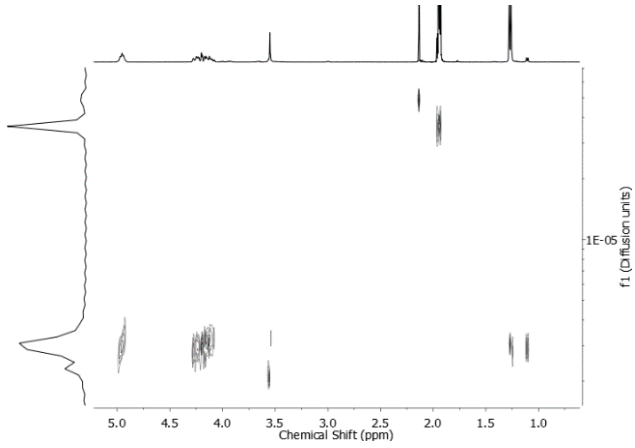

Figure S 13. DOSY spectrum of *hb*(PG_4-*co*-PEO_{45})-*g*-PPC_{349} (Table 1, sample 7) (CD3CN, 400 MHz).

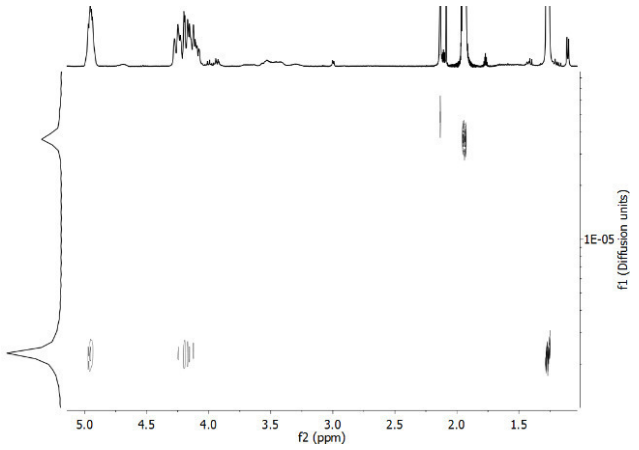

Figure S 14. DOSY spectrum of *hb*(PG$_4$-*co*-PBO$_{10}$)-*g*-PPC$_{146}$ (Table 1, sample 8) (CD3CN, 400 MHz).

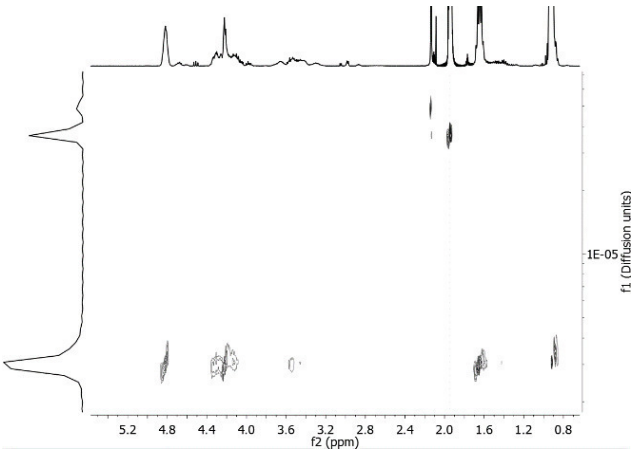

Figure S 15. DOSY spectrum of *hb*(PG$_4$-*co*-PBO$_{10}$)-*g*-PBC$_{66}$ (Table 1, sample 9) (CD3CN, 400 MHz).

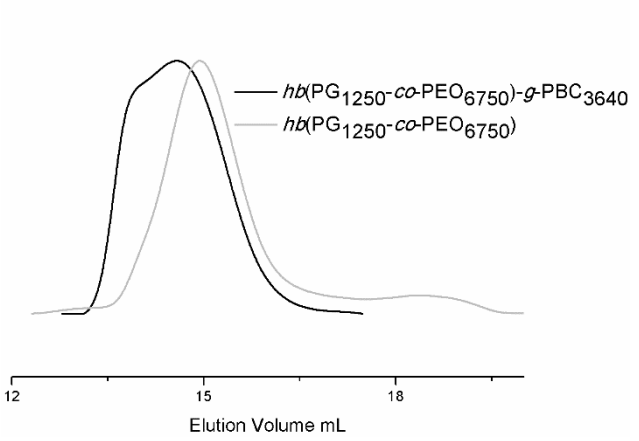

Figure S 16. SEC results of *hb*(PG$_{1250}$-*co*-PEO$_{6750}$)-*g*-PBC$_{3640}$ (Table 1, sample 6) and its macroinitiator in DMF.

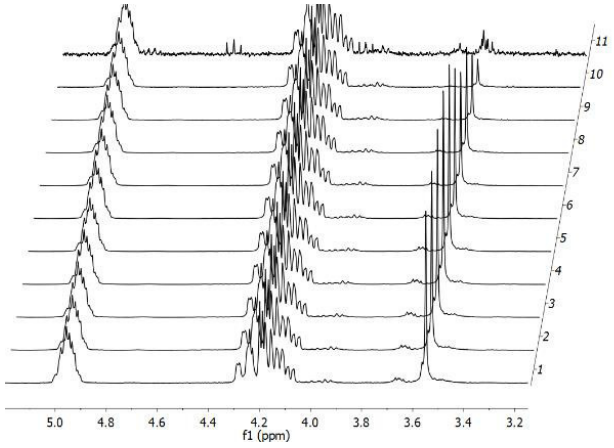

Figure S 17. ^{1}H NMR spectra of *hb*(PG$_4$-*co*-PEO$_{45}$)-*g*-PPC$_{349}$ (Table 1, sample 7) after separation with a preparative SEC. (300 MHz, CD_3CN).)

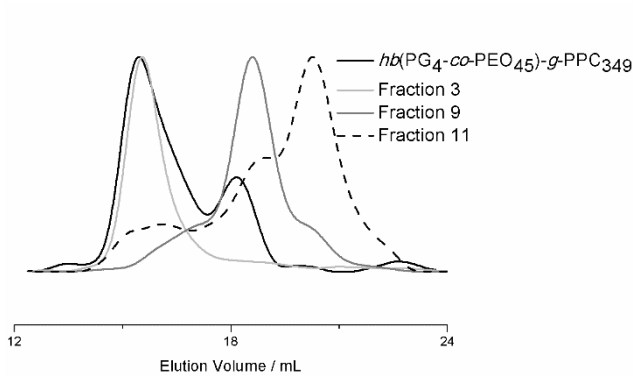

Figure S 18. SEC results for selected fractions of *hb*(PG$_4$-*co*-PEO$_{45}$)-*g*-PPC$_{349}$ (Table 1, sample 7) star polymers in DMF.

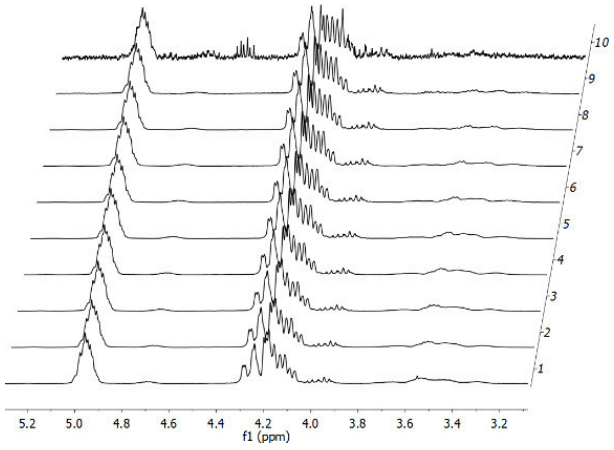

Figure S 19. ^{1}H NMR spectra of *hb*(PG$_4$-*co*-PBO$_{10}$)-*g*-PPC$_{146}$ (Table 1, sample 8) after separation with a preparative SEC. (300 MHz, CD_3CN).)

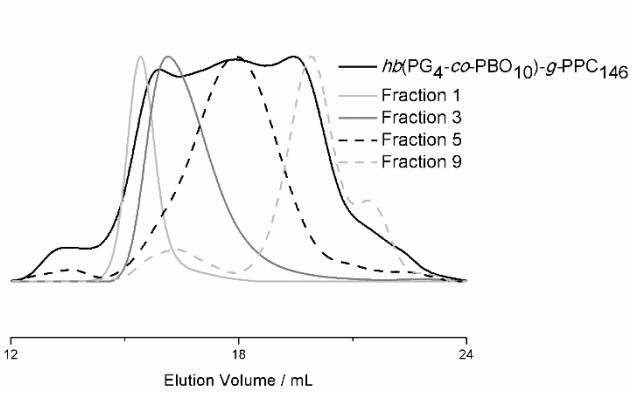

Figure S 20. SEC results for some fraction of *hb*(PG$_4$-*co*-PBO$_{10}$)-*g*-PPC$_{146}$ (Table 1, sample 8) star polymers in DMF.

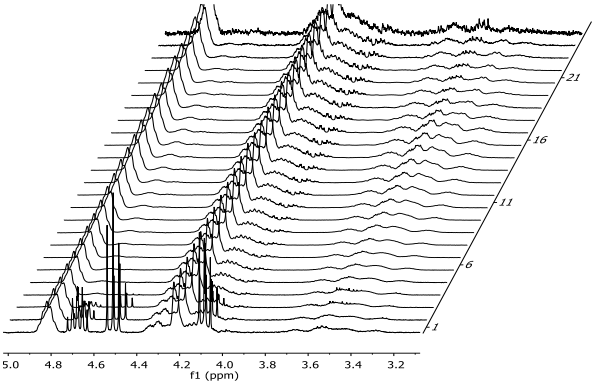

Figure S 21. ^{1}H NMR spectra of *hb*(PG$_4$-*co*-PBO$_{10}$)-*g*-PBC$_{66}$ (Table 1, sample 9) after separation via preparative SEC. (300 MHz, CD_3CN).)

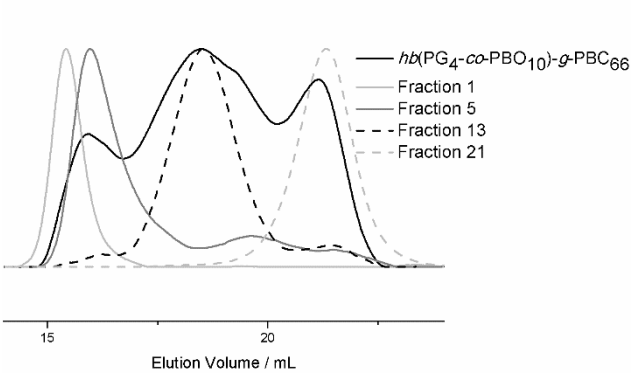

Figure S 22. SEC results for selected fractions of *hb*(PG$_4$-*co*-PBO$_{10}$)-*g*-PBC$_{66}$ (Table 1, sample 9) star polymers in DMF.

3.3 Ultra-high Molecular Weight Polystyrene Hyperstar Polymers with Hyperbranched Polyethylene Oxide as the Core

*Jan Seiwert[1], Pia Winterwerber[1], Holger Frey[1,]**

[1] Institute of Organic Chemistry, Johannes Gutenberg-University, Duesbergweg 10-14, D-55128 Mainz, Germany

In preparation.

This chapter summarizes research results that are also presented in Pia Winterwerber's bachelor thesis. The project was planned and supervised by the author of this thesis.

Abstract

A three-step core-first strategy to synthesize ultra-high molecular weight hyperstar polymers with hydrophobic polystyrene (PS) arms and a hydrophilic hyperbranched poly(ethylene oxide) (*hb*PEO) core is presented. First, two *hb*PEO polyether polyols with 800 and 2100 hydroxyl end groups for further functionalization were prepared by copolymerization of ethylene oxide with glycidol as a branching unit. Absolute molecular weight averages of 389 and 518 kg mol^{-1} were determined from on-line viscometry and a universal calibration. The degree of branching and the number of end groups were adjusted by variation of the comonomer ratio. Esterification of the hydroxyl end groups with 2-bromoisobutyryl bromide yielded multifunctional macroinitiators for atom transfer radical polymerization (ATRP). Subsequently, PS arms were grafted from the multifunctional macroinitiators, resulting in a core-shell structure. Successful copolymer formation was confirmed by ^{1}H NMR spectroscopy, SEC and differential scanning calorimetry. Separation of *hb*PEO core and PS arms by alkaline cleavage of the ester linkages allowed for precise SEC characterization of the PS arms and monitoring of the ATRP reaction kinetics.

Introduction

Polystyrene (PS) and polyethylene oxide (PEO) are among the most prominent types of commercial polymers, yet their material properties and therefore their scope of application differ greatly. The rigid, hydrophobic PS-based materials have found broad commercial use, e.g. for thermal, electrical and acoustic insulation as well as protective (food) packaging.[1] PEO on the other hand has become the gold standard polymer for pharmaceutical applications, and has versatile application in cosmetic and food products due to its excellent solubility in water and its very low toxicity.[2] Furthermore, it is employed for various industrial purposes, such as lubrication and defoaming.

The dissimilar couple of PEO and PS has been combined in a great variety of amphiphilic copolymer architectures. A vast amount of linear and star-shaped block copolymers, miktoarm star polymers and graft copolymers have been prepared.[3,4] Early works mostly rely on anionic polymerization to obtain well-defined copolymer structures. Since the 1990s, controlled radical polymerization techniques such as atom transfer radical polymerization (ATRP) and reversible addition–fragmentation chain transfer (RAFT) polymerization have gained in importance for the preparation of the polystyrene blocks.[3o)] PEO and PS blocks are largely immiscible. Their phase

behavior in bulk and the self-assembly of their amphiphilic copolymers in solution have been investigated extensively.[5]

A special class of copolymers are hyperstar (alias multiarm star) copolymers; i.e. polymers consisting of a (hyper)branched core and several to hundreds linear arms attached to it. These polymers can either be synthesized via the "core-first" or via the "arm-first" approach. The "core-first" strategy employs the core molecule as a multifunctional macroinitiator for the polymerization of the arms, whereas the "arm-first" method relies on prefabricated arms. They can be grafted onto the core or connected by crosslinking of the end groups. Various hyperstar copolymers with a branched PS derivative as a core and linear PEO arms as a shell have been synthesized.[4,6] These amphiphilic core-shell structures are potentially useful for encapsulation of hydrophobic compounds. Both "arm-first" and "core-first" strategies have been reported. These hyperstar copolymers mostly exhibit broad molecular weight distributions because neither multibranching self-condensing vinyl polymerization of chlorostyrene nor cross-linking of divinylbenzene results in well-defined hyperbranched polystyrene structures.

Hyperstar copolymers with linear polystyrene arms and a hyperbranched polyether core have been prepared via ATRP of styrene from polyglycerol or polyoxetane macroinitiators.[7,8] Rather small polyether cores with molecular weights below 50 kDa were employed, resulting in limited numbers of initiating moieties per polymer and polystyrene arms. Neither the hydrophobic polyoxetane nor the strongly polar polyglycerol matches the excellent solubility of PEO in both water and polar organic solvents.

In this work, we present the synthesis of amphiphilic, ultra-high molecular weight polystyrene hyperstar polymers with hyperbranched polyethylene oxide (*hb*PEO) as the core by combining anionic ring-opening polymerization (AROP) and ATRP (Figure 1). Random anionic ring-opening copolymerization of ethylene oxide with glycidol in dioxane as an emulsifying solvent and subsequent modification of end groups provides access to well-defined high molecular weight *hb*PEO macroinitiators with an adjustable number of end groups.[9,10] Polystyrene arms were grafted from the multifunctional macroinitiators via ATRP to attach a hydrophobic shell to the hydrophilic core in a controlled manner.

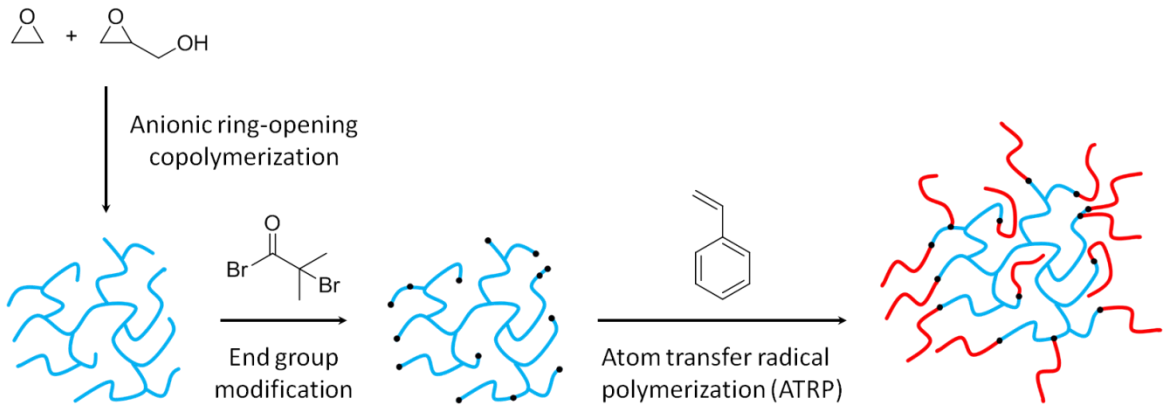

Figure 1. Synthesis scheme for the core-first preparation of *hb*PEO-*g*-PS hyperstar copolymers in three steps.

Experimental Part

Materials

Solvents and reagents were purchased from Sigma Aldrich or Acros Organics. Deuterated NMR solvents were obtained from Deutero. Glycidol purified by distillation over CaH_2 in vacuum. Dioxane was dried over sodium and distilled in vacuum prior to use. Styrene was distilled before use to remove the stabilizer. Other solvents and reagents were used as received.

Instrumentation

NMR spectra were recorded a *Bruker* Advance III HD 300 (5 mm BBFO head with z-gradient and ATM) at 300 MHz (^{1}H) and 75 MHz (^{13}C) as well as on a *Bruker* Advance III HD 400 (5 mm BBFO-SmartProbe with z-gradient and ATM) at 400 MHz (^{1}H) and 100 MHz (^{13}C). The residual signals of the deuterated solvent were utilized as an internal reference.

FTIR spectra were recorded on a Thermo Scientific iS10 FTIR spectrometer, equipped with a diamond ATR probe.

SEC measurements were performed in DMF (containing 0.25 g L^{-1} of lithium bromide). An integrated Agilent 1100 series instrument, equipped with a PSS HEMA column ($10^6/10^4/10^2$ Å porosity), UV and RI detector, was used. Linear poly(ethylene glycol) standards (Polymer Standards Service) were employed for calibration.

On-line viscometry measurements were performed at Polymer Standards Service. A PSS GRAM column (30/100/1000 Å porosity) equipped with a SECcurity GPC1260 Refractive Index RI detector

and a SECcurity on-line viscometer DVD1260 was employed. DMF containing 5 g L^{-1} LiBr was used as a solvent. Samples and solvent were weighed in accurately to generate precisely known sample concentrations of ~ 20 mg mL^{-1}. 100 µL Solution were injected eight hours after dissolving of the polymer. Measurements were performed at a flow rate of 1 mL min^{-1} and a temperature of 70 °C. Molecular weights were calculated from averaging the results of three measurements. An universal calibration based on poly(methyl methacrylate) standards was applied.

Differential scanning calorimetry was performed on a PerkinElmer 8500 thermal analysis system, equipped with a Perkin-Elmer CLN2 thermal analysis controller. The temperature range was from -90 to +140 °C at a heating rate of 10 K min^{-1}.

Synthetic Procedures

Hyperbranched Poly(ethylene oxide) (*Hb*PEO)

*Hb*PEO was synthesized as reported in previous work.[9] 66 mg (0.50 mmol, 1 eq.) Trimethylolpropane (TMP) and 17 mg (0.15 mmol, 0.3 eq.) potassium *tert*-butoxide were mixed in 1 mL MeOH. 3 mL Benzene were added and the mixture was stirred for 30 min. Solvents and volatiles were removed in high vacuum at room temperature overnight. The dried initiator salt was dissolved in 20 mL dioxane and 0.66 mL (10 mmol, 20 eq.) / 1.33 mL (20 mmol, 40 eq.) glycidol was added through a canula. 4.5 mL (90 mmol, 180 eq.) / 4.0 mL (80 mmol, 160 eq.) Ethylene oxide was added via vacuum distillation. The vacuum-sealed reaction flask was heated to 80 °C for 3 days. Subsequently, the polymerization was terminated with 5 mL MeOH. After neutralization with Dowex® 50WX8 ion exchange resin, the solution was filtrated and solvents were removed in vacuum. The crude polymer was dialyzed against MeOH (MWCO = 3000 Da) and dried in vacuum at 85 °C for 24 h. *Hb*PEO was obtained as a highly viscous, brown oil in 80-90 % yield.

Caution: In very few cases, the pressure evolving in the early stages of the reaction in the flask may lead to the spontaneous removal of the septum and release of ethylene oxide. Thus, the reaction has to be carried out in an appropriate fume hood, and the respective safety precautions should be taken. The amount of EO used did not exceed 5 g per batch in a 250 mL flask to guarantee a safe reaction.

^{1}H-NMR (DMSO-d_6, 400 MHz): δ (ppm) = 4.62 – 4.29 (m, br, OH); 4.04 – 3.02 (m, O-CH, O-CH_2).

^{13}C-NMR (DMSO-d_6, 100 MHz): δ (ppm) = 78.86 – 77.31 (m, Dendritic$_G$ CH); 73.22 – 72.09 (m, 2 Linear$_{G14}$ CH_2); 71.97 – 69.42 (m, 2 Dendritic$_G$ CH_2, 2 Linear$_E$ CH_2, Terminal$_E$ $\underline{C}H_2$-CH_2-OH, Terminal$_G$ CH, Terminal$_G$ CH_2); 69.41 – 68.14 (m, Linear$_{G13}$ CH_2, Linear$_{G14}$ CH-OH); 60.79 – 59.84 (m, Terminal$_E$ CH_2-OH, Linear$_{G13}$ CH_2-OH).

*Hb*PEO-Br Macroinitiator

The esterification of *hb*PEO was performed following a modified literature-known procedure.[7] *hb*PEO was dissolved in benzene and azeotropicly dried in high vacuum overnight. Then, the polymer was dissolved in dry pyridine and warmed to 50 °C. 2-Bromoisobutyryl bromide was added dropwise. After stirring over night at room temperature, the mixture was stirred over potassium carbonate for 20 min and filtrated. Pyridine was removed by azeotropic distillation with toluene. The residue was dissolved in toluene and dried over magnesium sulfate. After filtration, toluene was removed. The crude product was dialyzed against chloroform (MWCO = 2000 Da) and subsequently dried at 80 °C in high vacuum overnight to yield the pure *hb*PEG-Br macroinitiator.

^{1}H-NMR (DMSO-d_6, 300 MHz): δ (ppm) = 4.24 (s, CH_2-O-CO); 387 – 3.24 (m, polyether backbone); 1.89 (s, CBr-CH_3).

^{13}C-NMR (DMSO-d_6, 75 MHz): δ (ppm) = 170.6 (C=O); 78.4-64.8 (m, polyether backbone), 56.9 (C-Br); 30.3 (CBr-$\underline{C}H_3$).

N,N,N′,N′,N′′,N′′-Hexamethyl [Tris(2-aminoethyl)amine] (Me_6-tren)

Me_6-Tren was synthesized following a procedure by Singha and coworkers.[11] 206 mL Acetonitrile, 46 mL glacial acetic, 15.6 mL (226 mmol) aqueous formaldehyde solution (40 w%) and 1.09 g (7.7 mmol) tris(2-aminoethyl)amine were mixed. After stirring for one hour, 3.38 g (89.3 mmol) $NaBH_4$ were added at 0 °C. The mixture was stirred at room temperature for 72 h and the solvent was removed subsequently. The residue was alkalized (pH = 12) using 3 M NaOH solution and extracted with dichloromethane four times. The organic phases were collected and dried over $MgSO_4$. Dichloromethane was removed and the residue was dissolved in pentane. After filtration, the product was isolated by distillation under reduced pressure. Me_6-tren was obtained as a yellow liquid in 42 % yield.

^{1}H NMR (300 MHz, $CDCl_3$, δ): 2.66 – 2.60 (m, 6H, N-$(CH_2)_3$), 2.46 – 2.39 (m, 6H, $C\underline{H_2}$-N-CH_3), 2.26 (s, 18H, CH_3)

*Hb*PEO-*g*-Polystyrene Hyperstar Polymers

The following steps were performed under Argon atmosphere. 2 mL Anisole, 46 mg (0.2 mmol, 1 eq.) Me_6-tren, 26 mg (0.2 mmol, 1 eq.) CuBr and 5.0 mL (44 mmol, 220 eq.) styrene were mixed and degassed by bubbling Argon through the mixture for 30 min. In a separate flask, 98 mg *hb*$PEO_{0.16}$-Br / 80 mg *hb*$PEO_{0.30}$-Br macroinitiator (= 0.2 mmol C-Br initiator groups, 1 eq) was dissolved in 3 mL anisole, degassed and subsequently added to the mixture via cannula. The polymerization was started by immersing the reaction flask in an oil bath preheated at 70 °C. Samples were taken via syringe and frozen in liquid nitrogen. After 330 min, the polymerization was terminated by immersing the reaction flask in liquid nitrogen. The polymers were dissolved in tetrahydrofuran (THF), freed from copper ions by stirring over Lewatit ion exchange resin for 18 h and precipitated in cold methanol. After drying at 50 °C in vacuum overnight, *hb*PEO-*g*-PS was obtained as a colorless solid material.

^{1}H-NMR (300 MHz, $CDCl_3$, δ): = 7.43-6.30 (m, aromatic polystyrene side chain), 2.01-0.75 (m, aliphatic polystyrene backbone).

Separation of *hb*PEO core and PS arms

10-20 mg *hb*PEG-*g*-PS was dissolved in 1-2 mL THF and 0.5 mL 1 M KOH in MeOH was added. The mixture was heated to 55 °C overnight. After partial removal of the solvents, the polymer solution was precipitated in water. Drying in vacuum gave PS homopolymer as a colorless solid.

Results and Discussion

Hyperbranched Poly(ethylene oxide) Polyols

Hyperbranched PEO copolymers were prepared by anionic ring-opening multibranching copolymerization of ethylene oxide (EO) and glycidol (G) according to an established procedure reported in a previous work (Scheme 1).[9] Polymerization was performed in dioxane to obtain high molecular weights in the range of 389 to 518 kg mol^{-1}.

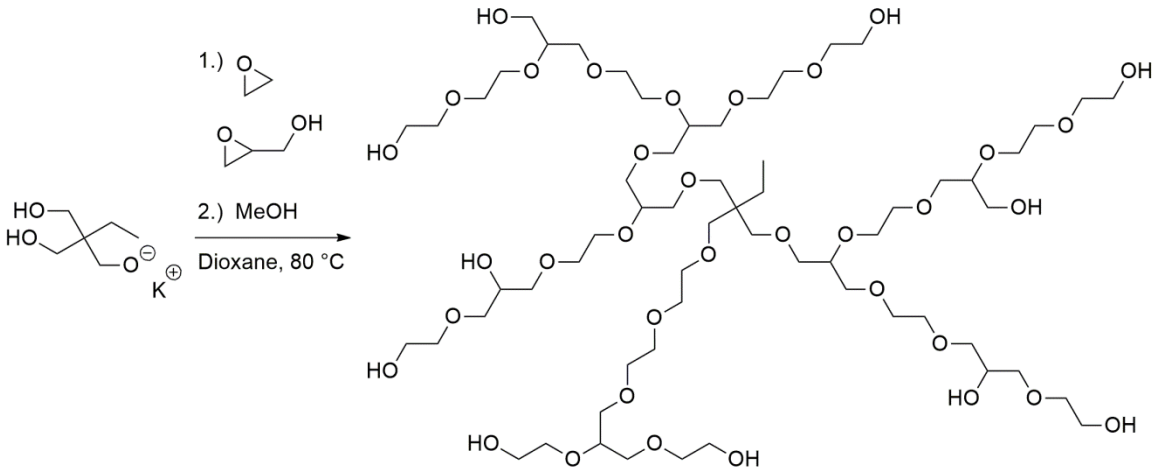

Scheme 1. Synthesis of hyperbranched polyether polyols from ethylene oxide and glycidol.

The characterization data for the hyperbranched polyether polyols is summarized in Table 1. Two copolymers with different EO/G ratios were synthesized to vary the number of hydroxyl end groups. Thereby, their influence on the synthesis of the ATRP macroinitiator and the following styrene polymerization could be investigated. Glycidol content ([*G*]) and degree of branching (*DB*) were determined by inverse gated ^{13}C NMR spectroscopy according to equation 1 and 2.[12]

$$[G] = \frac{[Dendritic_{\mathrm{G}}] + [Linear_{\mathrm{G13}}] + [Linear_{\mathrm{G14}}] + [Terminal_{\mathrm{G}}]}{[Dendritic_{\mathrm{G}}] + [Linear_{\mathrm{G13}}] + [Linear_{\mathrm{G14}}] + [Terminal_{\mathrm{G}}] + [Linear_{\mathrm{E}}] + [Terminal_{\mathrm{E}}]} \quad (1)$$

$$DB = \frac{2\,[Dendritic_{\mathrm{G}}]}{2\,[Dendritic_{\mathrm{G}}] + [Linear_{\mathrm{G13}}] + [Linear_{\mathrm{G14}}] + [Linear_{\mathrm{E}}]} \quad (2)$$

The first copolymer had a glycerol content of 16% and a DB of 0.17, whereas the second copolymer had a glycerol content of 30% and a DB of 0.28. EO and G can be copolymerized to very high molecular weights by employing dioxane as an "emulsifying" solvent.[9,13] In this manner, absolute average molecular weights of M_n(*hb*PEO$_{16G\%}$) = 389 000 g mol^{-1} and M_n(*hb*PEO$_{30G\%}$) = 518 000 g mol^{-1} were obtained, as determined by on-line viscometry and universal calibration. The molecular weight distributions ($Đ = M_w/M_n$) were rather broad with values of 2.8 for both polymers. However, dispersities were much smaller than expected for hyperbranched polymers exhibiting degrees of polymerization in this order of magnitude (DP_n(*hb*PEO$_{16G\%}$) ≈ 8·10^3, DP_n(*hb*PEO$_{30G\%}$) ≈ 1·10^4).[14] From the copolymer compositions and the absolute molecular weight values, the average numbers of hydroxyl end groups were calculated: 840 for *hb*PEO$_{16G\%}$ and 2100 for *hb*PEO$_{30G\%}$.

Table 1. Characterization data of the hyperbranched PEO copolymers.

Sample	G content[a]	*DB*[a]	M_n[b] kg mol^{-1}	*Đ*[b]	M_n[c] kg mol^{-1}	*Đ*[c]	*#OH*[d]
***hb*PEO$_{16G\%}$**	0.16	0.17	53	1.2	389	2.8	840
***hb*PEO$_{30G\%}$**	0.30	0.28	43	1.5	518	2.8	2100

[a] Determined from inverse gated (IG) ^{13}C NMR spectroscopy, [b] Apparent values determined from SEC (DMF, linear PEO standard), [c] Absolute values determined from on-line viscometry, [d] Calculated from IG ^{13}C NMR and on-line viscometry results.

*Hb*PEO-Br Macroinitiators

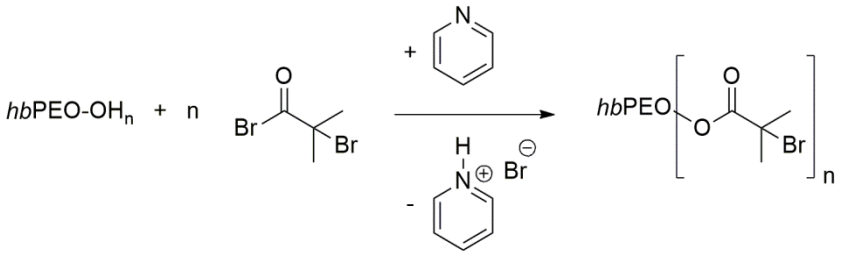

Scheme 2. Esterification of *hb*PEO with 2-bromoisobutyryl bromide.

ATRP initiator groups were attached to the polymer hydroxyl groups by Einhorn esterification of the hyperbranched PEO polyols with 2-bromoisobutyryl bromide (Scheme 2). This procedure was performed in analogy to the functionalization of other hyperbranched polyether polyols reported in the literature.[7] Successful functionalization was confirmed by ^{1}H NMR spectroscopy (Figure 2). The broad singlet (bs) at 1.88 ppm corresponds to the two methyl groups adjacent to the bromide substituent. The signal attributed to the terminal methylene groups of the polyether polyol is shifted downfield after esterification due to the electron-withdrawing effect of the ester moiety and can be identified at 4.32 ppm. The signal intensity ratio of 3:1 proves that all 2-bromoisobutyryl moieties are attached to the polyether polyol and no free low-molecular 2-bromoisobutyric acid is present. The hydroxyl proton signal at 4.5 ppm disappears from the spectrum after derivatization, indicating complete conversion of the hydroxyl groups.

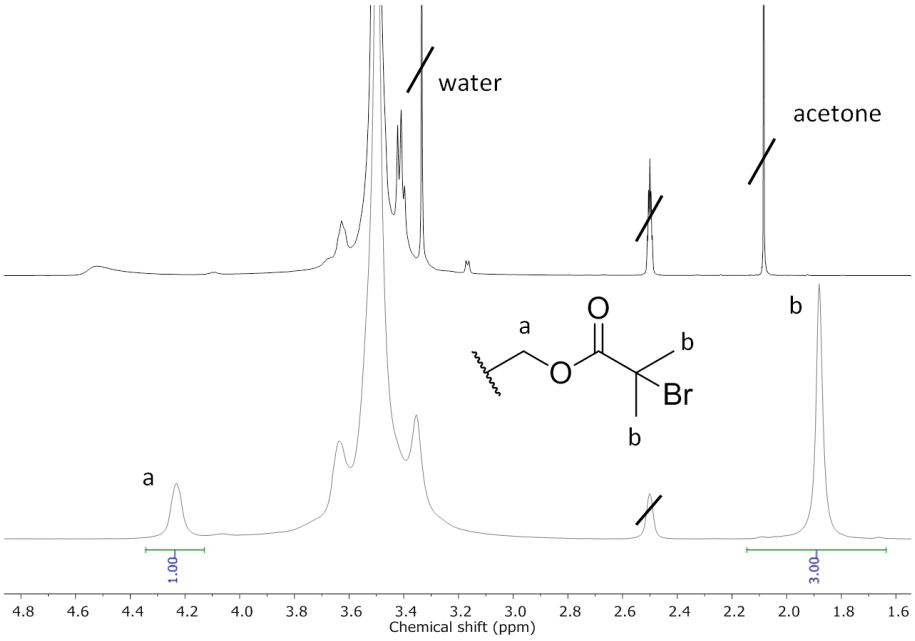

Figure 2. ^{1}H NMR spectra of *hb*PEO$_{16G\%}$ before (top) and after (bottom) esterification of the hydroxyl groups with 2-bromoisobutyryl bromide (DMSO-d_6, 300 MHz).

This finding was confirmed by ^{13}C NMR spectroscopy. Figure 3 reveals the disappearance of the characteristic terminal EO (60 ppm) and linear G signals (72 ppm). Terminal G units, which would result in a signal at 63 ppm, cannot be found at all (Figure 3, top). This can be ascribed to the high EO/G monomer feed ratio and the faster consumption of glycidol during the copolymerization.[15]

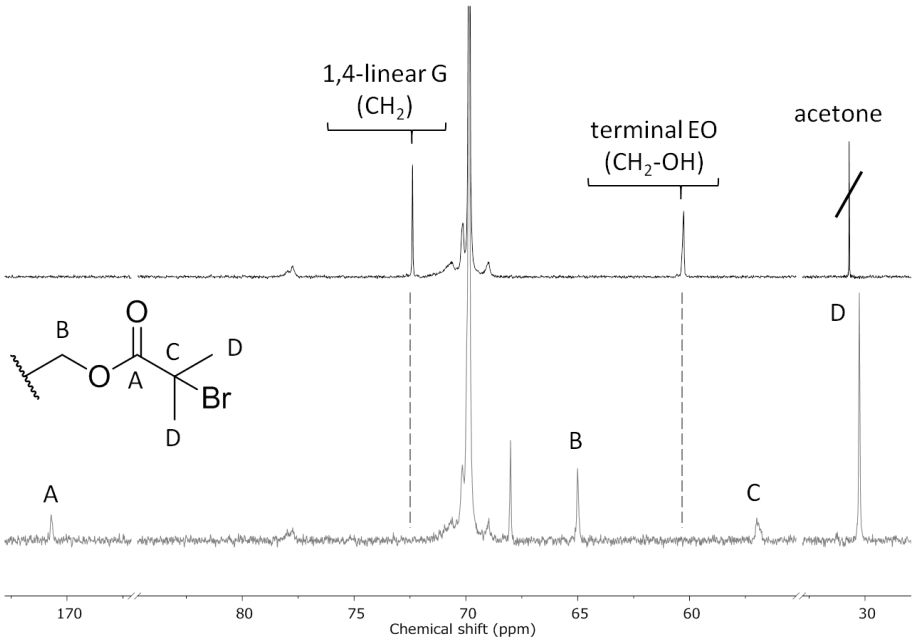

Figure 3. ^{13}C NMR spectra of *hb*PEO$_{16G\%}$ before (top) and after (bottom) esterification of the hydroxyl groups with 2-bromoisobutyryl bromide (DMSO-d_6, 75 MHz).

Characterization by FTIR spectroscopy was performed for comparison, revealing both the expected carbonyl absorption band at 1730 cm^{-1} and a weak, remaining hydroxyl band at 3500 cm^{-1} after modification (Figure 4). However, since the deviation is small and might result from residual water rather than incomplete conversion, quantitative modification was assumed for further calculations.

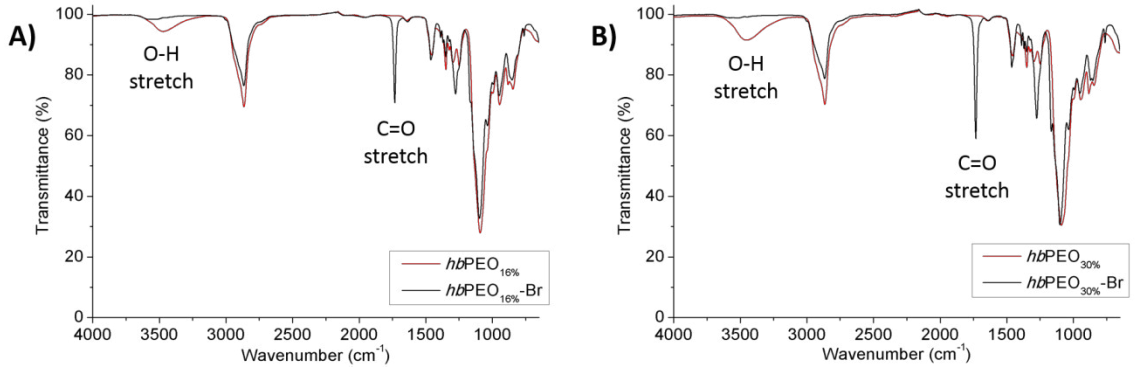

Figure 4. FTIR spectra of *hb*$PEO_{16G\%}$ (A) and *hb*$PEO_{30G\%}$ (B) before (red line) and after (black line) esterification of the hydroxyl groups with 2-bromoisobutyryl bromide.

*Hb*PEO-*g*-PS Hyperstar Copolymers

The *hb*PEO-Br macroinitiators were employed for the atom transfer radical polymerization (ATRP) of styrene, using CuBr and Me_6-tren as catalytic system. Me_6-tren is known to be a powerful ligand for ATRP that ensures both high catalyst activity and sufficient deactivation rates.[16] It was prepared from tris(2-aminoethyl)amine by reductive methylation, according to an established procedure.[11] For the ATRP of styrene, the initial molar ratio of monomer, to copper salt, ligand and macroinitiator was fixed at 220:1:1:1. Polymerization in bulk led to fast gelation of the reaction mixture and an insoluble product. Therefore, polymerizations were conducted using anisole as a solvent to prevent gelation. After termination of the polymerizations by immersing the reaction flask in liquid nitrogen, copper salts were removed from the reaction mixture using Lewatit ion exchange resin. The resulting *hb*PEO-*g*-PS hyperstar polymers were moderately soluble in chloroform, tetrahydrofuran and dimethylformamide. Solutions were slightly turbid, presumably due to self-aggregation of the immiscible *hb*PEO and the PS segments of the high molecular weight polymers. Chemical star-star coupling via free radical side reactions was excluded as a cause for the turbidity after characterization of the individual polystyrene arms (vide infra). NMR and SEC samples were filtered to obtain entirely clear solutions. The ^{1}H NMR spectra of the hyperstar polymers (Figure 5) show the aliphatic backbone and the aromatic side chain

signals of polystyrene. The polyether signal intensity is diminished for the hyperstar polymer with the *hb*PEO$_{16G\%}$ core (Figure 5, top). In the spectrum of the hyperstar polymer with the *hb*PEO$_{30G\%}$ core, the polyether backbone has vanished entirely (Figure 5, bottom). This can be explained by the high mass fraction of the PS shell and by potential shielding or poor solvation of the core.

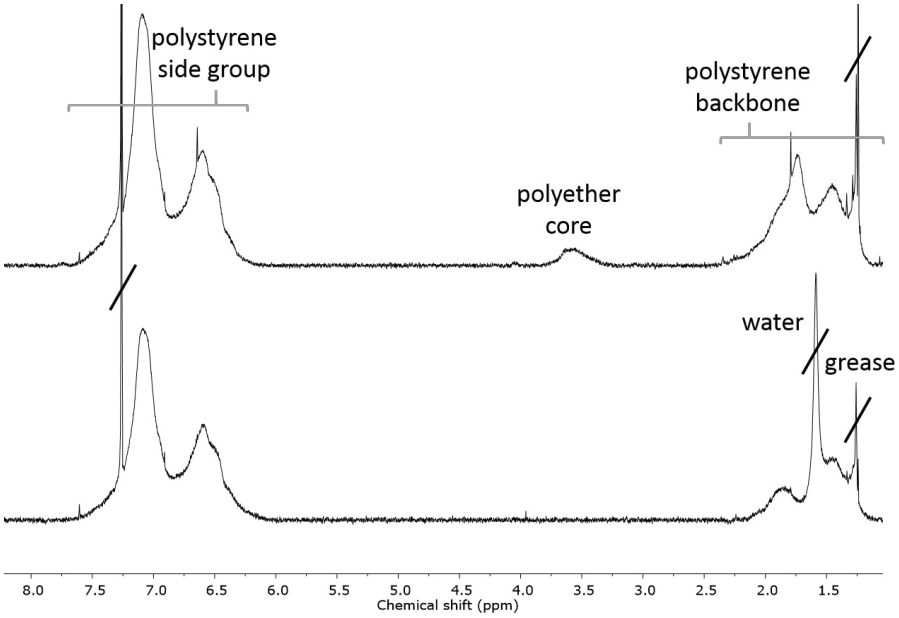

Figure 5. ^{1}H NMR spectra of *hb*PEO$_{16G\%}$-*g*-PS (top) and *hb*PEO$_{30G\%}$-*g*-PS (bottom), ($CDCl_3$, 300 MHz).

Thermal properties of *hb*PEO$_{16G\%}$-*g*-PS in bulk were determined by differential scanning calorimetry (DSC). The formation of a phase-separated block copolymer is unambiguously revealed by the occurrence of two distinct glass transition temperatures (T_g) at -43 °C for the polyether and 51 °C for the polystyrene segment that differ significantly from the transition temperatures of the individual homopolymers. The first T_g is 17 K higher than the T_g of the unmodified *hb*PEO$_{16G\%}$ polyether polyol and the second T_g is approximately 50 K below the T_g of a polystyrene homopolymer.

SEC (Figure 6) provides further evidence for the formation of *hb*PEO-*g*-PS hyperstar polymers. After the ATRP step, the traces are shifted to lower elution volumes in comparison to the *hb*PEO core polymers, implying a significant increase of the molecular weight. The traces of the hyperstar polymers reveal the same tailing as the curves of the *hb*PEO cores. However, no signs of low-molecular weight polystyrene homopolymers are found.

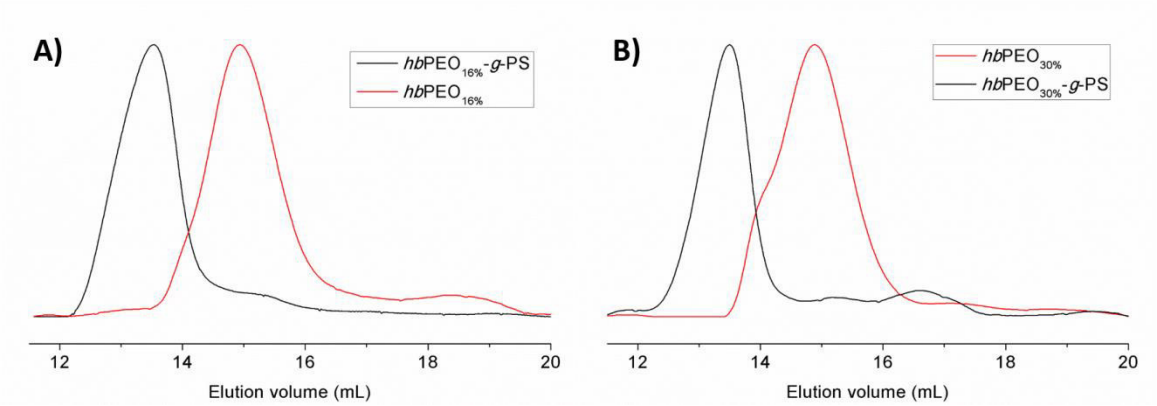

Figure 6. SEC traces (DMF) of *hb*PEO$_{16G\%}$ (A) and *hb*PEO$_{30G\%}$ (B) before (red line) and after (black line) grafting with polystyrene.

Due to the unusual copolymer architecture and the lack of an appropriate standard material, the SEC traces of the hyperstar polymers do not provide quantitative information about the degree of polymerization of the PS arms. Furthermore, the filtration required due to the poor solubility of the hyperstar polymers might affect the SEC measurements and lead to incomplete information. Therefore, the PS arms were separated from the hyperbranched polyether core by saponification of the connective ester groups and characterized individually, employing an appropriate polystyrene calibration. Capitalizing on this approach, we envisaged to elucidate the polymerization kinetics of the ATRP grafting-from step. Samples were taken from the reaction mixture during the polymerization at different reaction times, quenched, freed from copper salts and saponified. Subsequently, the isolated arms were characterized by SEC (Figure 7).

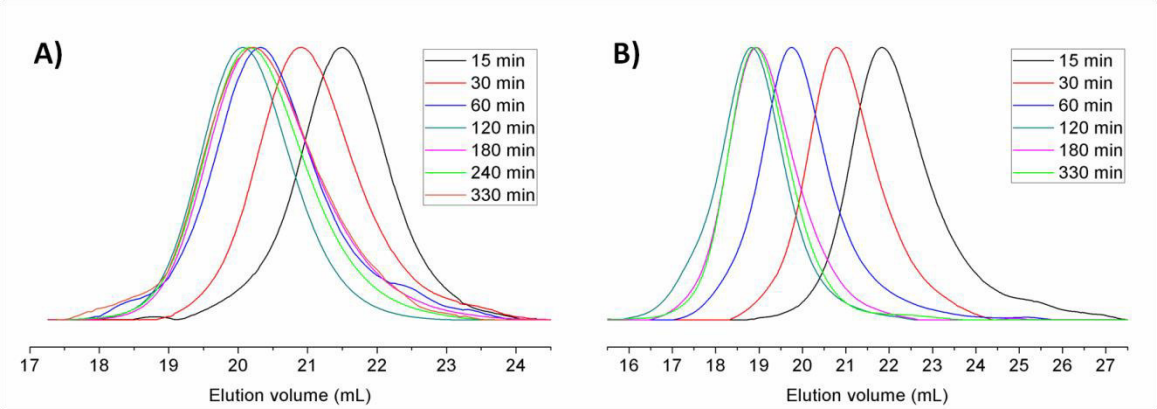

Figure 7. SEC traces (DMF) of PS arms grafted from *hb*PEO$_{16G\%}$ (A) and of PS arms grafted from *hb*PEO$_{30G\%}$ (B) at different reaction times.

Within the first 120 min of the ATRP, the PS arms of both hyperstar polymers grow continuously. *hb*PEO$_{30G\%}$-*g*-PS exhibits the linear correlation between degree of polymerization and reaction time expected for a controlled radical polymerization (Figure 8). For *hb*PEO$_{16G\%}$-*g*-PS, the expected linear dependence on time cannot be verified from the SEC data.

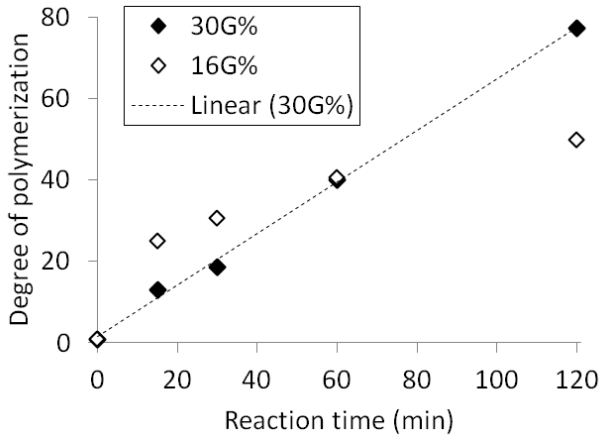

Figure 8. Degree of polymerization versus reaction time determined for the styrene polymerizations grafted from *hb*PEO$_{30G\%}$-Br (black) and *hb*PEO$_{16G\%}$-Br (white).

After 120 min both polymerizations reached a maximum molecular weight and no further growth was observed (Figure 7). The styrene arms grafted from *hb*PEO$_{30G\%}$-Br reached an average molecular weight of M_n = 8050 g mol^{-1}, corresponding to 35% styrene conversion (calculated from the degree of polymerization determined by SEC and the monomer to initiator ratio), at this point while the styrene polymerization grafted from *hb*PEO$_{16G\%}$-Br reached an average molecular weight of M_n = 5190 g mol^{-1} and 23% conversion. The small shift to higher elution volume in the SEC traces of samples collected after 120 min might result from inhomogeneities in the reaction mixture from which the samples were taken or non-uniform termination of the different samples. Depolymerization can be ruled out because the radical polymerization of styrene is irreversible. The *hb*PEO$_{16G\%}$-*g*-PS arms exhibit rather narrow molecular weight distributions with dispersities *Đ* ranging from 1.2 to 1.4. The *hb*PEO$_{30G\%}$-*g*-PS arms show higher dispersities in the range of 1.5 to 1.9. This can be ascribed to the higher grafting density of *hb*PEO$_{30G\%}$-*g*-PS causing sterical hindrance for the growth of some arms and an inhomogeneous overall chain growth. All SEC curves show monomodal distributions without minor maxima at higher molecular weights, eliminating radical recombination of two active polystyrene chain ends as a side reaction that would lead to covalent star-star coupling.

The poor solubility of the *hb*PEO-*g*-PS hyperstar polymers has hindered a comprehensive molecular weight characterization to date. However, theoretical molecular weights can be

calculated from the known average molecular weight values of the *hb*PEO-Br macroinitiators and the individual polystyrene arms, and the known number of initiator groups per macroinitiator. The resulting theoretical molecular weight values of *hb*$PEO_{16G\%}$-*g*-PS and *hb*$PEO_{30G\%}$-*g*-PS are $4.9 \cdot 10^6$ and $1.8 \cdot 10^7$ g mol^{-1}. Further studies to elucidate the true molecular weights of these exceptionally large hyperstar structures are in progress.

Conclusion

In summary, we have presented the synthesis of two ultra-high molecular weight *hb*PEO-*g*-PS hyperstar polymers with 800 and over 2000 PS arms employing a three-step core-first approach. In the first step, hydrophilic, hyperbranched PEO polyether polyols were prepared by anionic ring-opening copolymerization of ethylene oxide and glycidol. Subsequently, ATRP initiator groups were attached to the polymer via esterification of the hydroxyl groups with 2-bromoisobutyryl bromide. In the third step, hydrophobic polystyrene arms were grafted from the resulting multifunctional macroinitiator by controlled radical polymerization (ATRP). Mediocre solubility posed a challenge for the characterization of the resulting hyperstar polymers. NMR spectroscopy, SEC and DSC confirmed the successful copolymer formation. Separation of the polystyrene arms from the core permitted precise SEC characterization for the individual arms and monitoring of the polymerization kinetics. Molecular weights up to 5190 g mol^{-1} with dispersities *Đ* of 1.2 to 1.4 were found for *hb*$PEO_{16G\%}$-*g*-PS. *hb*$PEO_{30G\%}$-*g*-PS arms exhibited higher molecular weights up to 8050 g mol^{-1} with broader molecular weight distributions ranging from 1.5 to 1.9. From the characterization data of the individual *hb*PEO cores and the PS blocks, exceptionally high overall molecular weights of $4.9 \cdot 10^6$ and $1.8 \cdot 10^7$ g mol^{-1} were calculated for *hb*$PEO_{16G\%}$-*g*-PS and *hb*$PEO_{30G\%}$-*g*-PS, respectively. Further studies concerning the experimental determination of molecular weights, imaging of the copolymers, their phase behavior in bulk and their self-aggregation in solution are in progress.

The synthetic strategy described herein presents a universal concept for the synthesis of various ultra-high molecular weight hyperstar polymers. *hb*PEO-Br macroinitiators could be employed for the ATRP of other suitable vinyl monomers to tune the materials properties of the resulting hyperstar polymers.

Acknowledgment

The authors thank Dr. Jasmin Preis and Polymer Standards Service GmbH for on-line viscometry measurements.

References

1. a) J. Scheirs, D. B. Priddy, *Modern Styrenic Polymers: Polystyrenes and Styrenic Copolymers*, Chichester, UK, John Wiley & Sons, Ltd. **2003**; b) J. R. Wünsch, *Polystyrene: Synthesis, production and applications*, Shawbury, Shrewsbury, Shropshire, UK, Rapra Technology Ltd. **2000**;

2. a) C. Dingels, M. Schömer, H. Frey, *Chem. unserer Zeit.* **2011**, *45*, 338; b) J. Herzberger, K. Niederer, H. Pohlit, J. Seiwert, M. Worm, F. R. Wurm, H. Frey, *Chem. Rev.* **2016**, *116*, 2170;

3. a) R. S. Velichikova, Christova D. C., *Prog. Polym. Sci.* **1995**, *20*, 819; b) R. P. Quirk, J. Kim, C. Kausch, M. Chun, *Polym. Int.* **1996**, *39*, 3; c) K. Jankova, X. Chen, J. Kops, W. Batsberg, *Macromolecules.* **1998**, *31*, 538; d) M. Bednarek, T. Biedroń, P. Kubisa, *Macromol. Rapid Commun.* **1999**, *20*, 59; e) C. Gao, S. Li, Q. Li, P. Shi, S. A. Shah, W. Zhang, *Polym. Chem.* **2014**, *5*, 6957; f) D. Taton, E. Cloutet, Y. Gnanou, *Macromol. Chem. Phys.* **1998**, *199*, 2501; g) S. Angot, D. Taton, Y. Gnanou, *Macromolecules.* **2000**, *33*, 5418; h) R. Francis, D. Taton, J. L. Logan, P. Masse, Y. Gnanou, R. S. Duran, *Macromolecules.* **2003**, *36*, 8253; i) F. Candau, F. Afchar-Taromi, P. Rempp, *Polymer.* **1977**, *18*, 1253; j) S. Peleshanko, R. Gunawidjaja, S. Petrash, V. V. Tsukruk, *Macromolecules.* **2006**, *39*, 4756; k) Z. Li, P. Li, J. Huang, *J. Polym. Sci. A Polym. Chem.* **2006**, *44*, 4361; l) Z. Jia, Q. Fu, J. Huang, *Macromolecules.* **2006**, *39*, 5190; m) L. Chen, J. Huang, X. Wang, C. Lu, H. Zhang, G. Wang, *RSC Adv.* **2015**, *5*, 32358; n) C. M. Bates, A. B. Chang, N. Momčilović, S. C. Jones, R. H. Grubbs, *Macromolecules.* **2015**, *48*, 4967; o) K. Matyjaszewski, J. Xia, *Chem. Rev.* **2001**, *101*, 2921.

4. G. Lapienis, *Prog. Polym. Sci.* **2009**, *34*, 852.

5. a) K. Nakamura, R. Endo, M. Takeda, *J. Polym. Sci. Polym. Phys. Ed.* **1976**, *14*, 1287; b) C. Le Zhao, M. A. Winnik, G. Riess, M. D. Croucher, *Langmuir.* **1990**, *6*, 514; c) M. Wilhelm, C. Le Zhao, Y. Wang, R. Xu, M. A. Winnik, J. L. Mura, G. Riess, M. D. Croucher, *Macromolecules.* **1991**, *24*, 1033; d) R. Xu, M. A. Winnik, F. R. Hallett, G. Riess, M. D. Croucher, *Macromolecules.* **1991**, *24*, 87; e) R. Xu, M. A. Winnik, G. Riess, B. Chu, M. D. Croucher, *Macromolecules.* **1992**, *25*, 644; f) A. Jada, G. Hurtrez, B. Siffert, G. Riess, *Macromol. Chem. Phys.* **1996**, *197*, 3697; g) K.

Yu, A. Eisenberg, *Macromolecules.* **1996**, *29*, 6359; h) K. Yu, A. Eisenberg, *Macromolecules.* **1998**, *31*, 3509; i) L. Zhu, S. Z. D. Cheng, B. H. Calhoun, Q. Ge, R. P. Quirk, E. L. Thomas, B. S. Hsiao, F. Yeh, B. Lotz, *J. Am. Chem. Soc.* **2000**, *122*, 5957; j) L. Zhu, S. Cheng, B. H. Calhoun, Q. Ge, R. P. Quirk, E. L. Thomas, B. S. Hsiao, F. Yeh, B. Lotz, *Polymer.* **2001**, *42*, 5829; k) J. L. Logan, P. Masse, Y. Gnanou, D. Taton, R. S. Duran, *Langmuir.* **2005**, *21*, 7380; l) P. Bhargava, J. X. Zheng, P. Li, R. P. Quirk, F. W. Harris, S. Z. D. Cheng, *Macromolecules.* **2006**, *39*, 4880;

6. a) H. Durmaz, A. Dag, E. Erdogan, A. L. Demirel, G. Hizal, U. Tunca, *J. Polym. Sci. A Polym. Chem.* **2010**, *48*, 99; b) H. Durmaz, A. Dag, D. Gursoy, A. L. Demirel, G. Hizal, U. Tunca, *J. Polym. Sci. A Polym. Chem.* **2010**, *48*, 1557; c) V. Rodionov, H. Gao, S. Scroggins, D. A. Unruh, A. J. Avestro, J. M. Frechet, *J. Am. Chem. Soc.* **2010**, *132*, 2570; d) W. Li, K. Matyjaszewski, *Macromol. Rapid Commun.* **2011**, *32*, 74;

7. M. Morell, X. Fernández-Francos, J. Gombau, F. Ferrando, A. Lederer, X. Ramis, B. Voit, À. Serra, *Prog. Org. Coat.* **2012**, *73*, 62.

8. a) K. Jankova, M. Bednarek, S. Hvilsted, *J. Polym. Sci. A Polym. Chem.* **2005**, *43*, 3748; b) G. Jiang, L. Wang, W. Chen, *Eur. Polym. J.* **2006**, *42*, 3333; c) C. Liu, Y. Zhang, J. Huang, *Macromolecules* **2008**, *41*, 325.

9. I. Perevyazko, J. Seiwert, M. Schömer, H. Frey, U. S. Schubert, G. M. Pavlov, *Macromolecules.* **2015**, *48*, 5887.

10. S. Maier, A. Sunder, H. Frey, R. Mülhaupt, *Macromol. Rapid Commun.* **2000**, *21*, 226.

11. S. Ata, D. Mal, N. K. Singha, *RSC Adv.* **2013**, *3*, 14486.

12. a) D. Wilms, M. Schömer, F. Wurm, M. I. Hermanns, C. J. Kirkpatrick, H. Frey, *Macromol. Rapid Commun.* **2010**, *31*, 1811; b) H. Frey, D. Hölter, *Acta Polym.* **1999**, *50*, 67;

13. R. K. Kainthan, E. B. Muliawan, S. G. Hatzikiriakos, D. E. Brooks, *Macromolecules.* **2006**, *39*, 7708.

14. P. J. Flory, *J. Am. Chem. Soc.* **1952**, *74*, 2718.

15. D. Leibig, J. Seiwert, J. Liermann, H. Frey, **2016**, *submitted*.

16. W. Tang, Y. Kwak, W. Braunecker, N. V. Tsarevsky, M. L. Coote, K. Matyjaszewski, *J. Am. Chem. Soc.* **2008**, *130*, 10702.

4

HETEROFUNCTIONAL HYPERBRANCHED POLYETHER POLYOLS

4.1 Thioether-bearing Hyperbranched Polyether Polyols: A Versatile Platform for Orthogonal Functionalization

Jan Seiwert[1], Jana Herzberger[1,2], Daniel Leibig[1,2], Holger Frey[1,2,]*

[1] Institute of Organic Chemistry, Johannes Gutenberg-University, Duesbergweg 10-14, 55128 Mainz, Germany

[2] Graduate School Materials Science in Mainz, Staudinger Weg 9, 55128 Mainz, Germany

Submitted.

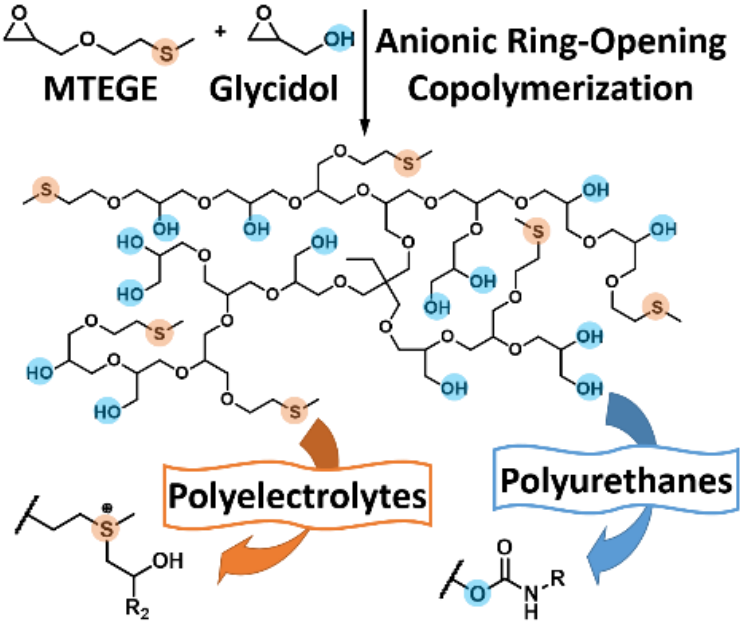

Abstract

The synthesis of thioether-bearing hyperbranched polyether polyols based on the copolymerization of AB/AB_2 type (cyclic latent) monomers is introduced. The polymers are prepared by anionic ring-opening multibranching copolymerization of glycidol, and the novel monomer 2-(methylthio)ethyl glycidyl ether (MTEGE), which is conveniently accessible in a single etherification step. Slow monomer addition provides control over molecular weights. Given the hyperbranched structure, moderate dispersities (Đ = 1.48 to 1.85) are obtained. *In situ* ^{1}H NMR copolymerization kinetics revealed reactivity ratios of $r_G = 3.7$ and $r_{MTEGE} = 0.27$. Using slow monomer addition, copolymer composition can be systematically varied, allowing for the adjustment of the hydroxyl/thioether ratio, the degree of branching (DB = 0.36 - 0.48), thermal properties and cloud point temperatures in aqueous solution in the range of 29 to 75 °C. Thioether oxidation enables tailoring the copolymers' solubility profile. Use of these copolymers as versatile, multifunctional platform for orthogonal modification is demonstrated. The methyl thioether group can be selectively alkoxylated, using propylene oxide, allyl glycidyl ether and furfuryl glycidyl ether, resulting in functional hyperbranched polyelectrolytes. These moieties tolerate urethane functionalization of the glycerol units.

Introduction

Since 1999 both linear and hyperbranched polyglycerols (PG) have been established as a multifunctional alternative to poly(ethylene glycol) (PEG), the gold standard polyether for pharmaceutical application.[1] Both polyethers share excellent biocompatibility and good solubility in polar solvents.[2] In addition, the compact, three-dimensional structure of hyperbranched polyglycerol (*hb*PG) adds several dendrimer-like features. Hyperbranched polyglycerol possesses a high number of hydroxyl groups as well as a lower intrinsic viscosity than PEG and does not crystallize.[3] In contrast to many other hyperbranched polymers, polyglycerol can be prepared with control over molecular weight and narrow to moderate molecular weight distributions using multibranching anionic ring-opening polymerization and slow addition of the glycidol monomer.[3, 4] The slow monomer addition (SMA) procedure enables complete incorporation of the initiating core molecule and lowers the probality of chain transfer reactions.[5] Similarly controlled multibranching polymerization procedures often involve specifically designed monomers or core molecules, ruling out large-scale applications of the resulting materials, whereas *hb*PG can be prepared on a kilogram scale from commercial reagents.[6]

Polyglycerol-based materials bearing different functional groups in addition to the many hydroxyl groups are of special interest, e.g., for biomedical purposes and surface modification.[7] They can be accessed via various synthetic strategies. Initiating the polymerization from a heterofunctional polyol results in *hb*PG polymers containing exactly one functional moiety at the focal point of the branched structure, such as a single alkyne, amine, cholesterol or catechol group.[8] Furthermore, *hb*PG end groups can be partly modified after polymerization to obtain a large variety of functional materials.[9] This strategy commonly requires multi-step procedures and thorough purification. Copolymerization of glycidol with functional glycidyl ethers on the other hand provides an elegant way of introducing certain functional groups into *hb*PG directly in a single step. Via this approach the introduction of allyl, alkyne, phenyl, ferrocene, maleimide, and catechol moieties as well as stimuli-responsive cleaving sites into the hyperbranched polyether structure was accomplished.[10–13]

In this work we present the synthesis of methyl thioether-bearing hyperbranched polyglycerol by random anionic copolymerization of glycidol and a novel comonomer: 2-(methylthio)ethyl glycidyl ether (MTEGE). The thioether side chain resembles methionine, an essential α-amino acid. Sulfur opens manifold possibilities for modification by either oxidation or alkylation.[14, 15] Recently, also alkoxylation of thioethers using miscellaneous epoxides has been explored as a convenient click functionalization.[16] This renders thioether-bearing hyperbranched polyglycerol a multifunctional platform for a wide range of further modifications.

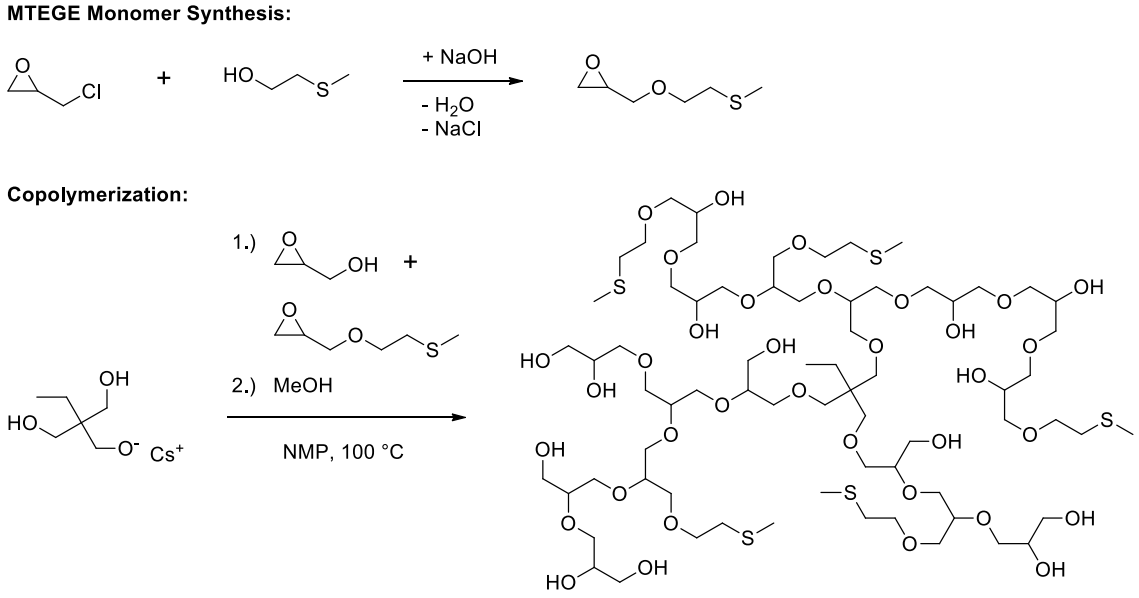

Scheme 1. Synthesis of hyperbranched copolymers from MTEGE and glycidol.

Experimental Section

Materials, instrumentation and further procedures are described in the Supporting Information.

Monomer Synthesis: 2-(Methylthio)ethyl Glycidyl Ether (MTEGE)

10 mL (115 mmol, 1 eq.) 2-(Methylthio)ethanol was placed in a three-necked flask equipped with a mechanical stirrer and a dropping funnel. 4,6 g (115 mmol, 1 eq.) crushed NaOH pellets were added and the mixture was stirred at room temperature until most NaOH was dissolved. After cooling to 0 °C, 18 mL (230 mmol, 2 eq.) epichlorohydrin (ECH) was added dropwise and the mixture was stirred for two days. Subsequently, the formed salt was removed via centrifugation. The organic phase was dried over $MgSO_4$. MTEGE was isolated by repeated, fractionated vacuum distillation (p = 0.006 mbar, T_b = 60°C) as a colorless liquid (yield: 50-60 %).

^{1}H NMR (400 MHz, $CDCl_3$, δ): 3.86 – 3.60 (m, 3H, CH-C<u>H</u>H-O, O-C<u>H$_2$</u>-CH$_2$); 3.43 (dd, J = 11.6, 5.9 Hz, 1H, , CH-CH<u>H</u>-O); 3.18 (ddt , J = 5.9, 4.2, 2.8 Hz, 1H, H$_2$C(O)C<u>H</u>); 2.82 (dd, J = 5.0, 4.2 Hz, 1H, <u>H</u>HC(O)CH); 2.72 (t, J = 6.7 Hz, 2H, CH$_2$-S); 2.64 (dd, J = 5.0, 2.8 Hz, 1H, H<u>H</u>C(O)CH); 2.17 (s, 3H, S-CH$_3$).

^{13}C NMR (100 MHz, $CDCl_3$, δ): 71.7 (CH-<u>C</u>H$_2$-O), 70.8 (O-<u>C</u>H$_2$-CH$_2$), 50.9 (H$_2$C(O)<u>C</u>H), 44.3 (H$_2$<u>C</u>(O)CH), 33.7 (CH$_2$-S), 16.2 (S-CH$_3$).

FDMS m/z: [M$^+$] calc. for $C_6H_{12}O_2S$, 148.06; found, 148.2.

Copolymerization of MTEGE and Glycidol

General procedure: In a Schlenk flask equipped with a magnetic stirrer, 67 mg (0.5 mmol, 1.0 eq.) trimethylolpropane (TMP) was dissolved in methanol, partly deprotonated with 28 mg (0.17 mmol, 0.3 eq.) cesium hydroxide monohydrate and dried in vacuum overnight at room temperature. Subsequently, the initiator was dissolved in 1 mL N-methyl-2-pyrrolidone and heated to 100 °C under argon atmosphere. In a separate flask, the monomers MTEGE and glycidol were mixed under argon atmosphere and diluted with NMP in a volume ratio of 1:1. The solution was added dropwise to the initiator at a rate of 0.2 mL h^{-1} using a syringe pump. The polymerization was terminated with methanol 1 h after finishing the monomer addition. After removal of the solvent, the resulting pale brown oil was precipitated from MeOH into cold diethyl ether and then dried in vacuum at 50 °C for 24 h (yield 80 - 90%).

^{1}H NMR (400 MHz, DMSO-d_6, δ): 4.85 – 4.08 (br, OH); 4.05 – 3.05 (m, O-CH, O-CH_2); 2.61 (t, J = 6.7 Hz, CH_2-S); 2.07 (s, S-CH_3); 1.38 – 1.18 (m, 2H, C$\underline{H}_2$-CH_3 (TMP)); 0.87 – 0.72 (m, 3H, CH_3 (TMP)).

^{13}C NMR (DMSO-d_6, 100 MHz, δ): 80.30 – 79.45 (m, CH $G_{1,3\text{-Linear}}$); 78.68 – 77.63 (m, CH $G_{Dendritic}$, CH M_{Linear}); 72.92 (s, 2 CH_2 $G_{1,4\text{-Linear}}$); 72.26 (s, 2 CH_2 $M_{Terminal}$); 72.04 – 70.41 (m, 2 CH_2 $G_{Dendritic}$, CH $G_{Terminal}$, CH_2 $G_{Terminal}$); 70.39 – 69.93 (m, 2 CH_2 M_{Linear}); 69.61 – 68.37 (m, CH_2 $G_{1,3\text{-Linear}}$, CH-OH $G_{1,4\text{-Linear}}$, O-C$\underline{H}_2$-CH_2-S M_{Linear}, O-C$\underline{H}_2$-CH_2-S $M_{Terminal}$); 63.12 (s, CH_2-OH $G_{Terminal}$); 61.56 – 60.70 (m, CH_2-OH $G_{1,3\text{-Linear}}$); 32.69 (s, CH_2-S M_{Linear}, CH_2-S $M_{Terminal}$); 15.28 32.69 (s, S-CH_3 M_{Linear}, S-CH_3 $M_{Terminal}$).

Results and Discussion

Monomer synthesis

2-(Methylthio)ethyl glycidyl ether (MTEGE) was synthesized from the commercially available reagents epichlorohydrin and 2-(methylthio)ethanol in a single, straightforward etherification step (Scheme 1). Successful synthesis was confirmed by ^{1}H and ^{13}C NMR spectroscopy (Figure S1) as well as mass spectrometry. Purification of the monomer by repeated fractionated distillation gave yields of 50 to 60% and allowed recollecting unreacted 2-(methylthio)ethanol. Column chromatography was found to be unsuitable for purification of MTEGE, due to side reactions with the column material (silica or aluminum oxide).

Copolymerization of MTEGE and Glycidol and Copolymer Characterization

The anionic ring-opening multibranching copolymerization of MTEGE with glycidol was realized in analogy to the established procedure for the synthesis of polyglycerol-based copolymers (Scheme 1).[10–12] A mixture of both monomers was added slowly to a cesium alkoxide initiator in *N*-methyl-2-pyrrolidone, at 100 °C. The copolymer composition was systematically varied from 10% to 40% MTEGE content. ^{1}H and quantitative Inverse Gated ^{13}C NMR spectroscopy prove controlled incorporation of the MTEGE comonomer (Figure S2, Figure S3). The slightly lower MTEGE contents determined from the ^{1}H NMR spectra can be attributed to an overlap of the polymer backbone signal between 3.05 and 4.05 ppm and the water signal at 3.33 ppm resulting from moisture in the NMR solvent. Average molecular weights can be calculated from the ^{1}H NMR spectra, as it is known for other polyglycerol copolymers prepared by slow monomer addition, using the methyl group of the initiator as a reference. Molecular weights in the range of 3890 to 5490 g mol^{-1} are found, matching the theoretical values well. Due to the low hydrodynamic volume of the compact,

hyperbranched polymer structure in solution, size-exclusion chromatography based on linear PEG standards yields lower apparent molecular weights ranging from 1060 to 2170 g mol^{-1}.[17, 5] Taking the hyperbranched structure into account, moderate, mostly monomodal molecular weight distributions with dispersity in the range of Đ = 1.48 to 1.85 were obtained (Figure S4 – Figure S7). Table 1 summarizes the characterization data for the *hb*(PG-*co*-PMTEGE) copolymers.

Table 1. Characterization data of the *hb*(PG-*co*-PMTEGE) copolymers.

#	Sample name[a)]	MTEGE % theo	MTEGE % [b)]	MTEGE % [c)]	DB% [c)]	M_n Theo / g mol^{-1}	M_n[b)] / g mol^{-1}	M_n[d)] / g mol^{-1}	Đ[d)]	T_g[e)] / °C	T_{cp}[f)] / °C
1	*hb*(PG_{44}-*co*-$PMTEGE_4$)	10	7	9	48	3370	3890	1060	1.85	-27	-
2	*hb*(PG_{36}-*co*-$PMTEGE_6$)	20	15	16	48	3690	3740	1750	1.51	-27	-
3	*hb*(PG_{46}-*co*-$PMTEGE_{13}$)	30	22	30	42	4950	5490	2170	1.48	-31	75
4	*hb*(PG_{32}-*co*-$PMTEGE_{18}$)	40	36	41	36	5320	5220	2160	1.58	-34	29

[a)] Terminology: Samples are named according to the number of comonomer units *hb*(PG_x-*co*-$PMTEGE_y$), where x is the absolute number of G units and y the absolute number of MTEGE units, calculated from ^{1}H NMR spectra, [b)] determined by ^{1}H NMR, [c)] determined by Inverse Gated ^{13}C NMR, [d)] determined by SEC, [e)] determined by DSC, [f)] cloud point temperatures, determined by turbidimetry.

The copolymerization kinetics of MTEGE and glycidol was investigated using *in situ* ^{1}H NMR spectroscopy. In order to ensure a safe reaction in the NMR tube, we altered the polymerization protocol described above and performed the copolymerization in deuterated DMSO-d_6 at 60 °C without slow monomer addition. *In situ* NMR spectroscopy allows monitoring the single monomer conversion in real time. Figure 1 and Figure S8 demonstrate that MTEGE is consumed somewhat slower than glycidol in a batch copolymerization. Since the monomer feed ratio shifts continuously and is observed during the entire course of the polymerization, a single experiment provides sufficient data to calculate reactivity ratios according to the Fineman-Ross formalism: $r_G = 3.7 \pm 0.3$ and $r_{MTEGE} = 0.27 \pm 0.02$.[18] This implies that batch copolymerization of glycidol and MTEGE leads to a gradient compositional profile with a PG-rich center and a PMTEGE-rich periphery. It should be noted, however, that both comonomers react sufficiently fast to avoid accumulation of the less reactive MTEGE in the reaction mixture when employing slow monomer

addition. Otherwise, the copolymers' composition would not equate the monomer feed ratio and residual monomer should have been found in the mixture after termination.[5]

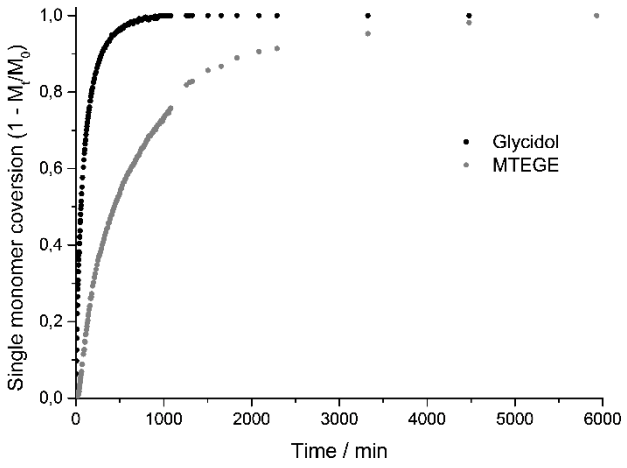

Figure 1. Single monomer conversion plot of glycidol and MTEGE in DMSO-d_6 at 60 °C versus time.

The degree of branching is a key parameter to describe the structure of a hyperbranched polymer. It can assume values between 0 (linear, no branching) and 1 (dendrimer-like, completely branched). For the *hb*(PG-*co*-PMTEGE) copolymers, inverse gated ^{13}C NMR spectroscopy reveals the characteristic signal pattern of a hyperbranched polyglycerol copolymer (Figure S3). The spectra enable to distinguish and quantify dendritic (D), linear (L) and terminal (T) repeating units. Due to the multiple chain ends of the branched structure, the spectra of the copolymers show considerably more terminal MTEGE units than the linear PMTEGE homopolymer (Figure S12). The degree of branching (DB) can be calculated according to Equation 1.[19]

$$DB = \frac{2D}{2D+L} \quad (1)$$

As expected, the DB decreases from 0.48 to 0.36 with increasing MTEGE content, because only glycidol can form dendritic repeating units, whereas MTEGE forms linear and terminal units exclusively.

The composition and the DB affect the thermal properties of the copolymers. DSC measurements reveal a decrease in the glass transition temperature from -27 °C to -34 °C with increasing MTEGE content. This finding can be ascribed to the reduced hydroxyl group density and therefore weaker hydrogen bonding as well as the flexible methyl-thioethyl chain.

Post-polymerization Modification

The two different kinds of functional groups of *hb*(PG-*co*-PMTEGE) offer the possibility for orthogonal modification. Treating the copolymers with acidified hydrogen peroxide solution for 30 min at room temperature selectively oxidizes the thioether moieties to the corresponding sulfoxides.[15] Complete disappearance of signals of the thioether-neighboring methylene and methyl groups in the ^{1}H NMR proves complete conversion (Figure S13). After oxidation, the methylene and methyl signals reappear at 2.78 - 3.10 ppm and 2.57 ppm. Converting thioethers into sulfoxides increases the local dipole moment of the group. On the macroscopic scale, one can observe the impact of the increasing polarity by temperature-dependent turbidimetry of aqueous copolymer solutions before and after oxidation. Figure 2 and Figure S14 show that before oxidation, *hb*(PG_{46}-*co*-$PMTEGE_{13}$) and *hb*(PG_{32}-*co*-$PMTEGE_{16}$) exhibit thermoresponsive solubility with demixing above a cloud point of 29 °C and 75 °C, respectively. By oxidizing the thioether moieties, however, both copolymers become completely water-soluble at all temperatures.

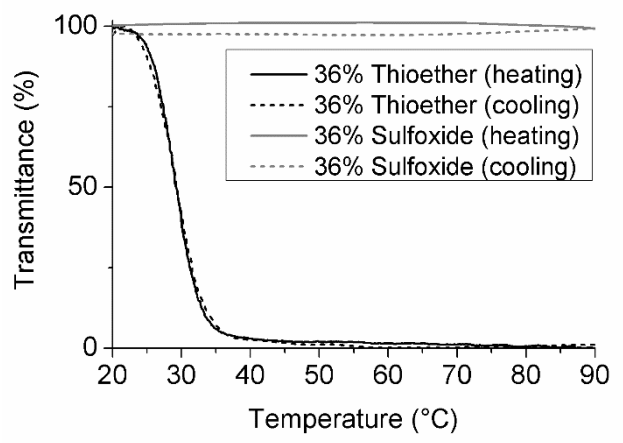

Figure 2. Intensity of transmitted laser light versus temperature for *hb*(PG_{32}-*co*-$PMTEGE_{18}$) in aqueous solution (c = 5 mg mL^{-1}) before and after oxidation of the thioether moieties.

Besides their oxidation-responsiveness, thioether groups can act as Lewis bases; e.g. they can open epoxide rings in a nucleophilic addition under acidic conditions, forming sulfonium cations.[16] Capitalizing on this feature, *hb*(PG-*co*-PMTEGE) was dissolved in glacial acetic acid to alkoxylate the thioether moieties within 24 h at room temperature using the commercially available epoxides propylene oxide, allyl glycidyl ether (AGE) and furfuryl glycidyl ether (FGE) (Figure 3). Allyl and furfuryl functionalized polymers are known for their use in thiol-ene click and Diels-Alder click chemistry.[20] By dialyzing the modified polymers against diluted hydrochloric acid, the acetate anions were exchanged with chloride anions. The thioether groups were converted into sulfonium cations with 96-99% conversion, as can be deduced from the signal shift

of the neighboring methyl group in the ^{1}H NMR spectra from 2.08 to 3.05 ppm. In addition, the characteristic signals of the attached methyl (1.22 ppm, Figure S15), allyl (5.17, 5.29 and 5.88 ppm, Figure S16) and furfuryl groups (4.46, 6.44, 7.64 ppm, Figure 3) appear after modification. Comparison of their intensity with the shifted thioether methyl signal confirms that under the acidic reaction conditions applied, the epoxides selectively react with the thioether moieties, but not with hydroxyl groups. Strikingly, this is exactly the opposite reactivity in contrast to the alkoxide-mediated ring-opening during the polymerization that leaves the thioether groups unchanged.

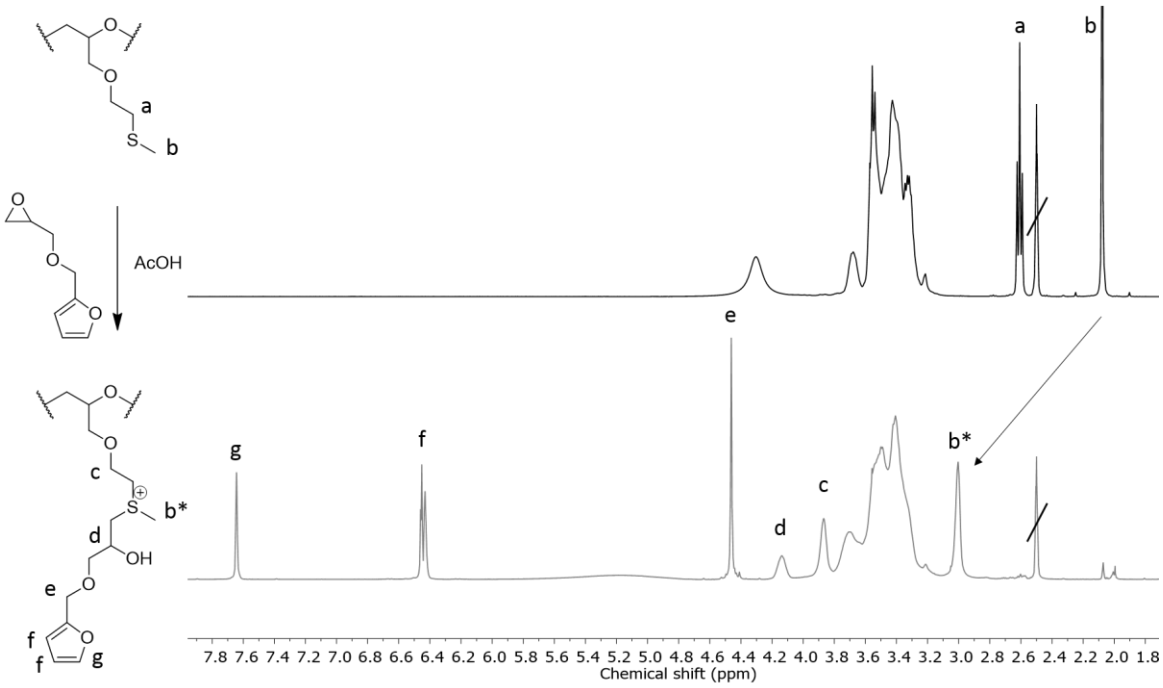

Figure 3. ^{1}H NMR spectra of *hb*(PG$_{46}$-*co*-PMTEGE$_{13}$) before (black, top) and after (grey, bottom) modification of the thioether groups with furfuryl glycidyl ether (400 MHz, DMSO-d_6).

As a proof of principle experiment to demonstrate that the hydroxyl groups can also be modified selectively, *hb*(PG$_{46}$-*co*-PMTEGE$_{13}$) was reacted with phenyl isocyanate as a model compound to obtain urethanes. Figure S17 shows the new aromatic and NH-signals of the phenyl urethane groups in the downfield area of the ^{1}H NMR spectrum between 6.74 and 8.15 ppm. Furthermore, the chemical shift of the thioether-related signals remains unchanged in the ^{1}H NMR and ^{13}C NMR (Figure S18) spectra, proving the selective modification of the hydroxyl groups. The urethane-functionalized polymer exhibits an increased glass transition temperature of 26 °C, due to reduced chain flexibility and increased hydrogen bonding. The material exhibits a strong UV signal in the

SEC due to the aromatic end groups, and the SEC trace is shifted towards higher molecular weights (Figure S19).

Conclusions

We have introduced hyperbranched, thioether-bearing polyether polyols as a versatile platform for modification, employing the easily accessible MTEGE as a new comonomer for anionic ring-opening multibranching polymerization of glycidol. A series of copolymers with systematically varied MTEGE incorporation between 7 and 36% was synthesized with good control over molecular weight, degree of branching and thermal properties. Real time NMR kinetic studies elucidated the reactivity ratios of the two comonomers, revealing a sufficiently small difference in reactivity that allows polymerization under slow monomer addition conditions.

Copolymerization of the hydrophilic glycidol with the hydrophobic MTEGE monomer permits tailoring the aqueous solubility, resulting in thermoresponsive behavior with cloud point temperatures in a wide temperature range between 29 and 75 °C. By oxidizing the thioether groups of the thermoresponsive copolymers with hydrogen peroxide, the solubility can be switched to fully water-soluble. This is an intriguing feature for potential application as an oxidation-responsive surface coating material. Functional sulfonium derivatives are conveniently accessible from the reaction of *hb*(PG-*co*-PMTEGE) with epoxides under acidic conditions. This was demonstrated using propylene oxide, allyl glycidyl ether and furfuryl glycidyl ether. Based on the great variety of available epoxides,[21] we envision *hb*(PG-*co*-PMTEGE) as a universal platform to create a library of heterofunctional hyperbranched polyelectrolytes and potentially as an unusual epoxy curing agent. Furthermore, the possibility to selectively modify the hydroxyl groups with isocyanates potentially renders these materials functional polyol building blocks for polyurethanes.

Acknowledgement

The authors thank Maria Golowin for technical assistance. J.H. is grateful to the Fonds der Chemischen Industrie for a scholarship. J.H. and D.L. acknowledge fellowships through the Excellence Initiative (DFG/GSC 266) in the context of MAINZ “Materials Science in Mainz”.

References

[1] a) D. Wilms, S. E. Stiriba, H. Frey, *Acc. Chem. Res.* **2010**, *43*, 129; b) M. Schömer, C. Schüll, H. Frey, *J. Polym. Sci. A Polym. Chem.* **2013**, *51*, 995; c) A. Thomas, S. S. Muller, H. Frey, *Biomacromolecules.* **2014**, *15*, 1935;

[2] R. K. Kainthan, J. Janzen, E. Levin, D. V. Devine, D. E. Brooks, *Biomacromolecules.* **2006**, *7*, 703.

[3] A. Sunder, R. Hanselmann, H. Frey, R. Mülhaupt, *Macromolecules.* **1999**, *32*, 4240.

[4] a) W. Radke, G. Litvinenko, A. H. E. Müller, *Macromolecules.* **1998**, *31*, 239; b) R. Hanselmann, D. Hölter, H. Frey, *Macromolecules.* **1998**, *31*, 3790; c) R. K. Kainthan, E. B. Muliawan, S. G. Hatzikiriakos, D. E. Brooks, *Macromolecules.* **2006**, *39*, 7708;

[5] J. Seiwert, D. Leibig, U. Kemmer-Jonas, M. Bauer, I. Perevyazko, J. Preis, H. Frey, *Macromolecules.* **2016**, *49*, 38.

[6] a) P. Bharathi, J. S. Moore, *Macromolecules.* **2000**, *33*, 3212; b) D. P. Bernal, L. Bedrossian, K. Collins, E. Fossum, *Macromolecules.* **2003**, *36*, 333; c) Y. Ohta, S. Fujii, A. Yokoyama, T. Furuyama, M. Uchiyama, T. Yokozawa, *Angew. Chem. Int. Ed.* **2009**, *48*, 5942; d) D. Konkolewicz, A. Gray-Weale, S. Perrier, *J. Am. Chem. Soc.* **2009**, *131*, 18075; e) J.-Y. Chen, M. Smet, J.-C. Zhang, W.-K. Shao, X. Li, K. Zhang, Y. Fu, Y.-H. Jiao, T. Sun, W. Dehaen, F.-C. Liu, E.-H. Han, *Polym. Chem.* **2014**, *5*, 2401; f) Y. Shi, R. W. Graff, X. Cao, X. Wang, H. Gao, *Angew. Chem. Int. Ed.* **2015**, *54*, 7631; g) A. B. Cook, R. Barbey, J. A. Burns, S. Perrier, *Macromolecules.* **2016**, *49*, 1296; h) X. Cao, Y. Shi, X. Wang, R. W. Graff, H. Gao, *Macromolecules.* **2016**, *49*, 760;

[7] a) M. Calderon, M. A. Quadir, S. K. Sharma, R. Haag, *Adv. Mater.* **2010**, *22*, 190; b) J. Khandare, M. Calderon, N. M. Dagia, R. Haag, *Chem. Soc. Rev.* **2012**, *41*, 2824; c) E. Moore, H. Thissen, N. H. Voelcker, *Prog. Surf. Sci.* **2013**, *88*, 213; d) H. Zhang, M. W. Grinstaff, *Macromol. Rapid Commun.* **2014**, *35*, 1906; e) E. Mohammadifar, A. Nemati Kharat, M. Adeli, *J. Mater. Chem. B.* **2015**, *3*, 3896;

[8] a) A. Zill, A. L. Rutz, R. E. Kohman, Am Alkilany, C. J. Murphy, H. Kong, S. C. Zimmerman, *Chem. Commun.* **2011**, *47*, 1279; b) A. M. Hofmann, F. Wurm, E. Huhn, T. Nawroth, P. Langguth, H. Frey, *Biomacromolecules.* **2010**, *11*, 568; c) C. Schüll, L. Nuhn, C. Mangold, E. Christ, R. Zentel, H. Frey, *Macromolecules.* **2012**, *45*, 5901; d) A. Thomas, H. Bauer, A.-M. Schilmann, K. Fischer, W. Tremel, H. Frey, *Macromolecules.* **2014**, *47*, 4557;

[9] a) S. Roller, H. Zhou, R. Haag, *Mol. Divers.* **2005**, *9*, 305; b) Tziveleka L. A., C. Kontoyianni, Z. Sideratou, D. Tsiourvas, C. M. Paleos, *Macromol. Biosci.* **2006**, *6*, 161; c) I. Papp, J. Dernedde,

S. Enders, R. Haag, *Chem. Commun.* **2008**, 5851; d) D. Gröger, M. Kerschnitzki, M. Weinhart, S. Reimann, T. Schneider, B. Kohl, W. Wagermaier, G. Schulze-Tanzil, P. Fratzl, R. Haag, *Adv. Healthcare Mater.* **2014**, *3*, 375; e) Q. Wei, S. Krysiak, K. Achazi, T. Becherer, P. L. Noeske, F. Paulus, H. Liebe, I. Grunwald, J. Dernedde, A. Hartwig, T. Hugel, R. Haag, *Colloids Surf. B Biointerfaces.* **2014**, *122*, 684; f) Y. Yu, H. Frey, *Langmuir.* **2015**, *31*, 13101; g) D. Pranantyo, L. Q. Xu, K. G. Neoh, E.-T. Kang, S. L.-M. Teo, *Ind. Eng. Chem. Res.* **2016**, *55*, 1890;

[10] A. Sunder, H. Türk, R. Haag, H. Frey, *Macromolecules.* **2000**, *33*, 7682.

[11] C. Schüll, T. Gieshoff, H. Frey, *Polym. Chem.* **2013**, *4*, 4730.

[12] A. Alkan, R. Klein, S. I. Shylin, U. Kemmer-Jonas, H. Frey, F. R. Wurm, *Polym. Chem.* **2015**, *6*, 7112.

[13] a) R. Klein, F. Übel, H. Frey, *Macromol. Rapid Commun.* **2015**, *36*, 1822; b) K. Niederer, C. Schüll, D. Leibig, T. Johann, H. Frey, *Macromolecules.* **2016**, *49*, 1655; c) C. Tonhauser, C. Schüll, C. Dingels, H. Frey, *ACS Macro Lett.* **2012**, *1*, 1094; d) R. A. Shenoi, J. K. Narayanannair, J. L. Hamilton, B. F. Lai, S. Horte, R. K. Kainthan, J. P. Varghese, K. G. Rajeev, M. Manoharan, J. N. Kizhakkedathu, *J. Am. Chem. Soc.* **2012**, *134*, 14945; e) R. A. Shenoi, I. Chafeeva, B. F. L. Lai, S. Horte, J. N. Kizhakkedathu, *J. Polym. Sci. A Polym. Chem.* **2015**, *53*, 2104; f) S. Son, E. Shin, B.-S. Kim, *Macromolecules.* **2015**, *48*, 600;

[14] a) H. G. Batz, V. Hofmann, H. Ringsdorf, *Makromol. Chem.* **1973**, *169*, 323; b) V. Hofmann, H. Ringsdorf, G. Muacevic, *Makromol. Chem.* **1975**, *176*, 1929; c) A. Napoli, M. Valentini, N. Tirelli, M. Muller, J. A. Hubbell, *Nat. Mater.* **2004**, *3*, 183; d) B. L. Allen, J. D. Johnson, J. P. Walker, *ACS Nano.* **2011**, *5*, 5263; e) P. Carampin, E. Lallana, J. Laliturai, S. C. Carroccio, C. Puglisi, N. Tirelli, *Macromol. Chem. Phys.* **2012**, *213*, 2052; f) J. R. Kramer, T. J. Deming, *Biomacromolecules.* **2012**, *13*, 1719; g) J. R. Kramer, T. J. Deming, *Chem. Commun.* **2013**, *49*, 5144; h) S. T. Hemp, M. H. Allen, A. E. Smith, T. E. Long, *ACS Macro Lett.* **2013**, *2*, 731; i) J. R. Kramer, T. J. Deming, *J. Am. Chem. Soc.* **2014**, *136*, 5547; j) M. C. Mackenzie, A. R. Shrivats, D. Konkolewicz, S. E. Averick, M. C. McDermott, J. O. Hollinger, K. Matyjaszewski, *Biomacromolecules.* **2015**, *16*, 236;

[15] A. R. Rodriguez, Kramer, JR, T. J. Deming, *Biomacromolecules.* **2013**, *14*, 3610.

[16] E. G. Gharakhanian, T. J. Deming, *Biomacromolecules.* **2015**, *16*, 1802.

[17] I. Perevyazko, J. Seiwert, M. Schömer, H. Frey, U. S. Schubert, G. M. Pavlov, *Macromolecules.* **2015**, *48*, 5887.

[18] M. Fineman, S. D. Ross, *J. Polym. Sci.* **1950**, *5*, 259.

[19] H. Frey, D. Hölter, *Acta Polym.* **1999**, *50*, 67.

[20] a) C. E. Hoyle, A. B. Lowe, C. N. Bowman, *Chem. Soc. Rev.* **2010**, *39*, 1355; b) K. Kempe, A. Krieg, C. R. Becer, U. S. Schubert, *Chem. Soc. Rev.* **2012**, *41*, 176; c) A. Gandini, *Prog. Polym. Sci.* **2013**, *38*, 1;

[21] J. Herzberger, K. Niederer, H. Pohlit, J. Seiwert, M. Worm, F. R. Wurm, H. Frey, *Chem. Rev.* **2016**, *116*, 2170.

Supporting Information

Materials

Solvents and reagents were obtained from *Sigma Aldrich* and *Acros Organics*, respectively. DMSO-d_6 and $CDCl_3$ were received from *Deutero GmbH*. MTEGE, Glycidol (96%) and *N*-methyl-2-pyrrolidone (99.5%) were dried over calcium hydride (CaH_2) and distilled in vacuum directly prior to use. Phenyl isocyanate was freshly distilled prior to use. Epichlorohydrin (99%), 2-(methylthio)ethanol (99%) and all other reagents and solvents were used as received.

Instrumentation

NMR spectra were recorded on a *Bruker* Advance III HD 400 (5 mm BBFO-SmartProbe with z-gradient and ATM) at 400 MHz (^{1}H) and 100 MHz (^{13}C). The residual signals of the deuterated solvent were utilized as an internal reference.

Analytical SEC measurements in DMF (containing 0.25 g L^{-1} of lithium bromide) were performed on an *Agilent* 1100 series instrument, including a *PSS* HEMA column ($10^6/10^4/10^2$ Å porosity) and UV and RI detector. Poly(ethylene glycol) standards (*Polymer Standards Service GmbH*) were employed for calibration.

Purification by SEC was performed in $CHCl_3$, at 25 °C and a flow rate of 3.5 mL min^{-1} using a LC-91XX Next Series Recycling Preparative HPLC Anlage by *Japan Analytical Industry Co. Ltd.*. A Jaigel-2H column (upper exclusion limit $5 \cdot 10^3$ g mol^{-1}) and a UV and RI detector were used.

Differential scanning calorimetry (DSC) was measured using a *PerkinElmer* 8500 thermal analysis system and a *PerkinElmer* CLN2 thermal analysis controller in the temperature range from -90 to +20 °C at a heating rate of 10 K min^{-1}.

Cloud points were observed by optical transmittance of a light beam (λ = 670 nm) through a 1 cm sample quartz cell containing the polymer solution in deionized water (5 mg mL^{-1}), in dependence of the solution temperature. A *Jasco* V-630 photospectrometer with a *Jasco* ETC-717 Peltier element was used. The heating and cooling rate was 1 K min^{-1}, and values were recorded in 1 K steps.

In situ ^{1}H NMR Kinetics

Copolymerization in the NMR tube was performed in DMSO-d_6 following a procedure described in previous work. 4.0 mg (0.03 mmol, 1.0 eq.) 1,1,1-Tris(hydroxymethyl)propane (TMP) and 1.7 mg (0.01 mmol 0.3 eq.) cesium hydroxide monohydrate were dissolved in methanol. Benzene was added and volatiles were removed in high vacuum overnight. The following operations were performed under Argon atmosphere. The dried initiator salt was dissolved in 0.5 mL DMSO-d_6. The solution was transferred to an NMR tube equipped with a Teflon stopcock. 60 µL (0.9 mmol, 30 eq.) glycidol and 0.6 mmol (20 eq.) MTEGE were added and the solution was degassed subsequently. The tube was sealed under vacuum and then placed in the NMR spectrometer at 60 °C. Spectra were recorded with 16 scans at 2-minute intervals during the first hour, at 5-minute intervals during the following 2 hours, at 10-minute intervals within the next 15 hours and extended afterwards.

Oxidation of the Thioether Groups

Oxidation of the thioether groups was performed following a modified procedure by Deming et al..[15] 100 mg *hb*(PG_{32}-*co*-$PMTEGE_{18}$) was dissolved in aqueous hydrogen peroxide solution (35%) and acidified with AcOH (1%). The mixture was stirred at room temperature for 30 min, quenched with 1 M aqueous sodium thiosulfate solution and dialyzed against deionized water (MWCO: 100 – 500 Da). Subsequently, the oxidized polymer was isolated by lyophilization in 80% yield.

Alkoxylation of the Thioether Groups

Alkoxylation of the thioether groups was performed following a modified procedure by Gharakhanian and Deming.[16] 100 mg *hb*(PG-*co*-PMTEGE) was dissolved in 6 mL glacial acetic acid. 3 Eq. (compared to the amount of thioether groups) propylene oxide, allyl glycidyl ether or furfuryl glycidyl ether were added and the mixture was stirred at room temperature for 24 h. Afterwards, the solvent and unreacted epoxide were removed in vacuum. The residue was dialyzed against 3 mM HCl_{aq} (MWCO: 100 – 500 Da) and freeze-dried subsequently. Hence, the alkoxylated polymer was obtained in 90-95% yield.

Urethane Formation

100 mg polymer was dried overnight in vacuum and dissolved in dry pyridine. Phenyl isocyanate (1.1 eq., compared to the amount of hydroxyl groups) was added and the mixture was stirred at room temperature for 4 hours. Then, pyridine and residual phenyl isocyanate were removed in vacuum. The residue was purified by preparative SEC and dried in vacuum subsequently, to yield the urethane-functionalized polymer.

Additional Characterization Data

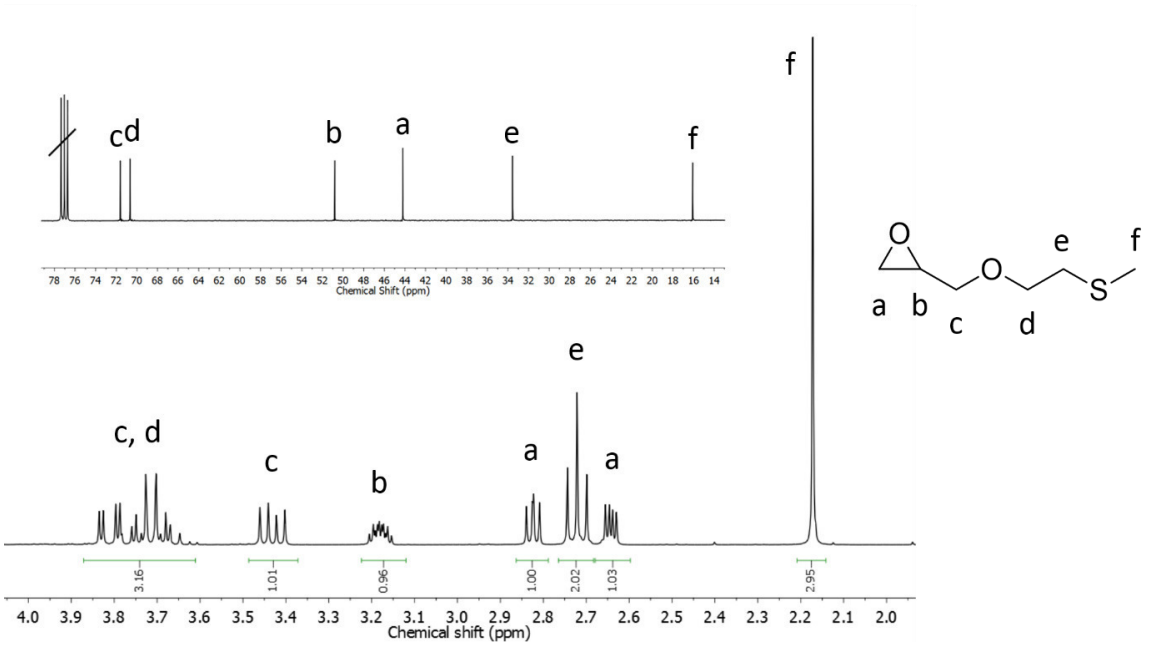

Figure S1. ^{1}H (bottom) and ^{13}C NMR (top) spectra of 2-(methylthio)ethyl glycidyl ether (MTEGE) (400/100 MHz, $CDCl_3$).

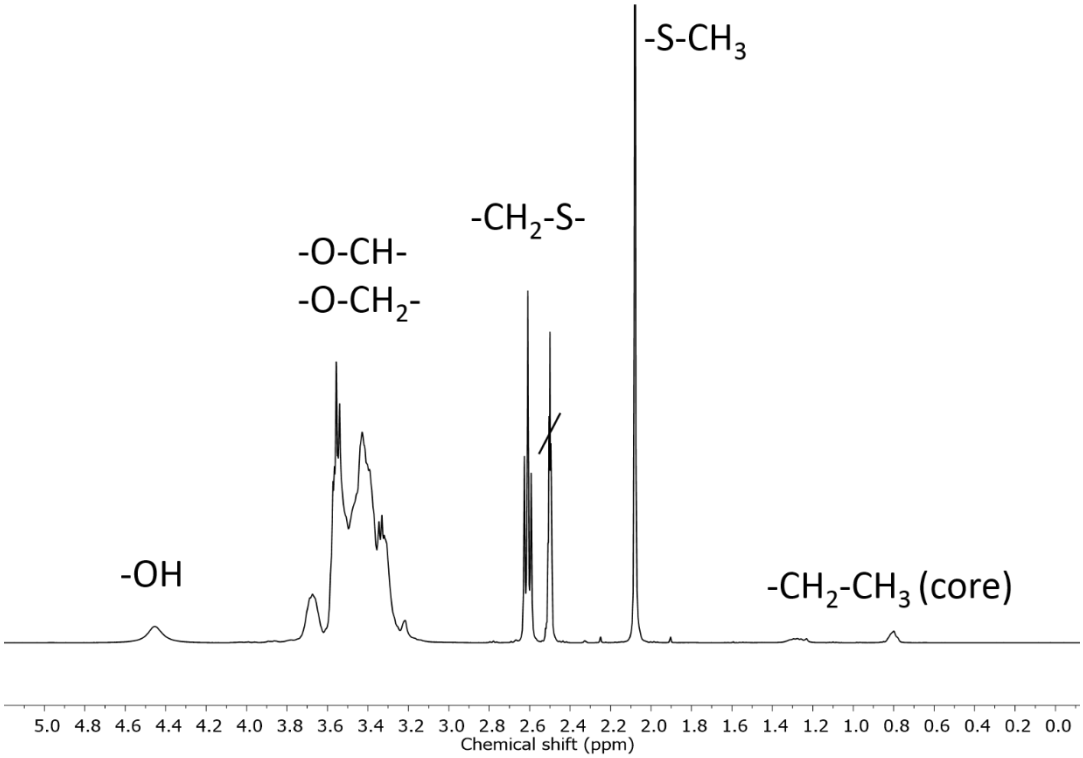

Figure S2. ^{1}H NMR spectrum of *hb*(PG$_{32}$-*co*-PMTEGE$_{18}$) (400 MHz, DMSO-*d*$_6$).

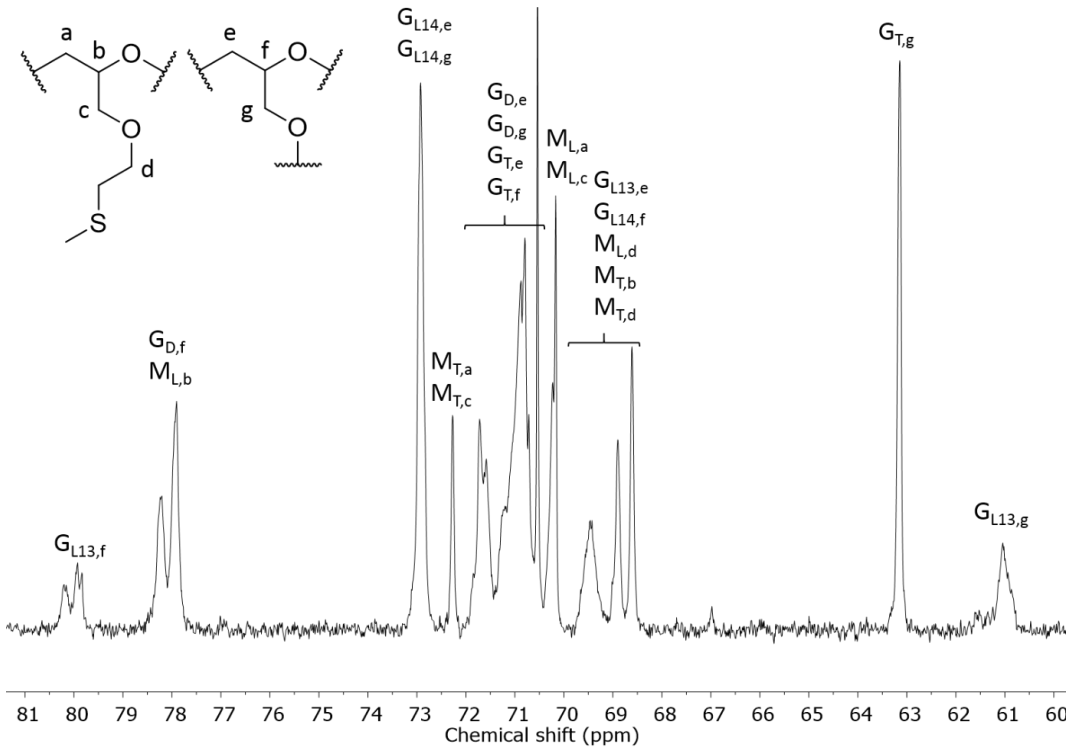

Figure S3. Signal assignment of dendritic (D), linear (L) and terminal (T) MTEGE (M) und glycerol (G) units of *hb*(PG-*co*-PMTEGE) in the ether region of the IG ^{13}C NMR spectrum (100 MHz, DMSO-*d*$_6$).

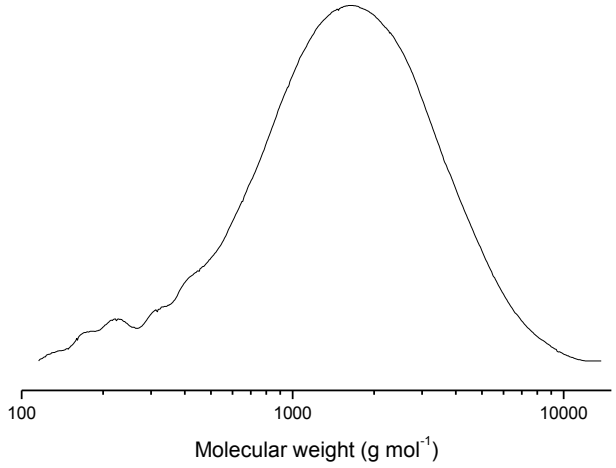

Figure S4. SEC trace (DMF, RI signal, PEG standard) of *hb*(PG_{44}-*co*-$PMTEGE_4$).

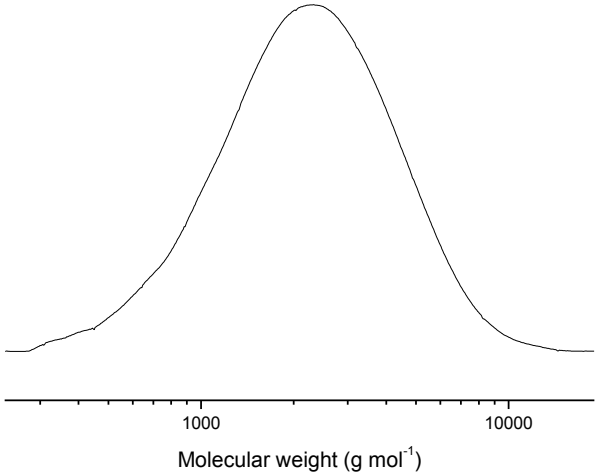

Figure S5. SEC trace (DMF, RI signal, PEG standard) of *hb*(PG_{36}-*co*-$PMTEGE_6$).

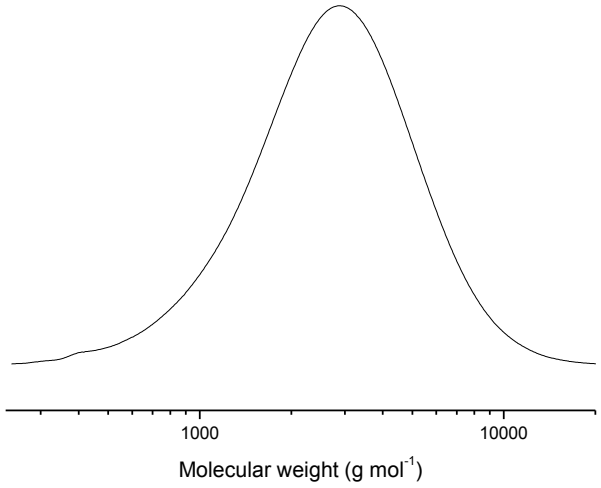

Figure S6. SEC trace (DMF, RI signal, PEG standard) of *hb*(PG_{46}-*co*-$PMTEGE_{13}$).

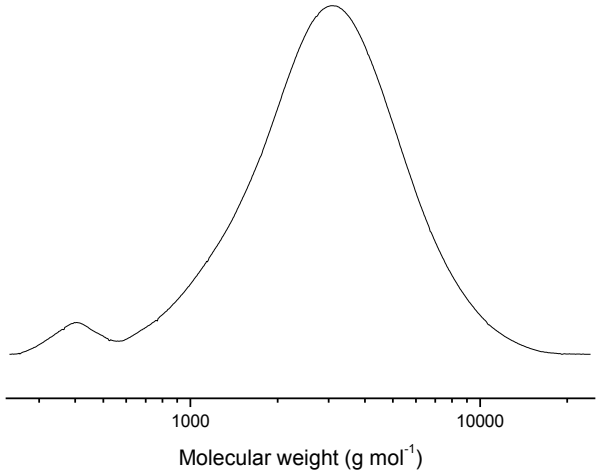

Figure S7. SEC trace (DMF, RI signal, PEG standard) of *hb*(PG_{32}-*co*-$PMTEGE_{18}$).

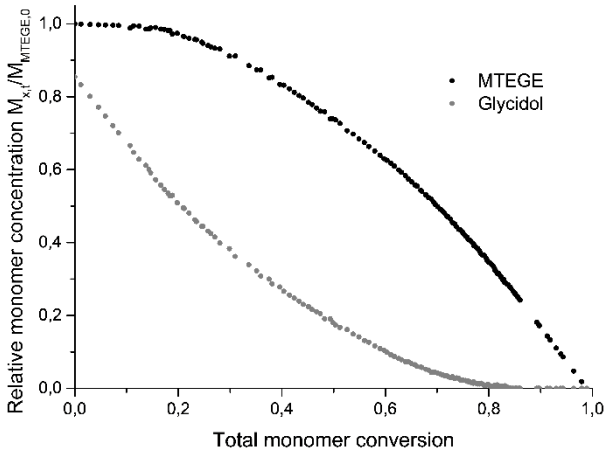

Figure S8. Relative single monomer conversion $M_x/M_{MTEGE,0}$ versus total monomer conversion.

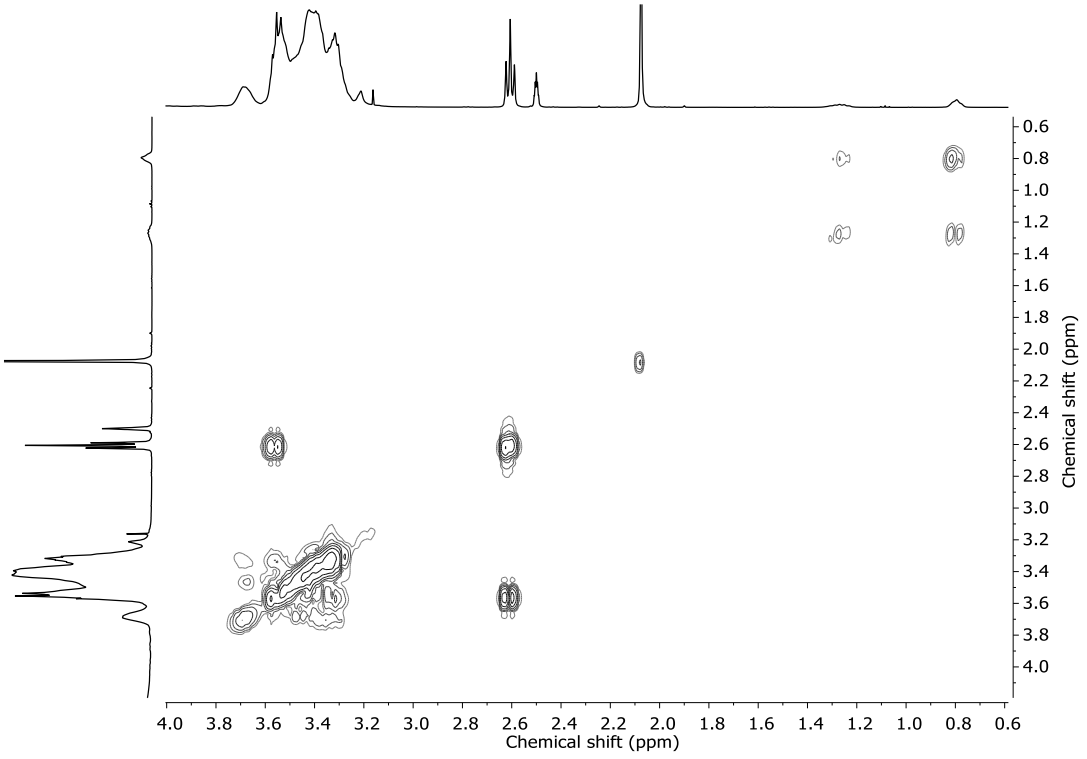

Figure S9. COSY NMR spectrum of *hb*(PG-*co*-PMTEGE) (400 MHz, DMSO-d_6).

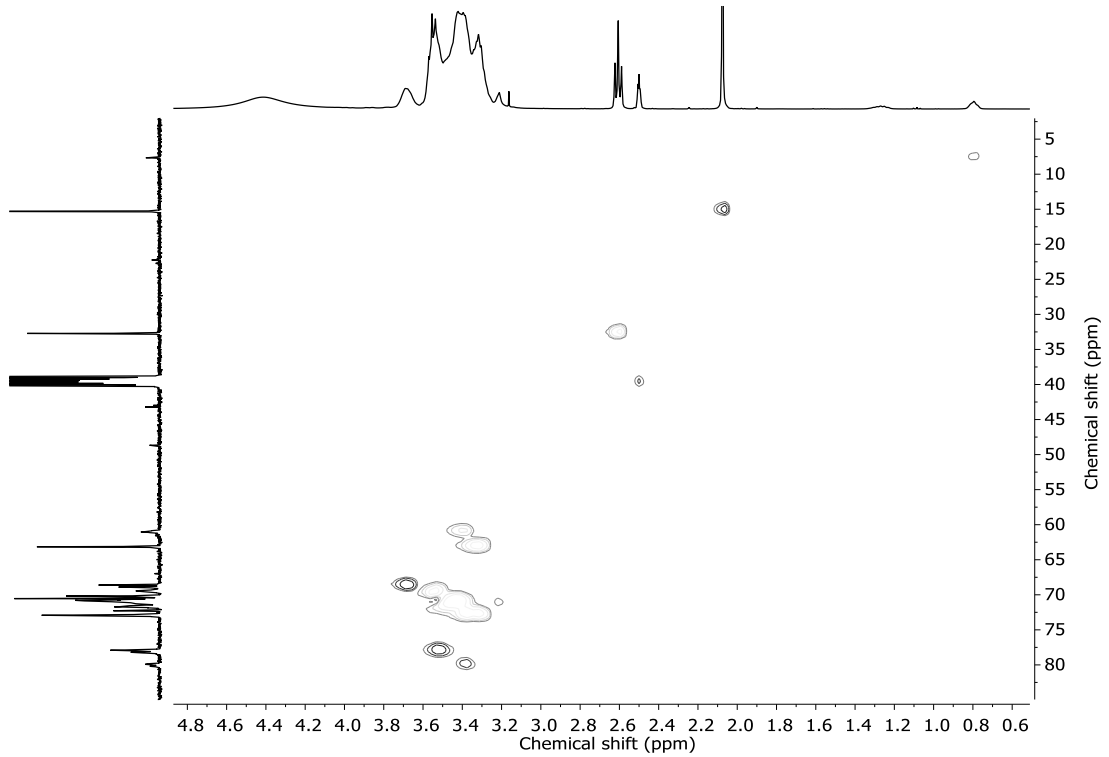

Figure S10. HSQC NMR spectrum of *hb*(PG-*co*-PMTEGE) (400/100 MHz, DMSO-d_6). Horizontal axis: ^{1}H NMR spectrum; vertical axis: ^{13}C NMR spectrum. Phase correlation is given by correlation of cross peaks (dark grey: methyl, methine, light grey: methylene).

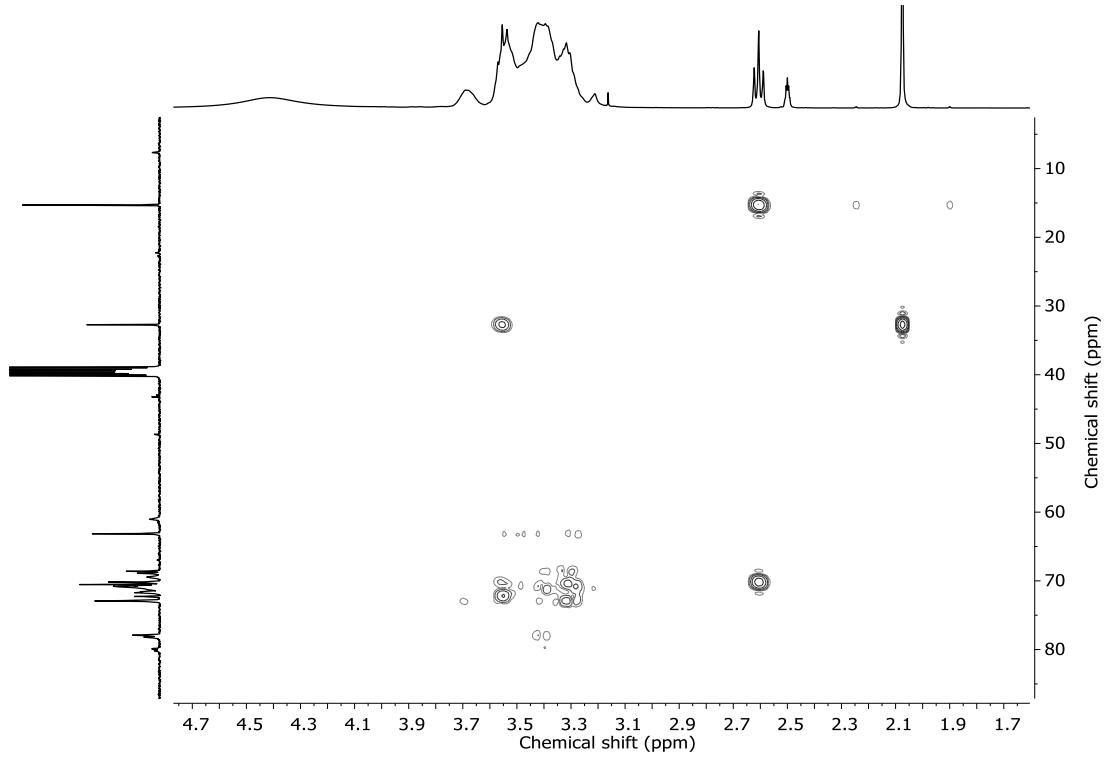

Figure S11. HMBC NMR spectrum of *hb*(PG-*co*-PMTEGE) (400/100 MHz, DMSO-d_6). Horizontal axis: ^{1}H NMR spectrum; vertical axis: ^{13}C NMR spectrum.

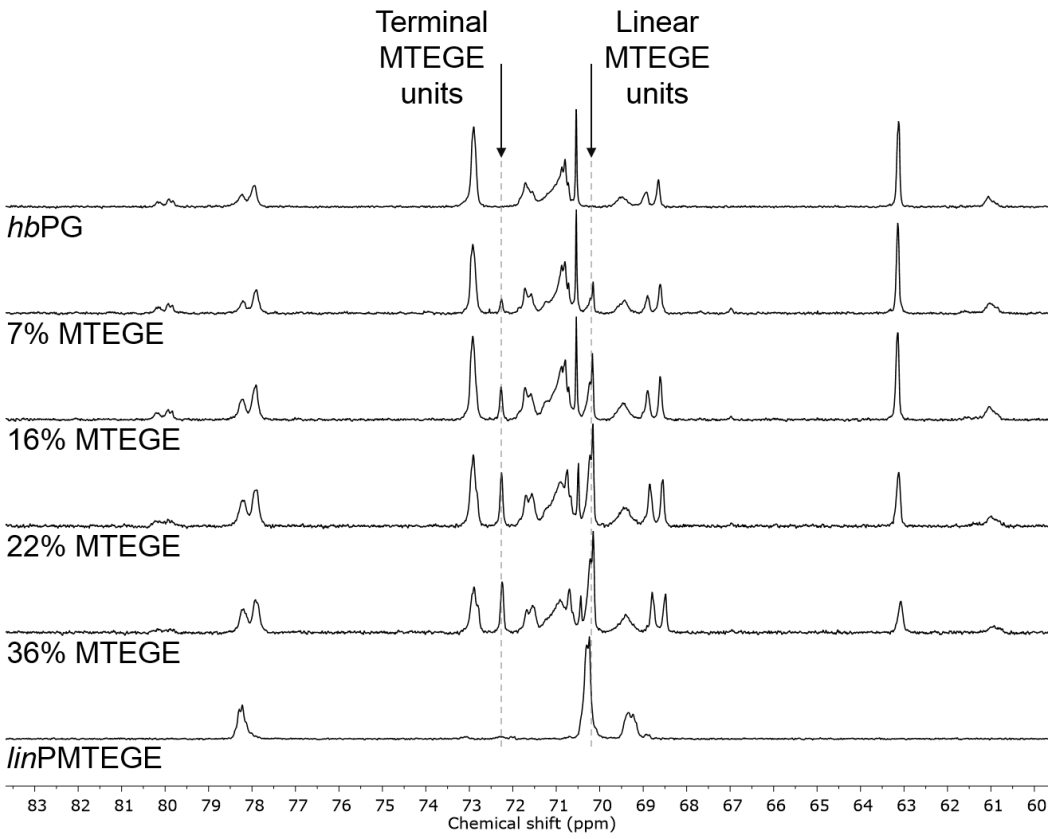

Figure S12. Inverse Gated ^{13}C NMR spectra of *hb*(PG-*co*-PMTEGE) copolymers with varying composition. Spectra of the two homopolymers for comparison (100 MHz, DMSO-d_6).

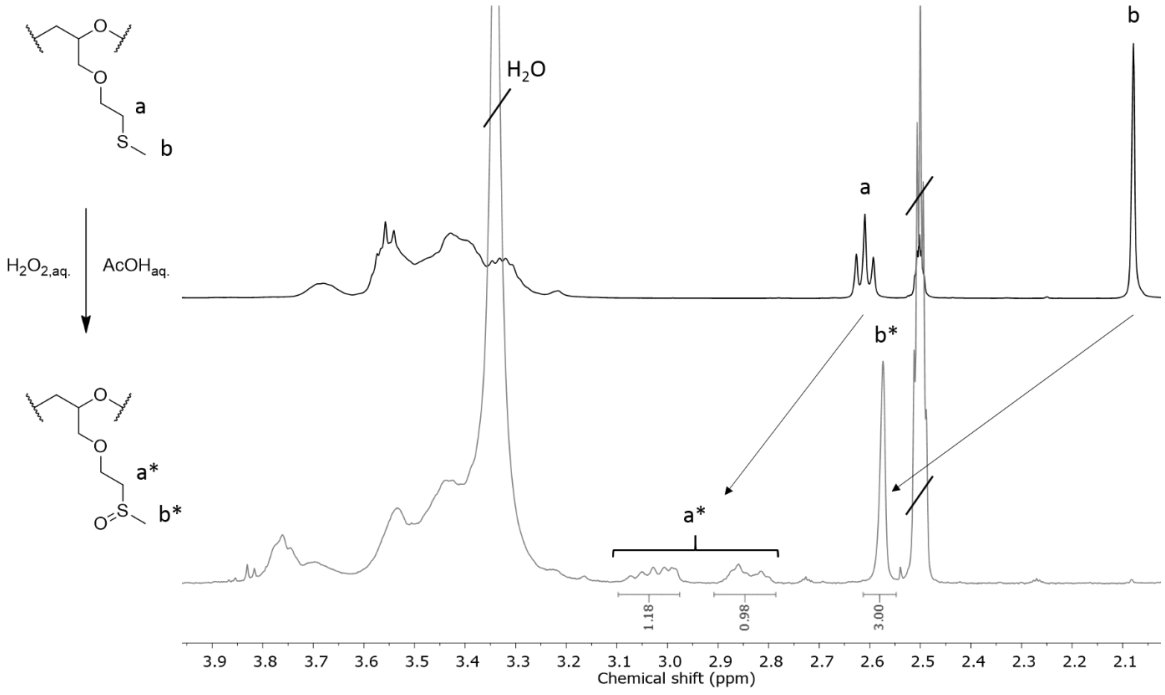

Figure S13. ^{1}H NMR spectra of *hb*(PG_{32}-*co*-$PMTEGE_{18}$) before (black, top) and after (grey, bottom) oxidation of the thioether groups (400 MHz, DMSO-d_6).

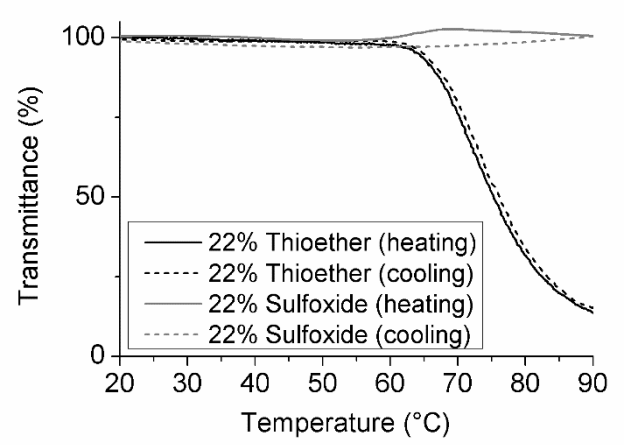

Figure S14. Intensity of transmitted laser light versus temperature for *hb*(PG_{46}-*co*-$PMTEGE_{13}$) in aqueous solution (c = 5 mg mL^{-1}) before and after oxidation of the thioether moieties.

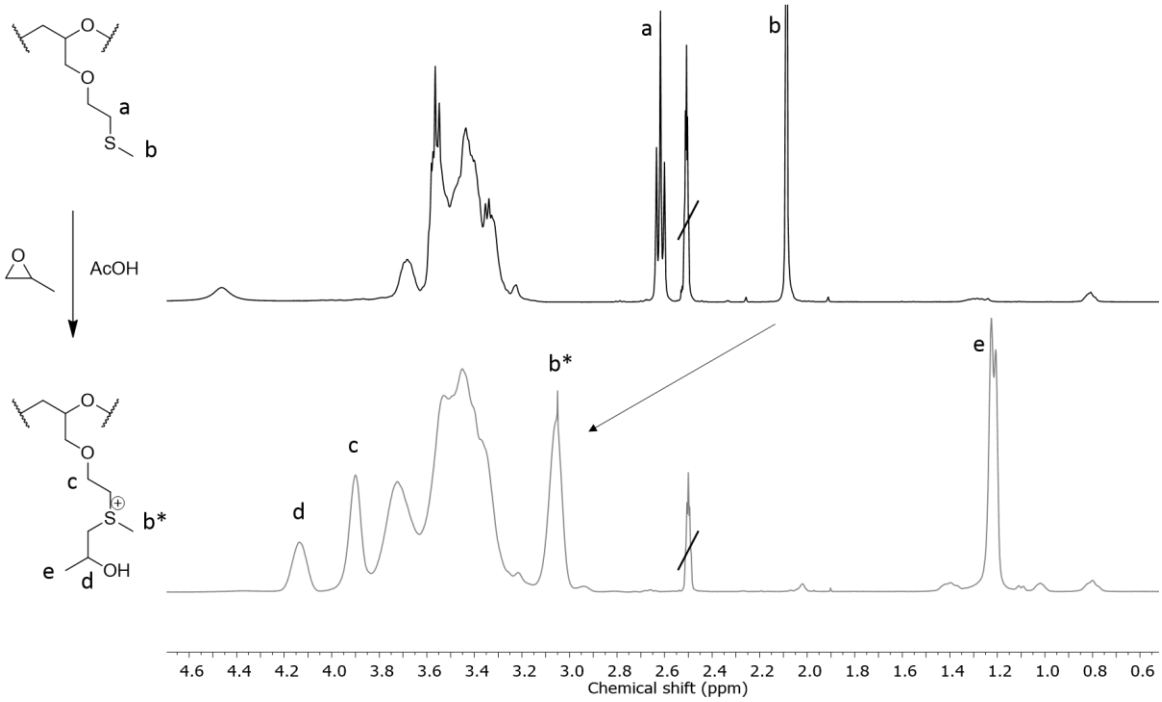

Figure S15. ^{1}H NMR spectra of *hb*(PG_{32}-*co*-$PMTEGE_{18}$) before (black, top) and after (grey, bottom) modification of the thioether groups with propylene oxide (400 MHz, DMSO-d_6).

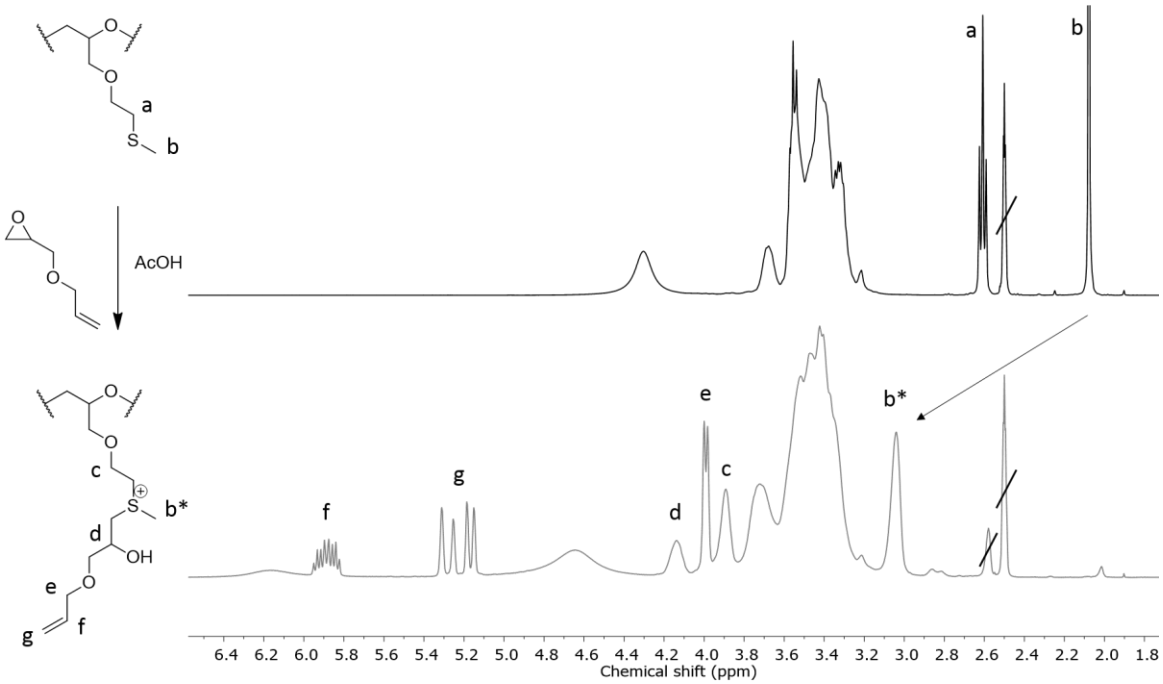

Figure S16. ^{1}H spectra of *hb*(PG$_{32}$-*co*-PMTEGE$_{18}$) before (black, top) and after (grey, bottom) modification of the thioether groups with allyl glycidyl ether (400 MHz, DMSO-d_6).

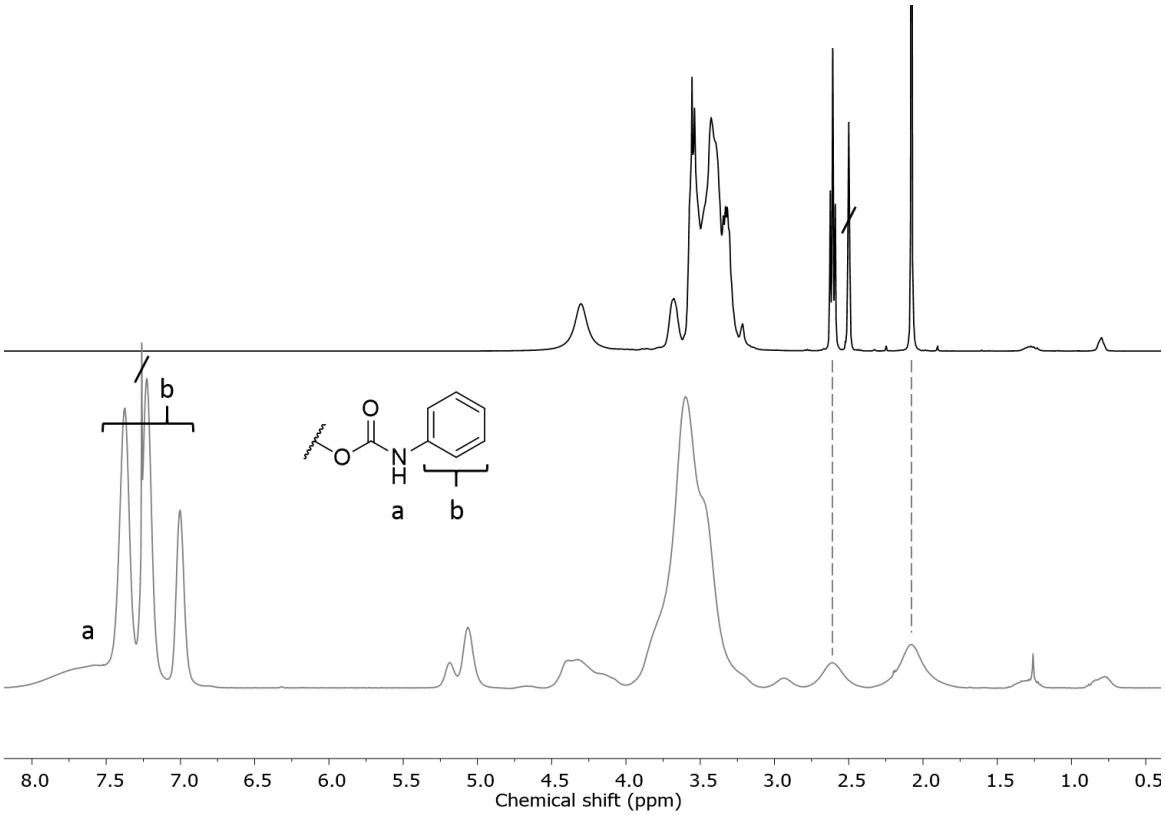

Figure S17. ^{1}H NMR spectra of *hb*(PG$_{46}$-*co*-PMTEGE$_{13}$) before (black, top) and after (grey, bottom) transforming the hydroxyl groups into urethane groups (400 MHz, top: DMSO-d_6, bottom: $CDCl_3$).

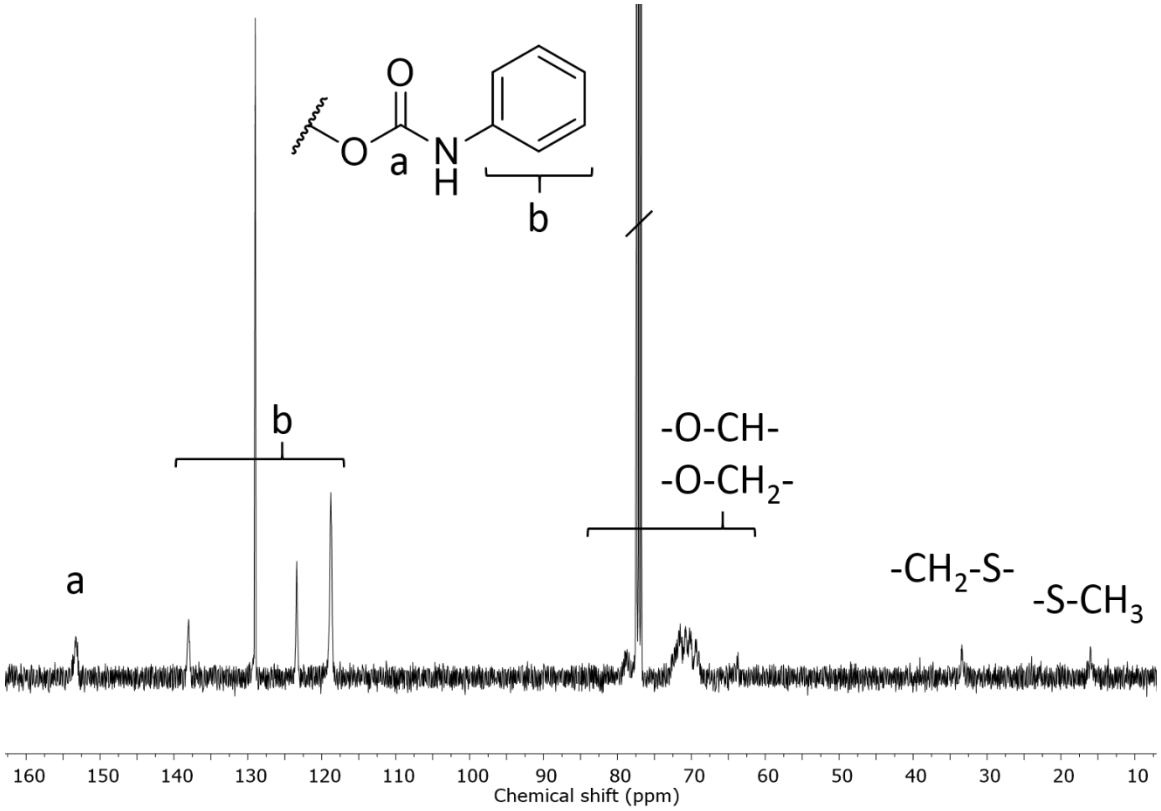

Figure S18. ^{13}C NMR spectrum of *hb*(PG$_{46}$-*co*-PMTEGE$_{13}$) after transforming the hydroxyl groups into urethane groups (100 MHz, DMSO-d_6).

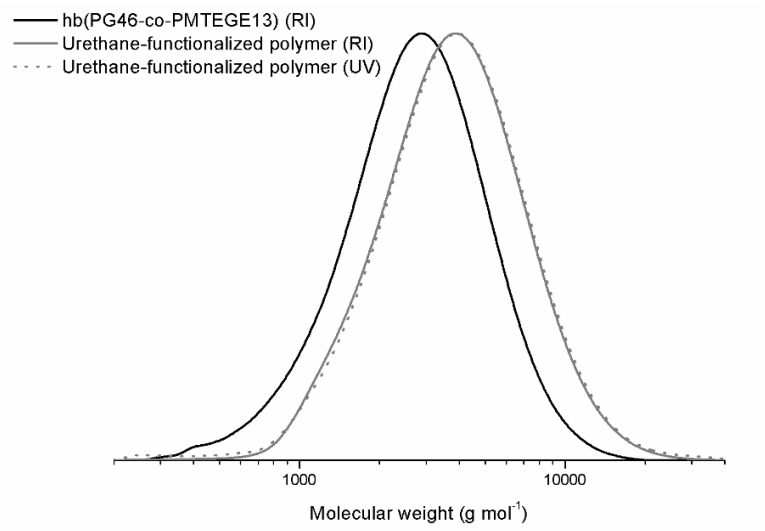

Figure S19. SEC traces (DMF, PEG standard) of *hb*(PG$_{46}$-*co*-PMTEGE$_{13}$) before and after modification with phenyl isocyanate.

A

APPENDIX

A.1 Hyperbranched Poly(propylene oxide): A Multifunctional Backbone-Thermoresponsive Polyether Polyol Copolymer

*Martina Schömer[1], Jan Seiwert[1], and Holger Frey[1,]**

[1] Institute of Organic Chemistry, Johannes Gutenberg-University, Duesbergweg 10-14, 55128 Mainz, Germany

Published in *ACS Macro Letters* **2012**, *1*, 888−891.

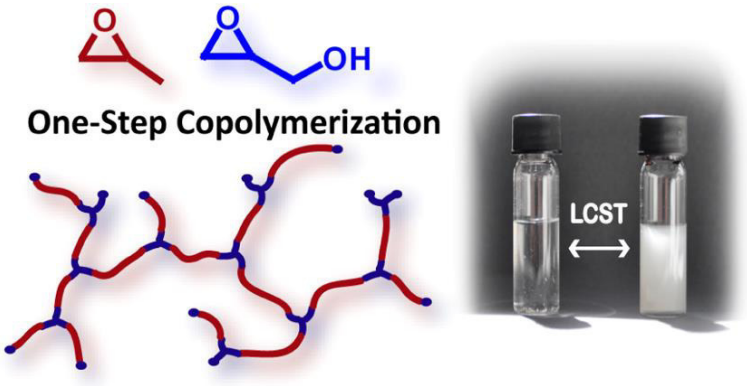

Abstract

Backbone-thermoresponsive hyperbranched poly(propylene oxide)-based polyether polyols have been synthesized by anionic ring-opening copolymerization of glycidol and propylene oxide. The number of functional hydroxyl end groups and the lower critical solution temperature (LCST) can be readily adjusted by varying the comonomer ratio. Molecular weights in the range of 1200−2000 g/mol were achieved. Hyperbranched polyether polyols with LCST values between 24 and 83 °C can be obtained in a convenient one-step reaction.

Introduction

Hyperbranched polymers have attracted broad attention, due to their unique molecular structures and distinct chemical and physical properties, as well as their numerous potential applications.[1–9] Among them, thermoresponsive polymers, which combine the advantages of a multifunctional structure with “smart” behavior are of particular interest. To date, two different strategies have been employed to prepare thermoresponsive hyperbranched polymers. One is the modification with temperature-responsive functional groups or oligomer segments.[10–14] The other option is the combination of hydrophobic and hydrophilic functionalities into a highly branched polymer backbone. This type of backbone-thermoresponsive hyperbranched polymer has been hardly investigated. Recently, some examples, prepared through proton transfer polymerization of diglycidyl ethers[15-17] or cationic polymerization,[18] were reported. Furthermore, poly(ether-ester)s[19] and poly(ether-amine)s[17,20,21] are known.

Here we report the synthesis of a backbone-thermoresponsive hyperbranched polyether by anionic polymerization. Combining the two commercially available monomers propylene oxide and glycidol allows for the generation of copolymers with adjustable functionality and lower critical solution temperature (LCST) in one single step. Both monomers have been combined before to generate linear structures and block architectures,[22–27] but a random copolymerization, as it has recently been reported for the monomer combination ethylene oxide/glycidol[28] has not been successful to date.

Results and Discussion

We present a straightforward random copolymerization protocol for the preparation of multifunctional and thermoresponsive poly(propylene oxide) (PPO) copolymers in one single step. The degree of functionality and the LCST can be controlled by the comonomer ratio. The synthetic route to the multifunctional hyperbranched PPOs is given in Scheme 1. The polymerization of propylene oxide (PO) and glycidol was carried out in bulk at 120 °C. These conditions result in an anionic ring-opening multibranching copolymerization.

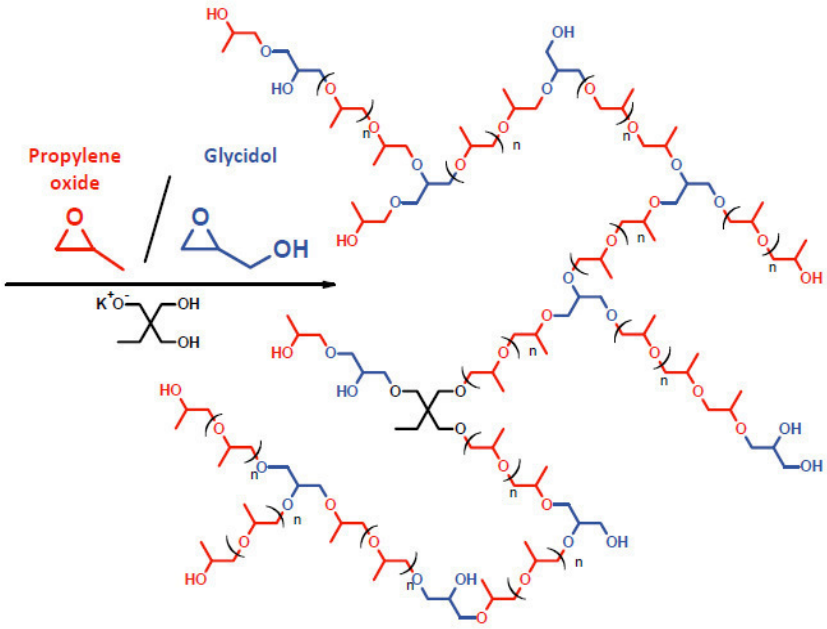

Scheme 1. Synthesis scheme for the anionic ring-opening multibranching copolymerization of propylene oxide and glycidol.

An alkoxide initiator first reacts with one of the monomers and opens the epoxide ring. Rapid proton transfer from the secondary alkoxide to a primary alkoxide (either intra- or intermolecular) leads to branching during the reaction, generating hyperbranched poly(propylene oxide) copolymers with glycerol branching units. Protic termination is necessary to release the hydroxyl groups. The copolymerization can be carried out without any solvent and hyperbranched PPO copolymers in 80–90% yield are obtained.

Surprisingly, chain transfer to the monomer propylene oxide (which is a well-known side reaction for poly(propylene oxide)synthesis) is not observed. Therefore, potassium can be used as a counterion, and the use of the larger but more expensive cesium (that would lower the rearrangement tendency) can be avoided.

The end group functionality of the resulting copolymer depends on the number of incorporated glycerol branching units (because each glycerol unit adds exactly one additional hydroxyl group) and can thus be directly adjusted by the comonomer ratio. Incorporated glycidol monomer may result in branching points (if both functional groups propagate) as well as linear or terminal units.

The hyperbranched structure of the obtained copolymers was confirmed by detailed NMR analysis. The assignment given in Figure 1 is based on literature data as well as twodimensional NMR spectroscopy that permits to correlate ^{13}C and ^{1}H NMR shifts (cf. Supporting Information, Figure S2). The occurrence of the methine carbon signal for the dendritic glycerol unit (78.0 ppm) is an unambiguous proof for the branched polymer structure together with the characteristic peak pattern of the PO methyl group (cf. Figure 1b).

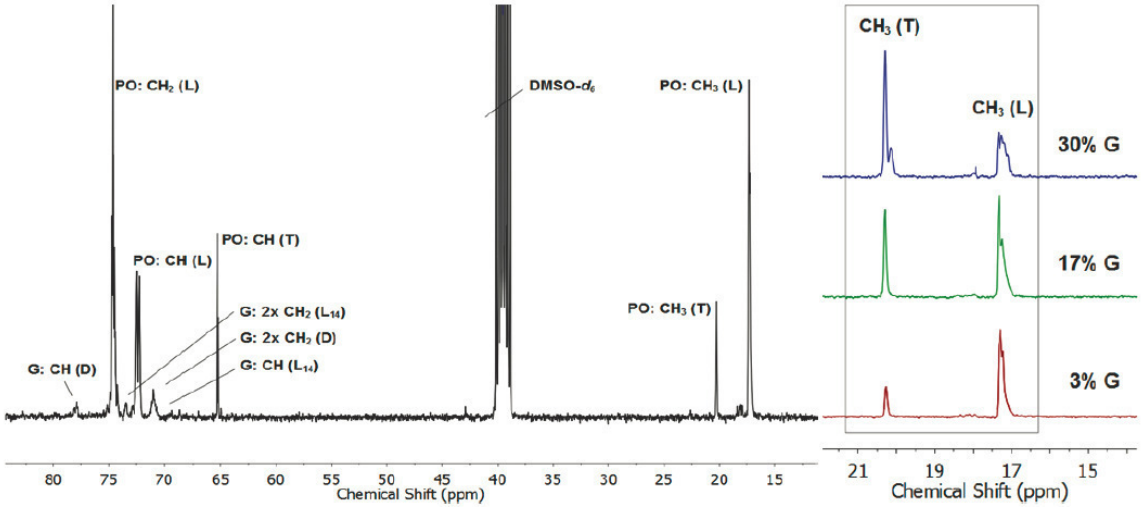

Figure 1. a) ^{13}C NMR spectrum (inverse gated) of *hb*PPO-*co*-PG sample (3% glycidol) with signal assignment; b) Comparison of the methyl region of ^{13}C IG NMR spectra (400 MHz) obtained from *hb*PPO-*co*-PG with different glycidol fractions.

The glycidol content was varied from 3 to 56%. With increasing glycidol fraction the degree of branching (DB) value increases, starting with only slightly branched polymers with 3% glycerol units up to hyperbranched polymers with higher glycerol contents. The DB was calculated using the equation introduced by Hölter and Frey for random copolymerization of AB/AB_2 systems:[29]

$$DB_{\mathrm{AB/AB_2}} = \frac{2D}{2D + L_{co}}$$

Details for the DB determination can be found in the Supporting Information. The calculated DB values are summarized in Table 1.

Introducing more glycerol units goes along with a rising number of end groups as each glycerol units adds exactly one additional hydroxyl end group. The methyl group of the propylene oxide unit shifts from 17.3 to 20.3 ppm when it is incorporated as a terminal unit, compared to the linear incorporation. In Figure 1b, a considerable shift of the intensities of the two resonances can be seen, which reflects the increase in terminal propylene oxide units, depending on the degree of branching.

Table 1. Characterization data for *hb*PPO_m-*co*-PG_n copolymers with varying monomer compositions.

Sample	G / mol% [a]	G (th.) / mol%	DB / % [b]	M_n / g mol^{-1} [c]	PDI [c]	T_g / °C	LCST / °C
hb$PPO_{0.97}$-*co*-$PG_{0.03}$	3	5	11	2000	1.48	-65	24
hb$PPO_{0.88}$-*co*-$PG_{0.12}$	12	10	18	1400	1.68	-62	33
hb$PPO_{0.83}$-*co*-$PG_{0.17}$	17	15	27	1350	1.65	-59	40
hb$PPO_{0.80}$-*co*-$PG_{0.20}$	20	20	37	1600	1.41	-54	43
hb$PPO_{0.70}$-*co*-$PG_{0.30}$	32	30	50	1700	1.69	-49	83
hb$PPO_{0.62}$-*co*-$PG_{0.38}$	38	40	53	1500	1.40	-48	--
hb$PPO_{0.44}$-*co*-$PG_{0.56}$	56	50	59	1160	1.63	-35	--

a) Determined from ^{1}H NMR; b) Determined from inverse gated ^{13}C NMR; c) Determined from SEC (solvent: DMF, linear PEO standard).

In contrast to previous reports on PPO star copolymers with hyperbranched polyglycerol as a core,[24] random hyperbranched PPO copolymers are formed, as it is evident from NMR spectra and the dependence of the end group structure on the comonomer composition. For the random copolymers, the PO/G ratio can be adjusted and the so far necessary multistep synthesis can be reduced to one single polymerization step.

The thermal behavior of the hyperbranched polyethers has also been investigated. Differential scanning calorimetry (DSC) has been used to quantifiy the thermal properties of the materials. With increasing glycerol content, the glass transition (T_g) increases from the Tg of the linear homopolymer PPO (−73 °C)[23] to the T_g of the hyperbranched homopolymer polyglycerol (−25 °C).[30] We ascribe this to the additional interaction of the increasing number of hydroxyl groups via

hydrogen-bonding in the multifunctional copolymers. In contrast to hyperbranched poly(ethylene oxide),[28] a completely amorphous and, thus, highly flexible hyperbranched polyether polyol is obtained.

Size exclusion chromatography (SEC) yields molecular weight distributions with M_w/M_n between 1.4 and 1.7 (Table 1, Figure S4). MALDI ToF mass spectrometry shows molecular weights in the same range and supports incorporation of both comonomers (cf. Figure S5, Supporting Information). Molecular weights are generally in the range of 1000−2000 g mol^{-1}, that is, in the same range as for numerous other hyperbranched materials.[6] It appears that the amount of initiator used does not permit to control molecular weights, in contrast to the hyperbranched polyglycerol homopolymer. Further work on this issue is under way. However, it is remarkable that hyperbranched PPO copolymers of moderate polydispersity index and adjustable functionality can be obtained, despite deviating from a slow addition protocol, as is typically employed to control the anionic hyperbranching homopolymerization of glycidol.[3,30]

In contrast to the PPO homopolymer, the hyperbranched polyethers are highly soluble in water under ambient conditions. This is attributed to the introduction of additional hydroxyl end groups as a consequence of the incorporation of glycidol as a comonomer. Interestingly, the hyperbranched PPO-based polyethers show temperature-sensitive solubility in aqueous solution with a lower critical solution temperature (LCST). The thermoresponsive behavior can be explained by the interplay of the hydrophilic groups (especially the hydroxyl end groups) and the hydrophobic methyl groups of the rather apolar PPO segments. At temperatures above the cloud point of the solutions, the hydrophobic domains cause a phase separation from water due to aggregation. This forces the polymer chain to undergo a coil-to-globule transition and consequently results in the observed macroscopic precipitation. For linear aliphatic polyether copolymers, a similar temperature-dependent solubility behavior in aqueous solution has been reported recently.[22,31] Cloud points of aqueous copolymer solutions have been investigated by turbidimetry measurement, using a temperature-controlled UV−vis spectrometer. Figure 2 shows the temperature dependence of the light transmission of aqueous polymer solutions and the dependence of the LCST on the glycerol content. As can be seen from Figure 2a, the LCST behavior can be controlled by variation of the comonomer content. With increasing fraction of the more hydrophilic glycerol units, the LCST of the hyperbranched PPO copolymers increases. At this point, we assume that the unusual curve shape of the copolymers with intermediate glycidol content has to be ascribed to the hyperbranched nature of the copolymers, as they differ from analogous linear copolymers.[22] Figure 2b shows the effect of the glycidol content on the LCST. The LCST value increases almost linearly with increasing content of the hydrophilic glycerol comonomer.

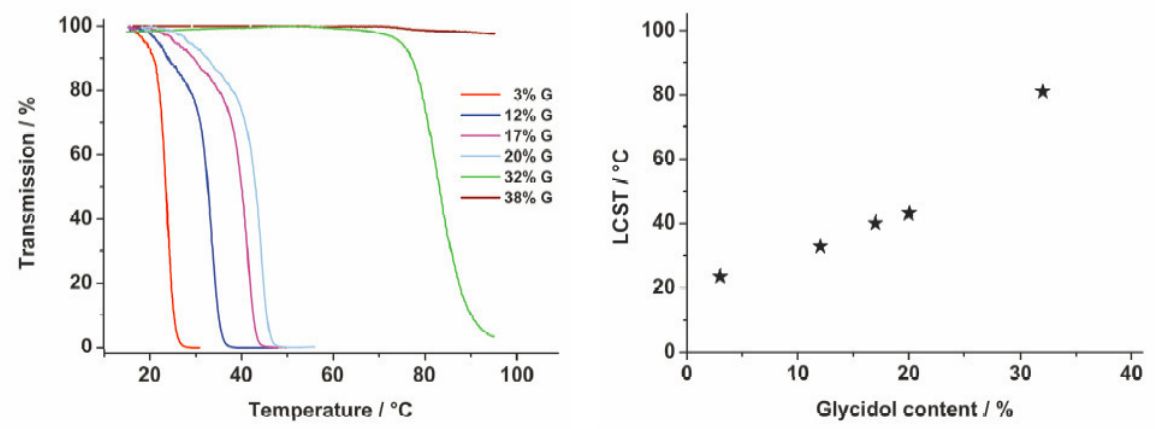

Figure 2. (a) Intensity of transmitted laser light vs temperature for *hb*PPO-*co*-PG copolymers of various compositions at a concentration of 5 mg mL^{-1} in aqueous solution. (b) Effect of glycidol content on LCST.

This is consistent with previous reports on linear random polyethers based on ethylene oxide and PO or other glycidyl ethers.[31,32] Our study demonstrates that this behavior is also found for hyperbranched polyethers. The interception with the y-axis (19.7 °C) corresponds to the LCST of a polymer with 0% of comonomer incorporated (PPO homopolymer) and is in good agreement with previous experimental results for the PPO homopolymer.[33]

Conclusion

In summary, we have introduced a new type of backbone-thermoresponsive hyperbranched polyether prepared by solvent-free anionic copolymerization of propylene oxide and glycidol in one single step. The copolymer composition and the LCST values can be readily adjusted by varying the comonomer ratio. In all cases monomodal, moderate molecular weight distributions with PDIs generally below 1.7 were obtained. The hyperbranched polyethers with thermoresponsive backbone possess an adjustable number of hydroxyl end groups that can be used for further functionalization or cross-linking. Their possible use as building blocks for stimuli-responsive hydrogels or nanoparticles in the biomedical field or as flexible polyol component for polyurethanes renders them interesting for further exploration.

Acknowledgment

M.S. and H.F. acknowledge funding of the Max Planck Graduate Center (MPGC) with the Johannes Gutenberg-University and the Graduate School of Excellence “Materials Science in Mainz/MAINZ”. The authors thank Sebastian Jäger for technical assistance.

References

1. Yan, D., Gao, C., Frey, H, Eds.; *Hyperbranched Polymers: Synthesis, Properties, and Applications*; Wiley: Hoboken, NJ, **2011**.
2. Calderón, M.; Quadir, M. A.; Sharma, S. K.; Haag, R. *Adv. Mater*. **2010**, *22*, 190−218.
3. Wilms, D.; Stiriba, S.-E.; Frey, H. *Acc. Chem. Res*. **2010**, *43*, 129−141.
4. Zhou, Y.; Huang, W.; Liu, J.; Zhu, X.; Yan, D. *Adv. Mater*. **2010**, *22*, 4567−4590.
5. Carlmark, A.; Hawker, C.; Hult, A.; Malkoch, M. *Chem. Soc. Rev*. **2009**, *38*, 352.
6. Voit, B. I.; Lederer, A. *Chem. Rev*. **2009**, *109*, 5924−5973.
7. Voit, B. *J. Polym. Sci., Part A: Polym. Chem*. **2005**, *43*, 2679−2699.
8. Gao, C.; Yan, D. *Prog. Polym. Sci*. **2004**, *29*, 183−275.
9. Voit, B. *J. Polym. Sci., Part A: Polym. Chem*. **2000**, *38*, 2505−2525.
10. Liu, H.; Chen, Y.; Shen, Z. *J. Polym. Sci., Part A: Polym. Chem*. **2007**, *45*, 1177−1184.
11. Kojima, C.; Yoshimura, K.; Harada, A.; Sakanishi, Y.; Kono, K. *Bioconjugate Chem*. **2009**, *20*, 1054−1057.
12. Kojima, C.; Yoshimura, K.; Harada, A.; Sakanishi, Y.; Kono, K. *J. Polym. Sci., Part A: Polym. Chem*. **2010**, *48*, 4047−4054.
13. Sun, X.; Zhou, Y.; Yan, D. *Macromol. Chem. Phys*. **2010**, *211*, 1940−1946.
14. Wang, H.; Sun, S.; Wu, P. *J. Phys. Chem. B* **2011**, *115*, 8832−8844.
15. Jia, Z.; Chen, H.; Zhu, X.; Yan, D. *J. Am. Chem. Soc*. **2006**, *128*, 8144−8145.
16. Chen, H.; Jia, Z.; Yan, D.; Zhu, X. *Macromol. Chem. Phys*. **2007**, *208*, 1637−1645.
17. Pang, Y.; Zhu, Q.; Zhou, D.; Liu, J.; Chen, Y.; Su, Y.; Yan, D.; Zhu, X.; Zhu, B. *J. Polym. Sci., Part A: Polym. Chem*. **2011**, *49*, 966−975.
18. Xia, Y.; Wang, Y.; Wang, Y.; Wang, D.; Deng, H.; Zhuang, Y.; Yan, D.; Zhu, B.; Zhu, X. *Macromol. Chem. Phys*. **2011**, *212*, 1056−1062.
19. Jia, Z.; Li, G.; Zhu, Q.; Yan, D.; Zhu, X.; Chen, H.; Wu, J.; Tu, C.; Sun, J. *Chem. Eur. J*. **2009**, *15*, 7593−7600.
20. Yu, B.; Jiang, X.; Yin, G.; Yin, J. *J. Polym. Sci., Part A: Polym. Chem*. **2010**, *48*, 4252−4261.

21. Pang, Y.; Liu, J.; Su, Y.; Wu, J.; Zhu, L.; Zhu, X.; Yan, D.; Zhu, B. *Polym. Chem*. **2011**, *2*, 1661.
22. Schömer, M.; Frey, H. *Macromolecules* **2012**, *45*, 3039−3046.
23. Istratov, V.; Kautz, H.; Kim, Y.-K.; Schubert, R.; Frey, H. *Tetrahedron* **2003**, *59*, 4017−4024.
24. Sunder, A.; Mülhaupt, R.; Frey, H. *Macromolecules* **2000**, *33*, 309−314.
25. Stolarzewicz, A.; Morejko-Buż, B.; Grobelny, Z.; Pisarski, W.; Frey, H. *Polymer* **2004**, *45*, 7047−7051.
26. Fröhlich, J.; Kautz, H.; Thomann, R.; Frey, H.; Mülhaupt, R. *Polymer* **2004**, *45*, 2155−2164.
27. Royappa, A. T.; Dalal, N.; Giese, M. W. *J. Appl. Polym. Sci*. **2001**, *82*, 2290−2299.
28. Wilms, D.; Schömer, M.; Wurm, F.; Hermanns, M. I.; Kirkpatrick, C. J.; Frey, H. *Macromol. Rapid Commun*. **2010**, *31*, 1811−1815.
29. Frey, H.; Hölter, D. *Acta Polym*. **1999**, *50*, 67−76.
30. Sunder, A.; Hanselmann, R.; Frey, H.; Mülhaupt, R. *Macromolecules* **1999**, *32*, 4240−4246.
31. Mangold, C.; Obermeier, B.; Wurm, F.; Frey, H. *Macromol. Rapid Commun*. **2011**, *32*, 1930−1934.
32. Louai, A.; Sarazin, D.; Pollet, G.; François, J.; Moreaux, F. *Polymer* **1991**, *32*, 703−712.
33. Mortensen, K.; Schwahn, D.; Janssen, S. *Phys. Rev. Lett*. **1993**, *71*, 1728.

Supporting Information

Instrumentation

^{1}H NMR and ^{13}C NMR spectra were recorded on a Bruker AC300 or AMX400 and were referenced internally to residual proton signals of the deuterated solvent. For SEC measurements in DMF (containing 0.25 g L^{-1} of lithium bromide as an additive), an Agilent 1100 series was used as an integrated instrument including a PSS HEMA column ($10^6/10^4/10^2$ Å porosity) and both, an UV and a RI detector. Calibration was achieved with poly(ethylene oxide) standards provided by Polymer Standards Service (PSS). Matrix-assisted laser desorption and ionization time-of-flight (MALDI-ToF) measurements were performed on a Shimadzu Axima CFR MALDI-TOF mass spectrometer, using dithranol (1,8,9-trishydroxyanthracene) as matrix. DSC curves were recorded with a Perkin Elmer DSC 7. Samples were dried for 24 h at 80 °C in vacuum before measurements. Cloud points were determined in deionized water at varying concentration and observed by optical transmittance of a light beam (λ = 632 nm) through a 1 cm sample quartz cell. The measurements were performed in a Jasco V-630 photospectrometer with a Jasco ETC-717 Peltier element. The intensities of the transmitted light were recorded versus the temperature of the sample cell. The heating/cooling rate was 1 K min^{-1} and values were recorded every 0.1 K.

Materials

All reagents and solvents were used as received, if not otherwise mentioned. Deuterated DMSO-d_6 was purchased from Deutero GmbH. Propylene oxide and glycidol were dried over CaH_2 and distilled under vacuum prior to use.

Synthesis of *hb*PPO-*co*-PG Copolymers

Typical procedure for the preparation of random copolymers of propylene oxide and glycidol: Here, an exemplary synthetic protocol is described for *hb*$PPO_{0.80}$-*co*-$PG_{0.20}$: A two-necked flask equipped with a septum, teflon seal and a magnetic stirrer was connected to a vacuum line. 45 mg (0.33 mmol) of 1,1,1-tris(hydroxymethyl)propane (TMP) was deprotonated with 0.3 eq. potassium *tert*-butoxide in methanol and dried azeotropically with benzene to remove the methanol together with formed *tert*butanol and other volatiles. 2.32 g (40 mmol) propylene oxide (PO) was transferred to an ampoule and subsequently to the reaction flask in vacuo. The flask was sealed

and 740 mg (10 mmol) freshly distilled glycidol was introduced through the septum via cannula. The reaction mixture was then immediately heated to 120°C and stirred for 18 h. After addition of an excess of methanol to quench the polymerization the solution the copolymer was precipitated in a mixture of hexane and isopropanol to afford the hyperbranched $PPO_{0.80}$-*co*-$PG_{0.20}$ in ca. 80-90% yield.

Caution: In very few cases the pressure evolving in the early stages of the reaction in the flask led to the spontaneous removal of the septum and release of PO. Thus, the reaction has to be carried out in an appropriate fume hood and according safety precautions should be taken. In general, the amount of PO used did not exceed 5 g per batch in a 250 mL flask to guarantee a safe reaction.

Supplementary Characterization Data

Figure S1 shows the ^{1}H NMR spectrum of a typical PPO-*co*-PG copolymer. Both the initiator core and the hydroxyl protons are clearly visible.

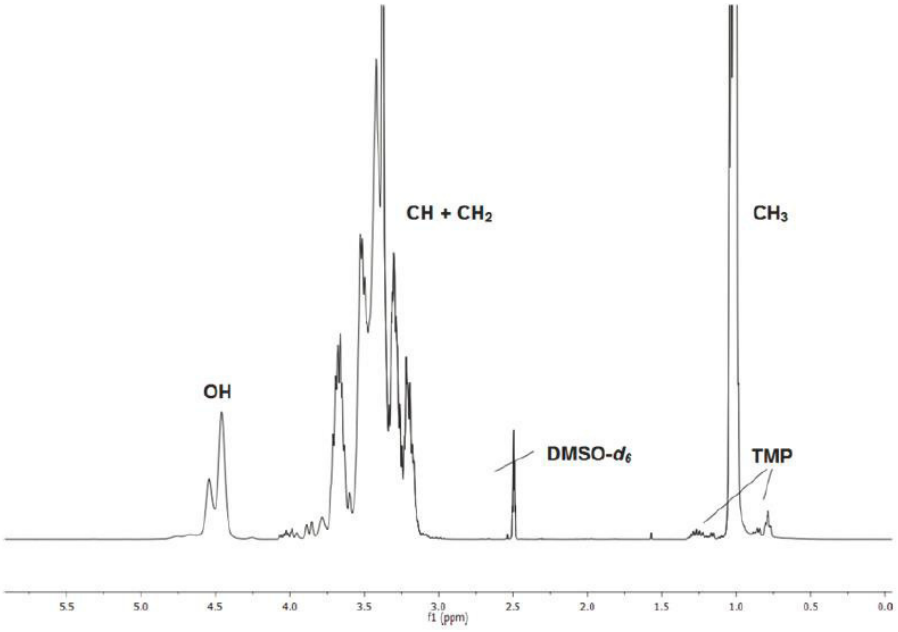

Figure S1. 1H NMR spectrum (400 MHz) of *hb*PPO-*co*-PG with a trimethylol propane core.

The fraction of glycerol units incorporated into the polymer was calculated by referencing to the methyl group of the initiator (0.78 ppm) and comparing this value with the integral of the methyl group of the propylene oxide units (0.99 - 1.05 ppm) and the methylene and methine groups of the polymer backbone (3.1-3.9 ppm). In addition, the total number of glycidol units of each macromolecule corresponds to the total number of hydroxyl groups (4.4 - 4.7 ppm) minus the number of hydroxyl groups introduced by the initiator moiety (assuming that the core is fully incorporated into the polymer distribution). In the case of a trimethylol propane core, $n(OH)_{core}$ equals a value of 3. The other five protons of each glycerol unit as well as three propylene oxide protons generate a broad resonance between 3.1 and 3.8 ppm. Hence, the ratio between propylene oxide and glycerol repeat units can be directly calculated.

$$\#PO = \frac{I_{Methyl}}{3}$$

$$\#G = \frac{I_{Backbone} - 3 \cdot \#PO}{5}$$

$$\#G = n(OH)_{total} - n(OH)_{core}$$

Both equations for the calculation of the number of glycidol units are in good agreement. These values become defective if the core is not fully incorporated into the polymer and/or if the intensity of the hydroxyl groups is very low (e. g., at low glycidol feed ratios).

$$DP_n = \#G + \#PO$$

$$\%G = \frac{\#G}{DP_n}$$

The overall degree of polymerization (DPn) is the sum of both comonomers, and the glycidol content is calculated by dividing the number of G units by the DP_n. All values are rounded to integer.

Figure S2 shows the HSQC (heteronuclear single-quantum correlation) spectrum of the sample with ca. 20% glycidol content. Methylene groups can be identified by their blue color, while red color represents the methine groups. The HSQC spectrum further confirms the assignments given in Figure 1 of the main manuscript.

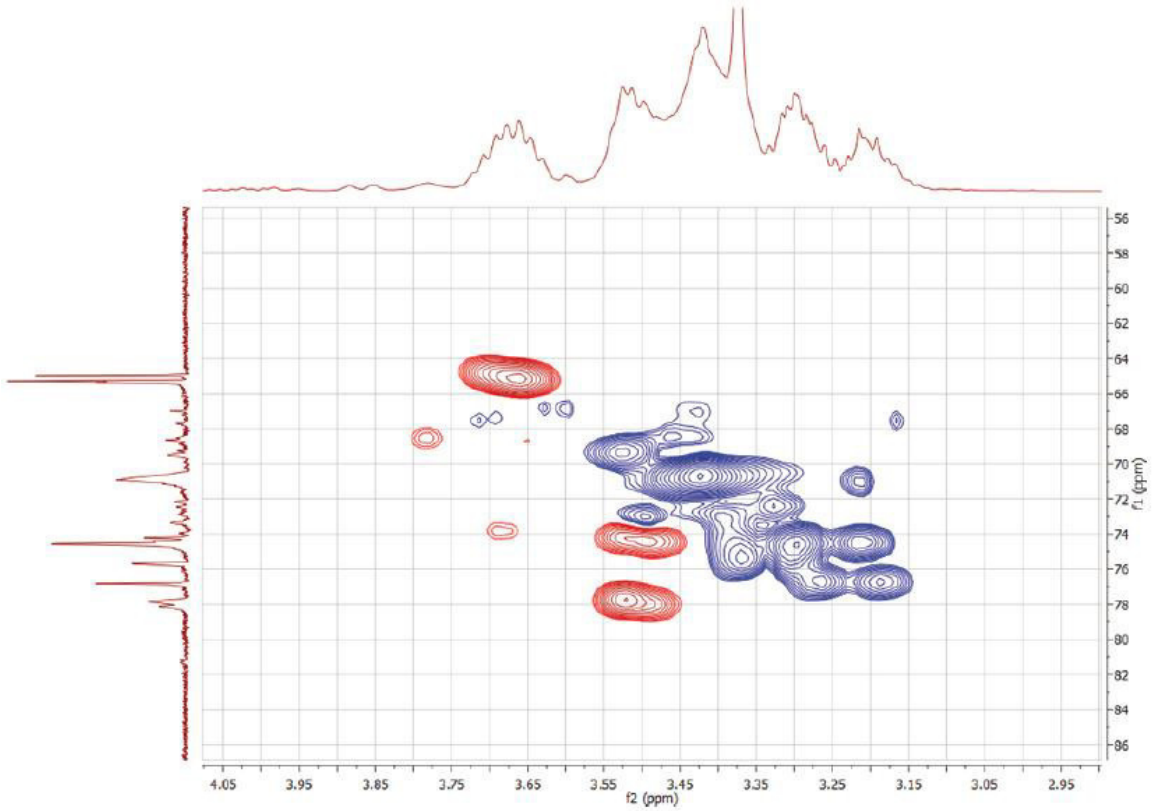

Figure S2. HSQC spectrum of *hb*PPO-*co*-PG with a glycidol fraction of 20%. ^{1}H- and ^{13}C NMR spectra can be found on the horizontal and vertical axis, respectively.

The degree of branching DB was calculated using the equation introduced by Hölter and Frey for random copolymerization of AB/AB_2 systems.[29]

$$DB_{\frac{\mathrm{AB}}{\mathrm{AB_2}}} = \frac{2D}{2D + L_{co}}$$

Figure S3 shows the experimental relation between the comonomer ratio (expressed as glycidol content) and the degree of branching.

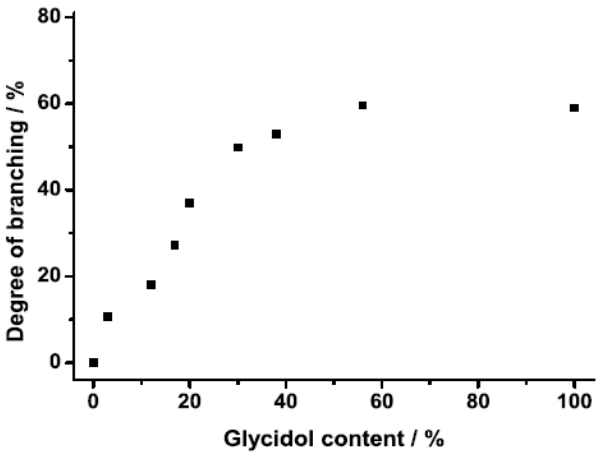

Figure S3. Plot of the degree of branching vs. the glycidol content (calculated from inverse gated ^{13}C NMR spectra).

It has to be taken into account that integrals obtained from inverse gated ^{13}C NMR spectroscopy may involve an error due to the noise level inherent to this technique. Partial overlap of the signals, particularly at high comonomer fractions, further complicates quantitative analysis.

Figure S4 shows typical SEC traces of *hb*PPO-*co*-PGs, measured in DMF with linear PEG standards.

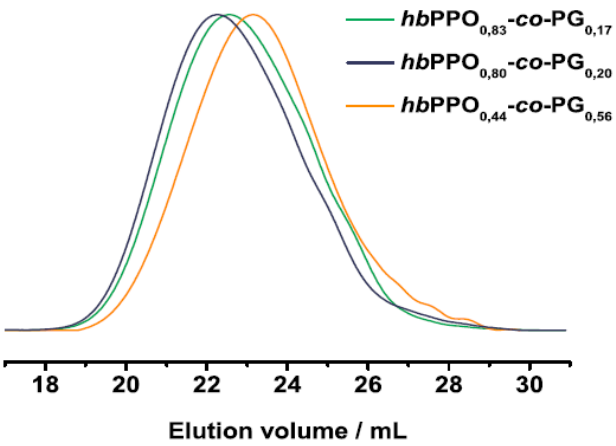

Figure S4. SEC traces (measured in DMF) of *hb*PPO-*co*-PGs with different glycidol fractions.

In addition to the NMR and SEC characterization the composition and molecular weight of the copolymers was also analysed by MALDI-ToF mass spectrometry. In Figure S5 the characteristic subdistributions for copolymers can be seen. Each series of colored dots represents a distribution with the same number of glycidol units but different PO contents. As the generally used initiator 1,1,1-tris(hydroxymethyl)propane (TMP) is not suitable for MALDI-ToF analysis because distinction between TMP-initiated polymer chains and those initiated by residual traces of water would not be possible (M(TMP) = 134.17 g/mol = 2 x M(PO) + M(H2O)) another initiator was chosen (1,3,5-tris-(hydroxymethyl)benzene) for the MALDI-ToF characterization. The incorporation of both comonomers and the initiator can be clearly seen. The molecular weights obtained by MALDI-ToF-MS are in the same range as the values obtained from SEC.

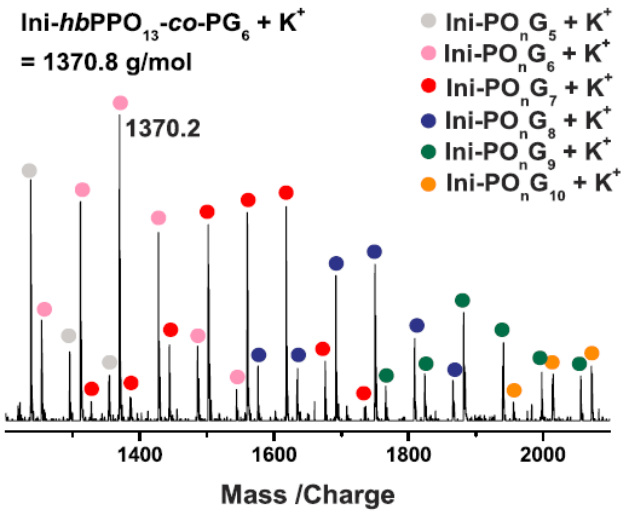

Figure S5. MALDI-ToF-MS spectrum of *hb*PPO$_{0.70}$-*co*-PG$_{0.30}$ (SEC: M_n = 1700 g mol^{-1}, PDI = 1.47) showing the characteristic subdistributions of copolymers.

A.2 List of Publications

Peer-reviewed Publications

"Hyperbranched Poly(propylene oxide): A Multifunctional Backbone-Thermoresponsive Polyether Polyol Copolymer"

M. Schömer, J. Seiwert, H. Frey, *ACS Macro Lett.* **2012**, *1* (7), 888–891.

"Controlled Synthesis of Multi-Arm Star Polyether-Polycarbonate Polyols Based on Propylene Oxide and CO_2"

J. Hilf, P. Schulze, J. Seiwert, H. Frey, *Macromol. Rapid Commun.* **2014**, *35* (2), 198-203.

"Hyperbranched Poly(ethylene glycol) Copolymers: Absolute Values of the Molar Mass, Properties in Dilute Solution, and Hydrodynamic Homology"

I. Perevyazko, J. Seiwert, M. Schömer, H. Frey, U.S. Schubert, G.M. Pavlov, *Macromolecules* **2015**, *48* (16), 5887-5898.

"Hyperbranched Polyols via Copolymerization of 1,2-Butylene Oxide and Glycidol: Comparison of Batch Synthesis and Slow Monomer Addition"

J. Seiwert, D. Leibig, U. Kemmer-Jonas, M. Bauer, I. Perevyazko, J. Preis, H. Frey, *Macromolecules* **2016**, *49* (1), 38-47.

"Polymerization of Ethylene Oxide, Propylene Oxide, and Other Alkylene Oxides: Synthesis, Novel Polymer Architectures, and Bioconjugation" (Review article)

J. Herzberger, K. Niederer, H. Pohlit, J. Seiwert, M. Worm, F.R. Wurm, H. Frey, *Chem. Rev.* **2016**, *116* (4), 2170-2243.

"Thioether-Bearing Hyperbranched Polyether Polyols: A Versatile Platform for Orthogonal Functionalization"

J. Seiwert, J. Herzberger, D. Leibig, H. Frey **2016**, *submitted*.

"Online NMR Copolymerization Kinetics of Glycidol with Ethylene Oxide, Propylene Oxide and 1,2-Butylene Oxide: From Hyperbranched to Hyperstar"

D. Leibig, J. Seiwert, J. Liermann, H. Frey **2016**, *submitted*.

"Multiarm Star Polyether-Polycarbonates Based on Hyperbranched Polyether Polyols, Carbon Dioxide and Tailored Epoxides"

M. Scharfenberg, J. Seiwert, M. Scherger, J. Preis, H. Frey **2016**, *submitted.*

“Ultra-high Molecular Weight Polystyrene Hyperstar Polymers with Hyperbranched Polyethylene Oxide as the Core”

J. Seiwert, P. Winterwerber, H. Frey **2016**, *in preparation*.

“Controlling the Molar Mass of Hyperbranched Poly(ethylene oxide) Copolymers via Polymerization under Slow Monomer Addition Conditions”

J.Seiwert, J. Vitz, T. Majdanski, T. Kaiser, U.S. Schubert, H. Frey **2016**, *in preparation*.

Conference Contributions

"Thermoresponsive Hyperbranched Poly(1,2-butylene oxide) by Random Anionic Copolymerization with Glycidol" (Poster)

J. Seiwert, M. Bauer, D. Leibig, H. Frey, *European Polymer Federation Congress*, Dresden/Germany **2015**.

"Tailoring Hyperbranched Polyether Polyols with Adjustable Degree of Branching and Hydrophilicity by Random Anionic Copolymerization of Alkylene Oxides and Glycidol" (Talk)

J. Seiwert, M. Schömer, M. Bauer, H. Frey, *250th American Chemical Society National Meeting*, Boston/USA **2015**.